Simulation-integrated Design of Dry Bulk Terminals

Teus van Vianen

Delft University of Technology

Cover design: Fourdesign

Simulation-integrated Design of Dry Bulk Terminals

Proefschrift

ter verkrijging van de graad van doctor
aan de Technische Universiteit Delft,
op gezag van de Rector Magnificus prof. ir. K.C.A.M. Luyben,
voorzitter van het College voor Promoties
in het openbaar te verdedigen op dinsdag 13 januari 2015 om 15:00 uur

door

Teunis Arie VAN VIANEN

Werktuigkundig ingenieur,
geboren te Brandwijk.

Dit proefschrift is goedgekeurd door de promotor:

Prof. dr. ir. G. Lodewijks

Samenstelling promotiecommissie:

Rector Magnificus	voorzitter
Prof. dr. ir. G. Lodewijks	Technische Universiteit Delft, Promotor
Dr. ir. J.A. Ottjes	Technische Universiteit Delft, Copromotor
Prof. dr.-Ing. H. Lieberwirth	Technische Universität Bergakademie Freiberg
Prof. dr. ir. A. Verbraeck	Technische Universiteit Delft
Prof. ir. T. Vellinga	Technische Universiteit Delft
Prof. ir. J.C. Rijsenbrij	Technische Universiteit Delft

TRAIL Thesis Series T2015/1, the Netherlands TRAIL Research School

TRAIL Research School
PO Box 5017
2600 GA Delft
The Netherlands
T: +31 (0) 15 278 6046
E: info@rsTRAIL.nl

ISBN: 978-90-5584-182-0

Printed in the Netherlands

To the memory of my father,
not only because I miss him
but also to be thankful that he
encouraged me to continue studying.

Preface

I am grateful to present my PhD thesis. During my PhD project I was supported, encouraged and challenged by many people. This preface is an excellent opportunity to express my thanks.

First of all, I would like to thank my promotor Gabriël Lodewijks. Despite his busy schedules he always made time for me to discuss my research and to push me into the right direction. By asking the right questions, he made sure that the outcome of the research is applicable for solving real problems. I am also thankful for his suggestions after reviewing papers which helped me a lot to formulate my sentences more accurate en more precise. I really appreciate the support of my copromotor Jaap Ottjes during my PhD research even after he has been retired. He helped me when I was stuck with my simulation models and always challenged me to check (and double check) that my models are correct. I want to thank him for reading my papers and thesis a couple of times. Although, I was not always happy when I received back this work fully red-colored with your remarks, it puts my writer's skills up to a higher level.

I would like to express my thanks to some persons in particular who work in the dry bulk industry; Jan de Wit, Daniël Mooijman, Ron Schuurmans and Koen van Horssen. I really appreciate the meetings with them and I am grateful for all operational data they provided. During meetings they challenged me to bridge the gap between the academic world and their daily challenges. During Daniël's MSc thesis project and afterwards he helped me with a lot with the analysis of data, developing simulation models and for giving valuable feedback. I want to thank Koen in particular for his work for the determination of the effective reclaiming capacity for bucket-wheel reclaimers.

Further, I would like to thank all other students who cooperate in this research as well. It was often a welcome break of my daily activities to supervise them and to discuss parts of my research project.

To my colleagues in the Maritime and Transport Engineering department, many thanks for our chats, discussions, international dinners and drinks. Moreover, it has enriched me to work together with people from so many nationalities. It has broadened my horizon about global issues and the impact of local media on our opinions. I also would like to thank Joan Rijsenbrij for his motivational talks and his contribution to my research. For the conversations with coffee on the early mornings with Dick, Hans and Jaap, I am going to miss their humorous look on daily news.

I would like to thank my family and friends for their support and questions about my research. It helped me a lot to step out of my research area and vocabulary to explain my PhD project to 'outsiders'. I am truly indebted to Chris for designing the cover and to Albert and Marlene who agreed to be my paranymphs during the PhD ceremony. In particular, I would like to thank my mother and in memory to my recently deceased father, for their support in my study and their interest in what I was doing.

I would like to thank Liesbeth for her encouragement and support during this project. I was quite often absent when I locked myself again in my office the entire day (and night) to perform the research and to write this thesis. To my daughters, Anna and Evi, from now I will have time again to visit all playgrounds in our neighborhood. Last, but certainly not least, I would like to thank God for given me the health, talent and perseverance to complete this PhD project.

Ridderkerk, September 2014

Teus van Vianen

Table of Contents

1 Introduction

1.1 A growing global demand for energy and steel

Coal and iron ore are essential base materials for the global production of electric energy and steel. Although the demand for renewable energy sources is growing and the requirements for greenhouse gas emission reductions are becoming stricter, coal will be required in the near future to meet the global demand for electrical power. Coal fired power plants are often the short term answer to power shortages (IEA, 2013).

Figure 1.1 shows the global energy demand broken down into the main primary energy fuels expressed in million tons of oil equivalents per year [Mtoe/y]. Global energy use decreased significantly in 2009 as a result of the financial and economic crisis, but it quickly resumed its long-term upward trend once economic recovery was underway. Crude oil remains the dominant fuel for power generation and coal is expected to remain the second main fuel for power generation throughout the period to 2035 (IEA, 2013).

Due to the lower calorific value of coal compared to crude oil, the required coal volumes will grow faster than the required oil volumes. The centre of gravity for energy demand is switching decisively to the emerging economies, particularly China, India and the Middle East. China is about to become the largest oil-importing country and India becomes the largest importer of coal by the early 2020s. The only region where coal demand declined is the United States. That drop is the result of the availability of cheap (shale) gas. Except this region, coal remains a cheaper option than gas for electricity generation. Policy interventions to improve efficiency, to reduce local air pollution and to mitigate climate change will be critical in determining its longer-term prospects (IEA, 2013).

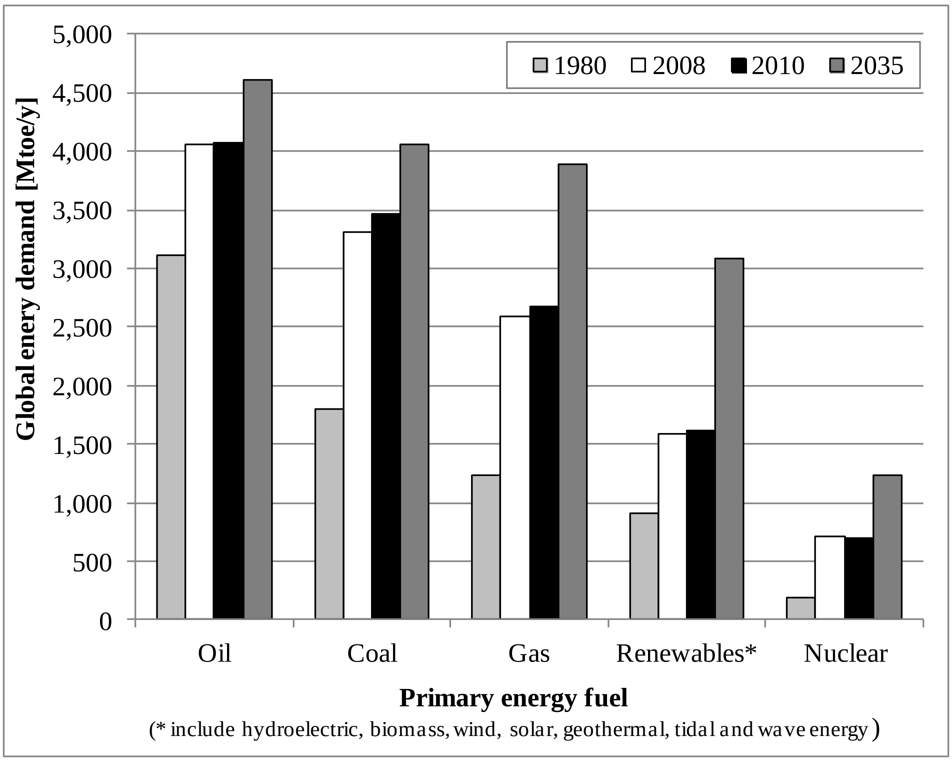

Figure 1.1: Global energy demand for the main energy fuels (in Mtoe/y), derived from IEA (2011)

The current state of the global steel industry shows a slower demand growth, overcapacity, low profitability and strengthening environmental regulations. However, future scenarios for the steel industry predict that urbanization and population growth will support the global steel demand growth for considerable time (Han, 2013).

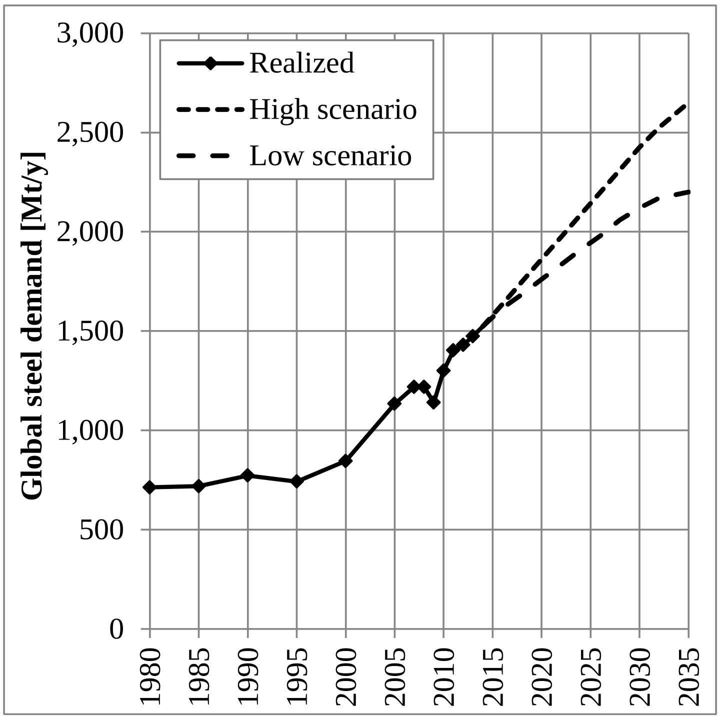

Figure 1.2: Realized and projected global steel demand, derived from Han (2013)

Figure 1.2 shows the realized global steel demands from 1980 until 2013 and two projected long term scenarios that were introduced by (Han, 2013), expressed in million tons per year [Mt/y]. Unfortunately, Han (2013) did not mention the reasons for the distinction between the two long term scenarios and did not provide regional developments. Sultoon (2013) stated that the projected global steel demand will be dominated by China, India, Japan and South Korea. European steel producers will probably be forced to relocate their production facilities due to Europe’s expensive energy policy and the low gas prices (caused by the shale gas boom in the United States) elsewhere in the world (DCI, 2013).

1.2 Seaborne trade flows for coal and iron ore

Steam (or thermal) coal is used for the production of electric energy and coking (or metallurgical) coal and iron ore are the ingredients for steel production. Coal and iron ore reserves and the industrial users are often located far apart. To connect the mines, where these dry bulk materials are excavated, with the coal-fired power plants and steelworks, freight trains are generally used for the transport over land and large bulk ships are used for the sea-transport.

Figure 1.3 and Figure 1.4 show historical seaborne trade flows for coal (divided in steam and coking coal) and iron ore respectively. The directions and thicknesses of the arrows indicate the orientation and volumes of the seaborne trade flows between different countries and continents. Both figures show the huge Asian demand for coal and iron ore. Coal is mainly shipped from Indonesia and Australia to Asia (dominated by China, Japan and South Korea) and iron ore is primarily shipped from Australia and Brazil to Asia.

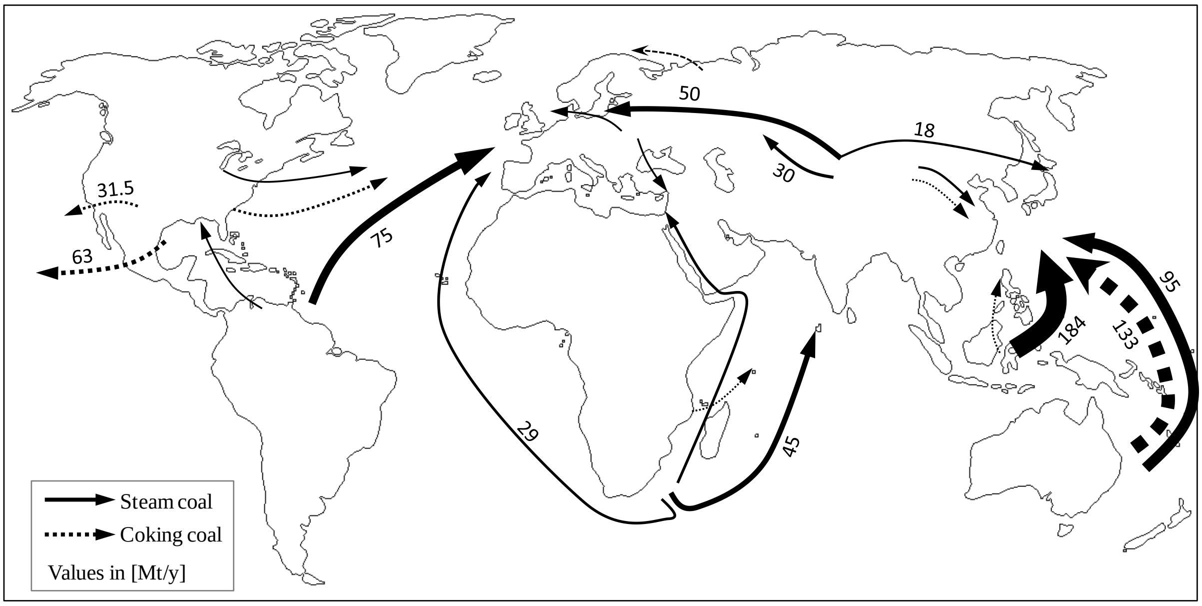

Figure 1.3: Seaborne trade flows for steam coal in 2010 (total 638 [Mt/y]), based on Haftendorn et al. (2012) and coking coal in 2012 (total 245 [Mt/y]), derived from Sultoon (2013)

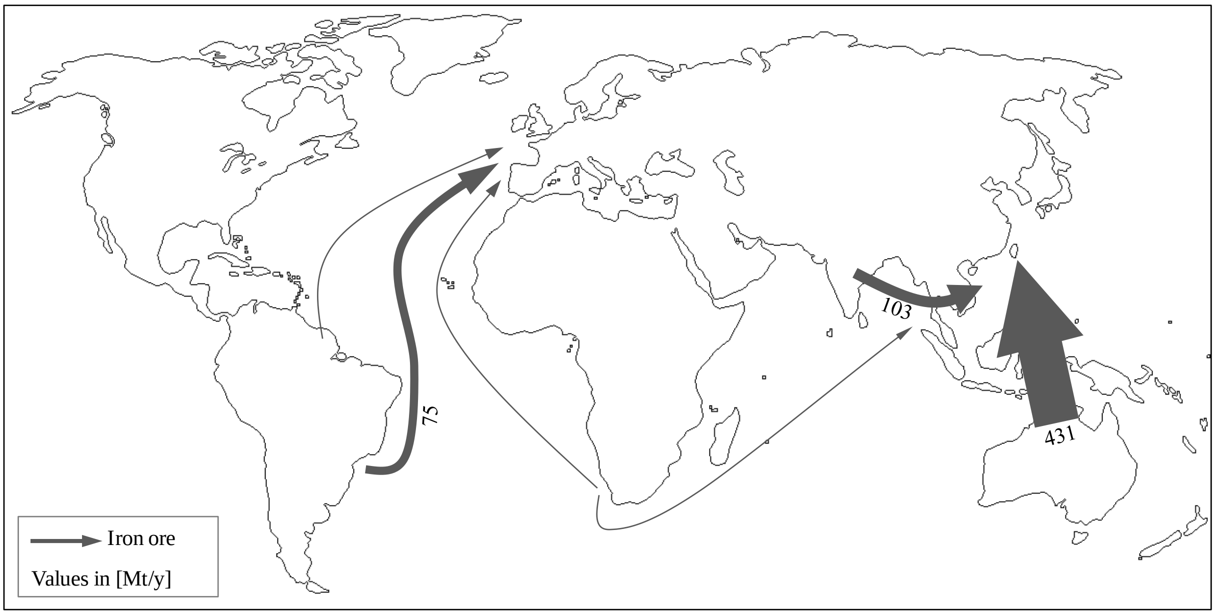

Figure 1.4: Seaborne trade flows for iron ore in 2010 (total 893 [Mt/y]), derived from Laugharne (2012)

Long term projections for seaborne trade flows are relevant for port development plans. Investments in port infrastructure are fixed investments with a long pay-back period. Analyzing the financial viability requires long term projections of port throughput (de Langen et al. 2012).

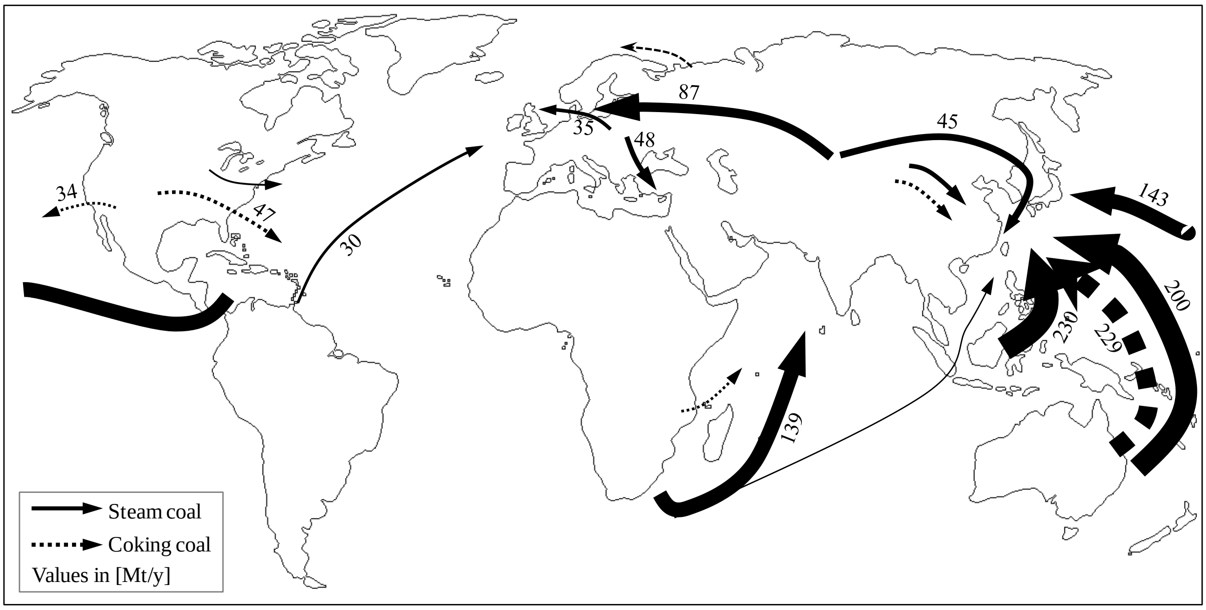

Figure 1.5: Projected seaborne trade flows for steam coal (total 1,009 [Mt/y]) and coking coal (total 391 [Mt/y] in 2030, derived from Haftendorn et al. (2012) and Sultoon (2013)

A limited number of research papers addressed long term projections for coal and iron ore. The aim for long term projections is to provide a 'sense of direction', precise figures are less relevant due to the uncertainty of future developments. Haftendorn et al. (2012) developed a numerical model for steam coal by including the major domestic markets together with the globalized seaborne market and incorporates geological, technical and economical data and mechanisms. The projected seaborne trade flows for steam coal in the year 2030 are shown in Figure 1.5 for the increasing demand scenario. This figure also shows the projected seaborne trade flows for coking coal in 2030 which were derived from (Sultoon, 2013).

From Figure 1.5 it can be derived that Australia and Indonesia remain the key players to deliver coal to Asia. The third most important exporter will be South Africa with an export level that doubles between 2006 and 2030. The good quality South African coal will be shipped to India, which is expected to be the largest coal importing country as from 2020. Russia and Poland will replace Europe's traditional coal supplier South Africa in 2030. Furthermore, a westwards shift from Colombian coal to Japan and South-Korea is expected.

Long term projections for the iron ore seaborne trade flows were not found. Han (2013) shows projections for the global steel demand, already shown in Figure 1.2. In 2030, the world population may reach 8 billion (was 6.9 billion in 2010), with 96% of growth coming from developing countries. India will overtake China with the largest population and the largest labor force in the world. Therefore, it is expected that India will see the largest growth in steel consumption. The Chinese steel consumption growth will slow down but China will still remain the biggest steel consumer in 2030 (Lloyd's Register, 2013). For the seaborne trade flows it is expected that India will not export iron ore to Asia anymore and Australia and Brazil will remain shipping iron ore to Asia. It is expected that iron ore will be shipped to India from South-Africa, Australia and Brazil.

1.3 Dry bulk terminals to tranship coal and iron ore

This research focuses on dry bulk terminals that handle coal and iron ore. Terminals dedicated for grain, the other dry bulk material that is shipped in large quantities around the world, are excluded in this research. To meet the growing global demand for energy and steel, the seaborne trade flows for coal and iron ore will have to increase. Dry bulk terminals are crucial nodes in the supply chain for these dry bulk materials. To facilitate the expected growing cargo flows, new dry bulk terminals have to be built or existing ones need to be expanded.

Dry bulk terminals will be faced in the future with a shortage of port areas that will result in an increase of the price per hectares to buy or rent these areas. Due to economies of scales for the transport of coal and iron ore, bulk ships will be even larger in future. The terminal's draft and the ship (un)loading equipment may possibly not be sufficient anymore. But also the environmental requirements will be stricter to reduce the CO_2 production and to prevent air and water pollution. Due to the aging of the population, terminal operators will face difficulties to maintain the number of skilled technical personnel.

Despite the expected increase of the seaborne trade flows for bulk commodities, a shortage of port area and skilled personnel and to cope with the requirement for less environmental impact, research on bulk terminal logistics is limited nowadays. Where the main focus on scientific research in the field of port logistics seems to be the container handling, more intensive research can be performed on dry bulk logistics considering the new approaches in modeling and simulation. Tools like used in container terminal simulation are beneficial for dry bulk terminals as well. Using simulation, future terminal layout modifications or new operational procedures can be evaluated to underpin investments, to improve the terminal performance and to train terminal operations planners.

Two primary terminal functions can be distinguished. The first one is to transship dry bulk materials between the different transport modalities and the second one is to store the materials temporarily to absorb unavoidable differences in time and quantities between incoming and outgoing flows. A dry bulk terminal contains three main subsystems; the seaside, landside and stockyard. The seaside and landside are the connections with the bulk supply chain where dry bulk materials are imported to or exported from the terminal. Based on the materials flow direction two terminal types exist; import and export terminals. At import terminals, dry bulk materials are supplied at the seaside and leave the terminal at the landside (Figure 1.6A). At export terminals, it is the other way around (Figure 1.6B). Figure 1.6 shows the division of the terminal into the three subsystems.

Dry bulk materials can directly be transferred (bypassed) between the different transport modalities without being stored at the stockyard. However, direct transfer is difficult to realize due to all kind of interruptions in the bulk supply chain. Most of the cargo is stored for a period of time in piles at the terminal's stockyard. Transportation of materials at terminals is generally performed using belt conveyors.

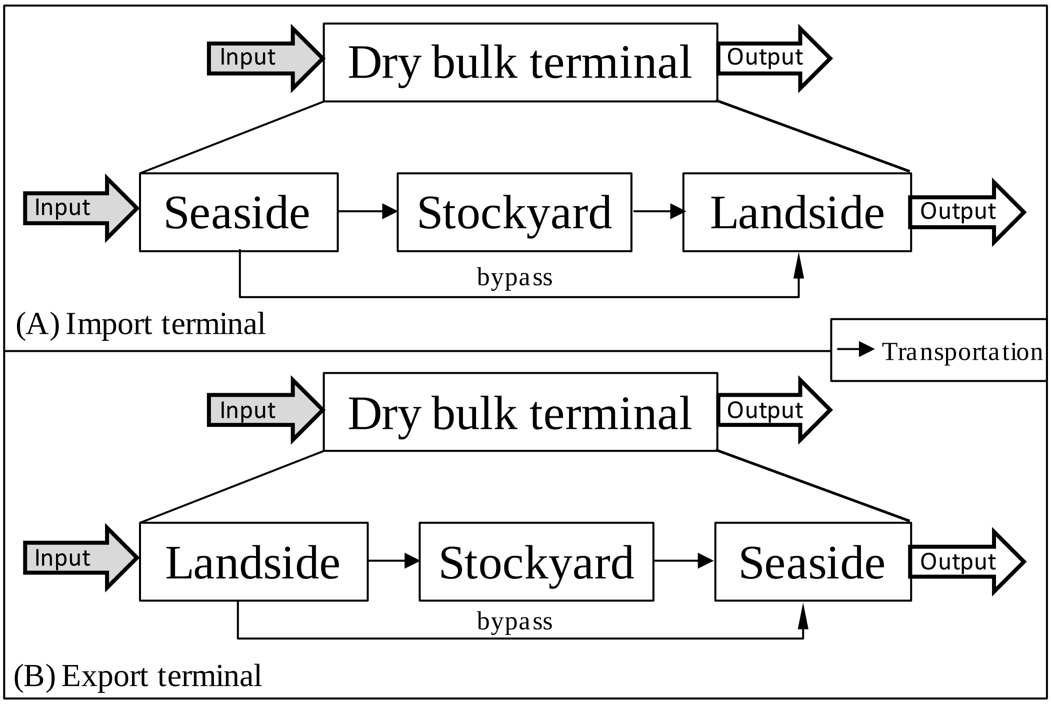

Figure 1.6: Distinction between import (A) and export terminals (B)

1.4 Problem statement

This section presents the problem statement for this thesis. In section 1.4.1 the available design methods are reviewed. Simulation models that were used for the design and optimization of dry bulk terminals are discussed in section 1.4.2. The formulation of the problem statement is given in section 1.4.3.

1.4.1 Available design methods

The most comprehensive design method for dry bulk terminals was already introduced by the United Nations Conference on Trade and Development in 1985 (UNCTAD, 1985). Unfortunately, this design method is not specific and detailed. It does not specify the required quay length, stockyard size, and machine types and how the transportation network of belt conveyors should be designed. These decisions are absolutely needed to realize feasible designs. Furthermore, several assumptions in this method do not comply with reality. For example, the UNCTAD method assumes that ship(un)loaders cannot operate at multiple berths, which is nowadays common practice. This assumption leads to an over-dimensioning of the number of expensive machines and berth lengths. Another example is the assumption that the unloading capacity remains constant during the unloading of the entire ship. In reality, when the holds are becoming empty the unloading capacity decreases significantly.

The proposed distributions for ship interarrival times and shiploads, which form the basis of the UNCTAD design method, seem to deviate significantly from real-world operations. Several factors were introduced (e.g., the through-ship factor and the berth-configuration factor) but specific values for these factors related to terminal types or terminal sizes are not given. Furthermore, the proposed stockpile type that forms the basis for one of the planning charts is a simplified representation of existing stockpiles. Another disadvantage of the UNCTAD method is that this method is only based on average values for the ship size and pile size. In short, the UNCTAD design method has been simplified to such an extent that application of it can lead to serious errors during the design process.

Memos (2004) extended the UNCTAD design method by adding specific equations for the determination of the required number of berths and storage area. Both equations show several factors (e.g., the fraction of time that berths are occupied and the peak factor to accommodate cargo peak flows). However, exact values for these factors are not given, only ranges are suggested. Ligteringen and Velsink (2012) and Willekes (1999) introduced rules-of-thumb values for some dry bulk terminal characteristics and presented overviews of installed equipment at dry bulk terminals. Willekes (1999) proposed equations to determine the nominal equipment capacities. These equations contain several efficiency factors whose exact values are difficult to determine.

1.4.2 Dry bulk terminal design and optimization using simulation

During daily operation several stochastic processes will affect the terminal operation. The late arrivals of ships may cause extra waiting times for other ships resulting in paying demurrage penalties to their ship-owners. Other stochastic processes are the variations in shiploads, storage times of dry bulk materials at the stockyard and equipment breakdowns. These stochastic processes must be considered to realize adequate designs. Simulation is a probate technique for performance analysis taking into account stochastic influences.

Many simulation models were developed to study optimization problems in planning and managing operations of existing dry bulk terminals. Baunach et al. (1985) used discrete event simulation techniques to study a proposed coal transshipment terminal to be built in Indonesia. The simulation model was used to compare alternative berth and equipment configurations and for the verification that the proposed equipment would operate effectively at the planned annual throughput. El Sheikh et al. (1987) used a simulation model to aid the planning of future berth requirements in a port. Park and Noh (1987) presented a port simulation model to simulate the future economic port capacity to meet projected cargo demand for the Port of Mobile in the United States. A more generic model was developed by Kondratowicz (1990) for simulating intermodal freight transportation systems. King et al. (1993) discussed a number of simulation models that were developed for direct use by clients to perform planning and de-bottlenecking studies.

Weiss et al. (1999) developed a simulation model to optimize the usage of receiving, storage, blending and shiploading facilities, assuming seasonal variations of production and shipping. Given a forecast, or the availability of new markets, future expansion requirements can be planned in an efficient way. The simulation model developed can also be applied as an operator training tool to let operators select operating strategies while abnormal occurrences are simulated. Dahal et al. (2003) presented the use of a genetic algorithm-based metaheuristic approach integrated in a discrete-event simulation model to solve specific design and operational problems. Sanchez et al. (2005) developed a simulation model to determine the number of berths to import coal for a power plant in Mexico.

Ottjes et al. (2007) used discrete-event simulation for designing and improving the operational control of large scale dry bulk terminals. The developed model is configurable with respect to terminal layout and different stochastic distribution types. Lodewijks et al. (2009) stated that discrete-event simulation can be used as a modern design tool for dry bulk terminals and used simulation to design a coal terminal by taking the availabilities for machines and belt conveyors into account. Boschert and Hellmuth (2010) presented a simulation tool for conveying systems to examine the flows of bulk materials. The authors stated that this tool will support optimizing the planning, design and implementation of conveyor systems. The tool is explained for the assessment of several design scenarios for a stockyard at a steel factory.

Cassettari et al. (2011) used simulation to determine the needed capacities for grab unloaders and required dome's storage capacity for a dry bulk terminal that feeds coal to a power plant. Cigolini et al. (2013) developed a simulation model for sizing the transshipment system for supplying coal to an Italian power plant.

1.4.3 Formulation of the problem statement

In section 1.4.1 it was introduced that there are a limited number of design methods available for dry bulk terminals. These design methods use several rules-of-thumb or average values without any stochastic as basis for design specifications. But for some aspects, for example, the determination of the required stockyard size and how to design belt conveyor networks, there are no references at all. In section 1.4.2, many simulation models were discussed that were used for the design and operation of specific (parts of) dry bulk terminals. However, these models cannot easily be adopted in a general design approach because these models were developed for specific companies or terminals and these models are not even available.

Dry bulk terminals have to be expanded or new terminals have to be built to meet the expected increase of the cargo flows, as introduced in section 1.2. Research is required to expand extisting design methods and to develop tools to support the design process.

1.5 Aim of the thesis

In this thesis the following main research question must be answered: "How to design dry bulk terminals? Rather then developing a new design method, existing design methods have to be expanded. In order to solve the main question, the following sub research questions must be answered:

1. Can characteristics from existing dry bulk terminals be used as design guidelines?
2. How should the terminal's seaside and landside be designed taking into account the stochastic arrival processes and shipload distributions?

3. How to size the stockyard required?
4. Which type and capacity of the stockyard machines are required to stack, reclaim and blend dry bulk materials?
5. How should the belt conveyor network be designed to connect all machines achieving sufficient connectivity, flexibility and operational predictability?
6. How to integrate the subsystems into the overall design of a dry bulk terminal?

1.6 Research methodology

Modeling and designing entire dry bulk terminals is complicated due to the dependencies between several terminal tasks. For example, a typical terminal performance indicator is the average waiting time of ships. But for the complete terminal, ships may wait for several reasons; due to limited service capacity at the terminal's seaside, due to an absence of available storage area or due to the fact that all stockyard machines are occupied. Our approach is first to decompose the terminal in its subsystems (seaside, stockyard and landside), analyze each subsystem and then connect the subsystems into a total terminal model.

Simulation tools will be developed to take the stochastic variations of the operational parameters, which occur during daily operation, into account. These simulation models have to be developed firstly, to assess the sensitivity of the operational parameters and secondly, to assess and evaluate terminal designs.

For the modeling and simulation the process-interaction approach will be followed. In this approach, introduced by Zeigler et al. (2000) and Fishmann (2001), the subsystem is virtually broken down into relevant element classes each with their typical attributes resulting in an object oriented data structure. For all active element classes process descriptions, which describe the functioning of these elements as a function of time, were defined. The benefit of using the process-interaction approach is that real-world operational processes can be translated into process descriptions, which allows an easy communication with terminal operators and permits the evaluation of the proper functioning of the simulation models based on experts' reviews.

1.7 Outline of the thesis

The thesis outline is graphically shown in Figure 1.7. Derived characteristics from existing dry bulk terminals will be presented in Chapter 2. In chapter 3, the seaside design is discussed and the landside design is addressed in chapter 4. In chapter 5, the determination of the required stockyard size is presented and the selection for the stockyard machines is provided in chapter 6. Chapter 7 focuses on the design and operation of belt conveyor networks. In a case study the redesign of a dry bulk terminal is discussed in chapter 8. Finally, in chapter 9 conclusions and recommendations for future research are provided.

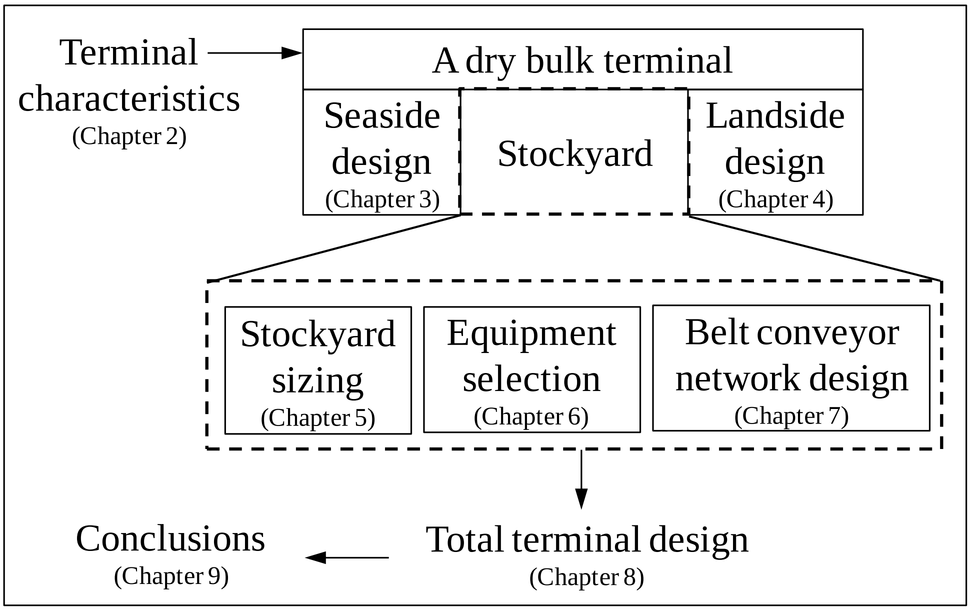

Figure 1.7: Thesis outline

2 Dry bulk terminal characteristics

This chapter is based on van Vianen et al. (2011a and 2011b).

Due to the absence of a comprehensive and detailed design method for dry bulk terminals, designs are nowadays forced to be based on rules-of-thumb, practical experiences and results obtained from dedicated simulation models. In this chapter, 49 terminals (import as well as export terminals with different sizes and locations worldwide) are studied to derive terminal characteristics like the quay length factor, storage factor and equipment utilizations. Various references are used such as terminal annual reports and websites, port authorities' information and Google Earth. The terminal characteristics derived match poorly with values proposed in literature. Using the proposed values for the quay length factor will lead to undersized quay lengths. Stockyard areas will be over-dimensioned; the storage factors determined are generally higher than the values proposed by Ligteringen and Velsink (2012). When values of equipment installation factors are used, specifications of machines may vary significantly considering the large range of these measured characteristics.

2.1 Introduction

Chapter 1 briefly discussed the absence of a comprehensive and up-to-date design method for dry bulk terminals. Despite this absence, many dry bulk terminals have been built during the last decades most likely based on rules-of-thumb and practical experiences. In this chapter, characteristics of existing dry bulk terminals will be derived. These characteristics are categorized for the seaside in section 2.2, for the landside in section 2.3 and finally for the stockyard in section 2.4. Unambiguous values per terminal type can then be used as guidelines for the (re)design process. A formulation of a terminal design when these terminal characteristics are applied is shown in section 2.5.

From 49 terminals that handle coal and/or iron ore detailed information was gathered. To cover the expected range of different terminal characteristics, import as well as export terminals from different sizes and different annual throughputs located all over the world, were investigated. The terminal's annual throughput ($\dot{m}$) was defined as the yearly amount of tons handled over the quay, expressed in million tons per year [Mt/y]. Values for the annual throughputs in 2008 were derived from terminal websites, annual reports, interviews, or acquired from port authorities. Data concerning machine types and capacities was collected from terminal websites or brochures, interviews or manufactures information. Terminal dimensions like the quay length and stockyard areas were measured using Google Earth (http://earth.google.com).

In this investigation, mainly technical aspects are considered. Economical performance indicators like profit margins or annual turnover are not considered due to the lack of available data. First of all, most of the terminal operators did not want share these numbers and secondly, these numbers cannot be determined easily. Many terminal operators belong to large conglomerates (steel producing companies or holding companies who own several terminals) and these companies do not present the economical data for individual terminals. The lack of this data hinders the comparison of terminal characteristics and economical performances. Nevertheless, the investigation is interesting enough to determine rules-of-thumb from the operation of exisiting dry bulk terminals.

Figure 2.1 shows the locations of the investigated import and export terminals around the world. The dot size represents the annual throughput. For the terminal names, locations and consulted references can be referred to Appendix A. Characteristics derived for the seaside, stockyard and landside will be presented in the next sections.

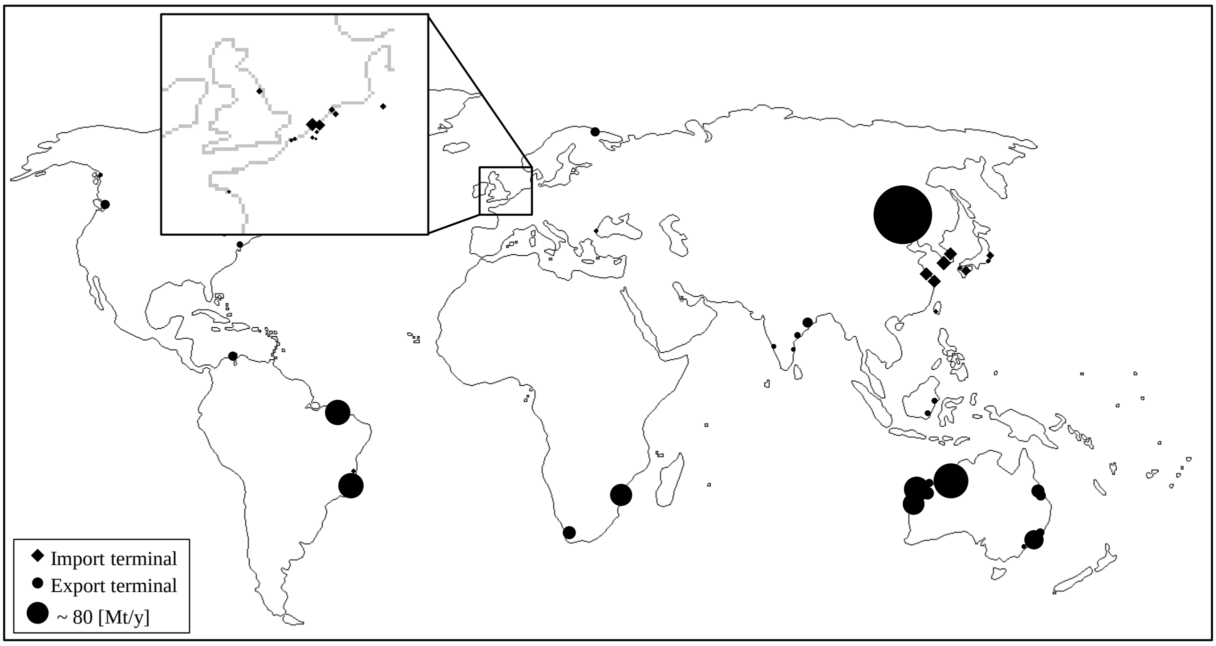

Figure 2.1: Investigated dry bulk terminals

2.2 Seaside

The maximum terminal's annual throughput relates to the terminal's quay length. Ligteringen and Velsink (2012) proposed that the quay length factor (f_{ql}) can be used as a design indicator.

This factor can be determined by dividing the annual throughput with the quay length, or expressed algebraically:

$$f_{ql} = \frac{\dot{m}}{L_q} \tag{2.1}$$

Where f_{ql} is the quay length factor expressed in kilotons per meter quay per year [$ktm^{-1}y^{-1}$], $\dot{m}$ is the annual throughput [Mt/y] and L_q [m] is the length of the quay. Ligteringen and Velsink (2012) suggested the following ranges for the quay length factor; for coal between 25 and 75 [$ktm^{-1}y^{-1}$] and for iron ore between 50 and 150 [$ktm^{-1}y^{-1}$].

Figure 2.2 shows the quay length factor determined per terminal together with suggested minimum and maximum values for both coal and iron ore. Due to the difference in bulk density between coal and iron ore, the commodity type should be considered as well in the quay length factor. The investigated export terminals handle either coal or iron ore. However, the majority of the analyzed import terminals handles both coal and iron ore over the same quay. A distinction per commodity cannot be made, only a combined value for the quay length factor was derived.

Figure 2.2 shows that the quay length factors vary considerably per terminal. Furthermore, the quay length factors for most import terminals are less than the proposed minimum value, especially for small terminals with a low annual throughput. At these terminals longer quays are installed than expected based on the suggested quay length factors. Using the suggested values will lead to undersized quays. Export terminals realize higher values for the quay length factor. The maximum value was not exceeded.

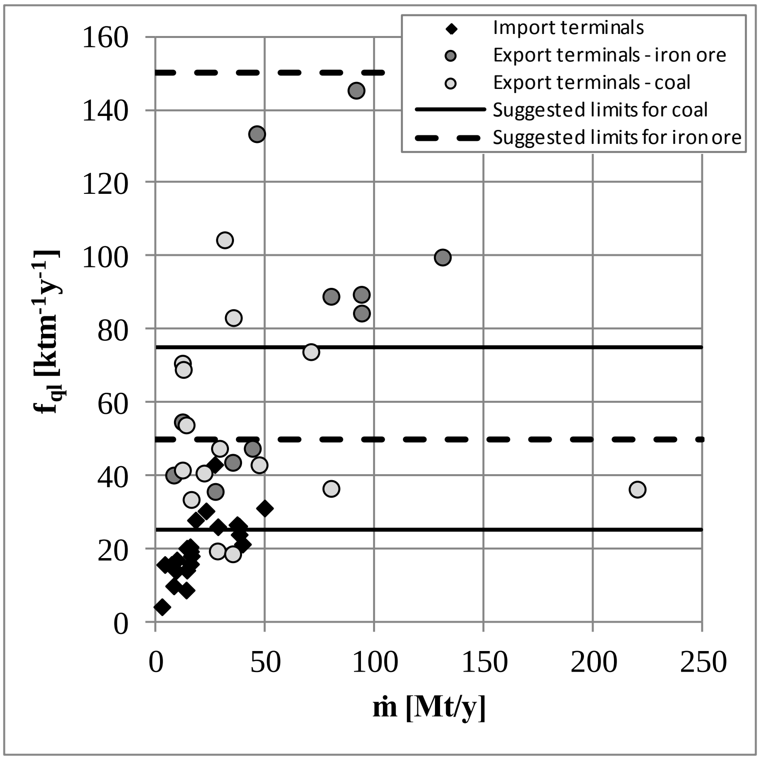

Figure 2.2: Quay length factors versus the annual throughput together with the suggested limits by Ligteringen and Velsink (2012)

Due to the stochastic ship arrival process, machines installed at the seaside to (un)load deep sea ships are not able to operate continuously. For each terminal, the seaside equipment installation factor (f_s) was determined by dividing the installed seaside capacity with the needed capacity to handle the annual throughput when the machines operate continuously (365 days per year and 24 hours per day). The installed capacities were collected from terminals websites, interviews with terminal operators or information and brochures from equipment manufactures. In Appendix A the references consulted are listed. This method was also applied to determine equipment installation factors for the landside, stacking and reclaiming equipment. Equation (2.2) shows the relation for the seaside equipment installation factor for (un)loading ships. Note that the equipment installation factors are a measure of the over-dimensioning of equipment installed.

$$f_s = \frac{Q_{installed}}{Q_{100\%}} \tag{2.2}$$

Where f_s [-] is the seaside equipment installation factor, $Q_{installed}$ [kt/h] is the installed terminal (un)loading rate (which is the product of the number of cranes and the technical capacity) and $Q_{100\%}$ [kt/h] is the terminal (un)loading rate needed when the (un)loading machines are 100% of the time in operation.

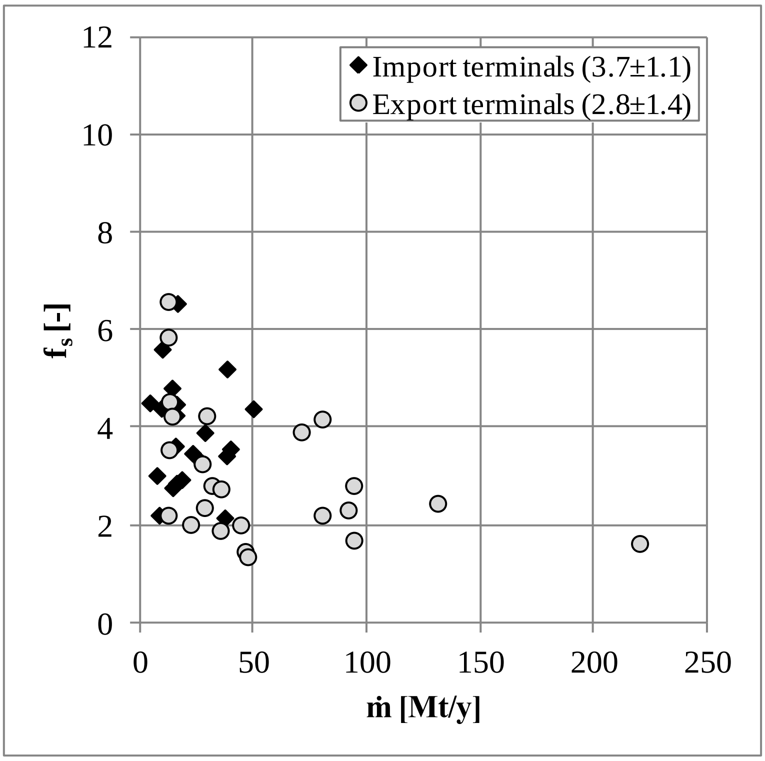

Figure 2.3: Seaside equipment installation factors versus the annual throughput

Figure 2.3 shows the seaside equipment installation factors versus the annual throughputs per terminal type. Average values and corresponding standard deviations are mentioned in the legend. From Figure 2.3 it can be concluded that the measured seaside equipment installation factors vary considerably per terminal. Due to this variation, the average value cannot easily be applied as design guidelines. From this figure, it can also be detected that the seaside equipment installation factor decreases when the annual throughput increases, that means that the installed equipment is more frequently used. Generally, seaside equipment at export terminals is more frequently used than seaside equipment at import terminals.

2.3 Landside

The landside equipment installation factor (f_l) [-] was determined per terminal by using the comparable method as explained in the previous section. In Figure 2.4 the measured factors are shown. From this figure it can be concluded that also these factors vary considerably per terminal. The variation of these measured factors is slightly less at export terminals compared to import terminals. Machines installed at the landside of export terminals are more frequently used than machines at import terminals.

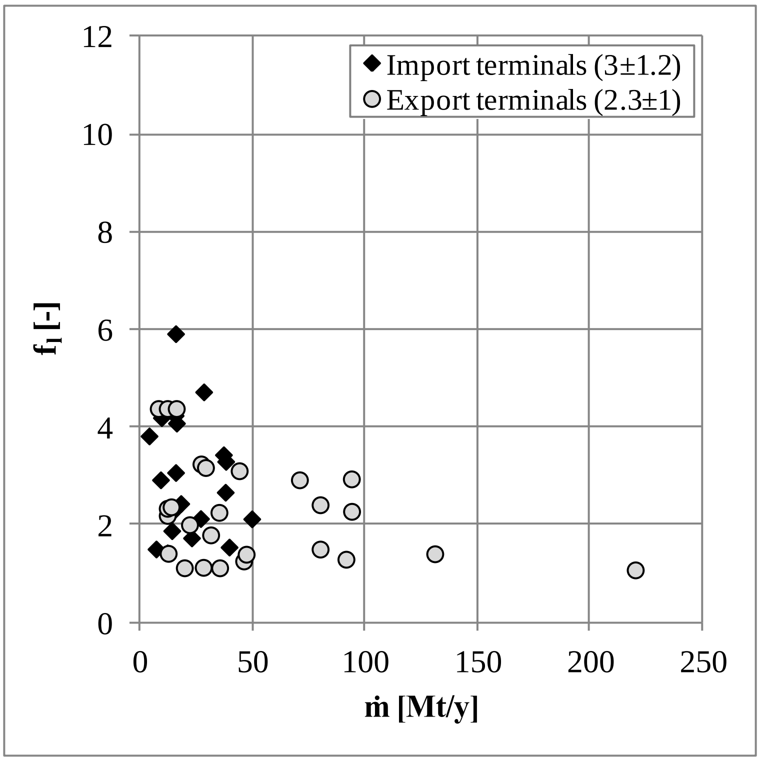

Figure 2.4: Landside equipment installation factors versus the annual throughput

2.4 Stockyard

Sizing the stockyard area is essential to realize a buffer between the varying input and output flows of dry bulk materials. If the storage capacity is insufficient the situation will occur where either bulk ships or industrial clients (steel factory or coal-fired power plant) are kept waiting for cargo. Ligteringen and Velsink (2012) proposed the storage factor as a design guideline for sizing the stockyard area. This factor represents the ratio between the annual throughput and the stockyard area, or expressed algebraically:

$$s = \frac{\dot{m}}{A} \tag{2.3}$$

Where s is the storage factor [$tm^{-2}y^{-1}$], $\dot{m}$ is the annual throughput [ty^{-1}] and A [m^2] is the stockyard area. When values for the storage factor and the required annual throughput are known, the stockyard area can be calculated.

Due to bulk density differences different values for the storage factor were suggested by Ligteringen and Velsink (2012): for coal between 15 and 25 [$tm^{-2}y^{-1}$] and for iron ore between 30 and 40 [$tm^{-2}y^{-1}$]. In this research, the storage areas for coal and iron ore on existing stockyards were determined per terminal using Google Earth. The storage factors determined are shown in Figure 2.5 together with the limits suggested by Ligteringen and Velsink (2012). Figure 2.5 shows the large variation of these storage factors and these storage factors determined are generally higher than the suggested values. From Figure 2.5 it can be concluded that the suggested limits are unrealistic. The higher values for the determined storage factor indicate that these terminals are able to realize a higher annual throughput per square meter than expected from literature. Using the suggested values from Ligteringen and Velsink (2012) will therefore lead to oversized stockyard areas.

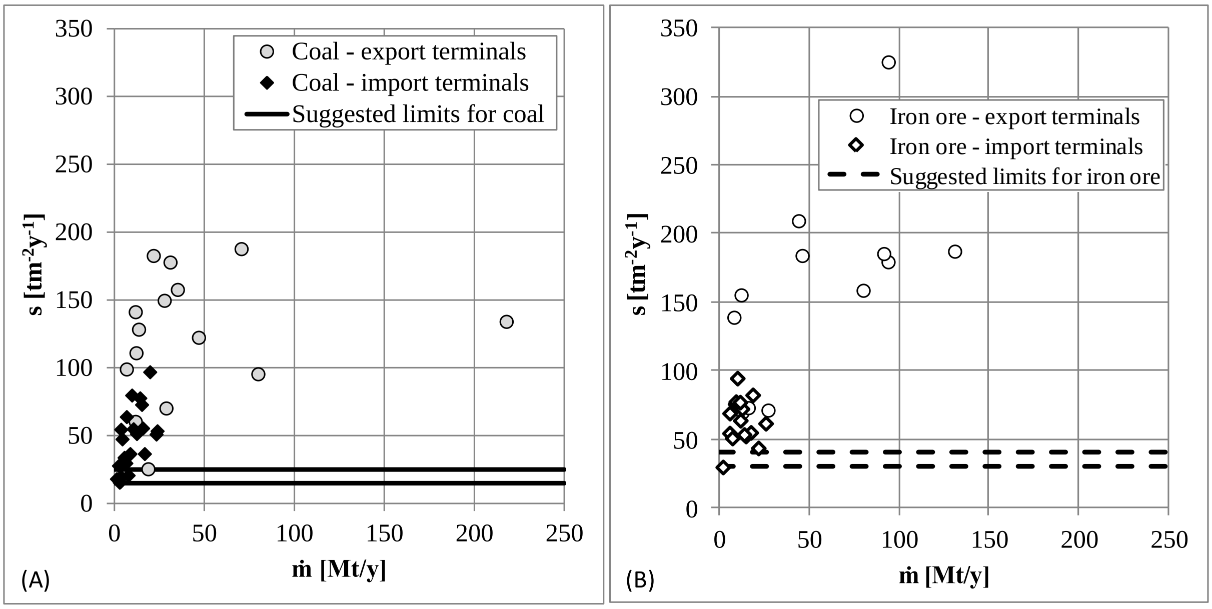

Figure 2.5: Storage factors for coal (A) and iron ore (B) together with the suggested limits as proposed by Ligteringen and Velsink (2012)

Bulk materials are stacked onto and subsequently reclaimed from piles at the stockyard. Common machines installed at stockyards are dual-purpose stacker-reclaimers or single-purpose stackers and reclaimers. Stacker-reclaimers combine the two functions of stacking and reclaiming into a single unit. Only one of these two functions can be fulfilled at a time. For each terminal the stacking equipment installation factor (f_{st}) [-] and the reclaiming equipment installation factor (f_r) [-] were determined by using the comparable method as described in section 2.2. In Figure 2.6A the stacking equipment installation factors are shown and the reclaiming equipment installation factors are listed in Figure 2.6B.

From Figure 2.6 it can be learned that both stacking and reclaiming equipment installation factors vary considerably. The stacking equipment installation factors are higher than the factors for the reclaiming equipment. Stockyard machines at export terminals are more frequently used than stockyard machines at import terminals. Apparently, the operation at export terminals can be better scheduled which results in less over-dimensioned machines.

Due to the large variation of the measured equipment installation factors, the average factors are not easily applicable for a correct determination of the required stacking and reclaiming capacity.

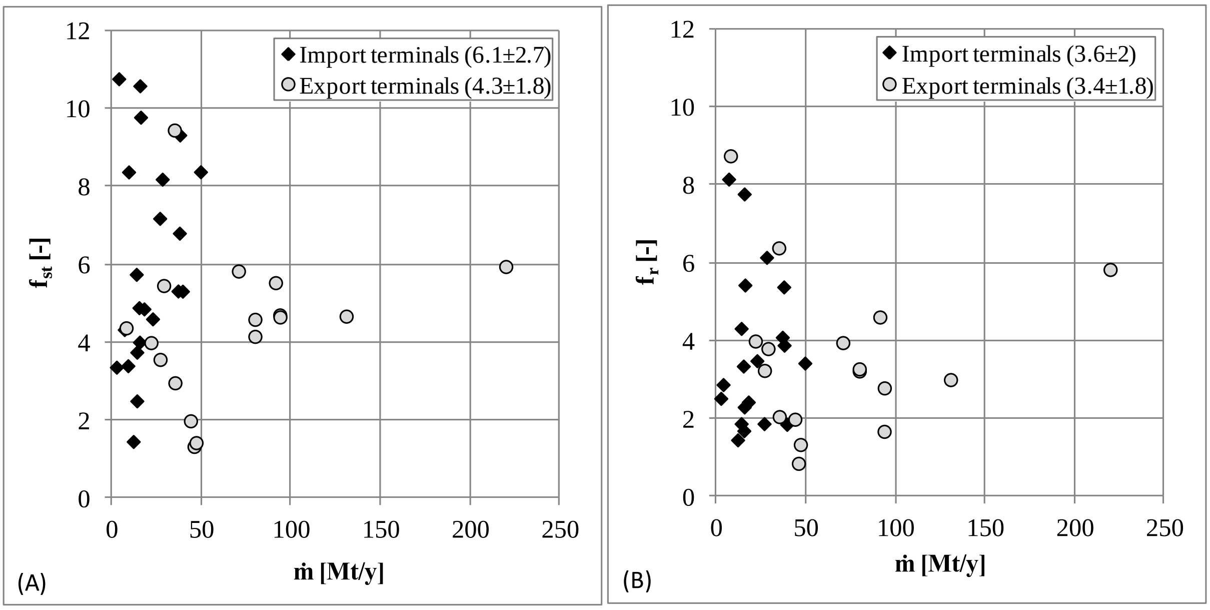

Figure 2.6: Stacking (A) and reclaiming (B) equipment installation factors versus the annual throughput

2.5 Terminal design: an example

In this section a terminal design is formulated using suggested values from literature and some terminal characteristics derived. In this case an import terminal has to be designed that has to handle an annual throughput of ten million tons of coal. In Table 2.1 the main requirements are listed. The predefined service times for both ships and trains need to be formulated in order to realize a competing terminal.

Table 2.1: Design requirements for the design of an import terminal

Parameter	Description	Value	Unit
$\dot{m}_{coal}$	Annual throughput of coal	10	[Mt/y]
sl	Average shipload	100	[kt]
$W_{s\text{-}ship}$	Predefined ship unloading time	60	[h]
tl	Average trainload	4	[kt]
$W_{s\text{-}train}$	Predefined train loading time	3	[h]
T_s	Material storage time[1]	0.2	[y]

[1] Time that a delivered shipload is stored at the terminal's stockyard

Step 1: Seaside design

For the terminal's seaside, the number of berths and the ship unloading capacity needs to be determined. The average ship interarrival time, the average shipload and the predefined ship unloading time determine the berth utilization. The number of berths is determined taking into account the values proposed for the maximum berth utilization. The berth utilization is expressed by the following equation, in analogy to the basic queuing theory formulation:

$$\rho = \frac{\lambda}{n_b \mu} \quad (2.4)$$

Where ρ [-] represents the berth utilization, λ [1/d] is the ship arrival rate, n_b [-] is the number of berths and μ [1/d] represents the ship unloading rate.

The ship arrival rate relates to the annual throughput, the number of operating days per year and the average shipload, or expressed algebraically:

$$\lambda = \frac{\dot{m}}{n_d sl} \quad (2.5)$$

Where λ [1/d] is the ship arrival rate, $\dot{m}$ [t/y] is the annual throughput, n_d [-] is the number of operating days per year and sl [t] is the average shipload.

The predefined ship unloading time and the number of operating hours per day determine the ship service rate. This relation is expressed by the following equation:

$$\mu = \frac{n_h}{W_{s-ship}} \quad (2.6)$$

Where μ [1/d] is the ship service rate, n_h [-] is the number of operational hours per day and $W_{s\text{-}ship}$ [h] is the average ship unloading time.

When assumed that the terminal operates 24 hours per day and 365 days per year, the berth utilization becomes for a single-berth 0.68. According UNCTAD (1985) the maximum berth occupancy for a single-berth is 0.4. A quay with two berths is needed; the berth utilization for this double-berth quay configuration becomes 0.34.

After the definition of the number of berths, the crane unloading rate should be determined. UNCTAD (1985) proposed a through-ship efficiency factor to express the ratio between gross and net ship servicing rates covering the total ship working time. Values between 0.3 and 0.7 are suggested by UNCTAD for the through-ship efficiency factor. The relation for the crane unloading rate is shown in equation (2.7).

$$Q_c = \frac{sl}{W_{s-ship}\eta} \quad (2.7)$$

Where Q_c [kt/h] is the crane unloading rate, sl [kt] is the average shipload, $W_{s\text{-}ship}$ [h] is the predefined ship unloading time and η [-] is the through-ship efficiency factor. For a through-ship efficiency factor of 0.5, the crane unloading rate becomes 3.3 [kt/h].

Step 2: Landside design

For this case, the number and capacity of train loading machines need to be determined. It was assumed that the set up time and the runaway time needed before and after loading was 30 minutes. There is 2 hours left to load trains with 4 kilotons within the predefined time. A net reclaiming capacity of 2 [kt/h] is required. Loading trains using a single train loader will result in 7,500 operational hours per year. Practical experience has shown that such a high machine utilization should be avoided. That's why two train loaders are proposed. An advantage of installing two loading machines is the redundant operation; when one loader breaks down, trains can still be served by the other machine.

Step 3: Stockyard sizing

The storage time of the material at the stockyard determines the storage capacity needed. As listed in Table 2.1, the predefined storage time is 0.2 [y], that means the stockyard area can five times be replenished per year. The minimum storage capacity becomes 2 million tons. Ligteringen and Velsink (2012) suggested values for the storage factor for coal (25 [$tm^{-2}y^{-1}$]) enabling a determination of the stockyard size required. By dividing the annual throughput with the proposed storage factor leads to a specification of 40 hectares needed.

Step 4: Stockyard machine selection

Practical experience has shown that typical stockyard machines are stacker-reclaimers. Such machines combine the two functions of stacking and reclaiming into a single unit. Stacker-reclaimers have limited boom length (e.g., 50 meter) and are generally mounted at rails between stockyard lanes. Typical lengths for lanes are in the order of 1 kilometer. A common lane's width is 50 meter. The stockyard area in reach of a single stacker-reclaimer becomes 10 hectares. In conclusion, four machines have to be installed to realize a stockyard area of 40 hectares that is directly accessible by stockyard machines.

For the determination of the name-plate capacity of the stockyard machines, the net capacities and utilization factors must be considered. The stacking capacity must correspond with the net ship unloading rate. For the reclaiming capacity, Willekes (1999) introduced a utilization factor of 0.7. The name-plate capacities for the stockyard machines become at least 3.3 [kt/h] for stacking to prevent a hindrance of the ship unloading speed and 2.9 [kt/h] for reclaiming.

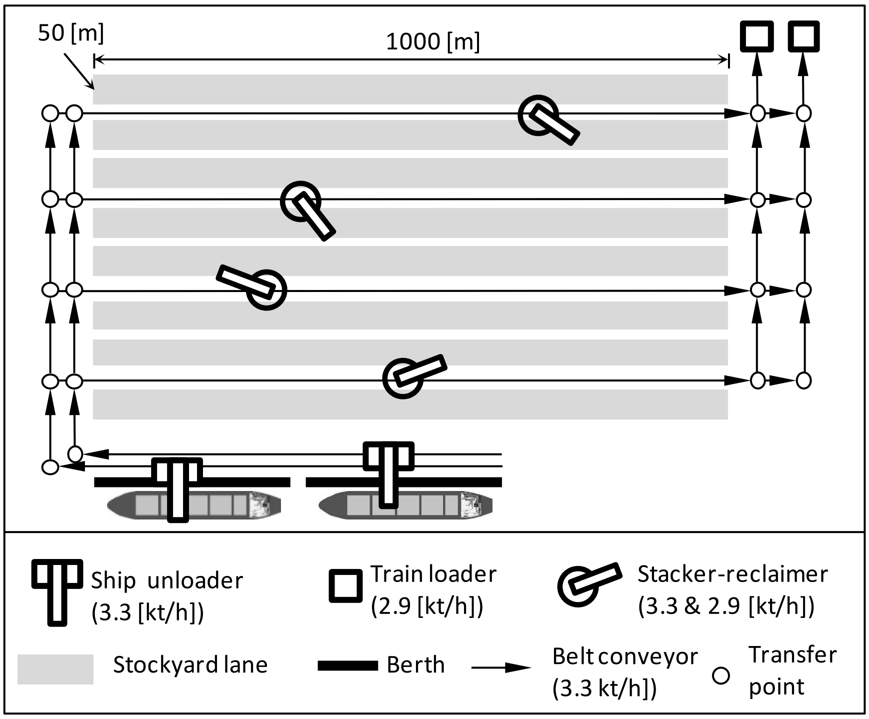

Figure 2.7: Schematic representation of the design for the import terminal

Step 5: Belt conveyor network design
Material needs to be transported between two ship unloaders, two train loaders and four stacker-reclaimers. To prevent that some activities cannot be performed simultaneously, a network that contains all possible connections is proposed. The connections between belt conveyors are shown as transfer points in Figure 2.7.

Although a terminal design can be formulated using known rules-of-thumb and practical experiences, many questions arose which does not give the impression that the best design is defined. More research is needed to answer these questions to realize adequate designs.

- What is the consequence on the terminal design when the stochastic variations in ship and train interarrival times, shiploads and storage times are considered?
- Do the suggested values for the berth utilization, storage factor and reclaiming efficiency cover experiences from terminal operators?
- How to dimension the length and water depth of the berths?
- Is it necessary to equip each berth with two unloading cranes to maintain ship servicing when one unloader breaks down and can unloaders be moved alongside the quay to help ship servicing at other berths?
- Can both required seaside and landside service demands be achieved using stacker-reclaimers?
- How does the stockyard size relate to different materials (iron ore and coal), different storage strategies (individual piles or combined piles) and additional stockyard activities like relocation?
- Which machines need to be selected when bulk materials must be blended and/or homogenized?
- What is the consequence on the terminal performance when a less extended belt conveyor network with limited flexibility in connections will be installed?

2.6 Conclusions

Characteristics from 49 dry bulk terminals were derived to investigate if these characteristics can be used as design indicators. The values determined for the quay length and storage factors match poorly with the suggested values by Ligteringen and Velsink (2012). At import terminals the quay length factors determined were less than the suggested values; using the suggested values will lead to undersized quay lengths. The storage factors derived were generally higher than the values proposed. Using the proposed storage factors by Ligteringen and Velsink (2012) will result in oversized stockyard areas.

To support the machine selection, equipment installation factors were determined. These values indicate the over-dimensioning of terminal equipment installed. Results have shown that the equipment installation factors determined vary significantly per terminal. Due to this large variation an accurate specification of machine capacity needed based on these factors is impossible. Although these factors can relatively easily been determined from terminal data it provides limited insight in the operational terminal efficiency. In Figure 2.8 the measured average equipment installation factors are shown together with the standard deviation of these average values categorized per subsystem for both import and export terminals. From this figure it can be concluded that stockyard machines are most over-dimensioned because the equipment installation factors show the highest values. The reason is that most investigated stockyard machines are dual-purpose stacker-reclaimers. These machines have to stack and reclaim sequentially without hindering the seaside and landside operation.

Applying the proposed and derived values for several rules-of-thumb during the formulation of a terminal design resulted in many outstanding issues and did not give the impression that an appropriate design was defined. Additional research is needed to enable the formulation of a more adequate design.

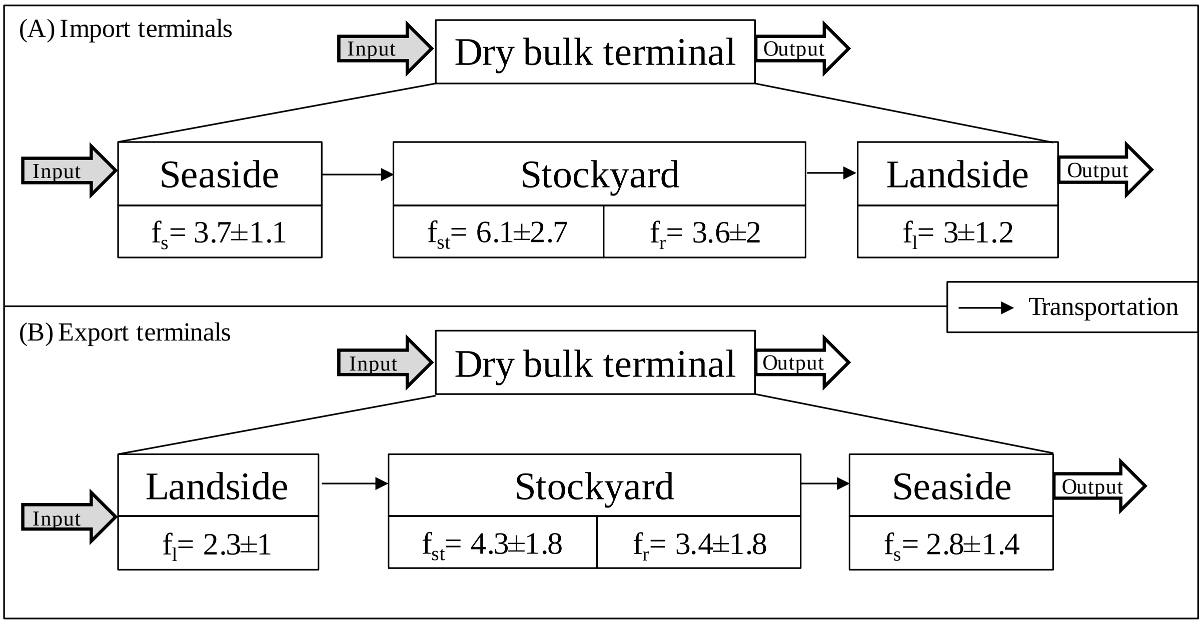

Figure 2.8: Overview of the average equipment installation factors, with standard deviations for the average values, for import terminals (A) and export terminals (B)

3 Seaside modeling and quay layout design

This chapter is based on van Vianen et al. (2012a).

In this chapter the seaside design and operation are discussed. The quay length is dimensioned and the number and capacity of ship (un)loading machines and quay conveyors are selected. Characteristics are derived for bulk ships and ship (un)loading machines. Although many researchers discussed the modeling of the seaside operation for container terminals, dry bulk terminals have received significant less attention in literature. A simulation model is developed to evaluate quay layouts and operational procedures. The operational procedures investigated concern the right positional orders of rail-mounted ship (un)loading machines, the number and capacity of quay belt conveyors, the significant draft of bulk ships and the variation of the unloading rate during ship unloading. In a case study, the seaside model was used to evaluate new quay layouts to facilitate the expected increase of the annual throughput for an import dry bulk terminal.

3.1 Introduction

At dry bulk terminals bulk ships, used for the sea-transport of dry bulk materials over long distances, are moored alongside quays to be serviced. Quay walls and ship (un)loading machines require very large investments and are crucial determinants for the service performance of dry bulk terminals.

In this chapter the seaside design will be discussed and quay operational procedures will be evaluated. A seaside design contains the quay length dimensioning and the selection of the number and capacity of ship (un)loading machines and connecting quay conveyors. In section 3.2 the main characteristics of bulk ships and machines are presented. A review of the literature that discussed the modeling of the seaside transshipment is given in section 3.3. Section 3.4 addresses the seaside modeling when the quay is divided in separate berths and the ships interarrival and service times can be represented by generalized distributions. In section 3.5 the ship arrival process at dry bulk terminals is discussed by presenting proposed and measured stochastic distributions and the parameters that affect the ship unloading rate. A simulation model to assess the continuous quay layout and operational procedures is introduced in section 3.6. In section 3.7 experimental results are shown and in section 3.8 the simulation model is used by evaluating the redesign of the quay layout of a terminal. Finally, the conclusions are presented in section 3.9.

3.2 Characteristics of bulk ships and ship (un)loading machines

For a seaside design, characteristics of visiting ships and seaside machines must be specified. The lengths of the visited ships determine the berth length needed. Berthing of ships with significant drafts can be limited by the water depth alongside the quay. The ship's beam, which is the overall width of the ship, specifies the required (un)loading machines' outreach. General characteristics will be derived for bulk ships (section 3.2.1), for ship unloading machines (section 3.2.2) and for ship loading machines (section 3.2.3).

3.2.1 Bulk ships

The required quay length relates to the number and length of the berthed ships that have to be served at the same time. From a Dutch terminal operator, names of 289 recently visited bulk ships carrying coal and iron ore were received. For these ships, values for the length, the draft and the beam were determined using the databases of Sea-web (http://www.sea-web.com) and Marinetraffic (https://www.marinetraffic.com). In Appendix B, an overview of the dimensions determined is listed. Figure 3.1 shows per ship its length (L_s) [m] versus its deadweight (dwt) in kilotons [kt]. The deadweight is the ship's carrying capacity including the weight of bunkers for fresh water, ballast water and fuel. The equations that describe the relation for the ship's length, beam and draft will be used later in this study in the simulation models developed.

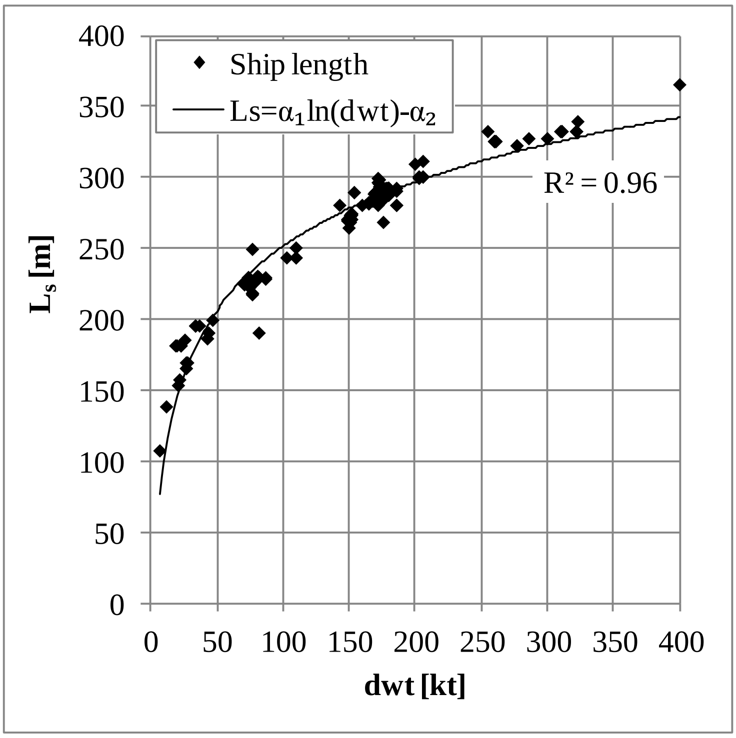

Figure 3.1: Ship's length versus the ship's deadweight

From the data presented in Figure 3.1, a relation was derived that expresses the relation between the ship's length and the ship's deadweight. Equation (3.1) shows this relation:

$$L_s = \alpha_1 \ln(dwt) - \alpha_2 \quad (3.1)$$

Where L_s [m] is the ship's length, dwt [kt] is the ship's deadweight, α_1 and α_2 are constants with the following values determined; 65.5 and 50 respectively. The correlation between equation (3.1) and the bulk ship data was determined and can be expressed with an R-squared value of 0.96.

In Figure 3.2, the ship beams and the ship maximum draft versus the ship deadweights are presented. The same method as mentioned above was used to determine relations for the ship's beam and the ship's maximum draft versus the ship's deadweight. These relations are shown in equation (3.2) and (3.3) respectively. The correlation coefficients between the equations and the dimensions measured are shown in Figure 3.2.

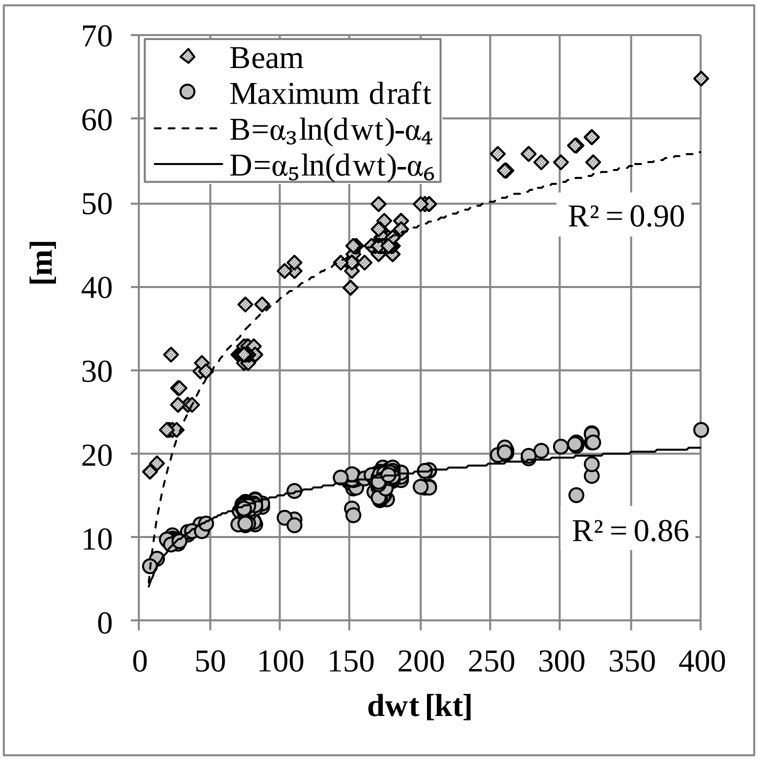

Figure 3.2: Ship's beam and ship's maximum draft versus the ship's deadweight

$$B = \alpha_3 \ln(dwt) - \alpha_4 \quad (3.2)$$

Where B [m] is the ship's beam, dwt [kt] is the ship's deadweight and α_3 and α_4 are constants with the following values determined; 12.7 and 20 respectively.

$$D = \alpha_5 \ln(dwt) - \alpha_6 \quad (3.3)$$

Where D [m] is the ship's maximum draft when the ship is fully loaded, dwt [kt] is the ship's deadweight and α_5 and α_6 are constants with the following values determined; 4.1 and 4 respectively.

Several ship registers classify bulk ships based on their deadweight. In Appendix B, ships are shown for each class to get an idea of the ship size per class. In Table 3.1 the common bulk ship classes are listed with a summary of the characteristics determined. Also the minimum and maximum numbers of holds of the ships per class are listed. Note that the class for the largest bulk ships is called Large Capesize in Table 3.1; other names like Valemax or Chinamax are also used to classify these ships.

Table 3.1: Classification and summary of the main characteristics for bulk ships (derived from several ship registers and own research)

	Deadweight [kt]	Length [m]	Beam [m]	Draft [m]	# holds [-]
Handysize	10-35	125-200	18-28	7-11	3-6
Handymax	35-55	175-200	22-32.2	8-13	5-7
Panamax	55-90	225	< 32.31	12-15	5-9
Small Capesize	90-150	225-280	32.31 - 45	13-17	7-9
Large Capesize	>150	280-365	45-65	16-22.5	7-10

In this research a material is defined as a bulk commodity (iron ore or coal) and a grade belongs to a material but contains specific characteristics (e.g., angle of repose, lump size and abrasiveness). Grades must be transported and stored separately to prevent mixing between grades. Generally bulk ships contained only one material but can be loaded with multiple grades. The terminal operator, who provided the names of the visited ships, provided also data that covers details of the unloading process during three years of operation from 791 bulk ships. The provided data is listed in Table B.2 (Appendix B). From this data, the different number of grades per ship was determined and is presented with a histogram in Figure 3.3. From this figure it can be learned that 40% of the unloaded ships was filled with one grade and only 2% of the ships contains more than five different grades.

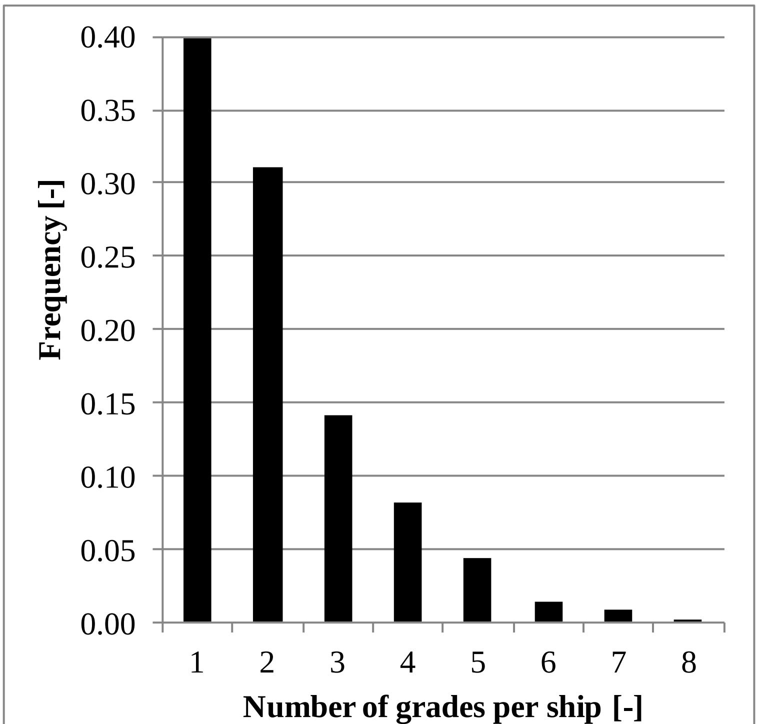

Figure 3.3: The number of grades per ship based on 791 unloaded bulk ships

3.2.2 Ship unloading machines

Two types of ship unloading machines exist; mobile (rubber tyred or pontoon mounted) and rail-mounted harbor cranes. Mobile harbor cranes are more flexible but limited in unloading capacity. Rail-mounted cranes can only move alongside the quay and cannot pass each other giving more complexity when dividing over various ships. Grab unloading is the most widely used method for ship unloading. Figure 3.4 shows different types of grab unloaders, a rail-mounted crane and two slewing cranes mounted on a pontoon. The slewing cranes directly transfer the material from the bulk ship into barges.

Figure 3.4: A rail-mounted grab crane and pontoon-mounted slewing grab cranes unload a bulk ship simultaneously (Courtesy of EMO BV)

In the last decades more and more continuous unloaders were built. Figure 3.5 shows two continuous unloaders mounted on a jetty enabling mooring ships at both sides. Advantages of such machines are the higher unloading efficiency (approximately 65% compared with to 50% for grab unloaders), the greater environmental protection (less dust, spillage and noise) and the easier automation (Ye, 2004). However, continuous unloaders are more expensive due to the higher mass and higher technical complexity, are inflexible for unloading different materials, are less reliable (more moving parts), have limited possibilities for the direct transfer of materials and need more energy per ton handled.

Generally, ship unloading machines are manually operated. The operational efficiency depends on the crane driver's proficiency. However, recent developments show a driverless grab unloading operation at the German Hansaport (iSAM, 2010) and the Chinese Luojing ore terminal (ABB, 2008). The objectives for automation are an increase of the unloading efficiency and a reduction of the personnel costs. The technology applied contains a real-time measurement of the grab position, the hatch position (due to tide changes and ship movements) and the cargo distribution within the hold (iSAM, 2010). Ye (2004) discussed the automatic mode for continuous unloaders. These machines are equipped with hatch shape scanning sensors and mechanical limit switches to prevent collisions. In the automatic mode, specific algorithms are applied to realize a constant feed quantity during unloading.

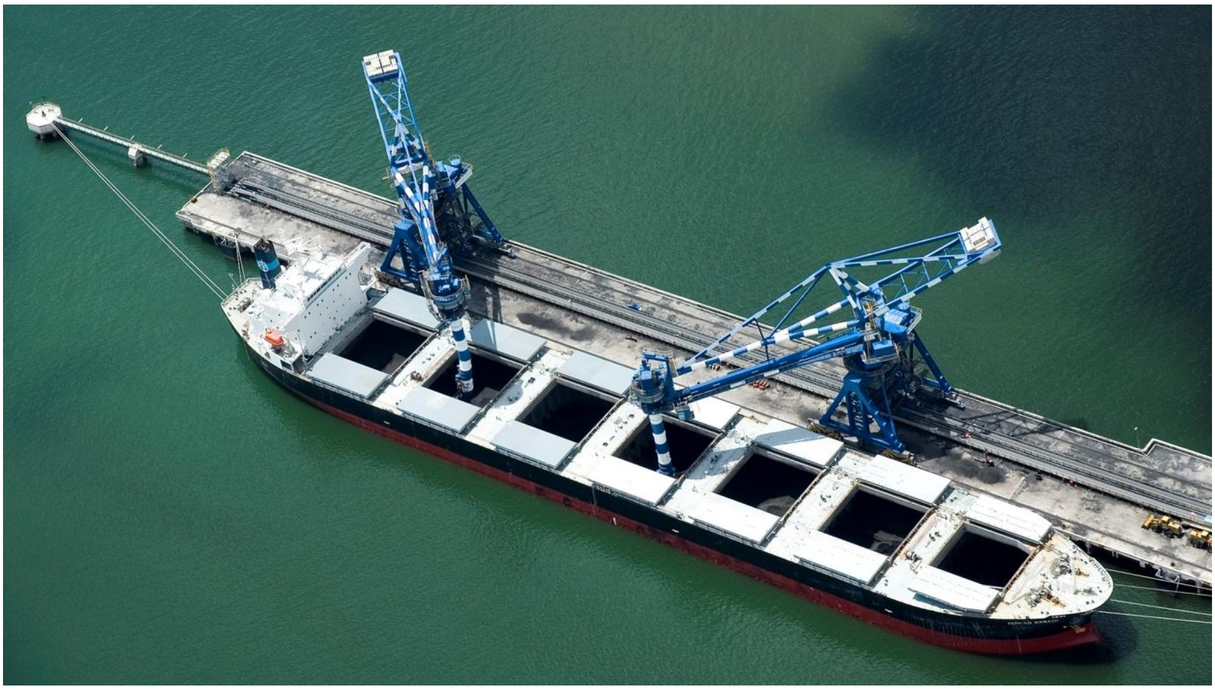

Figure 3.5: Two continuous ship unloaders installed at a jetty (Courtesy of ThyssenKrupp)

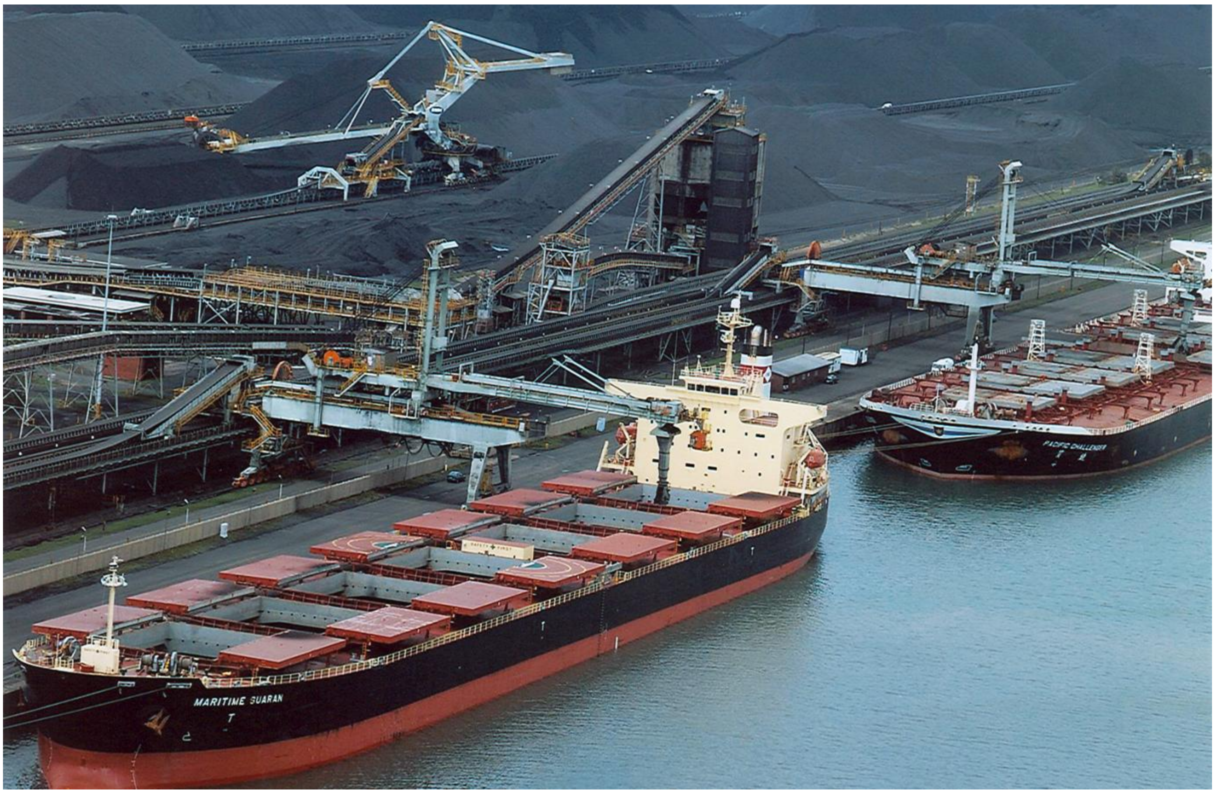

Figure 3.6: Bulk ships are being loaded (Courtesy of the Richards Bay Coal Terminal)

3.2.3 Ship loading machines

Ship loading machines are simple in comparison with ship unloading machines. Loaders normally require a belt conveyor and a loading chute. Loading capacities are usually limited by other parts of the terminal such as conveyors and reclaimers. Normal capacity ranges between 1 and 7 kilotons per hour [kt/h], in special cases even 16 [kt/h] for loading very large bulk ships, are possible. High loading speeds are limited by the rate at which the ship can be de-ballasted. Several ship loading machine types exist. Figure 3.6 shows travelling loading machines operated simultaneously. Other machine types, like the linear, quadrant or dual-quadrant machines, were introduced and described by Soros (1991 and 1993).

3.3 Seaside modeling: a literature review

Modeling the seaside operation is essential for realizing realistic quay designs. Compared to the significant amount of research on the transshipment of containers at container terminals, a limited number of papers discussed the seaside operation at dry bulk terminals. The seaside modeling of container terminals will be investigated to find possible analogies that can be applied to dry bulk terminals. Comprehensive overviews on applications and optimization models for the operations management in container terminals were given by Vis and De Koster (2003), Stahlbock and Voβ (2008) and Bierwirth and Meisel (2010). Several sub problems were distinguished; the assignment of ships to berthing locations alongside the quay (the berth allocation problem), the assignment of cranes to ships (the quay crane assignment problem) and the determination of cranes operating plans (the quay crane scheduling problem). Sections 3.3.1 until 3.3.3 review the literature available for these sub problems and section 3.3.4 evaluates this survey and indicates the approach used in this chapter.

3.3.1 Berth Allocation Problem

The berth allocation problem covers the mooring of a set of ships within the boundaries of the quay and within the planning horizon. For each ship additional data like the ship’s length, its draft, the expected time of arrival, and the projected handling time must be given. Several spatial constraints restrict the feasible berthing positions according to a preset partitioning of the quay into berths.

According to Imai et al. (2005) the following layouts can be recognized:

- Discrete quay layout (Figure 3.7A): the quay is divided into a number of berths and only one vessel can be served at each single berth. Either the quay construction causes the partitioning into berths or berths are applied to ease the planning problem.
- Continuous quay layout (Figure 3.7B): the quay has no spatial constraints and vessels can berth at arbitrary positions. Berth planning is more complicated but the quay can better be utilized.
- Hybrid quay layout (Figure 3.7C): the quay is partitioned into berths but large vessels may occupy more than one berth and small vessels may share a berth.

Han et al. (2006) and Zhou et al. (2006) included spatial constraints into their models to ensure that ships are moored at positions with sufficient water depth. Many models were developed to minimize the sum of the ships waiting and handling times. Schonfeld and Frank (1984) employed analytical models, Lai and Shih (1992), Legato and Mazza (2001 and 2013), Henesey et al. (2004) and Canonaco et al. (2008) developed simulation models and Dragovic et al. (2006) developed an analytical model based on queuing theory.

Many authors suggested the First-Come-First-Served (FCFS) method to determine the ship service order; Lai and Shih (1992), Botter et al. (2005), Singh et al. (2010), Hartmann et al. (2011) and Umang et al. (2013). The Earliest-Due-Date (EDD) method when ships with the earliest due date for completion are firstly berthed was suggested by Lai and Shih (1992) and Hartmann et al. (2011). Barros et al. (2011) proposed a high demurrage ship algorithm for the ship service order. The demurrage cost for each arrived ship must be calculated. The total terminal cost can then be minimized by serving high-cost ships earlier than low-cost ones.

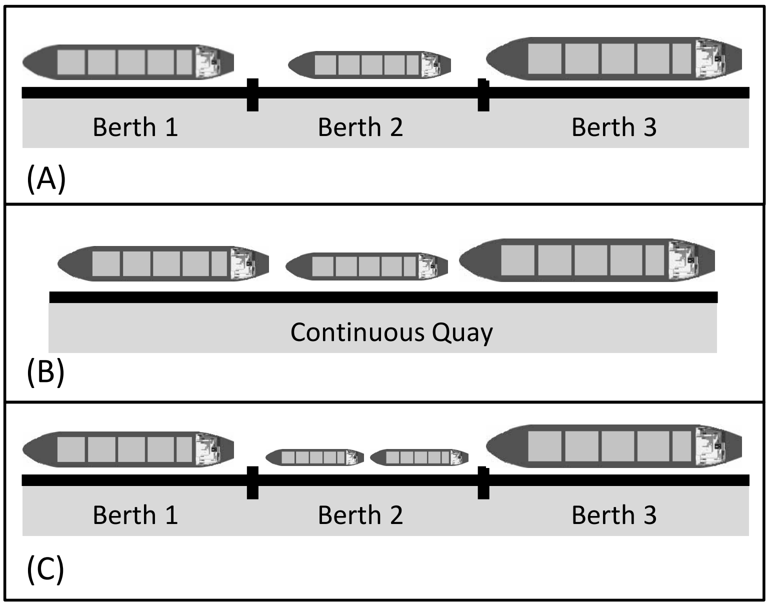

Figure 3.7: Different quay layouts: (A) the discrete quay layout, (B) the continuous quay layout and (C) the hybrid quay layout (derived from Imai et al., 2005)

Umang et al. (2013) and Robenek et al. (2013) studied the berth allocation problem explicitly for bulk ports by taking the cargo type (liquid bulk and dry bulk) into account. Conveyors or pipelines have to be selected for the transport of cargo between the seaside and predefined stockyard locations. In both papers it was assumed that the entire shipload was stored at one location. The authors stated that solving the problem for multiple storage locations per ship would be complicated. Two exact methods based on mixed integer linear programming were proposed. Heuristic approaches based on squeaky wheel optimization (Umang et al., 2013) and critical-shaking neighborhood search (Robenek et al., 2013) were applied to solve the problem in large scale environments.

3.3.2 Quay crane assignment problem

In the quay crane assignment problem (QCAP) cranes are assigned to ships in such a way that all required transshipments can be fulfilled. In the case for a discrete quay layout (Figure 3.7A), where each berth holds a set of dedicated cranes, an explicit assignment of cranes is not required (Bierwirth and Meisel, 2010). Typical objectives of the QCAP aim to minimize crane productivity losses by reducing the number of crane setups and crane travel times. The QCAP can contain the following requirements:

- The number of cranes assigned to a ship can be fixed during ship serving (the time-invariant assignment: Oğuz et al., 2004) or can change during ship serving (the variable-in-time assignment: Park and Kim, 2003).

- In some cases, a minimum number of cranes per ship throughout the handling time needs to be predefined. According Imai et al. (2008) and Legato and Mazza (2013), this number can be agreed in contracts between ship-owners and terminal operators.
- Meisel and Bierwirth (2006, 2009) modeled the decrease of crane productivity due to the hindrance of rail-mounted cranes.

Crane assignment for unloading barges was discussed by Bugaric and Petrovic (2007). These authors assessed two different crane operating strategies. In the first strategy, two cranes work independently at two separated berths (discrete quay layout). In the second strategy, the cranes are able to travel between berths realizing barge unloading of barges with two cranes (continuous quay layout). The authors defined two unloading stages. During unloading the first 80% of the load, both cranes operate simultaneously on the same barge. During the remaining stage, the ship is emptied using one crane. Simulation results showed that the total unloading capacity increased when the second strategy was applied. In Bugaric et al. (2012), a third crane was added to the quay. When the continuous quay layout will be applied the unloading capacity can further be increased compared to installing a third crane for the discrete quay layout.

Kim et al. (2011) extended the crane assignment problem with the selection of the transportation route to transport the unloaded material from the seaside to the stockyard. The authors proposed a heuristic approach that covered berth allocation, crane assignment and transportation route selection. Robenek et al. (2013) proposed the assignment of a fixed number of moveable cranes to ships. This number was defined as a function of the ships length.

3.3.3 Quay crane scheduling problem

The objective of the quay crane scheduling problem (QCSP) is to determine the sequence of the discharging and loading operations to minimize the ship service time. During ship serving, the difference between the maximum and minimum amount of cargo in the holds should not exceed a certain limit to maintain the balance required for safety and to prevent an exceeding of ship strength limitations (Kim et al., 2011). Daganzo (1989) was the first one who discussed the QCSP by proposing an algorithm that determined the number of cranes for multiple ships such that the overall workload was balanced. Peterkofsky and Daganzo (1990) extended this algorithm by assigning cranes to individual holds with the objective to minimize the ships departure times. The following quay crane scheduling principles were formulated by Daganzo (1989) and Peterkofsky and Daganzo (1990):

- A crane should not be idle if there is work to do.
- If multiple cranes work on a ship, one of them should work on the ‘maximum hold’, which is the hold that requires the most time to be finished.
- The holds of the earliest ship to depart allow the least flexibility to be assigned, this ship has priority to be serviced.
- The holds with the largest workload and the least amount of simultaneous crane access allow the least flexibility.

Han et al. (2010) introduced a berth and crane scheduling problem with stochastic ship arrival and handling times. Ships arrive with different priority levels depending on the relative customer importance. Their proposed method allows the movement of cranes to new arrived ships even if the task on their original assigned vessel was not finished. Applying this method will lead to more setup times because of the more frequent changes but brings more flexibility into the system.

3.3.4 Evaluation of modeling approaches

In the previous sections, a significant number of papers that discussed the seaside transshipment of cargo in ports was reviewed. For the discrete quay layout the planning problem is relatively easy and queuing models can be applied when generalized distributions are used to represent the ship arrival and service times. The quay and cranes performance can be increased when the continuous quay layout is applied and when the number of cranes assigned to ships may vary during the ship's service time. However, the planning of the seaside operation becomes more complicated, especially when rail-mounted cranes are used because these cranes cannot pass each other.

Modeling the ship arrival process is needed to realize accurate seaside designs. The stochastic processes that describe the ships interarrival and service times need to be investigated. If these processes match with generalized distributions queuing theory can be applied otherwise simulation is required.

Although many papers discussed the seaside operation at container terminals, these methods cannot easily be adapted to dry bulk terminals. The main difference is the operational behavior. At dry bulk terminals a continuous flow of dry bulk materials used a fixed infrastructure of belt conveyors versus the discontinuous transport of standardized load units at container terminals using individual transportation equipment. Bulk ships contain different grades of material. To prevent mixing, these materials must be handled and transported separately. The transportation capacity of the belt conveyors may hinder the cranes operating speed. Consequently, the number and capacity of the quay belt conveyors must be considered as well to realize adequate terminal designs.

Another difference is the longer operational times for ships at dry bulk terminals (up to several days) compared to ship turnaround times of 24 hours at container terminals. For a long time a part of the belt conveyor network is claimed and is not available. Another difference is the way of storing cargo; containers are stacked individually at the stockyard for a couple of days while bulk material is stored in large piles for a longer time, even up to several months. When a container is discharged from the stockyard, its location can immediately been occupied by another container. For dry bulk terminals, the pile's area is not changed when a portion of a pile is reclaimed while the stored capacity has been decreased.

3.4 Seaside modeling: application

Queuing theory can be applied to model the ship arrival process when ships can only moor at dedicated berths; each berth holds its own cranes and the stochastic variations can be represented by generalized distributions. Queues of waiting ships will occur whenever the current demand for ship serving exceeds the current capacity to provide that service. In section 3.4.1 the seaside modeling when the quay consists of a single berth is introduced. The multiple-berth layout is discussed in section 3.4.2. A method for the determination of the number of berths is presented in section 3.4.3.

3.4.1 Single-berth quay

A single-berth quay layout can be represented by a single-server queuing model. Equation (3.4) can be used to determine the average ship waiting time related to the server's utilization, the server's rate and the interarrival and service time distributions. Equation (3.4) was derived from Jagerman et al. (2004) for the G/G/1-queuing model and is an extension of the M/G/1 equation, also known as the Pollaczek-Khintchine formula. This equation is formulated in the same form as the Pollaczek-Khintchine equation in Tijms and Kalvelagen (1994).

$$W_t = \tfrac{1}{2}\left(c_X^2 + c_Y^2\right)\left(\frac{\rho}{1-\rho}\right)\frac{1}{\mu} \tag{3.4}$$

Where W_t is the average ship waiting time [h], c_X and c_Y [-] denote the coefficient of variation of the interarrival time X and the service time Y respectively, ρ [-] represent the berth utilization and μ is the service rate [1/h].

The coefficients of variation (c_X and c_Y) depend on the distribution type. The following values for these coefficients were presented; for a Negative Exponential Distribution (NED): 1 (Adan and Resing, 2002 and Jagerman et al., 2004), for an Erlang-k: √1/k (Adan and Resing, 2002) and for a deterministic (D) distribution: 0 due to the lack of stochastic variation.

For several combinations of the interarrival time and service time distributions, values for the term '½ ($c_X^2 + c_Y^2$)' were determined by using the above mentioned values for the coefficients of variation. These values determined are shown in Table 3.2.

From Table 3.2, it can be seen that the average waiting time reaches its maximum value when both distributions are negative exponential distributed (NED – NED). When the stochastic variation reduces (which is the case for an Erlang-2 distribution) the average waiting time reduces as well. When both distributions are deterministic ships do not have to wait due to stochastic variations.

Table 3.2: Determined values for ½ ($c_X^2 + c_Y^2$)

IAT Dist	W_sDist		
	NED	Erlang-2	D
NED	1	¾	½
Erlang-2	¾	½	¼
D	½	¼	0

3.4.2 Multiple-berth quay

A quay with multiple berths, each berth has its own handling equipment, allows simultaneous service of ships. When the interarrival times and the service times can be represented by a negative exponential distribution, there is an analytical solution available. Table 3.3 lists the equations for an M/M/n-queuing model. However, for all other combinations of distributions there are no analytical solutions and other solutions available. The solution for M/M/n queuing models will be used in this thesis for the verification of the simulation models.

Equations (3.5) and (3.6) were used to assess multiple-berth quays. From four M/M/n-queuing models the average waiting time was determined as function of the inverse service rate (W_t [1/μ]). Using equations (3.5) and (3.6) assume that berthing of ships occur according the FCFS-berthing method, each berth has a similar service capacity and ships can moor at each berth. Figure 3.8 shows the ship average waiting time versus the average berth utilization (ρ). As expected, the average waiting time decreases when the number of berths increases.

Especially, the reduction of the waiting time for a double-berth quay (M/M/2) compared to a single-berth quay (M/M/1) is significant.

Table 3.3: Overview of solutions for multiple-server queuing models

Queuing Model	Solution	Reference
M/M/n	$$W_t = \Pi_W \left(\frac{1}{1-\rho} \right) \frac{1}{n\mu} \quad (3.5)$$ Where Π_W is the delay probability [-], n is the number of servers [-] and c_u is the number of customers in the queuing system [-] $$\Pi_W = \frac{(n\rho)^n}{n!} \left((1-\rho) \sum_{c_u=0}^{c_u-1} \frac{(n\rho)^{c_u}}{c_u!} + \frac{(n\rho)^n}{n!} \right)^{-1} \quad (3.6)$$	Many references, e.g., Adan and Resing (2002)
M/G/n	Approximations, numerical solutions, queuing tables and simulation	Boxma et al. (1979), UNCTAD (1985), Gross et al. (2008) and Hillier and Lieberman (2010)
G/G/n	Some steady-state results and simulation	Gross et al. (2008), Hillier and Lieberman (2010)

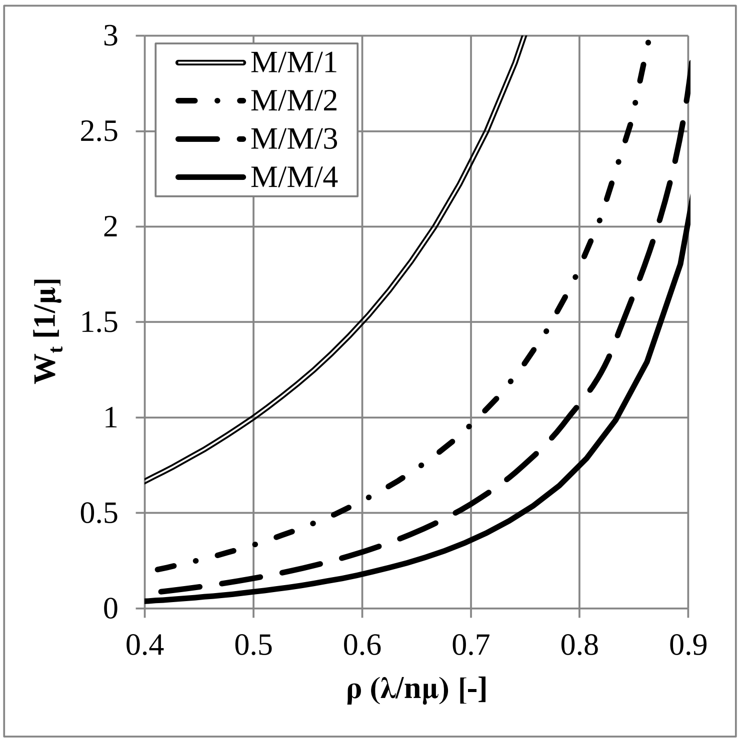

Figure 3.8: The average waiting time versus the average berth utilization for the multiple-berth quay layout

3.4.3 Determination of the number of berths

From Figure 3.8 it can be concluded that an increase of the number of berths will lead to a decrease of the average ship waiting times. However, installing multiple berths require substantial investments. This section introduces a method that determines the number of berths by taking the ships waiting costs and berth costs into account.

Several cost functions were derived to determine the initial number of berths. Huang and Wu (2005) presented an overview of these cost functions. One of the first developed cost functions was proposed by Plumlee (1966), this function is shown algebraically in equation (3.7):

$$TC = C_{ws}\lambda W_t + C_b n_b \left(1-\rho\right) \quad (3.7)$$

Where TC stands for total costs per day [k€/d], C_{ws} represents the daily costs per waiting ship [k€/d], λ is the ship arrival rate [1/d], W_t is the average ship waiting time [d], C_b is the daily cost per berth due to its unoccupancy [k€/d], n_b is the number of berths [-] and ρ is the average berth utilization [-].

To get an idea about the impact on the total daily costs when multiple berths are installed, the total daily costs were determined for two different quay layouts. For the first layout it was assumed that this layout contains two berths. It was assumed that this layout could be represented by an M/M/2-queuing system. The second quay layout contains three berths; an M/M/3-queuing system will be used. It was assumed that in both layouts the same ship arrival pattern and shipload distribution were used. Besides, at each berth the same service capacity was installed. For the daily ship waiting cost (C_{ws}) a value of 10 [k€/d] was used, which corresponds to the actual price for Panamax ships in October 2014. Two different values were taken for the daily berth cost (C_b). The first value for the daily berth cost was the same as for the daily ship waiting cost ($C_{ws} = C_b$).

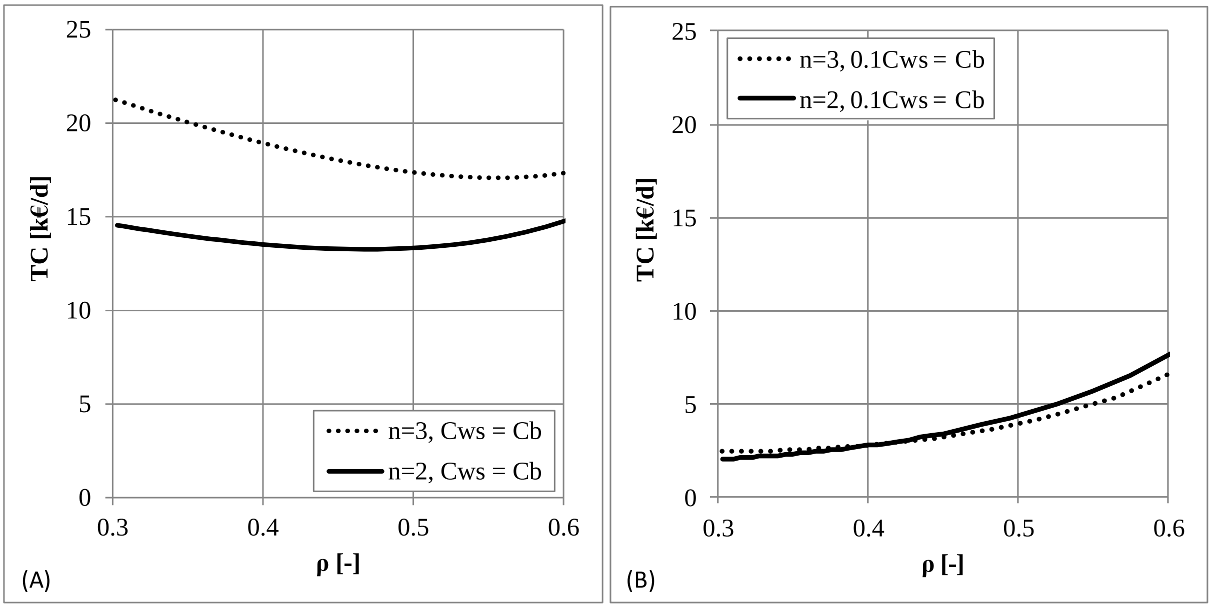

Figure 3.9: Total daily cost versus the average berth utilization for two or three berths and two different values for the daily berth costs (C_b) as function of the daily ship waiting costs (C_{ws}): (A) $C_{ws}= C_b$ and (B) $0.1C_{ws}= C_b$

Using the above mentioned daily berth and ship waiting costs the total daily cost as function of the average berth utilization was determined, these are shown in Figure 3.9A for cases with a different number of berths. In Figure 3.9B the daily costs versus the average berth utilization are shown when the daily berth costs (C_b) are only a tenth of the ship waiting costs ($0.1C_{ws} = C_b$). From Figure 3.9 it can be learned that installing an third berth will only result in a reduction of the total daily costs when the daily berth costs are significantly lower than the daily ship waiting cost.

3.5 Ship arrival process

This section introduces the parameters needed for the modeling of the ship arrival process. In section 3.5.1 the interarrival time distributions are discussed and the ship service time distributions are investigated in section 3.5.2. The parameters that affect the ship unloading time are derived in section 3.5.3.

3.5.1 Ship interarrival time distribution

In many studies, especially for container terminals, analytical distributions were applied to represent the ship interarrival times (IAT). Table 3.4 presents an overview of these suggested distributions. When distributions were derived from real-world data, the number of ships (n_s) is listed in Table 3.4. The cargo type discussed in the papers is also listed.

Table 3.4: Overview of proposed interarrival time distributions (IATDist)

IATDist	Reference	n_s [-]	Cargo[1]	IAT Dist	Reference	n_s [-]	Cargo[1]
Weibull	Tengku-Adnan et al. (2009)	408	DB	NED	Kia et al. (2002)	372	C
Weibull	Tahar and Hussain (2000)	-	C	NED	Demirci (2003)	297	C
Erlang-2	UNCTAD (1985)	-	DB	NED	Pachakis and Kiremidjian (2003)	142	C
Erlang-k	Kuo et al. (2006)[2]	7,729	C				
NED	UNCTAD (1985)	-	DB	NED	Van Asperen et al. (2003)	-	LB
NED	Radmilovich (1992)	-	-	NED	Dragovic et al. (2006)	711	C
NED	Kozan (1997)	679	C	NED	Bugaric and Petrovic (2007)	-	DB
NED	Shabayek and Yeung (2002)	12,610	C	NED	Legato and Mazza (2013)	1030	C

[1] Where C stands for containers, DB for dry bulk and LB for liquid bulk.
[2] Kuo et al. (2006) discovered for the arriving of container vessels in the port of Kaohsiung that the ship interarrival time distribution followed an Erlang-k distribution. The distribution coefficient (k) tends to decrease as the system's scale grows. The interarrival time at the public container terminal appears to be more scattered than at dedicated container terminals.

Most papers used the negative exponential distribution (NED) to represent the ship interarrival times. The arrival process can then be represented by a Poisson arrival process. The ships arrive randomly and independently. The proposed NED distribution for container terminals is remarkable. At container terminals, ship arrivals are scheduled and therefore expected not random. However, Pachakis and Kiremidjian (2003) stated that the superposition of several independent container shipping lines with uniformly arrival rates yields approximately a Poisson arrival pattern.

Table 3.4 lists a limited number of papers presenting interarrival time distributions for bulk ships. To expand this overview, empirical data of ship interarrival times from five dry bulk terminals that handle mainly coal and/or iron ore was investigated. The terminal operators did not want to be named explicitly due to commercial interests. That’s why the terminal names are replaced by T1 until T5. Interarrival time distributions were derived from the operational data and these distributions are shown as histograms in Figure 3.10 until Figure 3.12. In Table C.1, in Appendix C, details are listed for these interarrival time distributions.

Similarities between measured interarrival time distributions and proposed distributions for dry bulk terminals (see Table 3.4: Weibull, Erlang-2 and NED) were investigated. The first reason was to verify if distributions proposed do correspond with real operational data and secondly, if regularities can be distinguished between the distribution and terminal type. Such regularites can then be used for the design of new terminals which lack the availability of historical data.

In this thesis chi-square tests are used for curve fitting between measured and analytical distributions. The chi-square test can be applied to binned data like the histograms as shown in Figure 3.10 until Figure 3.14. A chi-square test is sensitive to the choice for the bin size, using too small bin sizes will result in wrong chi-square values. That’s why minimum bin sizes that contain at least five measured events (interarrival or service times) are realized by combining bins. In Figure 3.12B an example for the reduction of the number of bins is shown for the histogram as presented in Figure 3.12A.

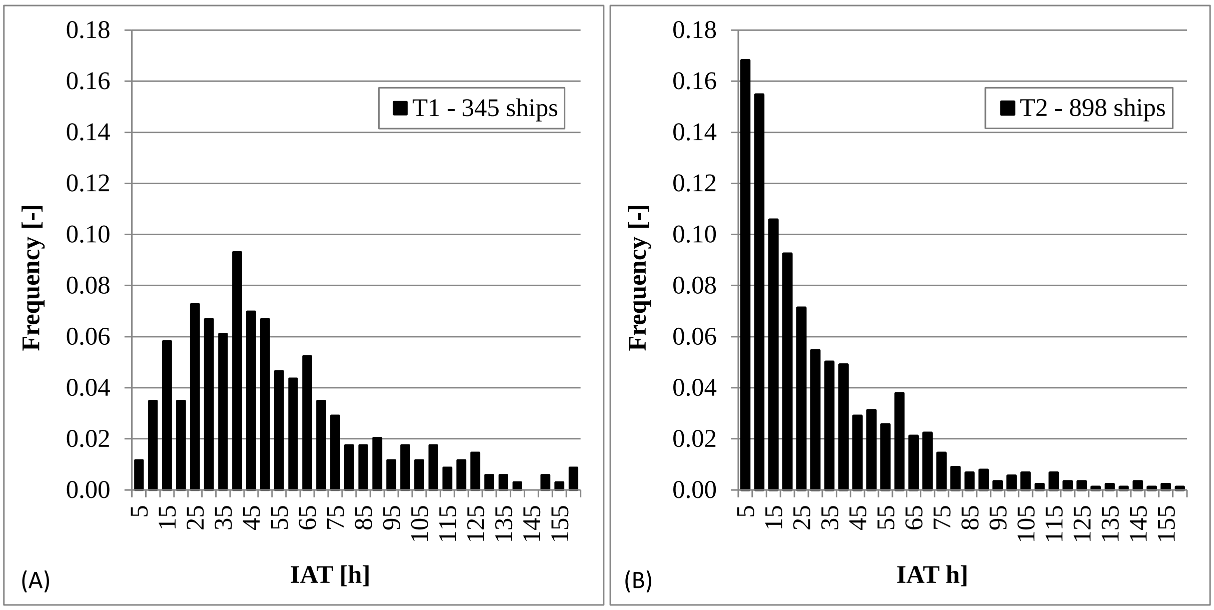

Figure 3.10: Measured interarrival time distributions for terminals T1 (A) and T2 (B)

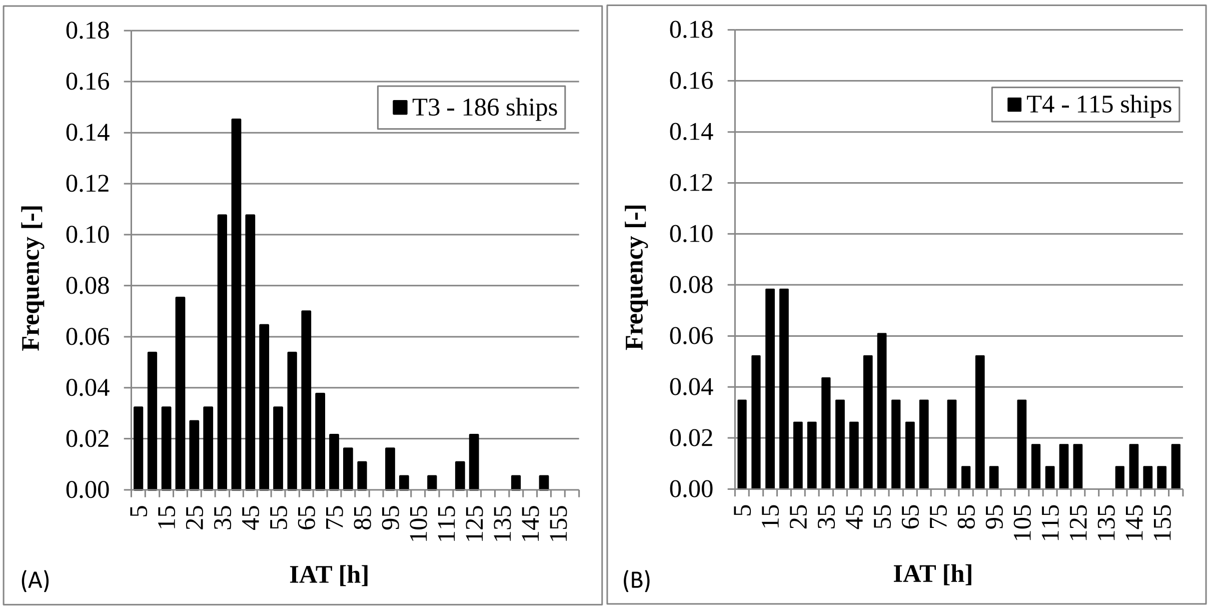

Figure 3.11: Measured interarrival time distributions for terminals T3 (A) and T4 (B)

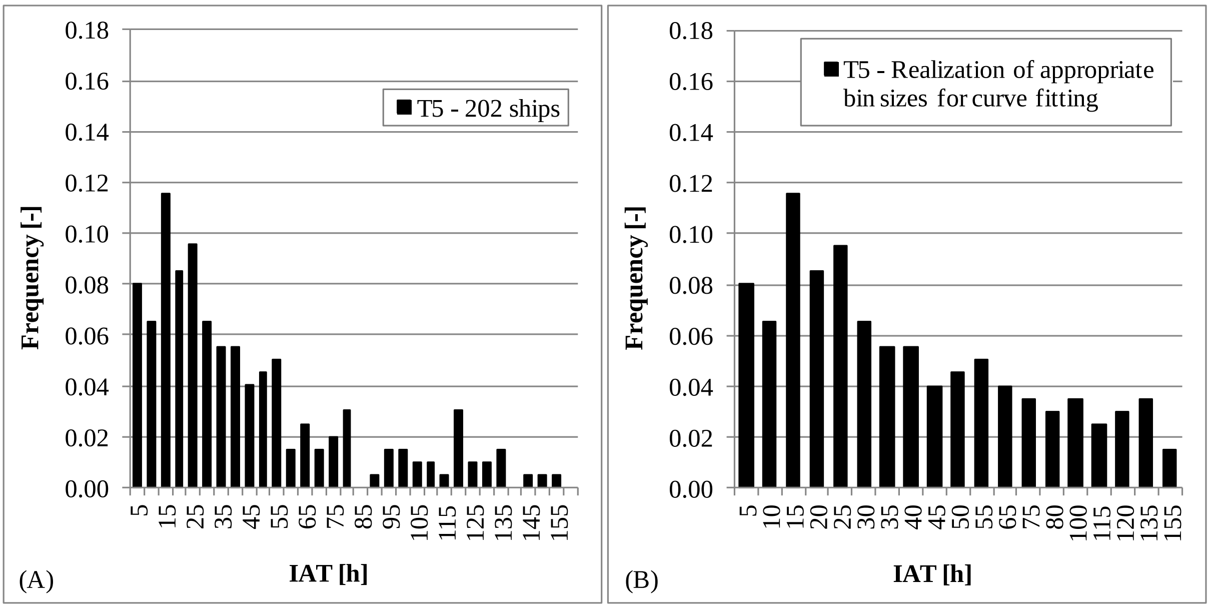

Figure 3.12: Measured interarrival time distribution for terminal T5 (A) and (B) shows the reduction of the number of bins to realize an appropriate number per bin

Results for the distribution fit are listed in Table 3.7. This table lists per terminal the main characteristics and the best fitted distribution out of the Weibull, Erlang-2 or NED. The measured distribution fits with an analytical distribution when the chi-square value (χ^2) equals or is less than the critical value ($\chi^2_{0.05}$). From Table 3.5 it can be concluded that the proposed NED, Weibull and Erlang-2 distributions correspond with measured interarrival time distributions for terminals T2, T4 and T5 respectively. However, the measured distributions for T1 and T3 cannot be fitted within a 95% confidence level with one of these analytical distributions.

Table 3.5: Results for the interarrival time distribution fit

Terminal	Figure	Characteristics	$\dot{m}$ [Mt/y]	n_s [-]	Best fitted distribution	χ^2 [-]	$\chi^2_{0.05}$ [-]
T1	3.8A	Single-user import	18	345	Weibull / Erlang-2	41.6 / 76.7	33.9
T2	3.8B	Multi-user import	37	898	NED	25.6	32.7
T3	3.9A	Single-user export	44	186	Weibull / Normal	43.4 / 60.1	27.6
T4	3.9B	Multi-user import	16	115	Weibull	30.1	30.1
T5	3.10	Multi-user import	12	202	Erlang-2	26.9	30.1

In accordance to Kuo et al. (2006) it seems that the stochastic variation increases when the system's scale grows. Regularities between measured distributions and terminal type can hardly be distinguished; for one multi-user import terminals an NED distribution satisfies while for the other multi-user import terminal the interarrival times are Erlang-2 distributed. The absence of a clear relation between distribution and terminal type complicates the design process for new terminals. When the distribution type is unknown, different types should be tested and being discussed with the terminal operator. When terminals have to be expanded, it is recommended to use historical data and assume that this dataset satisfies also in the future.

3.5.2 Ship service time distributions

The time needed to load or unload ships is called the ship service time (W_s). The handling of containers at the terminal's seaside has similarities with bulk ship unloading; in each crane cycle a container is handled or a certain tons of material is unloaded from the hold. Other similarities are that the handling capacity per crane reduces when multiple cranes are deployed at a ship and the crane cycle time increases when the ship becomes more emptied. Table 3.6 lists an overview of proposed service time distributions for both container and dry bulk cargo. When distributions were derived from real-world data, the number of ships (n_s) is listed.

Table 3.6: Overview of proposed service time distributions (W_sDist)

W_sDist	Reference	n_s [-]	Cargo[1]	W_sDist	Reference	n_s [-]	Cargo[1]
Normal	Tahar and Hussain (2000)	150	C	Erlang-k	Shabayek and Yeung (2002) [k:117]	12,610	C
	Bugaric and Petrovic (2007)	-	DB		Kozan (1997) [k:4]	679	C
NED	Radmilovich (1992)	-	-		Kia et al. (2002) [k:4]	372	C
	Demirci (2003)	297	C		Altiok (2000) [k:4]	248	DB
Beta	Legato and Mazza (2013)	1,030	C		Dragovic et al. (2006) [k: 3,7,12]	711	C
Gamma	Jagerman and Altiok (2003)	304	DB		UNCTAD (1985) [k:2]	-	DB

[1] Where C stands for containers and DB for dry bulk.

The proposed service time distributions were compared with the measured service time distributions from three of the already introduced dry bulk terminals (T2, T4 and T5). Figure 3.13 and Figure 3.14 show these measured service time distributions. Details for these service time distributions are listed in Table C.2 (Appendix C). The chi-square method was used to fit these measured distributions with one of the analytical distributions proposed for dry bulk terminals (Erlang-k, Normal and Gamma). Results for the distribution fit are listed in Table 3.7.

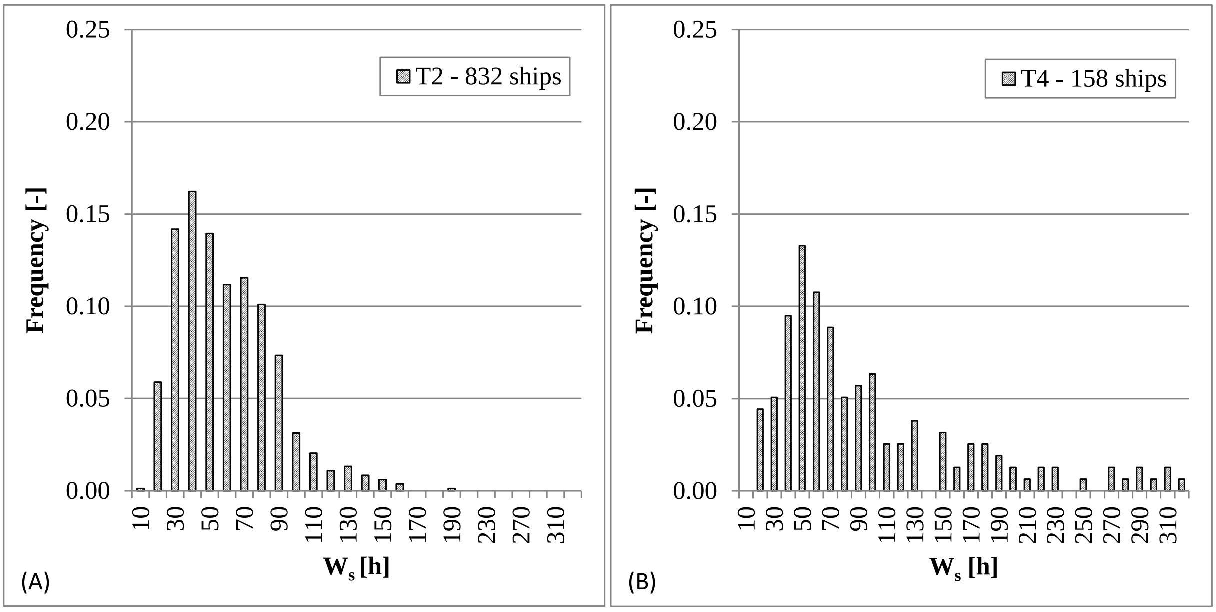

Figure 3.13: Measured service time distribution for terminals T2 (A) and T4 (B)

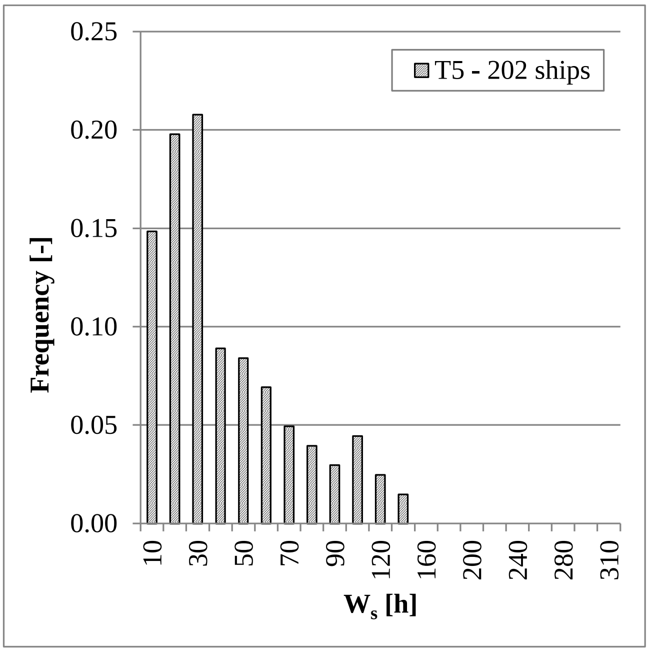

Figure 3.14: Measured service time distribution for terminal T5

All three service time distributions show the best fit with an Erlang-2 distribution. However, only the measured service time distribution for T5 can be represented within a 95%

confidence level by an Erlang-2 distribution. The measured average ship service time (W_s) and the average shipload of the visited fleet per terminal are also listed in this table.

Table 3.7: Results for the service time distribution fit

Terminal	Figure	Best fitted distribution	χ^2 [-]	$\chi^2_{0.05}$ [-]	W_s [h]	Shipload [kt]
T2	3.11A	Erlang-2	259.4	36.4	55	103
T4	3.11B	Erlang-2	48.6	27.6	94	69
T5	3.12	Erlang-2	15.9	19.7	39	24

From Table 3.7 it can be concluded that only one real-world service time distribution could be represented by an analytical distribution (terminal T5). Therefore, the accuracy of the seaside designs will increase when empirical shipload data and realistic ship service rates are used to represent the service times. For an indication of the sensitivity of the results when analytical or empirical distributions are used, is referred to section 4.5, where for a case this aspect will further be investigated. Details for the shiploads of the visited bulk ships at the dry bulk terminals investigated are listed in Table C.3 (Appendix C).

3.5.3 The ship unloading rate

As stated before, the ship service rate and the shipload determine the ship service time. Due to the lack of available ship loading data only the ship unloading process was investigated. The dataset as listed in Table B.2 (Appendix B) contains sufficient data for this analysis. The average unloading rate (Q_u) during the unloading of an entire bulk ship was determined by dividing the shipload by the service time registered. Note that in the average unloading rate the free-digging unloading capacity (when cranes can operate at maximum speed) and the reduced capacity (when crane have longer cycle times to unload the material that is stored in the lower part of the hold) are included.

In Figure 3.15, the measured unloading rates during unloading of iron ore (A) and coking coal (B) are shown. In Figure 3.16, the unloading rates during steam coal unloading are given versus the shiploads. From these figures it can be concluded that the unloading rate as function of the shipload vary significantly. A distinct relation cannot easily be derived and more research is required. In this section, parameters that affect the ship unloading rate will be investigated.

It is expected that the shipload and the number of active cranes during ship unloading will be relevant parameters. However, also the cargo type, the number of grades, the number of holds and the unloading sequence (covering the order and quantities of unloaded materials per hold) may affect the ship unloading rate. Data from the unloading process of terminal T2 was analyzed because only this dataset showed the fraction of time that quay cranes were active per ship. This dataset also contains information about the total service time, the ship's deadweight, the shipload, the number of grades and the number of holds per ship. The unloading sequence is not considered in this analysis due to the unavailability of data.

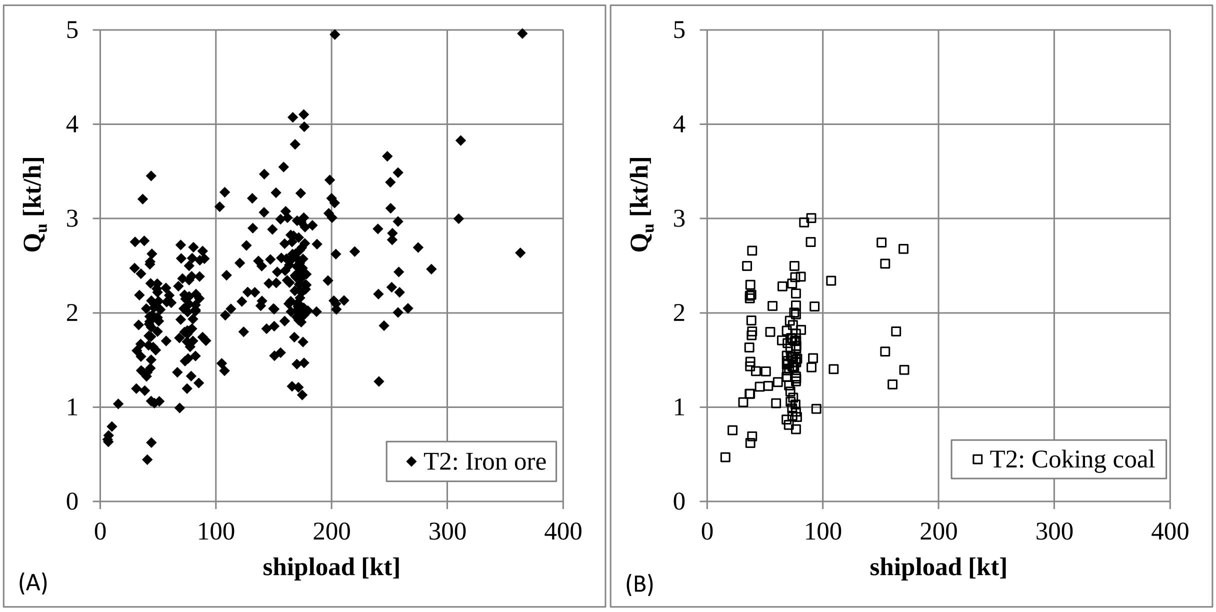

Figure 3.15: Measured unloading rates versus the shiploads for the unloading of iron ore (A) and coking coal (B)

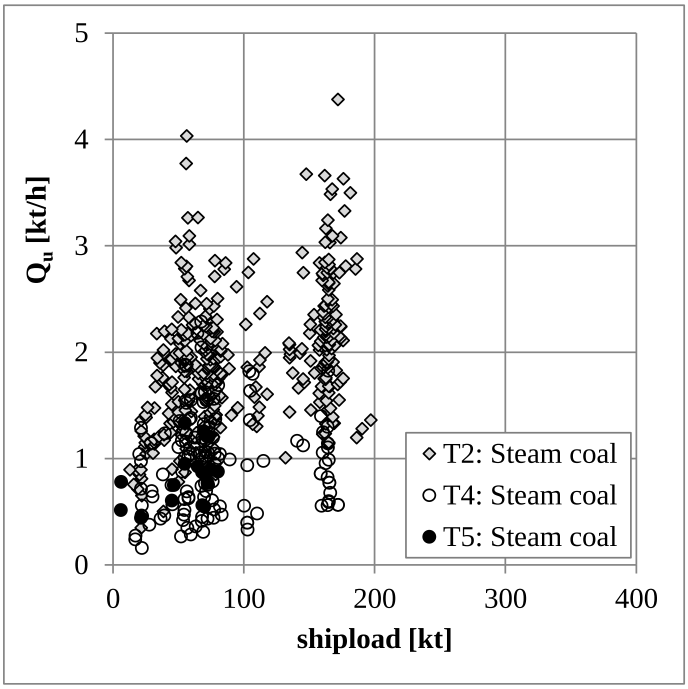

Figure 3.16: Measured unloading rates versus the shiploads for steam coal

From the dataset a multiple linear regression model was composed to determine the impact of each of the parameters (ship's deadweight, shipload and the number of materials, holds and active cranes) on the unloading rate. A multiple linear regression model was selected because it attempts to model the relationship between multiple explanatory variables (the relevant parameters) and the response variable (the unloading rate) by fitting a linear equation to the observed data. For the exclusion of irrelevant parameters the analysis of variance was used. The regression analysis has shown that the ship's deadweight, the shipload and the number and capacity of active quay cranes per time unit determine the unloading rate. The number of grades and the number of holds do not contribute significantly to the estimation of the unloading rate. Equation (3.8) shows the relation derived for the unloading rate based on the form of a multiple linear regression model.

$$Q_u = \beta_0 + \beta_1 dwt + \beta_2 sl + \sum_{c=1}^{c=4} Q_c f_{qc,c} + \varepsilon \tag{3.8}$$

Where Q_u is the unloading rate [kt/h], dwt is the ship's deadweight [kt], sl is the shipload [kt], Q_c is the determined unloading rate per crane [kt/h], $f_{qc,c}$ [-] is the fraction of time that a crane was active during unloading and c [-] is the number of cranes, for terminal T2 four. The parameters $\beta_0 - \beta_2$ and ε are regression parameters. Table 3.8 lists the values determined.

This determination of the ship unloading rate was used to exclude the parameters which are not relevant (cargo type, number of grades and holds) for the simulation model developed.

Table 3.8: Determined values for the unloading rate estimation

Parameter	Value	Unit	Parameter	Value	Unit
β_0	-11	[kt/h]	Q_2	0.969	[kt/h]
β_1	1.83	[h^{-1}]	Q_3	1.315	[kt/h]
β_2	0.74	[h^{-1}]	Q_4	1.190	[kt/h]
Q_1	0.732	[kt/h]	ε	0.35	[kt/h]

3.6 Simulation-based approach

From the previous section it can be concluded that for multiple-berth quays only analytical solutions exist when the interarrival times and service times are negative exponential distributed, the M/M/n-queuing model. However, from the measured distributions (see sections 3.5.1 and 3.5.2) it can be learned that NED distributions do not always correspond with real-world applications. Moreover, specific operational procedures like a limited water depth, the hindrance of ship serving due to the lack of transportation capacity, the cranes setup times and the varying unloading rates can hardly be considered analytically.

To consider the above mentioned seaside operational procedures and to take the real-world stochastic variations for the ships interarrival times, shiploads and equipment break downs into account, theoretical or formula based examinations cannot be used. Simulation proved to successful in the formulation and evaluation of quay side designs for container terminals, see for example the work of Saanen (2004). Also in this thesis simulation will be used to determine the parameters that affect the terminal's quay side design. Furthermore, simulation will be used to assess improvements of the seaside operation to increase the annual throughput of materials over the quay and to reduce the average time that ships spend in the port.

As already mentioned in the first chapter, the process-interaction method will be followed to develop the simulation models. Real-world operational processes have to be translated into process descriptions for simulation elements. In a research environment like this PhD project, the elements' processes need to be expanded, detailed and merged during time. Furthermore, in the field of dry bulk terminals there are hardly 'on the shelf' packages available to be selected. Within the department this research was performed, TOMAS has already succesfully been applied for design studies of a specific dry bulk terminals, see Ottjes et al., (2007) and Lodewijks et al., (2009). TOMAS, which is developed and introduced by Veeke and Ottjes

(1999), supports process interaction simulation and is a simple, open and flexible tool. The simulation models will be built in Delphi® (that uses the programming language Pascal) and TOMAS will be used for the simulation application.

In section 3.6.1, the simulation model dedicated for the terminal's seaside is introduced and the verification and validation of this model is discussed in section 3.6.2.

3.6.1 Seaside model

The seaside model is applicable for both import and export terminals. In this section, the model will be explained for import terminals. Ships are moored alongside the quay and cranes transfer the cargo from the ships to the quay conveyors. In the simulation model developed it was assumed that there was no direct transshipment of materials from seagoing vessels to inland ships. The quay conveyors transport the material to the stockyard. The seaside model is generic; the number of berths, cranes and quay conveyors can be varied. It was assumed that the number of cranes is at least the number of quay conveyors and the number of cranes is at least the number of berths. In this section a brief description of the seaside simulation model is introduced. Readers who are interested in specific details for the seaside model are referred to Appendix D. In Section D.2, the process interaction approach (proposed by Zeigler et al., 2000) is followed to present details of the seaside model.

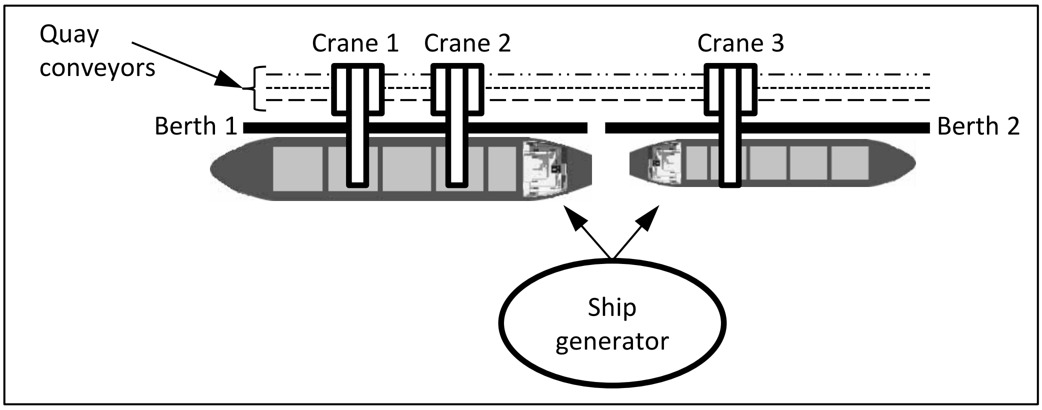

Figure 3.17: Schematic representation of the seaside simulation model (description follows in text)

Figure 3.17 shows an arbitrary layout of the seaside model where ships can moor at two berths. Also the main elements; a ship generator, ships, berths, cranes and quay conveyors are shown in this figure. The cranes are able to move alongside the quay to operate at both berths but cannot pass each other. Each crane is able to transfer the cargo to one of the quay conveyors. The ship generator creates ships. To each ship specific attributes are assigned; the arrival time, the shipload, the number of grades and the maximum number of cranes allowed during unloading. The number of cranes per ship is a parameter of the simulation model. In this case, it was assumed that maximum two cranes can unload ships with a shipload less than 60 [kt] and maximum four for larger ships. Based on the shipload, the ship's length, beam and draft were calculated using equations (3.1) until (3.3). The objective for each berth is to check if a new arrived ship can be moored and to assign cranes to ships. Cranes perform the ship serving operation and check, after finishing, if it can continue unloading with another ship to comply with the first quay crane scheduling principle as mentioned in section 3.3.3. Details of the algorithms developed are briefly discussed from now.

Berth's algorithm *SelectShip*

Each berth contains an algorithm *SelectShip* that selects a new arrived ship to moor when the berth's water depth is sufficient and a quay conveyor can be assigned to the ship. Basically, the following assigning rules were implemented:

- For the ship service order, the First-Come-First-Served method was used in accordance to many other references (see section 3.3.1).
- If a ship contains one grade and there are two quay conveyors and two cranes available, two quay conveyors are assigned.
- If a ship contains multiple grades, the maximum number of quay conveyors to be assigned equals this number when these quay conveyors are available.
- If there is no quay conveyor available but two quay conveyors are assigned to another ship; one quay conveyor, originally assigned to the ship in operation, is reassigned to the newly arrived ship.

Berth's algorithm *CraneAssignment*

The objective of the *CraneAssignment* algorithm is to assign cranes in the right geographic positional order to berthed ships. Each ship gets at least one crane when berthed. When there is no idle crane available, the ship that is served with more than one crane will be selected and a crane will be released from this ship. Cranes will be (re)assigned alongside the quay to maintain the right positional order. An example of the cranes repositioning is shown in Figure 3.18. A new ship (ship 4) arrives and can be assigned to berth 3. At berth 1, two cranes unload ship 1. Crane 3 has to be moved to berth 3 and crane 2 has to be moved to berth 2. The time needed for the cranes to travel to other berths is called the setup time.

Crane's algorithm *Process*

In the simulation model, two different operational crane procedures were implemented. The time-invariant assignment (Oğuz et al., 2004) where the number of cranes do not change during ship unloading and the variable-in-time crane assignment (Park and Kim, 2003) where the number of cranes varies during ship unloading. To monitor the unloading progress, the number of cranes and the number of quay conveyors during a time interval (e.g., 1 hour) must be determined. Based on these numbers and the ship unloading stage, the ship unloading capacity during this time interval will be determined. The shipload will be reduced stepwise with the unloading capacity.

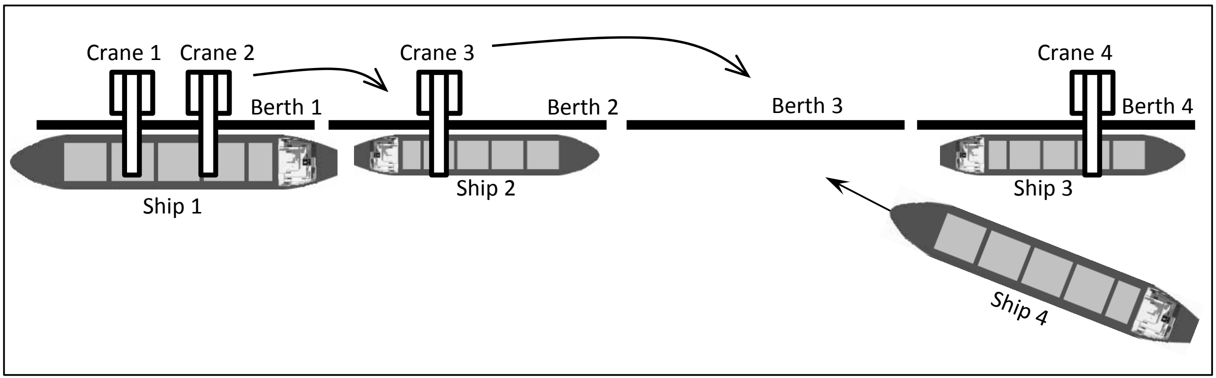

Figure 3.18: Repositioning of cranes alongside the quay

Verschoof (2002) introduced a variation of the unloading rate during the unloading time due to the ship characteristics. The author presented three different unloading stages based on the unloading of iron ore from a medium-sized bulk ship using grab cranes. The unloading stages are shown in Figure 3.19A. These stages were determined under good unloading conditions that mean a capable crane driver, good bulk material handling properties, good weather and no hindrance of cranes due to transportation of the material. During the free-digging stage, cranes operate at maximum speed by grabbing the material out of the upper part of the hold. When the shipload reduces, the grabs have to sink further into the hold which decreases the unloading capacity. During the cleaning stage, a dozer is brought into the hold to move the remaining material to the mid where the material can be picked up by the grab unloader.

The unloading curve, as presented in Figure 3.19, corresponds with practical experiences of terminal operators. However, measurements during daily operations were not available to verify the unloading curve presented by Verschoof (2002). The terminal operators, with whom I have had a close cooperation, do register the productivity rates for the unloading machines but do not assign these rates to individual ships. Especially, when cranes are moved frequently to other ships the determination of an unloading curve for individual ships can be a tough job. That’s why in this research, the unloading curve as presented by Verschoof (2002) will be used to determine the reduction of the unloading rate per ship.

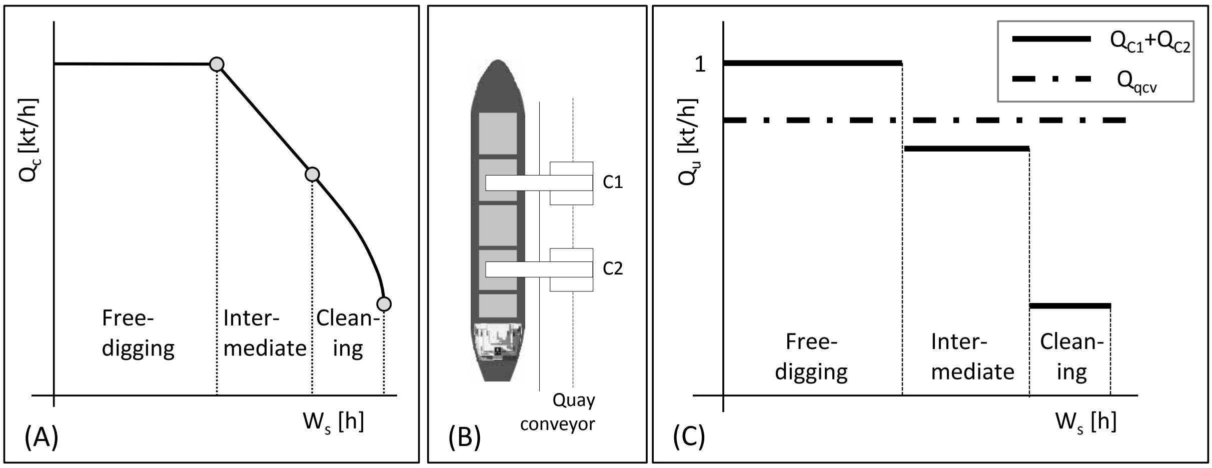

Figure 3.19: Determination of the unloading capacity. (A) shows the progress of the capacity during unloading (derived from Verschoof, 2002), (B) shows an example when two cranes unload a ship and one quay conveyor is used for the transport and (C) shows the limitations for the ship unloading capacity during the service time

Figure 3.19B and Figure 3.19C show an example for the determination of the ship unloading capacity (Q_u). Two cranes and one quay conveyor are assigned to a ship. In the free-digging stage, the combined unloading rate of the cranes ($Q_{C1+}Q_{C2}$) exceeds the transportation rate of the quay conveyor (Q_{qcv}). During this stage, the ship unloading capacity is limited by the transportation rate. For the rest of the unloading time, the ship unloading capacity is limited by the cranes capacities.

Crane’s algorithm *Reschedule*

When a ship is emptied and there are other ships being unloaded, the reschedule algorithm figures out whether this crane can be moved to another ship. A crane will not be moved to a ship that is already in the cleaning stage. Ship unloading during the cleaning stage with multiple cranes does not make any sense. If another ship can be unloaded with an extra crane, the cranes are reassigned over the berthed ships. The time needed to travel to another berth is a parameter (called the setup time) and is fixed for all cranes.

3.6.2 Verification and validation

According to Kleijnen (1995), all simulation models developed have to be verified to check the correct translation of the conceptual model into computer code and to determine whether these models performed as intended. The conceptual model for the seaside model is shown in Figure D.2 in Appendix D and the process descriptions are listed in the corresponding tables in Appendix D.

Verification of the seaside model was realized firstly with the verification of a correct processing of the operational processes using the tracing function of the simulation software. Secondly, simulation results for a simplified case, with an arbitrary number of four berths, were compared with analytical results. For the analytical results, an M/M/4-queuing model was used because from Table 3.3 it can be concluded that for an M/M/n-queuing model only analytical solutions exist.

Simulation results were obtained for a quay layout with four berths, each berth is equipped with one server (a crane together with a quay conveyor). For this verification the discrete quay layout was applied and the seaside operation was simplified; ships were loaded with only one grade, all shiploads are possible (sampling values for the shipload from the negative exponential distribution may result in exceptional shiploads), the service capacity remains constant during the ship serving operation (that means that the unloading curve as shown in Figure 3.19A was not taken into account), there was no water depth limitation and maximum one crane was assigned to each ship.

After each simulation run, the average ship waiting time and the average ship service time are measured. To realize accurate average values (with a low standard deviation); the impact of single random generated values should be diminished. A certain runtime is required. The run time is represented by the number of ships that have to be processed per simulation run. By increasing the number of ships, the run time will be increased as well. For this verification study, input files that contain 2,500 ships are used. This number is based on the specification for the required simulation outcome as it is mentioned in section 3.7.1.

For the verification study, ship arrival times and shiploads are sampled from negative exponential distributions. To start the random generations, ‘seeds’ are needed. A seed is an integer to set the generator to a random starting point for generating a series of random numbers. Different replications can then be realized by varying seed values. In this verification study, but also for the other simulation modesl in this thesis, ten replications will be used. The accuracy of a single average value is then determined by taken the variations of ten replications into account. The average values for the simulation results are shown in Figure 3.20 as single dots and the variation within the ten replications are shown with error bars.

From Figure 3.20 it can be concluded that despite the small deviation between simulation results and analytical results, the seaside model provides realistic outcomes. For the verification of this model the runtime satisfies but as it can be seen from Figure 3.20, for high values of the server utilization it is suggested to increase the run time to reduce the variation around the average values.

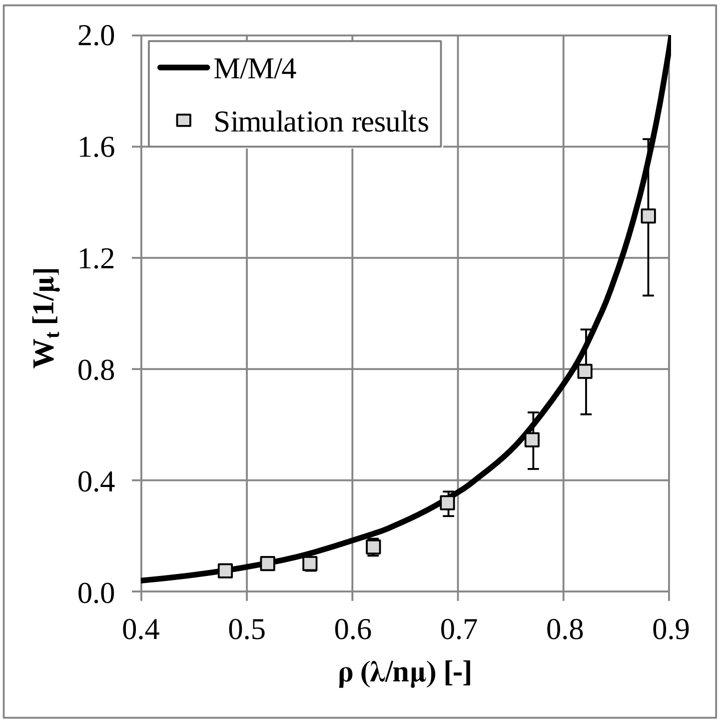

Figure 3.20: Verification of the seaside model by comparing analytical results obtained using an M/M/4-queuing system with simulation results for a 4-berth quay

The seaside model was developed in close cooperation with experts from the dry bulk industry; expert validation was applied. The processes implemented in the simulation models were compared with real terminal operations and (intermediate) outcomes of the model were discussed with terminal managers. For example, the case study, as presented in section 3.8, is based on a study performed at terminal T2 to investigate the possibilities to increase the quay productivity.

3.7 Simulation experimental results

In this section results from experiments are shown. The following experiments were performed; a discrete quay layout versus a continuous quay layout (section 3.7.2), the impact of the limitation of the water depth alongside the quay (section 3.7.3) and the consequence of the number and transportation rate of the quay conveyors (section 3.7.4). Results for these experiments were determined using the simulation model that was presented in the previous section. The average time that ships spend in the port (W_{ship}) [h] was used as key performance indicator. The ship port time includes the waiting time before being serviced and the service time. In the simulation model, the waiting time and service time for each ship is logged and is available for further analysis. But as first indication it was assumed that the average ship port time provides sufficient insight. The annual throughput ($\dot{m}$) was varied and the average ships port time was determined at the end of the simulation runs.

A seaside layout was defined as to be comparable with the quay layout of a large-sized Dutch import terminal to perform the experiments on. Using this quay layout, the experimental results can discussed with the terminal operator and a comparison with real-world operation can be made.

3.7.1 Input parameters and run control

Table 3.9 lists the input parameters for the experiments. The reduction of the crane unloading capacity during ship unloading was simplified in this case and is graphically shown in Figure 3.23A. Historical data of unloaded ships at terminal T2 (see Figure 3.23B, details for this histogram are listed in Table C.3 in Appendix C) was used as input for the shipload distribution.

Table 3.9: Input parameters for the simulation experiments

Parameter	Value	Unit	Parameter	Value	Unit
Number of berths	4	[-]	Maximum draft alongside the quay	20	[m]
Number of cranes	4	[-]	Cranes unloading rate (Q_c)	2	[kt/h]
Number of quay conveyors	4	[-]	Quay conveyors transportation rate (Q_{qcv})	2.5	[kt/h]
Ship interarrival time distribution	NED	[-]	Unloading efficiencies	Figure 3.23A	
			Average shipload	103	[kt]
Cranes setup times	0.5	[h]	Shipload distribution	Figure 3.23B	

For the interarrival time distribution a negative exponential distribution (NED) was used. Using this distribution type indicates that ships arrive randomly at the terminal, which contradicts the fact the ship arrivals are planned. Late arrivals of intercontinental ships are known in days in advance allowing terminal operations planners to adjust their plans. However, if a terminal operator has to service many ships from different clients the deviations from plan for individual ships introduce so many dispersion that when the ship arrival process is analyzed afterwards, it seems that ships arrive randomly. At these terminals, it is not an exception that the quay is empty for a couple of days while a week later ships have to wait offshore because the quay is fully occupied.

The terminal operations planners have hardly any influence in preventing such variations. One of the reasons is that in contracts between terminal operators and ship-owners demurrage penalties are included. Demurrage means an agreed amount payable to the ship-owner in respect to the delay of the ship beyond the laytime. The laytime is the period of time agreed between the terminal operator and the ship-owner for loading or unloading. Informing ship-owners in advance about extra waiting times does not automatically result in a reduction of ship's sailing speed but can even cause an increase of the speed to maximize the demurrage incomes for the ship owners.

Values for the shiploads are generated using a table-type distribution. Such distribution contains several classes with different ranges for the shiploads and the probability for this class. Within each class, values are uniformly distributed. For example, a class is defined with ranges of 50 and 100 [kt] with a probability of 0.2. For a generated shipload, the probability is 20% that its load is between the 50 and 100 [kt]. Ranges and probabilities for classes are represented by empirical data. In this case, the historical data from Figure 3.23B was used as input for six different classes.

For the generation of a single ship, its arrival time and its shipload are separately generated. However, does this assumption correspond with real operations? One would expect a certain interarrival time between large bulk ships to prevent excessive waiting times. From terminal T2, historical data was used to investigate a possible relation between the ships interarrival times and shiploads. In Figure 3.21 shiploads are listed during time (only an arbitrary time interval from the first three months in 2008 is shown) when ships arrived at the anchorage position offshore. In Figure 3.21 generated data is also presented when the arrival times and shiploads are separately generated. From both historical and generated data several cases can be distiquished when large ships arrive close after each other. For example, a case is shown for historical data (circled with the letter A within the circle) and a case (with letter B) for the generated data. While a clear relation between the ships interarrival times and shiploads cannot be distinguished, the ships arrival times and shiploads will be generated separately in this research.

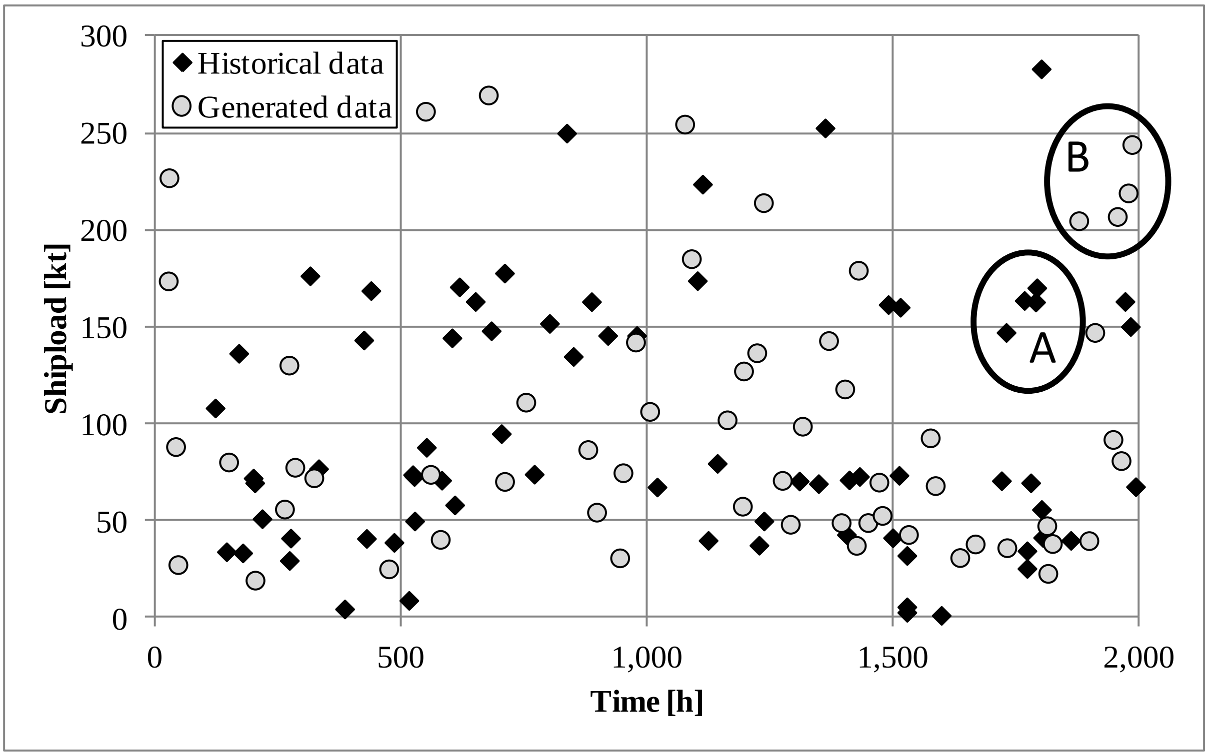

Figure 3.21: Comparison of historical data for the ship arrival times with corresponding shipload and generated data when the arrival times and shiploads are generated separately

Due to the fact that stochastic distributions are applied in the experimental results, the run time and accuracy have to be determined. The results for the run control are displayed in Figure 3.22 using boxplots. Boxplots (also called wisker plots) are used in this thesis in several places to display the variations for several key performance indicators measured. The spacings between the different parts of the box indicate the degree of dispersion and the skewness in the data. The bottom and top of the box represent the first and third quartiles of the measured data. The line within the box represents the median of the measured values. The ends of the wiskers correspond with the minimum and maximum values for the ten replications.

To determine the run time required the following method was applied. The seaside model was fed with ten different input files for three different numbers of ships (580, 1,450 and 2,500). These inputfiles were generated on beforehand each with different values for the seeds for random generation of the arrival times and shiploads. Subsequently, the seaside model was run ten times (each run with its own input file) and per run the average ship port time was registered. From this data, boxplots are designed, which are shown in Figure 3.22. There was no warm up time (time that the simulation will run before starting to collect results) included. The registration starts immediately which represent the situation of an empty quay, because such situations occur frequently during real operations.

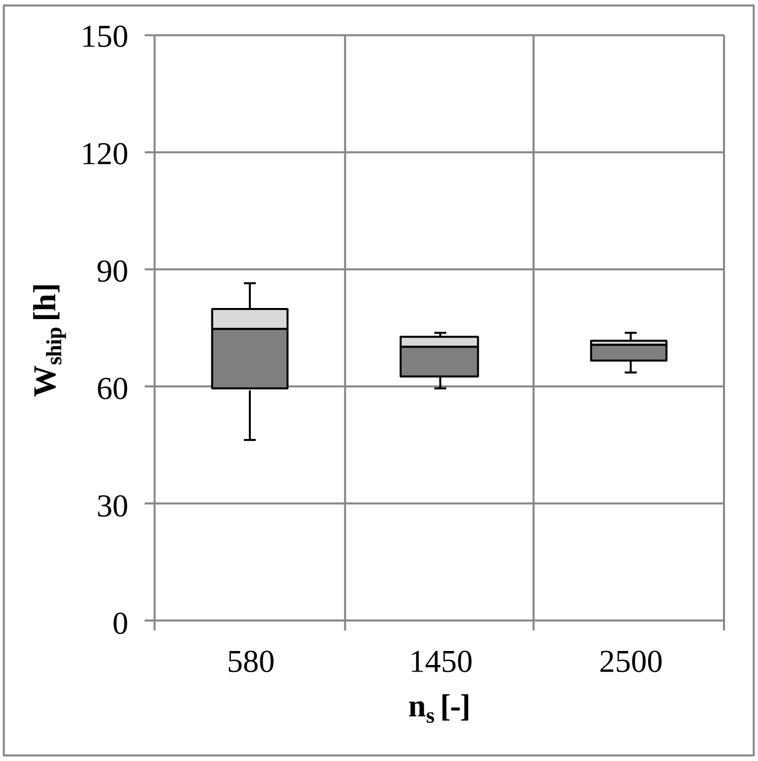

Figure 3.22: Determination of the number of ships per simulation run and the accuracy of the average ship port time determined for a specific case as shown in Figure 3.24A

For the required accuracy of the average ship port time, it was assumed that a run time is acceptable when the standard deviation of the average ship port time is within the 5%. The dispersion of the measured data for the different numbers of ships is shown in Figure 3.22 and the average, minimum and maximum ship port times for the ten replications are listed in Table 3.10. Also the standard deviations (StDev) for the average values and the standard deviation as percentage of the average ship port times are listed in Table 3.10. From Table 3.10 it can be concluded that when a simulation run of 2,500 ships is used, the standard deviation of the average ship port time is within the 5%. For the experimental results and the case study in this chapter, input files that contain 2,500 ships are applied.

Table 3.10: Accuracy of the average ship port time for different number of ships with ten replications

n_s [-]	W_{ship} [h]	$W_{ship-min}$ [h]	$W_{ship-max}$ [h]	StDev [h]	StDev in [%] of W_{ship}
580	74.8	59.5	87.1	7.9	10.6
1,450	69.4	62.8	74.2	4.2	6.1
2,500	71	67.0	74.0	2.0	2.8

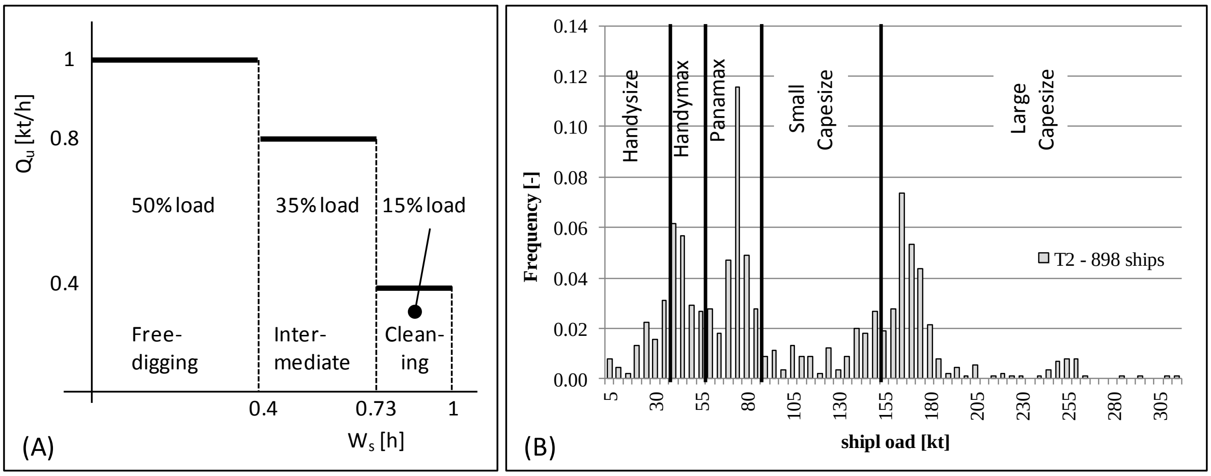

Figure 3.23: Cranes unloading efficiencies (A) and the shipload distribution (B) based on historical data from terminal T2

3.7.2 Discrete or continuous quay layout

Two different quay layouts were investigated; the discrete quay layout and the continuous quay layout. These quay layouts were introduced and shown in Figure 3.7. From both layouts the average ship port time was determined by varying annual throughput between 25 and 50 [Mt/y]. The results are shown in Figure 3.24A. When the continuous quay layout will be applied, ships were unloaded by multiple cranes which results in a reduced average ship port time.

For both layouts, the required quay length was determined. For the discrete quay, the required quay length is four times the maximum ship length (which was: 322 [m]) plus an extra safety distance for secure berthing of ships (assumed in this study: 20 [m]). The required quay length becomes for the discrete quay layout 1,368 meter to enable that all ships can moor at each berth.

For the continuous quay layout, the occupied quay length was registered during the simulation runs. The occupied quay length for 98% of the cases that at least one ship was moored at the quay was assumed as sufficient. This means that in 2% of the cases a ship has to wait before being serviced due to the lack of available quay length. Figure 3.24B shows the 98^{th} percentile of the total occupied quay length versus the annual throughput. From this figure it can be concluded that less quay length is claimed when the continuous quay layout is applied. Furthermore, a reduction of the annual throughput leads to a reduction of the quay length occupied during time. The explanation for the equal values of the occupied quay length from an annual throughput larger than 41 [Mt/y] is that it did not happen that four ships, with maximum ship length, berth at the same time during simulation.

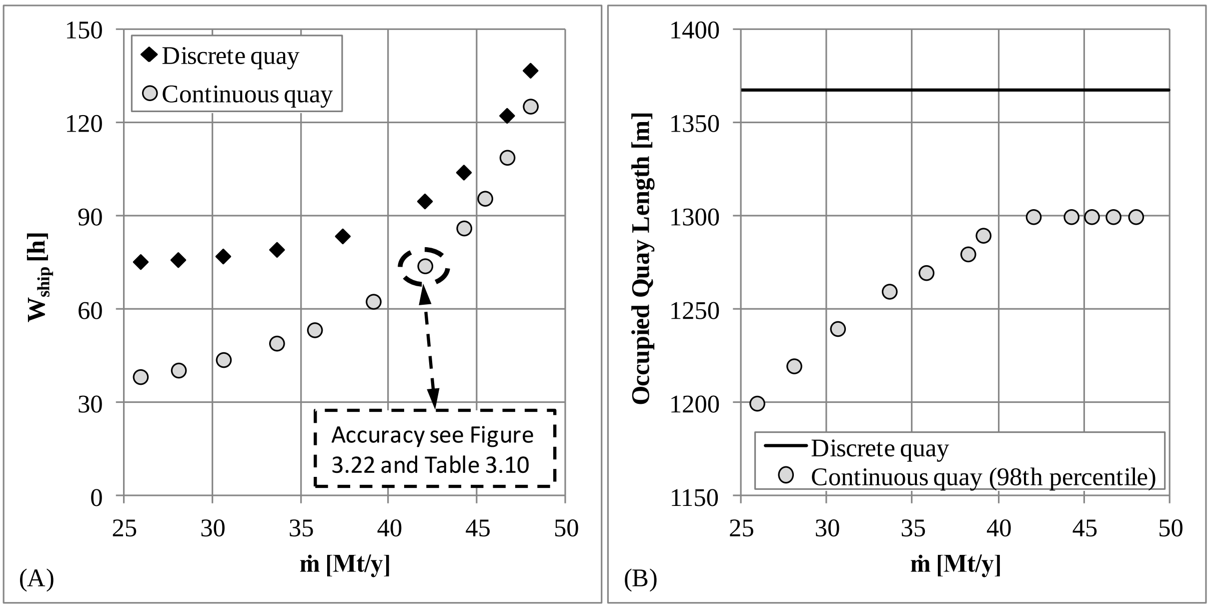

Figure 3.24: Average ship port time versus the annual throughput (A) and the occupied quay length (B) for two quay layouts

3.7.3 Water depth limitation

The realization and maintenance of large water depths alongside the quay are expensive. Experiments were performed to investigate the increase of the average ship port time when not each berth contains sufficient water depth that all ships can be moored. The maximum ships draft of the generated ships was registered. From these drafts a cumulative distribution function was derived that is shown in Figure 3.25B. The maximum ship's draft was 20 [m]. A scenario was evaluated where at two berths, only ships with a maximum draft of 15 [m] can moor. From Figure 3.25B, it can be determined that at least 40% of the total ships can only moor at the deep water berths (with a draft up to 20 meter). For this scenario the average ship port time was determined and presented as "*Draft limit"* in Figure 3.25A. From this figure it can be concluded that for the evaluated scenario a limitation of the water depth at two berths will only increase the average ship port time for high values of the annual throughput.

3.7.4 Quay conveyor transportation rate

When multiple cranes can be used to unload a ship and these cranes transfer material to a single quay conveyor, the transportation rate of this conveyor may limit the ship's unloading rate. The impact of the belt conveyor transportation rate on the average ship port time was investigated for two scenarios. In the first scenario, the conveyors' transportation rates were increased from 2.5 [kt/h] to 4 [kt/h] to study the possible reduction of the average ship port time. In Figure 3.26A the results are shown. As expected, an increase of the transportation rates leads to a reduction of the average ship port time. For example, for an annual throughput of 39 [Mt/y] the average ship port time decreased with 13%.

For a second and third scenario, the number of quay conveyors was reduced from four to three. For the second scenario the conveyors' transportation rates remained 2.5 [kt/h]. For the third scenario these rate were increased to 4 [kt/h]. For both scenarios the average ship port times were determined and are shown together with the already determined results for four quay conveyors with a transportation rate of 2.5 [kt/h] in Figure 3.26B (*Qqcv = 2.5 [kt/h] (4x)*). As expected, the average ship port time increased when the number of quay conveyor decreases.

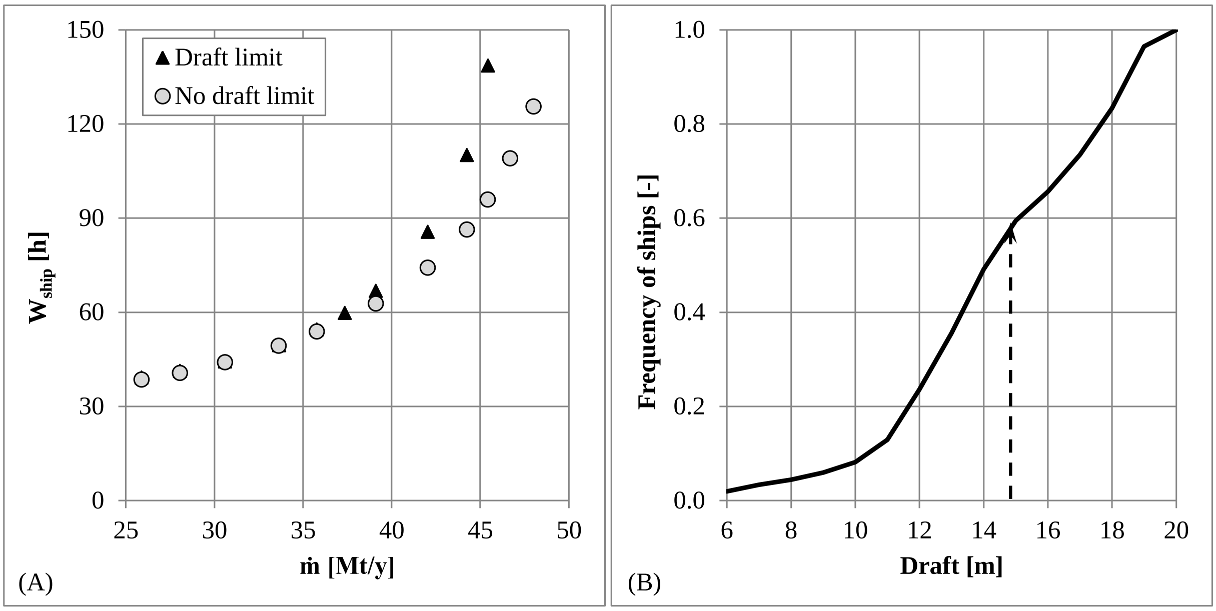

Figure 3.25: Average ship port time versus the annual throughput as function of the draft limitation (A) and the cumulative ship's draft distribution (B)

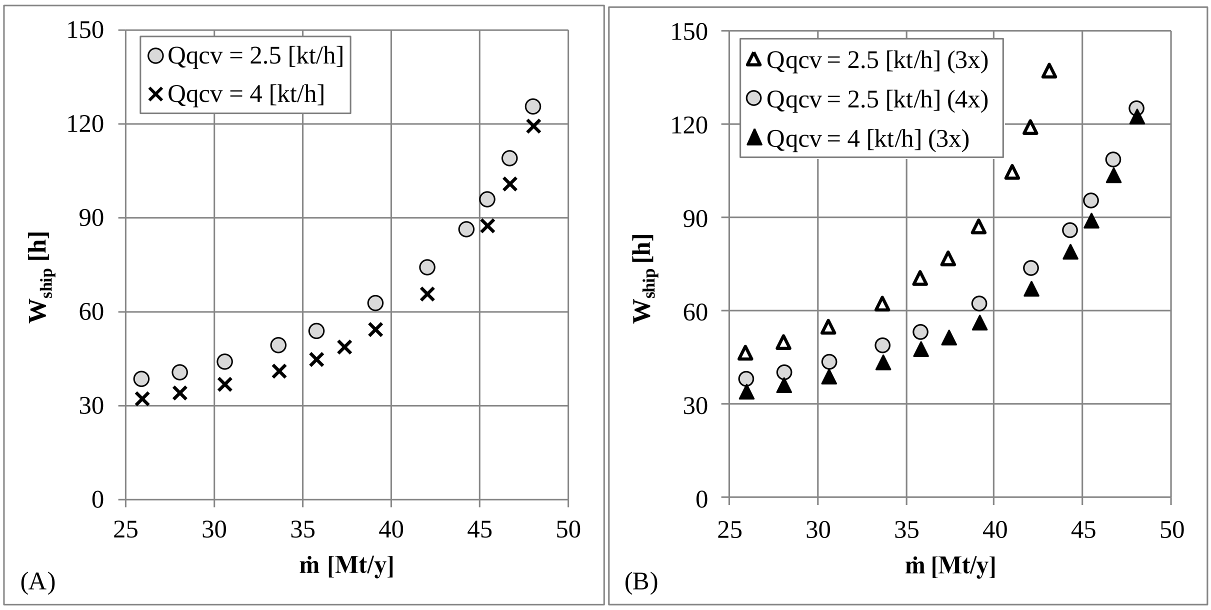

Figure 3.26: Average ship port time versus the annual throughput for an increase of the conveyors transportation rate (A) and a decrease of the number of quay conveyors (B)

When the transportation rate for three quay conveyors was increased to 4 [kt/h], the average ship port time can be reduced compared to installing four quay conveyors with a rate of 2.5 [kt/h]. The reduction of the average ship port time can be explained by the sums of the transportation rates. Note that for the increased transportation capacity of the quay conveyors, the other belt conveyors and stockyard machines require also a capacity of 4 [kt/h].

3.8 Case study: quay side redesign

A case study was defined to demonstrate the use of the simulation model. For an import terminal the terminal's seaside must be redesigned to facilitate an expected growing cargo flow. Projections for the expected growing cargo flow vary but the most optimistic scenario shows an increase of the terminal's annual throughput to 45 [Mt/y]. Currently, the terminal operator realizes for an annual throughput of 32 [Mt/y] an adequate service, expressed in an average ship port time of 75 hours, to ship-owners and industrial clients. This average ship port time may not be increased in the future to prevent that industrial clients select competing terminal operators to handle and store their materials.

In Table 3.11 the main characteristics for the terminal under study are listed. The terminal operator already applied the continuous quay operation and planned to retain the existing cranes and quay conveyors. Furthermore, it was assumed that the actual interarrival time distribution and shipload distribution will remain the same in future. From Table 3.11 it can be learned that ships with a draft more than 18 meter can only moor at one berth. Currently, cranes with different unloading capacities are used. The same input file as introduced in section 3.7.1, which contained 2,500 ships, was used to represent the ship arrival process.

To facilitate the expected cargo flows, the following redesign options were considered; install an extra quay conveyor and/or an extra crane and increase the water depth of all berths to 23 meter resulting that all ships can then moor at each berth. The simulation model was used to quantify the impact of these redesign options and to investigate if the average ship port time of maximum 75 hours could still be guaranteed for the increased annual throughput. From the redesign options, several quay layouts were defined. These layouts were based on the actual layout with extra equipment or an increased water depth. In Table 3.12 layouts characteristics are listed. For each layout the average ship port time as function of the annual throughput was determined. The results are shown in Figure 3.27A.

Table 3.11: Terminal characteristics

Parameter	Value	Unit	Parameter	Value	Unit
Number of berths	4	[-]	Maximum draft alongside the quay	3 berths: 18 and 1 berth: 23	[m]
Number of cranes	4	[-]	Cranes unloading rate (Q_c)	2 cranes: 1.4 and 2 cranes: 2	[kt/h]
Number of quay conveyors	3	[-]	Quay conveyor transportation rate (Q_{qcv})	2.5	[kt/h]
Quay length	1,350	[m]	Unloading efficiencies	See Figure 3.23A	
Ship interarrival time distribution	NED	[-]	Shipload distribution	See Figure 3.23B	
Cranes setup time	0.5	[h]	Average shipload	103	[kt]

Table 3.12: Characteristics of the investigated quay layouts

Layout	Characteristics
Actual	Actual layout, details see Table 3.11
A	Actual layout with an extra quay conveyor (Q_{qcv}: 2.5 [kt/h]) and no draft limitation
B	Actual layout with an extra quay conveyor (Q_{qcv}: 2.5 [kt/h]) and an extra crane (Q_c: 2 [kt/h])
C	Actual layout with an extra quay conveyor (Q_{qcv}: 2.5 [kt/h]), an extra crane (Q_c: 2 [kt/h]) and no draft limitation

From Figure 3.27A it can be learned that the annual throughput of 32 [Mt/y] can be increased to approximately 34 [Mt/y] when layout A will be used still guaranteeing the average ship port time of maximum 75 hours. Furthermore, this figure shows that an increase of the annual throughput to 45 [Mt/y] is only possible when an extra crane and an extra quay conveyor will be installed and when all berths are deepened to 23 meters (layout C).

The average ship port times versus the annual throughputs are shown as single results in Figure 3.27A. Each point represents the average value of the port times of individual ships. The histogram shown in Figure 3.27B shows the variation of the individual ship port times for the specific case when the actual layout was applied and an annual throughput of 34 [Mt/y] (see the circled result in Figure 3.27A). The large variation of the individual ship port times can be explained by the variation in shiploads, the waiting time of ships (some ships do not have to wait while others have to wait several days) and the use of cranes during unloading.

Using the simulation model to determine the average ship port time as function of the annual throughput for several scenarios enables the terminal operator to quantify each design option and to select an appropriate design to facilitate the handling of the expected annual throughput. In this case, layout C, where an extra quay conveyor and an extra crane are added to the actual layout and where all ships can moor at each berth, is needed to handle the 45 [Mt/y]. It is expected that this maximum annual throughput will not be reached in one year; layouts A and B can be used for the definition of the intermediate design stages.

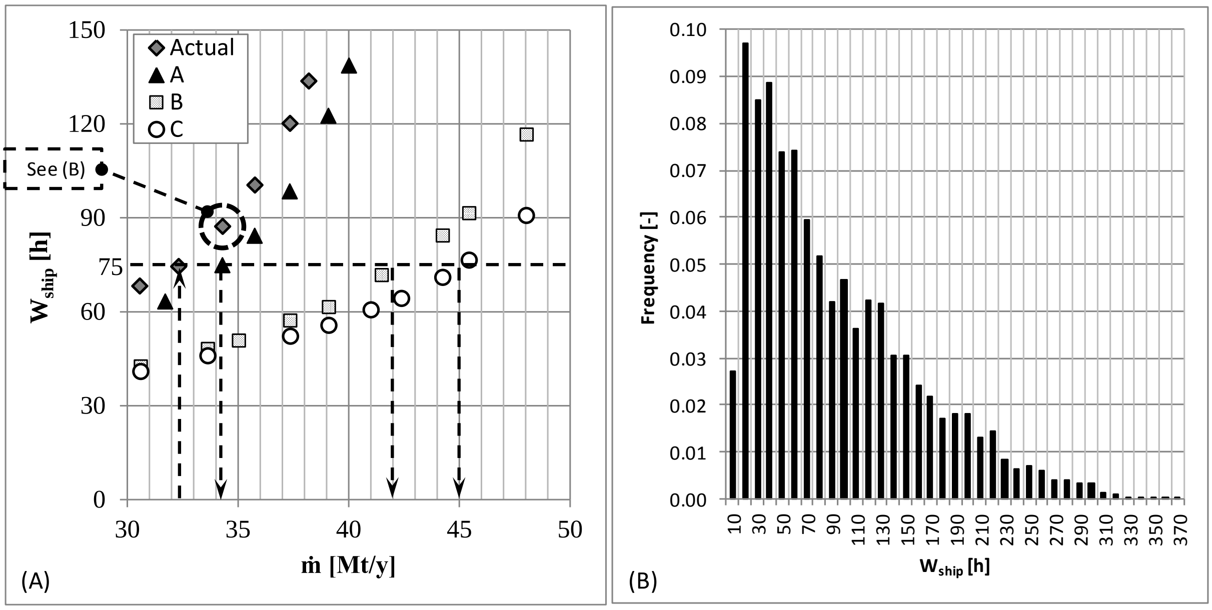

Figure 3.27: Average ship port time versus the annual throughput for several quay layouts (layout characteristics are mentioned in Table 3.12) in (A) and (B) shows a histogram of the individual ship port times for the circled result in (A)

3.9 Conclusions

Quays and cranes are expensive assets and a correct dimensioning is crucial. Bulk ships' characteristics are required for an accurate specification of the berth's length, berth's water depth and quay cranes' outreach. The number of berths, the number of cranes and the cranes' and quay conveyors' capacities must be selected in such a way that a predestined average ship port time can be guaranteed.

The analysis of ship unloading data has shown that the ship unloading rate relates to the ship's deadweight, the shipload to be serviced and the use and capacity of the cranes during the unloading operation. Parameters like the number of grades and the number of holds did not contribute significantly to the estimation of the unloading rate.

Modeling the seaside operation is needed for the selection of the handling capacity required. Although many researchers discussed the modeling of the seaside operation for container terminals, dry bulk terminals have received significant less attention in literature. Models developed for container terminals can be used but should be adapted to the typical bulk handling characteristics for crane assignment, crane productivity, material transportation and dedicated stockyard operational procedures.

Real-world stochastic variations of the interarrival and service times do hardly correspond with proposed distributions. Furthermore, regularities between measured distributions and terminal type were not discovered. A seaside simulation model was developed to model the terminal's seaside and to evaluate the continuous quay operation when cranes serve ships at multiple berths, the hindrance of the crane's handling due to a limited number and capacity of quay conveyors, the limitation of mooring ships at berths with insufficient water depth and the variation of the cranes' capacity during (un)loading of ships.

When the variation of the stochastic processes increases equipment with higher capacities should be installed to meet the predefined quay performance. When the continuous quay layout is applied cranes and berths are better utilized and less quay length is needed compared to the discrete quay layout. A partly limitation of the water depth will decrease the quay performance especially for higher values of the berth occupancy and the quay conveyors transportation rate must be selected such that cranes are hardly hindered, even during the free-digging stage of unloading. The seaside model developed is used in a case study to evaluate several seaside designs to increase the quay's annual throughput without exceeding a predestined average ship port time.

For the expansion of the design methods concerning the terminal's seaside, the following additions are formulated based on the research performed in this chapter:

1. The continuous quay layout, when cranes move alongside the quay to service multiple ships, is preferred to the discrete quay layout. This operation will result in reduced quay length required and higher cranes utilizations.
2. The specification of the water depth alongside the quay should be made taken into account the ships that have to be serviced and the probability that a number of the large ships will call at the same time.
3. Due to the impact of stochastic variations on the quay side design, use historical disturbances to represent the ship interarrival times and shiploads. When there is no historical data available, determine the sensitity when different analytical distributions (e.g., NED, Erlang-2, Weibull or Gamma) are used and discuss the results with terminal operators.
4. For the selection of the number and capacity of the quay conveyors, make the trade-off that either each crane has its own quay conveyor or reduce the number of quay conveyors and allows that several cranes can dump material onto the same quay conveyor. The capacity per quay conveyor should probably be increased to meet the service demands required.

4 Landside operation and machine specification

In this chapter the determination of the number and capacity of (un)loading machines for serving the landside transportation modalities and the machines' locations at the terminal are investigated. Characteristics from inland ships and freight trains are determined to realize accurate landside designs. Comparable to the terminal's seaside the handling capacity installed of the landside depends strongly on the stochastic variations in inland ships' and trains' interarrival times and service times. Real-world distributions for these stochastic processes are analyzed and compared with analytical distributions. This analysis has shown that the measured distributions can hardly be represented by analytical distributions. Using empirical distributions will result in more accurate landside designs. The simulation model developed in chapter 3 was used in a case study to select railcar unloading machines at an export terminal.

4.1 Introduction

At the terminal's landside multiple transportation modalities are generally applied to deliver or export dry bulk materials. Figure 4.1 shows a schematic representation of common used landside connections. Railcars coupled in freight trains are generally used for the transport over long distances between mines and terminals. When industrial clients are not directly located near import terminals, trains and (inland) ships realize the transportation of materials to the industrial clients. Belt conveyors are used to transport materials over short distances, generally less than five kilometers although there are also systems with lengths more than 20 kilometers.

For the transport of bulk materials from mines to export terminals, overseas customers assign freight forwarders. These agents assign a number of rolling-stocks (locomotives and railcars) which are lined up empty at marshalling rail yards in ports pending on the allocation of the mine. The trains traverse and arrive at specified mines, load the material, return to the port and unload at the export terminal where the material is stacked in stockpiles. The shipment can start after all required material is stacked (Kozan and Liu, 2012).

For import terminals, freight forwarders receive orders from industrial clients to deliver material at a predefined time at their facilities. The freight forwarder defines the train's journey time and determines in consultation with terminal operators when railcars must be loaded. Just before the loading time, the empty railcars are railed from the marshalling yard to the terminal. After loading, the train is railed to the industrial client, unloaded and returned to the marshalling yard. When inland ships are used, the requested loading time is reported by freight forwarders to terminal operators a couple of days before loading. The terminal operator schedules the loading to be performed during a specific working shift, which lasts for example eight hours. Before the working shift starts the inland ship must be moored at the loading berth. The terminal operator has some flexibility to perform loading during the shift. Empty coastal ships wait offshore before being loaded. When material is transported using belt conveyors, agreements are generally made about the time when materials have to be delivered to prevent a running out of stock at the client's facility.

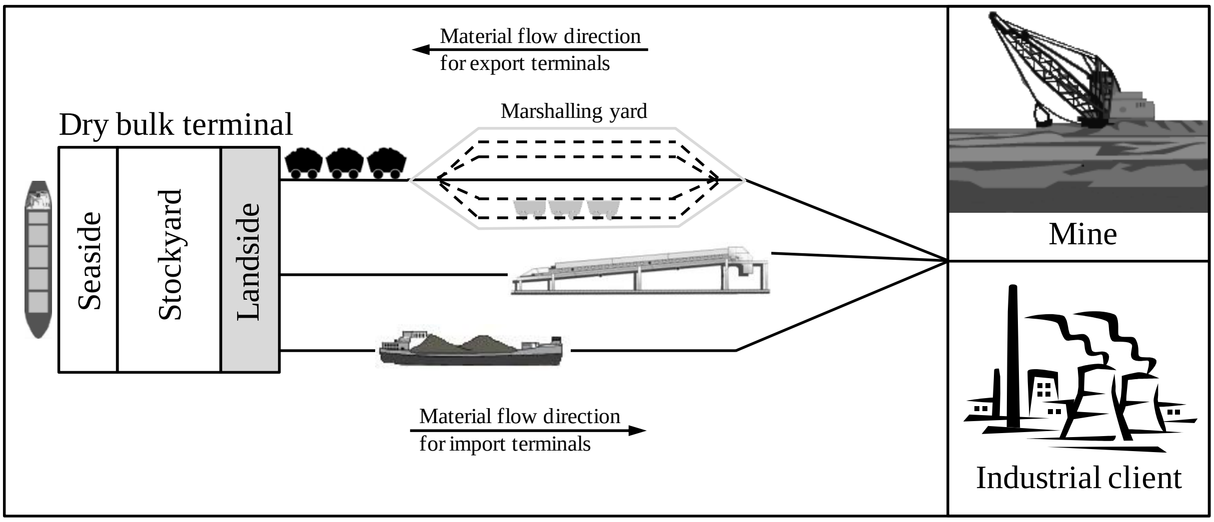

Figure 4.1: Transport between the terminal's landside, mines and industrial clients

In this chapter the specification and selection of landside machines is addressed. In this research the landside design is limited by the determination of the number and capacity of the (un)loading machines and their locations at the terminal. In section 4.2 the main characteristics of the landside operation are presented. Several papers that discussed the landside operational scheduling are reviewed in section 4.3. Measured distributions of the interarrival and service times are investigated and compared with analytical distributions in section 4.4. The impact of using analytical distributions to represent the interarrival and service times instead of measured distributions is addressed in section 4.5. A case study where unloading machines at an export terminal are specified is presented in section 4.6. Finally, the conclusions are presented in section 4.7.

4.2 Characteristics of the landside operation

In most countries, shippers have access to rail, in fewer countries they have access to the sea, and in a very few countries they have access to inland shipping (Bontekoning et al., 2004). For long distances and when river delivery is possible, barge delivery is usually the most practical mode with the lowest cost per ton kilometer (McCartney, 1996). However, recent trends show that despite having extensive river networks, rail transport is becoming more and more popular. Probably due to the global climate change the water depth in the rivers will vary more frequently in future. Industrial clients located upstream are asking for shorter delivery times and a higher delivery reliability, which can better be achieved by rail transport.

4.2.1 Inland ships

Inland shipping is applied in for example Western-Europe (Rhine and Maas River), United States (Mississippi and Ohio River) and China (Yangtze River and Yellow River). In Europe, inland ships and barges (see for an example Figure 4.2) pushed by tug boats are used for the inland river transport. In the United States only convoys of barges are used. More and more inland shipping is developed in upcoming economies like Brazil, India, and Venezuela. General characteristics for inland ships and barges are listed in Table 4.1.

Table 4.1: Main characteristics of inland ships and barges

	Europe[1]	China[2]	United States[3]
Length [m]	39 – 140	35 – 75	59.4 – 60.9
Beam [m]	5 – 15	3.5 – 16	10.7
Draft [m]	2.5 – 4	1.3 – 3.5	3.6 – 4.3
Load [kt]	0.25 – 3	0.3 – 3	1.9 – 2.1
Maximum number of barges in pushed convoys [-]	6	16	40

[1] Based on the CEMT-classification originated from 1992 (Conférence Européenne des Ministres des Transports)
[2] Based on regulations published in 2004 from the Ministry of Transport of the People's Republic of China
[3] Derived from 4490 barges which are listed in the barge register of the Ingram barge company (https://www.ingrambarge.com)

4.2.2 Barge (un)loading machines

For barge loading continuous loading machines are used in general. Figure 4.2 shows a barge loader that can move alongside the quay. Continuous loaders generally consist of a portal and a boom that can be raised or lowered. Bulk materials are fed to this machine using belt conveyors and dumped through a telescopic loading chute into barges. To fill the barge over its entire length, the barge may move alongside the quay (barge hauling system) or the loading machine moves. For unloading barges two primary machine types exist; grab unloaders or continuous bucket unloaders (see Figure 4.3). Grab unloaders have already been discussed in section 3.2.2. In the continuous bucket unloader, buckets are dragged through the material in the barge and are emptied after passing the discharge sprout (McCartney, 1996).

Barge (un)loading machines are generally installed at dedicated quays to prevent hindering the servicing of deep sea bulk ships. The draft of barges is limited and deep berths are not needed.

4.2.3 Rail transport

Railcars can be classified based on their discharge functionality. Hopper cars (made from steel or aluminum) must be unloaded by rotary car dumpers (Figure 4.5). Rotary car dumpers are also called tipplers. Other railcars use self-discharging side doors or bottom discharge doors to unload. The maximum carrying capacity (payload) varies between 65 and 115 tons per railcar. The total length of dry bulk trains varies per country. In Western-Europe and India the maximum length is 700 [m] but in Australia the maximum train length can even reach 2,500 [m] (Theis, 2009).

Figure 4.2: Barge loading machine (Courtesy of EECV)

Figure 4.3: Continuous bucket unloader at the Bontang coal terminal (Courtesy of ThyssenKrupp)

4.2.4 Railcar (un)loading machines

For railcar loading and unloading, a certain capacity must be installed to realize a specified turnaround time. According McCartney (1996), tariff agreements for most coal train operations in the United States specify that the turnaround time onsite may not exceed a fixed period, usually 4 hours, to avoid incurring monetary penalties.

In railcar loading machines (Figure 4.4) material is conveyed up and stored temporarily in a silo above the loading position. One of the used loading systems is based on batch-weighing. Batches are pre-weighed in hoppers before being transferred into railcars. Using this method, trains can be loaded with high loading rates (even up to 13 [kt/h]) with sufficient accuracy to avoid overloading railcars or preventing railcars to be significantly underutilized. It has been demonstrated that the amount of material transferred into weigh bins can be controlled within the 0.5% of the desired weight. Another loading method is volumetric loading. A railcar is positioned under a single silo and its weight is constantly measured using a weighbridge (Walker and Miller, 2004).

Figure 4.4: Railcar loading machines (Courtesy of EMO BV)

Railcar unloading machines have to be selected based on the railcar type. The selection for the railcar has to depend on the haul distance combined with climate conditions. Railcars subject to freezing are easier to unload when top dumped (McCartney, 1996). In bottom dump unloaders, railcars are positioned individually over an unloading hopper and the discharge doors are opened. A car shaker, which is a heavy vibrating mass or a robotic wagon vibrator (Morrison, 2009) can be placed in contact with the railcar. The flow out of the railcar will be improved especially when the material is wet or frozen (McCartney, 1996). Rotary car dumpers use top dumping with either flat bottom railcars or hopper cars. Railcars coupled with rotary couplers allow unloading without uncoupling. An automatic (electric or hydraulic powered) train positioner moves the coupled railcars through the dumper and positions automatically each railcar. This railcar is then rotated over the centerline of the coupling to 140 – 160 degrees before the material flows out (McCartney, 1996).

Figure 4.5: Rail cars unloading at the Richards Bay coal terminal (Courtesy of RBCT)

The rail network layout at dry bulk terminals can be designed in different ways. Balloon loops allow trains to reverse direction without shunting or even stopping. Advantages are a continuous operation and an easy passage of arriving and leaving trains. A disadvantage is that a balloon loop needs a lot of space because trains cannot make sharp turns. Furthermore, driving of trains produce noise in balloon loops as well as wear on wheels and rails. An alternative is realizing a stub rail with sufficient free length to park the train (or a part of the train) after being serviced. After shunting, the train passes the (un)loader in reverse direction or uses a bypass track to pass the (un)loading machine. Advantages are the minimum space requirement and the minimal noise level. Disadvantages are the production losses, the extra (un)locking actions of locomotives, the hindrance of arriving and leaving trains and the eventual compilation of train sets afterwards.

4.2.5 Truck transport

At mines, haul trucks are used for the transport of dry bulk material from excavators to the storage area. These huge trucks (the payload per truck can even exceed 350 tons) are not allowed to enter the public roads. The maximum road truck payload is limited by regulations which differ per country. For example, in Europe the maximum truck weight is limited to 50 tons. According McCartney (1996) highway trucks are used to transport coal between mines and moderate to small coal-fired power plants within a range of 80 kilometers. Trucks can be loaded from above using wheel loaders, silos, hoppers or batch-weighing loading machines. Trucks for coal transportation are generally rear dumpers or bottom dumpers. The material is unloaded into hoppers or directly onto stockpiles (McCartney, 1996).

4.3 Landside transport operation: a literature review

An accurate landside operation is crucial for terminal operators. A delay can result in a too late delivery of materials at clients' facilities, which may affect the terminal reputation and reduce the terminal attractiveness for freight forwarders. Next to the limited number of research papers that discussed explicitly the dry bulk terminal's landside operation, research papers that discuss the barge and rail operation of containers will be reviewed as well.

4.3.1 Barge operation

In some papers the optimum barge fleet was determined or barge assignment procedures were discussed. O'Brien and Crane (1959) presented results of a study that considered the scheduling of a barge line. The barge company used four tugs and a large number of barges for the inland shipping of coal in the United States. A Monte Carlo simulation was used to determine the optimum barge fleet using four tugboats. Vukadinović and Teodorović (1994) developed a model using fuzzy logic for the decision making process concerning the number of barges left at or taken from ports. Swedish (1998) used a discrete-event simulation model for the determination of the proper fleet size for the transport of coal from several mines to multiple distribution sites. The simulation model developed could also be used to assess allocation methods for barges to tugboats. Taylor et al. (2005) presented a simulation-based barge scheduling model to assist in barge dispatching and tug boat assignment problems for inland waterways. The simulation model developed was implemented at a barge line generating optimized barge schedules.

Some research papers discussed the barge scheduling for container transport. Douma et al. (2009) considered the alignment of barge rotations (sequence of terminal visits) with the quay schedules of container terminals in the port of Rotterdam. Each barge has to make a rotation along several terminals to (un)load containers. However, there is no central trusted party that coordinates the activities for both terminal operators and shippers because terminal operators and shippers want to stay autonomous and do not like to share information that possible undermines their competitive position. The authors proposed a multi-agent method using the maximum time that a barge has to wait until it will be serviced. This research was extended by considering the cooperation of the terminal operators on the efficiency of the barge alignment process in Douma et al. (2011). The paper provided possibilities to improve the barge scheduling process.

4.3.2 Rail operation

Many research papers discussed the scheduling of railway operations, see for example the extensive overview of Narayanaswami and Rangaraj (2001). Only a limited number of papers discussed the rail operation of freight trains loaded with dry bulk materials. Kozan and Liu (2012) proposed a demand-responsive decision support system by integrating the operations of coal shipment, coal stockpiles and coal railing from mines to ports into one system. Trains from different railway tracks were treated as critical resources in a cyclic-job-shop-scheduling environment with multiple resources and blocking constraints. An integrated train-stockpile-ship timetable was created and optimized for improving the overall efficiency of the transportation system. The authors claimed that the methodology proposed will provide better decision making on assigning rail rolling-stock. The integration of train timetabling and stockyard management in an export terminal was also discussed by Abdekhodaee et al. (2004). These authors used discrete event simulation to demonstrate the potential improvement.

Leech (2012) proposed for export terminals two rail operation modes: regular railing to dedicated stockpiles or scheduled railing to cargo assembled stockpiles. For regular railing the stockyard acts as a buffer between the relatively constant mining process and the irregular shipping operation. This approach tends to higher storage ratios. For scheduled railing the transportation is scheduled to meet the arrival of the ship. The potential downside for this mode is the greater level of complexity in the rail operation planning and the greater demand for rail rolling stock. The storage ratio tends to be smaller.

4.3.3 Evaluation of modeling approaches

To deliver an acceptable service to industrial clients and freight forwarders the number and capacity of the landside machines must be specified carefully by taking the stochastic arrival and service processes into account. Available literature about inland shipping discussed mainly the determination of the correct fleet size and barge scheduling protocols for assigning barges to tugboats. A limited number of papers addresses the railing of dry bulk materials. Some papers propose the integration of the rail operation with the terminal operation to prevent large ship waiting times.

Measured distributions for the landside interarrival and service times have to be investigated and will be compared with analytical distributions. If these real-world distributions correspond with analytical distributions, analytical distributions can be used to determine the number and capacity required for the landside equipment. If not, empirical distributions must be applied and in accordance to other authors (e.g., Swedish (1998), Taylor et al. (2005) and Abdekhodaee et al. (2004)) simulation can be used to realize more accurate designs.

4.4 Landside stochastic distributions

This section evaluates the distributions needed as input for simulation to assess landside designs. In section 4.4.1, the interarrival time distributions of landside transportation modalities are discussed and in section 4.4.2, the service time distributions for these modalities are presented.

4.4.1 Interarrival time distributions

There were no papers found that suggest distribution types for the interarrival times of cargo trains at dry bulk terminals. A limited number of papers elucidates the interarrival time distribution for passenger trains. Burkolter (2005) proposed an exponential distribution to represent the train arrivals at basic infrastructure elements like switches. Grubor et al. (2013) analyzed the regional railway traffic in Serbia. Passenger trains operate according to a planned timetable. However, the interarrival times of freight trains show stochastic variation and these trains do not operate according to the predefined timetable. The authors proposed an exponential distribution to represent the interarrival times of freight trains.

The dry bulk terminals T2, T3 and T4 provided operational data of their landside arrival processes. These datasets were used to determine real-world distributions. It was assumed that trains were immediately served after arriving at the terminal. In Figure 4.6 and 4.7 the measured interarrival time distributions are presented.

Terminals T2 and T4 are both multi-user import terminals but the train interarrival time distributions (Figure 4.6A and Figure 4.7) show differences. These differences can be explained by the number of railcar loaders installed. At terminal T2, three railcar loaders allow a simultaneously loading of rail cars. At terminal T4 one railcar loader is installed. Terminal T3 is an export terminal. From T3’s train interarrival time distribution (see Figure

4.6B) it can be concluded that the train arrival process is more or less scheduled (regular railing mode). The majority of the trains arrive between 4 and 6 hours after the previous ones. However, due to loading delays at mines or disturbances during railing over around 800 kilometers, stochastic variation is introduced.

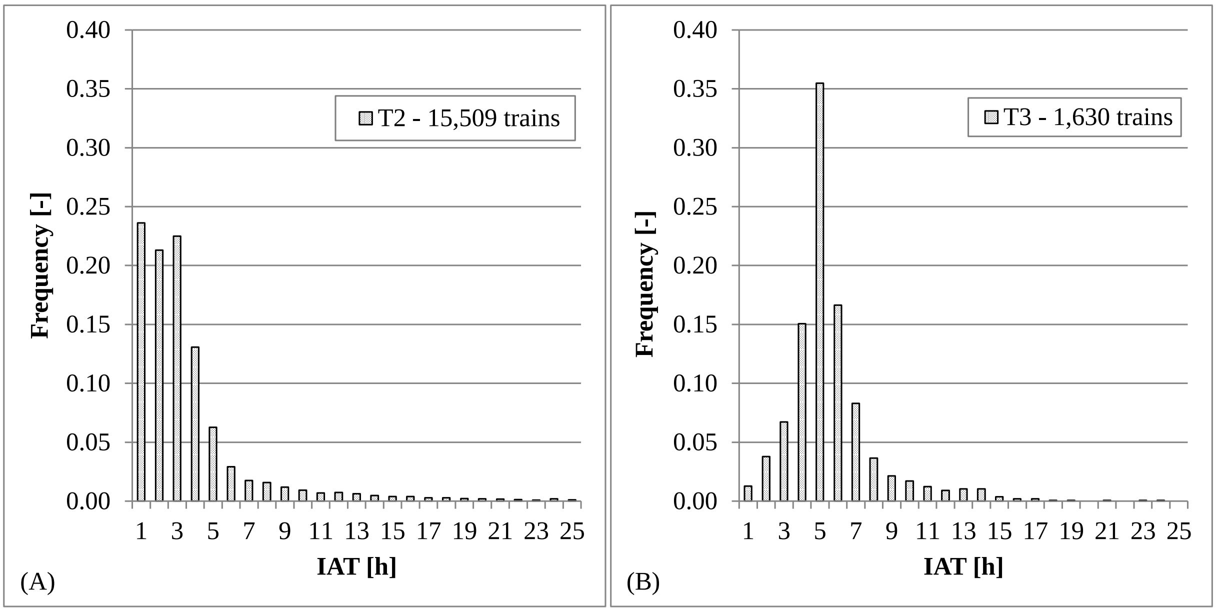

Figure 4.6: Measured interarrival time distributions for train arrivals at terminals T2 (A) and T3 (B)

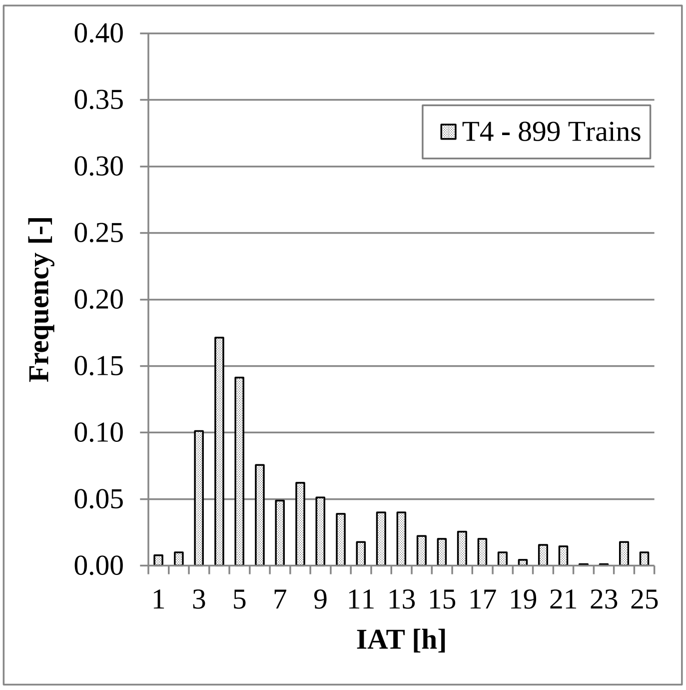

Figure 4.7: Measured interarrival time distribution for train arrivals at terminal T4

At import terminals T2 and T4 inland ships, coastal ships and belt conveyors are also used to transport materials from the stockyard to industrial clients. Appendix C shows the measured interarrival time distributions for these modalities. In accordance to the previous chapter the chi-square test was applied to check if the measured distributions match with one or more of the following analytical distributions: the negative exponential distribution, Erlang-k, Normal, Beta, Gamma and Weibull. Results for the distribution type fit are listed in Table 4.2. From this table it can be concluded that only the measured interarrival time distribution for coastal ships at T2 can be represented by one of the investigated distributions because only for this measured distribution the chi-square value (χ^2) is less than the critical chi-square value ($\chi^2_{0.05}$).

Table 4.2: Results for the interarrival time distribution fit (figures that start with the annotation C are shown in Appendix C)

	Transportation modality	Figure	n_s [-]	Best fitted distribution	χ^2 [-]	$\chi^2_{0.05}$ [-]
T2	Trains	4.6A	15,509	NED	2005	36.42
	Inland ships	C.1A	18,393	NED	2464	36.42
	Coastal ships	C.3	663	NED	31.42	42.56
	Belt conveyors	C.2A	409	NED	324	36.42
T3	Trains	4.6B	1,630	Normal	1952	28.85
T4	Trains	4.7	899	Erlang-2	291	43.19
	Inland ships	C.1B	1,209	NED	83.97	37.65
	Belt conveyors	C.2B	233	Erlang-2	240	19.68

4.4.2 Service time distributions

No papers were found that propose distribution types for the landside service times at dry bulk terminals. From the terminals of the previous section, service time distributions were derived for each transportation modality. For trains the measured service time distributions are shown in Figure 4.8 and 4.9. For the remaining transportation modalities the measured distributions are shown in Appendix C.

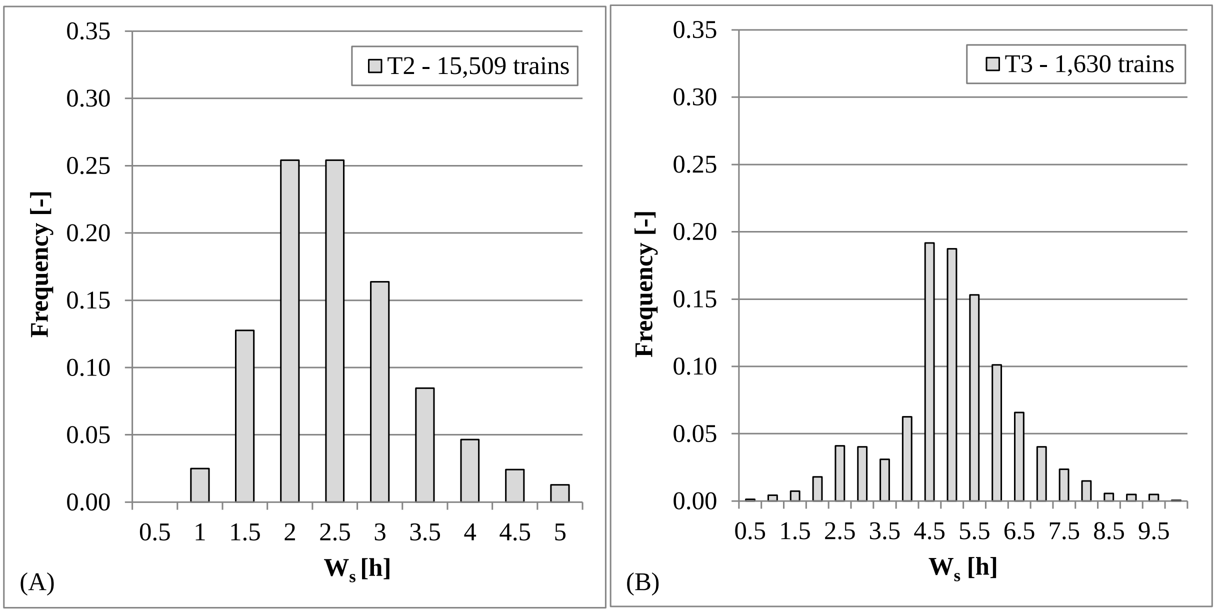

Figure 4.8: Measured train service time distributions for terminals T2 (A) and T3 (B)

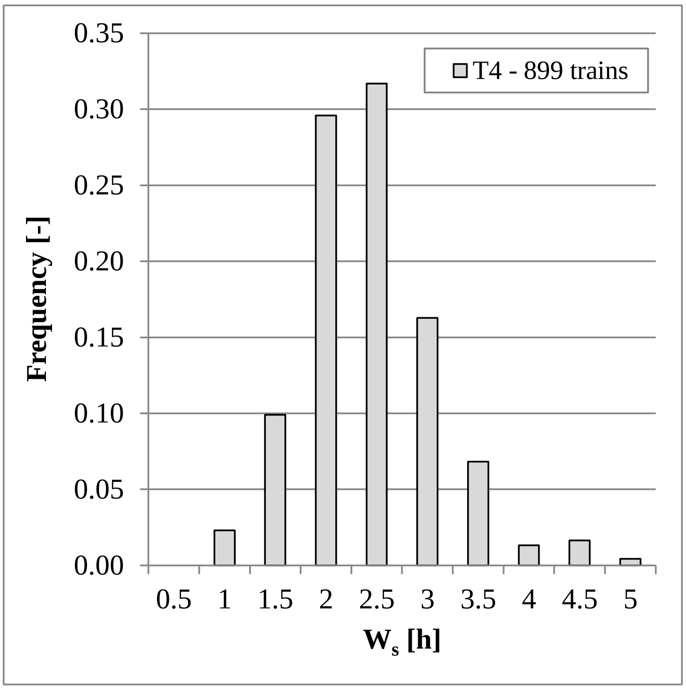

Figure 4.9: Measured train service time distribution for terminal T4

The chi-square test was also applied to check the potential fit of the service time distributions for measured landside transportation modalities with following, generally accepted in terminal seaside modeling, analytical distributions; the negative exponential distribution, Erlang-k, Normal, Beta, Gamma and Weibull. Results for the distribution fit are listed in Table 4.3. In this table also the average service times (W_s) and the average load per transportation mode is listed. From Table 4.3, it can be learned that only the measured service time distributions for the transport of bulk materials to the coal-fired plants using belt conveyors can be represented by one of the investigated analytical distributions. For both terminals the chi-square values (χ^2) for the measured distributions are less than the critical chi-square values ($\chi^2_{0.05}$).

Table 4.3: Results for the service time distribution fit (figures that starts with the annotation C are shown in Appendix C)

	Transportation modality	Figure	Best fitted distribution	χ^2 [-]	$\chi^2_{0.05}$ [-]	W_s [h]	Load [kt]
T2	Trains	4.8A	Normal	8461	18.31	3.5	2.8
	Inland ships	C.4A	Erlang-2	1715	18.31	2.8	2.2
	Coastal ships	C.6	Erlang-2	98.69	19.68	47.3	14.3[1]
	Belt conveyors	C.5A	Gamma	11.03	15.51	15.8	12.2
T3	Trains	4.8B	Normal	866	22.36	5.1	9.8
T4	Trains	4.9	Normal	1081	15.51	2.2	2.4
	Inland ships	C.4B	Erlang-2	116	23.68	4.5	2.3
	Belt conveyors	C.5B	Beta	9.80	14.07	6.7	4.9

[1] Note that the average shipload for coastal ships at terminal T2 is relatively low due to the fact that also inland ships were loaded by the loading machine dedicated for coastal ships.

4.5 Using analytical or measured distributions

The impact of using analytical distributions to represent the interarrival and service times instead of using measured distributions is investigated in this section. The simulation model as described in chapter 3 was used. For this analysis the measured data from the train arrival process during 6 years of operation at terminal T2 was used. Figure 4.6A shows the measured interarrival time distribution and in Figure 4.8A the measured service time distribution is presented. From Table 4.2 and Table 4.3 it can be concluded that these measured distributions do not sufficiently fit with the investigated analytical distributions.

The simulation run time required for the seaside model was already determined in section 3.7.1. In this section, it was mentioned that input files that contained 2,500 ships realize a maximum standard deviation around the average ship port time of 2.8%. The input files used in this section and in the case study (as mentioned in the next section) contain more than 15,000 simulation elements (trains). Thanks available large size of the input files sufficiently accurate values will occur.

For a specific case with two servers (representing two railcar unloaders installed) the average train waiting time as function of the inverse of the service rate (W_t [1/μ]) was determined when measured or when analytical distributions were used. For the analytical distributions a negative exponential distribution was applied to represent the trains interarrival times and a normal distribution represents the trains service times. The results are shown in Figure 4.10.

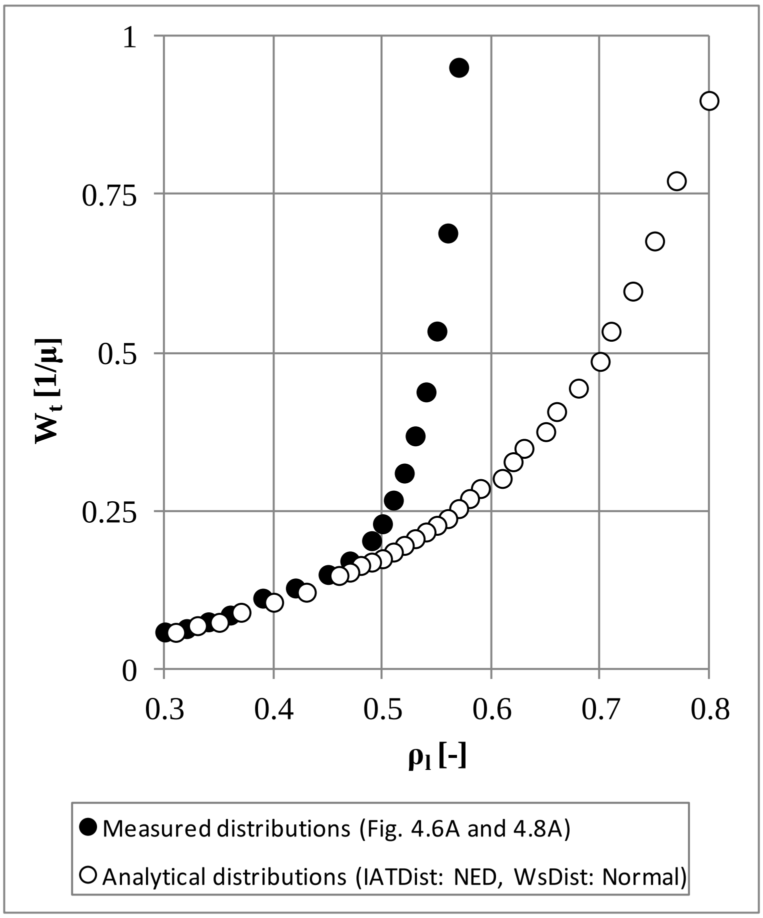

Figure 4.10: The average waiting time as function of the service time versus the landside machines utilization when analytical or measured distributions are used

From Figure 4.10 it can be concluded that for values for the landside machines utilization (ρ_l) higher than 0.5, a difference arises in the performance for both cases. This can be explained by the fact that the measured distributions show more variation than the analytical distributions. Rail car unloaders installed at export terminals show such high utilization values; values of 0.7 are not exceptional. When the capacity for such machines must be specified using analytical distributions will lead to an insufficient capacity specification.

4.6 Case study: selection of railcar unloading machine(s)

A case study was defined to specify railcar unloading machines for an export terminal. This terminal has to be developed in two stages. During the first stage, the terminal has a maximum annual throughput of 6 [Mt/y]. The terminal operator planned to expand later to 15 [Mt/y], the second stage. For the train arrival process it was assumed that the train interarrival times could be represented with the measured distribution of terminal T3 (shown in Figure 4.6B). To represent the train service times, a uniform trainload distribution between 9 and 11 [kt] was assumed and the capacity remains constant during unloading. Furthermore, it was assumed that the technical availability of railcar unloaders was 0.95. The maximum turnaround time of trains in the port should not exceed six hours. In Table 4.4, the input parameters are listed. The simulation model of chapter 3 was used for the determination of the average train port time (W_{train}) [h] as function of the annual throughput. The results are shown in Figure 4.11.

Table 4.4: Input parameters for the case study

Parameter	Value	Unit
Train interarrival time distribution	See Figure 4.6B	
Trainload distribution	Uniform	
Trainload limits	9-11	[kt]
Maximum turnaround time	6	[h]

Figure 4.11 shows for three scenarios the average train port time versus the annual throughput. The first scenario, shown with the series "*Scenario 1: 1x2 [kt/h]*" in Figure 4.11, was defined as a single unloading machine with an unloading capacity of 2 [kt/h]. When this machine will be used, the average train port time does not exceed the 6 hours for an annual throughput of 6 [Mt/y]. However, for the second stage (up to an annual throughput of 15 [Mt/y]) this machine cannot unload trains within the predefined turnaround time.

Another scenario is to install a railcar unloader with an unloading capacity of 3 [kt/h], shown with the series "*Scenario 2: 1x3 [kt/h]*" in Figure 4.11. For this machine, the maximum turnaround time can be realized for both stages. However, a disadvantage is that the transportation rates for the belt conveyors and the stacking rates of the stockyard machines must be increased as well to 3 [kt/h].

The third scenario is to install an extra unloader of 2 [kt/h], shown with the series "*Scenario 3: 2x2 [kt/h]*" in Figure 4.11, for the second stage to realize train unloading within the predefined turnaround time and for an annual throughput of 15 [Mt/y]. For the capacity specification, the rail layout at the terminal must be considered as well. When a stub rail configuration will be used, extra time for shunting (in the order of 30 minutes) must be included in the train port time. The railcar unloader capacity must be increased for the machines with a capacity of 2 [kt/h] to meet the maximum turnaround time.

The final selection must be based on machines capacities determined together with an economic assessment that includes stockyard machines, belt conveyors and infrastructural requirements for the rail layout. Due to the lack of investment costs for for machines and rail infrastucture such economical assessment (for example the Net Present Value approach) is not included in this research.

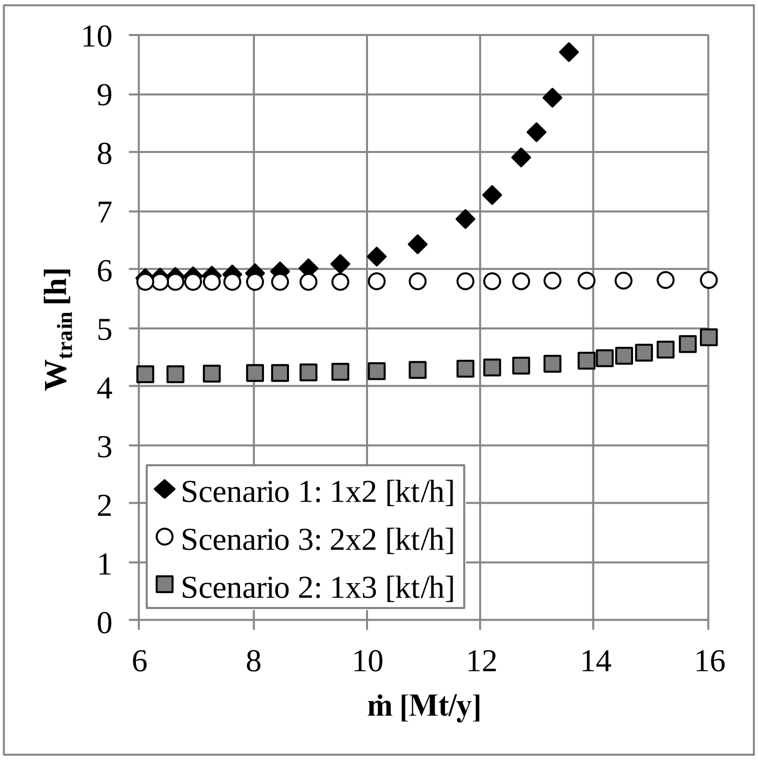

Figure 4.11: Average train port times versus the annual throughput for the three scenarios investigated

4.7 Conclusions

Many transportation modalities are used at the terminal's landside. When river delivery is possible, using inland ships will result in the lowest cost per ton kilometer. However, railing realizes shorter delivery times and a higher delivery reliability. Operational data from three terminals that covered the arrival and service processes of landside transportation modalities was investigated. From this data, distributions were determined. These measured interarrival and service times distributions show hardly a fit with one of the investigated (most commonly proposed) analytical distributions. Especially for higher machines utilization values, using analytical distributions will result in a machine selection with insufficient capacity. The simulation model developed in chapter 3 was used for a specific case to determine the number and capacity for railcar unloading machines at an export terminal. A final selection must be made taking into account the rail layout at the terminal (balloon loop or stub rail) and investments costs for the unloading machines, belt conveyors and stacking equipment.

As an addition for the design methods concerning the terminal's landside:

1. Measured distributions for the interarrival and service times for the landside transportation modalities do show a large variation. Using empirical data is recommended to realize accurate specifications for the number and capacity of landside machines.

5 Stockyard sizing

This chapter is based on van Vianen et al. (2014a).

In this chapter simulation is applied to determine the stockyard size required. To determine the parameters that affect the required storage size, the storage factor was derived analytically. This factor defines the ratio between the annual throughput and the required stockyard size. Simulation is required for stockyard dimensioning when including the stochastic variations in the ship interarrival times, ship sizes and bulk material storage times. In addition, specific operational procedures that potentially increase the storage capacity were investigated. In a case study, the stockyard model developed was applied by sizing the required stockyard area for a specific import terminal.

5.1 Introduction

The dry bulk supply chains typically include a number of transportation processes which are decoupled by buffer storage facilities located at dry bulk terminals in ports (Leech, 2012). These buffers are essential for absorbing unavoidable differences between incoming and outgoing flows of bulk materials (Lodewijks et al., 2009). Due to the large volumes of coal and iron ore and the possibility to store these dry bulk materials in open air, stockyards are generally used. Piles are sprayed with mixtures of water and wax-containing substances to accelerate crust formation on stockpile surfaces and to avoid wind erosion (FAM, 2010). Stockyard sizing is crucial during the (re)design of dry bulk terminals. An undersized stockyard results in excessive ship waiting times and forces terminal operators to pay penalty costs (demurrage) to ship owners. An oversized stockyard obstructs the recovery of the huge investment costs. Figure 5.1 shows an example of a stockyard where dry bulk materials are stored in segregated piles on several stockyard lanes.

In this chapter simulation will be used to determine the required stockyard size. In section 5.2 methodologies for sizing intermediate buffers at dry bulk terminals and related engineering applications like open pit mines, production and processing systems are provided. The analytical derivation of the 'storage factor' as the ratio between the terminal's annual throughput and the required stockyard size is presented in section 5.3. In section 5.4, the simulation-based approach to include the stochastic processes at dry bulk terminals (like the ship arrival process, ship sizes and storage times) in the determination of the required stockyard size is introduced. Simulation results are discussed in section 5.5. Finally, conclusions are presented in section 5.6.

Figure 5.1: A stockyard with lanes and segregated piles (Courtesy of EMO BV)

5.2 Literature review

In essence, the sizing of a stockyard has similarities with the sizing of a warehouse. The scientific literature about inventory theory used for sizing warehouses is immense, see for a literature review Gu et al. (2010). However, a clear method that can be used for sizing the stockyard area of dry bulk terminals is unavailable. This will be further discussed in this section.

5.2.1 Stockyard sizing at dry bulk terminals

At export terminals, stockpiles are assembled from dry bulk material delivered by trains, trucks or belt conveyors from mines. If the stockpile is completely assembled, which takes usually some days, then the pile can be reclaimed from the stockyard and loaded into a bulk ship (Boland et al., 2011). After the sea-voyage, dry bulk materials are unloaded and stacked at the import terminal's stockyard. Here the bulk materials are stored longer in comparison to the export terminals. Storage times of several months are not exceptional. End users, who generally operate coal-fired power plants or steel factories, buy speculative inventory to protect themselves against uncertain demand and store these materials close to their production facilities. Piles are gradually reclaimed from the import terminal in small batches and transported by trains, barges or belt conveyors to industrial clients.

Several authors applied queuing theory to determine the optimal number and size of stockpiles in export terminals (Binkowski et al. (1999), Ayu and Cardew-Hall (2002) and Abdekhodaee et al. (2004)). However, idealized assumptions are required to use the proposed methods. For assigning stockpiles to specific locations in the stockyard, similarities can be found to two-dimensional strip packing problems (Boland et al., 2011). Each stockpile consumes the entire width of a stockyard lane and the required stockpile length depends on its volume. Substantial literature is available about mathematical models and heuristic methods for packing a finite number of rectangles into a limited area see for an overview Lodi et al. (2002). Nevertheless, the stockyard operation is more complex than any of the 2D packing problems considered in literature. The size of stockpiles as a function of time is generally unknown because it depends on the individual pile's storage time and the availability of stockyard machines to reclaim.

Some design guidelines were found for stockyard sizing. In chapter 2 the storage factor was discussed. However, from Figure 2.4 it can be concluded that the storage factors for 49 dry bulk terminals around the world vary considerably per terminal and are significantly higher than the suggested values. Consequently, using the suggested values from Ligteringen and Velsink (2012) will lead to oversized stockyard areas. Lodewijks et al. (2009) suggested a rule-of-thumb that a possible stock of about 10% of the annual throughput seems to be accepted in the dry bulk industry. Kraaijveld van Hemert (1984) suggested that the required storage capacity could be defined by assessing the out of phase of the import fluctuations and consumption fluctuations. A rough assumption for a coal-receiving terminal is a minimum storage capacity of two months of the annual throughput, which equals about 17% of the annual throughput. UNCTAD (1985) provided guidelines for export stockpile dimensioning as a function of the annual throughput and the average shipload. Using this guideline for an annual throughput of 4 million tons and an average shipload of 100,000 tons will result in a stockyard size for 650,000 tons, which is 16% of the annual throughput.

5.2.2 Storage allocation strategies

Different policies for assigning storage locations to piles were introduced by Leech (2010); the cargo assembly mode (CAM) and Identity Preserved (ID). For CAM, materials are stored in piles based on their grade and for the ID-storage policy segregated piles are formed for individual clients. The CAM storage policy, which was called the fixed-facility-location by Umang et al. (2013), is generally applied at export terminals, where materials from a limited number of mines are stored. Stockpile duplication, where for each grade two different locations are reserved, is the key strategy to avoid network utilization conflicts (Leech, 2012). When the ID-storage policy is applied several piles can contain the same grade but the pile owners are different. The ID-storage policy is generally applied at multi-user import terminals where customers' materials have to be stored individually to prevent mixing and to realize material tracking and tracing. The potential downside of the latter storage policy is that it demands a more extended belt conveyor network, the operational planning becomes more complicated and more storage area is required.

Discrete-event simulation was used for an export terminal to study the issue where to store the arriving material (Dipsar and Altiok, 1998). The stockyard has to store two types of ore (wet and dry) and the stockyard operation is driven by the demand from bulk ships. A decision support system for intelligent stockpile building in the ore stockyard of the Ponta da Madeira terminal in Brazil was introduced by Molck et al. (2001). Heuristic search techniques guided by fuzzy evaluation functions were used to select the destination and origin stockpiles.

Robenek et al. (2013) studied the integrated problem of berth allocation and yard assignment in the context of bulk ports. The authors assumed that a cargo type (in their case liquid and dry bulk) is stored at its specific location. According to the authors, the mathematical formulation of the integrated problem was complex. The model developed has to be extended by including the uncertainty in ship arrival times and delays in handling operations due to the breakdown of equipment.

5.2.3 Safety stock at open pit mines

At open pit mines, a safety stock of bulk material is kept to prevent a shortage of material delivery due to the variations in time and quantities between the incoming and outgoing flows. This stock is called safety stock and literature about the determination of safety stock was investigated. At open pit mines the more or less continuous supply from the mines forms the input for the stock and material is exported in portions. Generally, materials are railed from the mines to export terminals and the train departures from mines are usually scheduled. However, due to all kind of disturbances (e.g., delay on return trips) these departure times vary from the scheduled ones.

Computer simulation was used to determine the optimum safety stock of silos at open pit mines (Chu and Ermolowich (1980) and Bradly et al. (1985)). Interactions between silos and the loading and unloading stations were governed by complex operating rules that enforced using simulation. Sarkar and Gunn (1994) formulated the pile scheduling at an open pit mine as a standard integer-programming model and solved this problem using a linear programming package. However, this solution applies for a limited number of piles (in the paper six) but in large-scale import dry bulk terminals hundreds of piles have to be stored at the same time.

5.2.4 Inventory models in operations research

A large number of references in operations research focused on classical inventory models to ensure a designated service level with preferably low inventory; see for an overview Kleijn and Dekker (1999) and Gu et al. (2010). Schmidt et al. (2012) assessed mathematical methods for calculating safety-stock using simulation. Safety-stock can be calculated by multiplying the safety factor, which depends on the required service level based on normal distributed demand, with the standard deviation of this demand during the replenishment time. A mathematical model was presented by Orbán-Mihályko and Lakatos (2004) to determine the size of intermediate storage aiming to buffer the operational differences between batch and continuous subsystems in the processing industry. This paper assumed the arrival of batches as a Poisson process, the batch sizes were also governed by an exponential distribution and to assure a continuous output, a specific reliability level has been considered.

5.2.5 Evaluation and selection of the modeling approach

As stated the sizing of a stockyard has similarities with the sizing of a warehouse. Although many methods were published to determine the size of intermediate buffers in a warehouse, a methodology that can directly be implemented for dry bulk terminals was not found. The position of dry bulk terminals in its supply chain causes the establishment of a strategic stock, which is contrary to the objective of minimizing inventory. Furthermore, several stockyard operations for housekeeping like the relocation of piles and specific terminal characteristics such as pile geometries, the large number and different sizes of grades make it an impossible task to come up with an analytical model.

Stockyard sizing depends on the storage strategy applied. For export terminals (with the CAM-storage policy and limited number of grades) the required area per grade relates to the imbalance between supply and demand. Several solutions exist to prevent a flooding of the stockyard; direct transfer of materials from freight trains directly into bulk ships, or storing materials longer at the mine or storing material temporarily in rail cars. This research focuses on the stockyard sizing for import terminals where materials are stored individually, the ID-storage policy. The storage factor, which is the ratio between the terminal's annual throughput and the total stockyard size, is possibly a powerful guideline for stockyard design. However, research is required to determine correct values that allow its calculation.

5.3 Storage factor

Little's law (1961) can be used for an analytical derivation of the storage factor. This law states that under steady state conditions, the average number of units L in a queuing system equals the average arrival rate λ at which units arrive, multiplied by the average time W units spend in the system, or expressed algebraically:

$$L = \lambda W \tag{5.1}$$

For dry bulk terminals, the number of units L can be interpreted as the average quantity of bulk materials at the terminal C [t]. The average arrival rate can be interpreted as the annual throughput $\dot{m}$ [t/y]. The average time units spend in the system is the average storage time of bulk materials at the stockyard T_s [y]. Note that at container terminals the term dwell time is used to express the time that a container is stacked at a yard. For the case of a dry bulk terminal, equation (5.1) can be reformulated:

$$C = \dot{m} T_s \tag{5.2}$$

The storage factor s expresses the ratio between the terminal's annual throughput and the total storage area A [m^2]. This can be formulated as follows:

$$s = \frac{\dot{m}}{\mathrm{A}} \tag{5.3}$$

The following relation for the storage factor can be derived by combining equations (5.2) and (5.3):

$$s = \frac{C}{A}\frac{1}{T_s} \tag{5.4}$$

Where the ratio C/A [tm^{-2}] indicates the mass per square meter and the second term ($1/T_s$) indicates the number of replenishments per year of dry bulk materials at the stockyard.

For the calculation of the required pile's length on a stockyard lane, the relation between the pile mass and pile geometry is required. UNCTAD (1985) assumed that bulk materials are stored in trapezoidal shapes. However, in practice stockpiles show end cones because of the shear effect of the bulk materials during stacking. In Figure 5.2A a three-dimensional representation of the trapezoidal stockpile with end cones is shown. The perpendicular view and the top view are shown respectively in Figure 5.2B and Figure 5.2C. For the stockpile shape of Figure 5.2, equation (5.5) expresses the relation for the pile's mass algebraically.

$$m = hl\rho\left(w - \frac{h}{\tan(\alpha)}\right) + \frac{1}{3}\rho\pi\left(\frac{h^3}{\tan^2(\alpha)}\right) + \rho h\left(w - \frac{2h}{\tan(\alpha)}\right)\frac{h}{\tan(\alpha)} \tag{5.5}$$

Where m is the pile's mass [t], h is the pile's height [m], which is normally limited by the stacking height of the stacker and/or reclaimer, l is the length of the trapezoidal part [m], ρ is the bulk density [t/m^3], w is the pile's width [m] and α is the material's angle of repose [°].

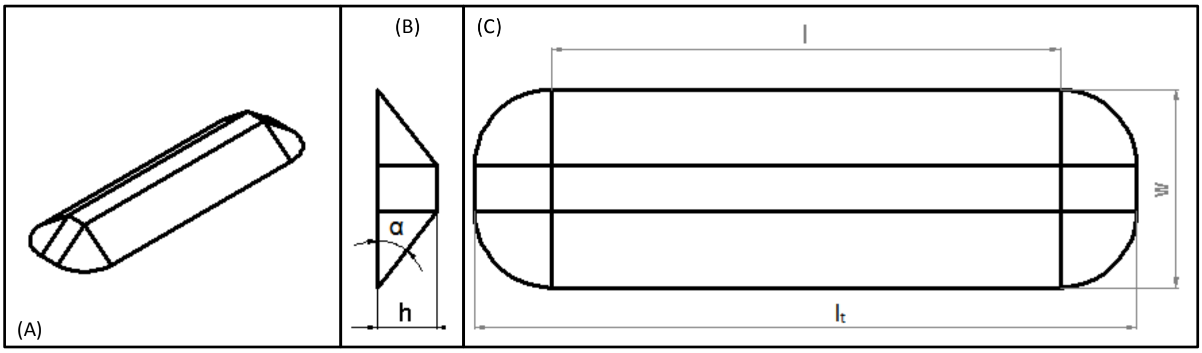

Figure 5.2: Trapezoidal stockpile with end cones

At dry bulk terminals, bulk materials are generally stored in individual piles to prevent contamination and mixing. A clear distinction between different shipments must be realized. Generally, a distance (d) of at least two meters is applied at the stockyard. If more piles are stored at a single lane then the ratio C/A [tm^{-2}] decreases due to the increase of the number of empty spaces. When each pile contains an empty space and all piles are stored over the entire lane width, the ratio C/A can be determined using equation (5.6), where l_t is the total pile's length [m] (see Figure 5.2):

$$\frac{C}{A} = \frac{m}{(l_t + d)w} \tag{5.6}$$

The dependency of C/A on the piles mass and the relation between the piles mass and the storage time (T_S) on the storage factor were investigated and shown in Figure 5.3. The used parameters are listed in Table 5.1.

Table 5.1: Used parameters for the analytical determination of the storage factor

Parameter	Description	Value	Unit
w	Width	60	[m]
h	Height	18	[m]
α	Angle of repose	38	[°]
ρ	Bulk density	0.8	[t/m^3]
d	Separation distance	2	[m]
T_s	Average storage time	0.1 – 0.3	[y]

The ratio C/A decreases significantly for small piles and goes to an asymptotic limit for large-sized piles, see Figure 5.3A. For the input parameters as listed in Table 5.1 the asymptotic limit will be around 8.8 [tm^{-2}].

As expected, the values for the storage factor decrease when the average storage time increases and when the pile's mass decreases, as it is shown in Figure 5.3B. The amount of stored material at the stockyard varies during daily operation due to stochastic variations in ships' interarrival times, ship sizes and piles storage times. The impact of these variations on the required stockyard size cannot be determined analytically. Therefore simulation will be used to take the stochastic processes into account.

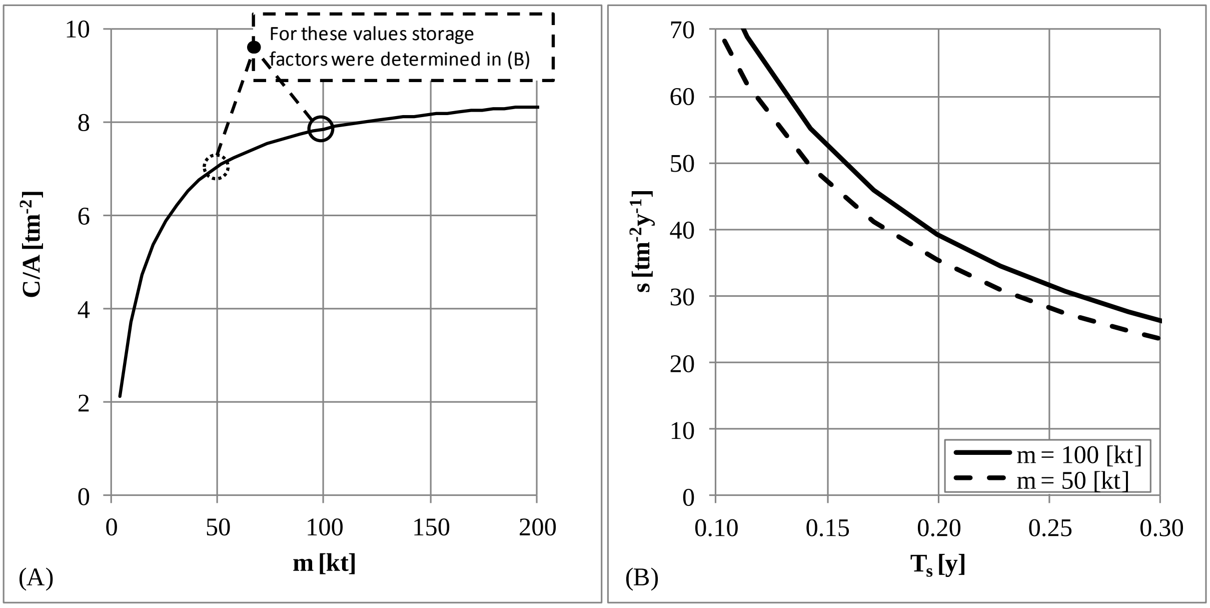

Figure 5.3: Mass per square meter versus pile mass (A) and the storage factor versus the average storage time (B)

5.4 Simulation-based approach

In this section the simulation based approach will be introduced. In section 5.4.1 the simulation model will be discussed. Section 5.4.2 introduces several terminal operational procedures which can be applied to increase the storage capacity. During daily operations several stochastic processes will affect the amount of bulk materials at the stockyard. The ship arrival process was already discussed in chapter 3. The variation in piles storage times will be addressed in section 5.4.3. The verification of the stockyard model is presented in section 5.4.4 and the validation of the simulation model is listed in section 5.4.5.

5.4.1 Stockyard model

The stockyard model was developed to be used for both import and export terminals. In this section the import terminal will be discussed. The cargo flow has the opposite direction for export terminals. A simplified representation of the simulation model is shown in Figure 5.4, where Figure 5.4A shows the main element classes (ship generator, train generator, lane, bulk ships, freight trains and strips). Figure 5.4B shows the queues used in the simulation model and Figure 5.4C shows an example of the progress of the pile's load during the storage time when small batches of material were reclaimed from the stockyard. The pile's storage time differs per pile and is drawn from a storage time distribution. Bulk handling activities are called jobs. At the terminal's landside different transport modalities can be used (trains, inland ships or belt conveyors). In this section, it was assumed that only freight trains are send to the terminal to pick up the material. Specific details for the stockyard model can be found in Appendix D, section D.3.

Queues
The queues used to control the stockyard model are represented in Figure 5.4B. When there is area available to store a newly arrived job, this job is moved into the job queue (JobQ). When there is no area available, jobs are stored temporarily in the job waiting queue (JobWQ). Each lane contains specific queues to store empty strips (MyESQ), full strips (MyFSQ) and all strips (MySQ). Strips are dedicated pieces of stockyard lanes where or material can be stored on (in a pile) or dedicated pieces to realize empty spaces between different piles. Piles stored at the stockyard are moved into a specific queue, the MyPilesQ. Figure 5.4B shows the elements in corresponding queues.

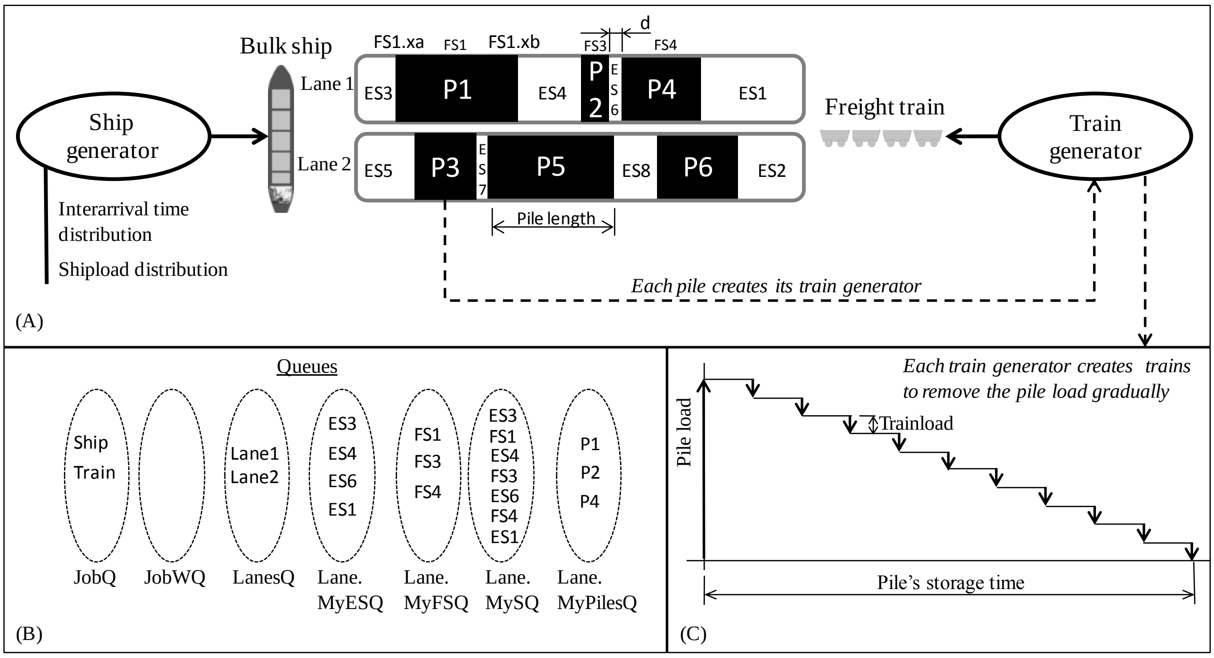

Figure 5.4: Schematic representation of the simulation model (description follows in text)

Ship generator
The ship generator creates ships based on predefined interarrival time distribution and shipload distribution. To store the shipload at the stockyard, the required pile length is determined using equation (5.6). A created ship is put in the JobQ when there is stockyard space available; otherwise this ship is stored in the waiting queue (JobWQ).

Train generator
The train generator generates a number of trains to reclaim the pile in small portions (see Figure 5.4C). The train generator samples the pile's storage time out of the storage time distribution. The pile's storage time is the total time a pile is stored at the stockyard, which is the time between the moment a pile is stacked and the moment that the last tons of material is reclaimed. The number of trains per pile is determined by dividing the ship's load with the maximum trainload (in this case 4 [kt]). The interarrival time between two successive trains is

assumed to be constant and can be determined by dividing the pile's storage time by the number of trains.

Lane

The stockyard is represented by several lanes with specific length and width. The dimensions and pile locations, represented with rectangular full strips (P1 – P6 in Figure 5.4A), are registered. Strips that do not contain materials are called empty strips (ES1 – ES8). By bookkeeping the start positions (xa) and end positions (xb) of the full strips and empty strips, the exact locations and loads of the bulk materials are registered.

Each lane checks one after the other if a new arrived job (ship or train) in the JobQ can be handled. If true, the job is removed from the JobQ. To assign a pile to a specific lane, the pile is moved into the lane's MyPilesQ. A full strip and a new empty strip, which represents the empty space between piles with distance (d), are created. Another empty strip, with sufficient free length is searched and the start and end positions are updated. When a pile is formed at the lane, a train generator is created. If the selected job is a train, the full strip is searched where the requested material is stored and the dimensions and mass are updated. If the remaining mass of the full strip equals zero then this full strip and its left empty strip are removed after leaving the corresponding queues.

5.4.2 Operational procedures to increase the storage capacity

The storage capacity can be increased by distributing the shipload across multiple storage locations, by clearing the pile's area directly when material is reclaimed or by relocating piles.

Shipload splitting

To prevent that ships have to wait until the entire load can be stored in one pile, the shipload can be split in multiple piles enabling distributing material over the stockyard. By the terminal operator of terminal T2 operational data was provided that contains the piles' load after stacking the material at the stockyard. From this data a histogram was composed that shows the frequency of the load per pile (the pile's load represents it size in tons). This histogram is shown in Figure 5.5. Although there is a large variation in pile loads, the maximum pile's load was determined as the 95^{th} percentile of all piles. The 95^{th} percentile of the maximum pile load for coal piles was 105 [kt] and for iron ore piles 175 [kt]. The maximum pile's load is an input parameter in the simulation model.

Clearing pile's area

Two different clearing methods (methods for removing material from piles and clearing the area for new piles) are implemented. In the first method, the pile's area is directly cleared when material is reclaimed and in the second method the pile's area is cleared when the entire pile load is exported. Both methods occur at stockyard operation and relate to the used reclaiming machine. For example, wheel loaders reclaim piles from the front resulting in a decrease of the pile's length each time when material is reclaimed. When rail-mounted bucket wheel reclaimers are used the stockpile is reclaimed layer for layer and the pile's area is cleared when all material is reclaimed (Knappe, 1995).

Relocation of piles

The piles lengths vary due to the variation in shiploads and the pile's area clearing method. When small piles are relocated, large free areas can arise and new incoming material can be stored. However, relocation introduces extra costs for terminal operators because they get only paid for the handling of the material from the seaside to the stockyard and from the stockyard to the hinterland. To minimize these relocation costs, the pile with the least mass must be relocated. Figure 5.6 shows an example of the pile relocation.

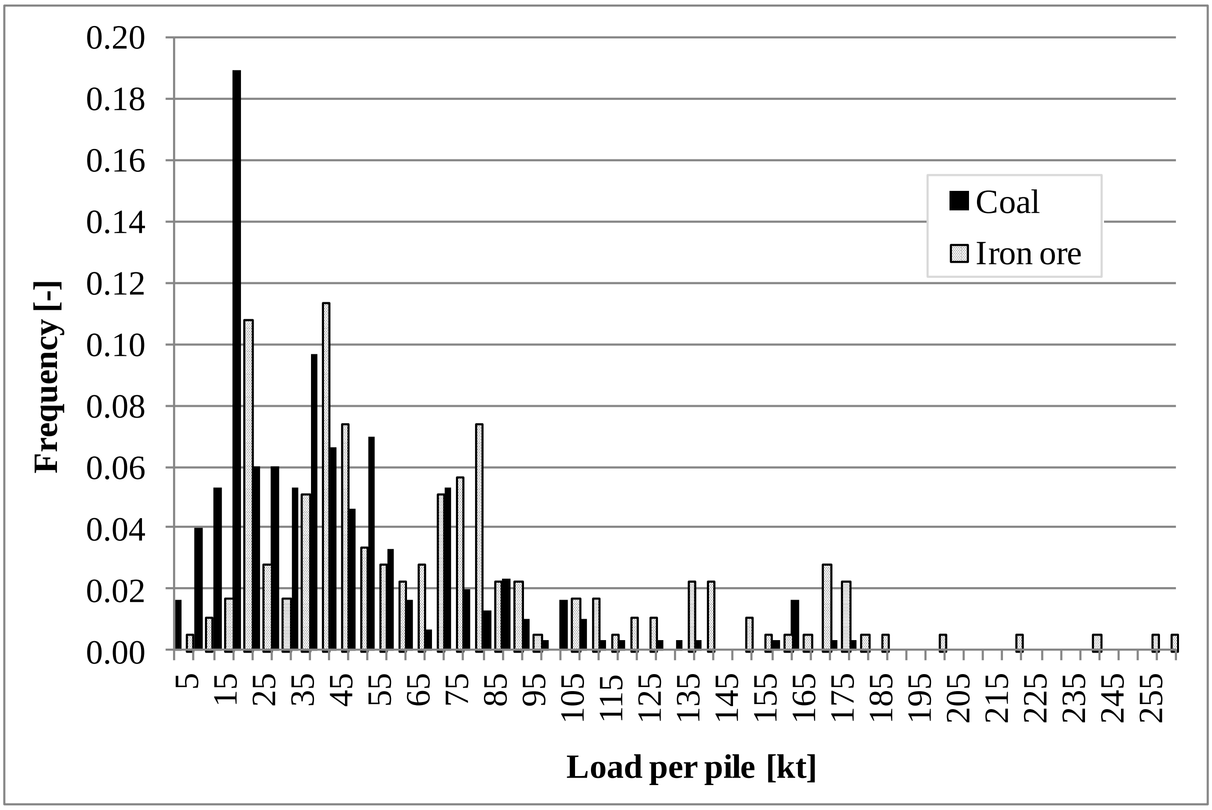

Figure 5.5: Histogram of maximum pile's load for coal and iron ore based on 479 stored piles at the stockyard of terminal T2

In the simulation model the relocation algorithm is implemented as follows:

- Find the piles with masses that do not exceed the predefined value for the maximum tons (e.g., 50 [kt]) to prevent that a too large pile is relocated. In the case as shown in Figure 5.6, piles B and C are candidates to be relocated.
- Detect for these piles the length that comes available at the stockyard. If this length exceeds the required length for the new pile and the relocated pile can be stored somewhere else, put this pile in a separate queue.
- Select the pile that contains the least mass in this queue and relocate this pile. In the case as shown in Figure 5.6, pile B contains less mass than pile C. Pile B will be relocated to realize sufficient free area to store pile A.

5.4.3 Storage time distribution

The average pile's storage time and the storage time distribution were investigated for terminal T2. A storage time distribution was derived from 8,500 piles during nineteen years of operation. Figure 5.7 shows this storage time distribution. The average pile's storage time was 0.2 years. The chi-square test was used to check whether this measured distribution corresponds with an analytical distribution. This distribution fit has shown that the storage time distribution does not fit exactly with an analytical distribution. The distribution type that comes closest was the negative exponential distribution (NED) (χ^2 for the real-world distribution in Figure 5.7: 832.2 [-] and $\chi^2_{0.05}$ for the generalized NED: 101.58 [-]). This distribution type together with an Erlang-2 distribution and a table-type input distribution were implemented in the simulation model. The table-type distribution enables an exact specification of the storage times of the delivered material. When the storage times are unknown on beforehand, one of the generalized distribution types can be used to generate storage times.

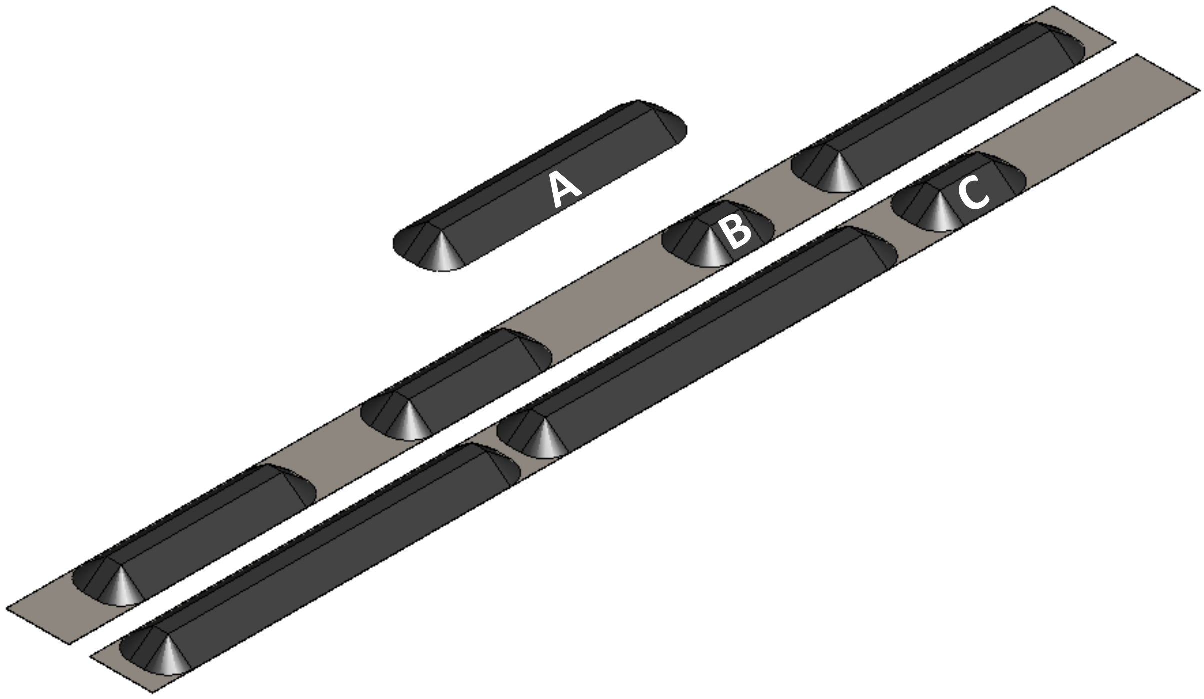

Figure 5.6: Explanation of the pile relocation procedure to realize sufficient length at an empty space to store the materials of pile A

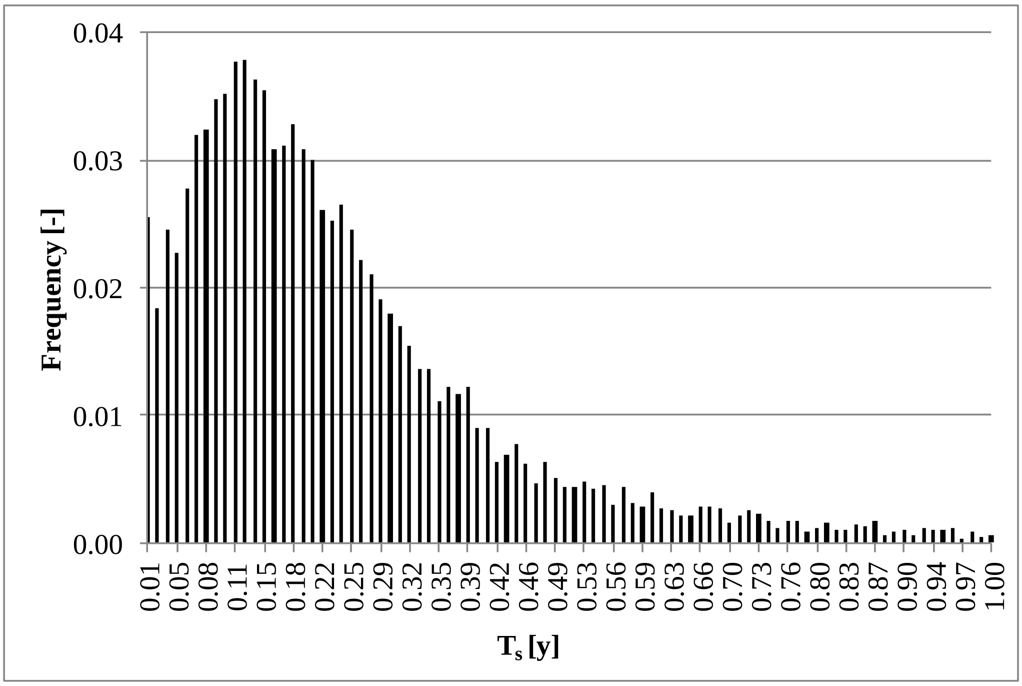

Figure 5.7: Measured storage time distribution for 8,500 piles stored at the stockyard of terminal T2 during nineteen years of operation

5.4.4 Verification

Verification of the stockyard model was realized using the tracing function of TOMAS and by comparing simulation results for the storage factor with analytical determined storage factors. Figure 5.8 shows this comparison where the analytical results, represented by the series "*m = 100 [kt]*", were already shown in Figure 5.3B. The simulation results were retrieved using the input parameters of Table 5.1.

The difference between both series in Figure 5.8 can be explained by the fact that the simulation model uses two stockyard lanes and that the lane length was not a multiple of the pile's length. The entire stockyard area was not fully occupied which leads to a reduction of the storage factors. The ratio between the analytically determined storage factors and the simulated results had an average value of 0.95 (with a standard deviation of 0.003). Although the values are not exactly the same, the trends are identical which indicates that the simulation model gives a satisfactory representation of reality.

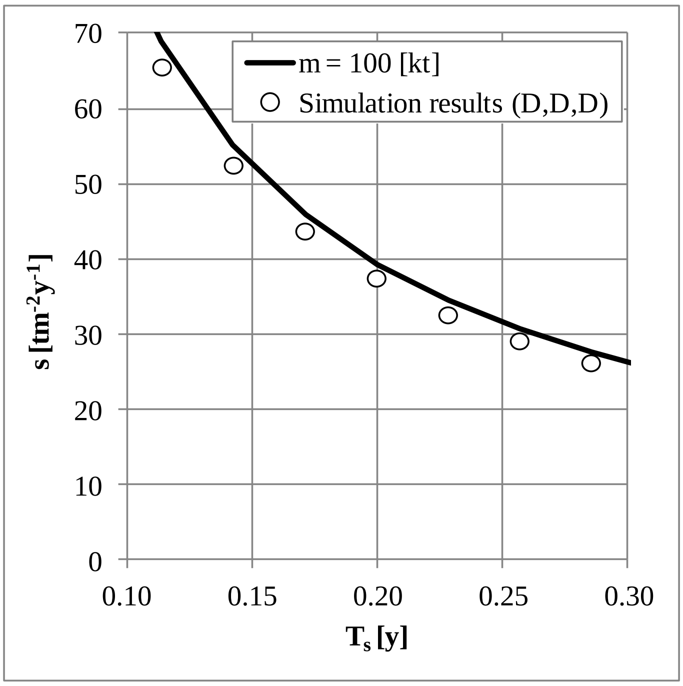

Figure 5.8: Verification of the stockyard model. Simulation results were obtained with deterministic interarrival time, shipload and storage time distribution (D,D,D) to make verification possible

5.4.5 Run control of the stockyard model

The stockyard model is developed to determine the relation between the stockyard area and the annual throughput. The simulation model starts empty, resulting that the first ships that deliver material do not have to wait before delivering their material. However, in real-operations an empty stockyard will not occur. To compensate this difference two options can be selected. The first one is to include a warm up time and starts registering the performance indicators after a certain time (for example, when the stockyard is half full). The second solution is to use a long simulation runtime that the advantage of starting the simulation empty is averaged. In this research, the second option is selected because the moment from where registering must start cannot be determined so easily. For example, start registering after a predefined stored volume will vary the warm up time for small or large stockyards significantly. Moreover, the computational time needed to simulate a relatively large number of simulation elements is minimal; for 2,500 ships the simulation time becomes 35 seconds.

In this section the accuracy of the annual throughput is determined as function of the stochastic variations in ships interarrival times, shiploads and material storage times and by taken the start with an empty stockyard into account. The input parameters for the investigation of the run time required are listed in Table 5.2. Ten replications were applied each containing different seed values to generate ships arrival times, shiploads and piles storage times. For each replication the annual throughput was increased gradually and at the end of the simulation run the average ship waiting time was measured. Subsequently, the maximum value for the annual throughput when the average ship waiting time does not exceed two hours (two hours was selected to specify the transition between waiting and no waiting of ships for area available) was selected. The dispersion of the annual throughputs is presented in boxplots (see Figure 5.9) and average, minimum and maximum values together with standard deviations are listed in Table 5.3.

Table 5.2: Used parameters for the run control of the stockyard model

Parameter	Description	Value	Unit
n_l	Number of lanes	4	[-]
Ll	Stockyard lane length	1,200	[m]
w	Width	60	[m]
h	Height	18	[m]
α	Angle of repose	38	[°]
ρ	Bulk density	0.8	[t/m^3]
d	Separation distance	2	[m]
T_s	Average storage time	0.2	[y]
sl	Average shipload	100	[kt]
IATType	Interarrival time distribution	NED	
SlType	Shipload distribution	Derived from T2 (see Figure 3.21B)	
T_sDist	Storage time distribution	Erlang-2	
StoragePolicy		Identity preserved	

Table 5.3: Accuracy of the average annual throughput for different number of ships with ten replications and a stockyard size of 29 hectares

n_s [-]	$\dot{m}$ [Mt/y]	$\dot{m}_{min}$ [Mt/y]	$\dot{m}_{max}$ [Mt/y]	StDev [Mt/y]	StDev in [%] of $\dot{m}$
300	8.94	6.47	10.87	1.46	16.3
500	8.82	7.59	10.41	0.84	9.5
700	8.79	8.05	9.54	0.42	4.8
900	8.79	8.18	9.18	0.37	4.2
1,100	8.73	8.28	9.33	0.33	3.8
1,500	8.69	8.29	9.11	0.25	2.9
2,500	8.76	8.55	9.13	0.18	2.0

For the required accuracy of the annual throughput in relation to the stockyard area, it was assumed that a number of ships is acceptable when the standard deviation of the average annual throughput is within the 2.5%. The reason for this requirement is that a relatively small stockyard size with limited annual throughput was investigated but this requirement will also result for larger stockyards in accurate values for the average annual throughput.

From Table 5.3 it can be concluded that when a simulation run of 2,500 ships is used, the standard deviation of the average annual throughput is within the 2.5%. For the experimental results and the case study in this chapter, input files that contain this number of ships are used.

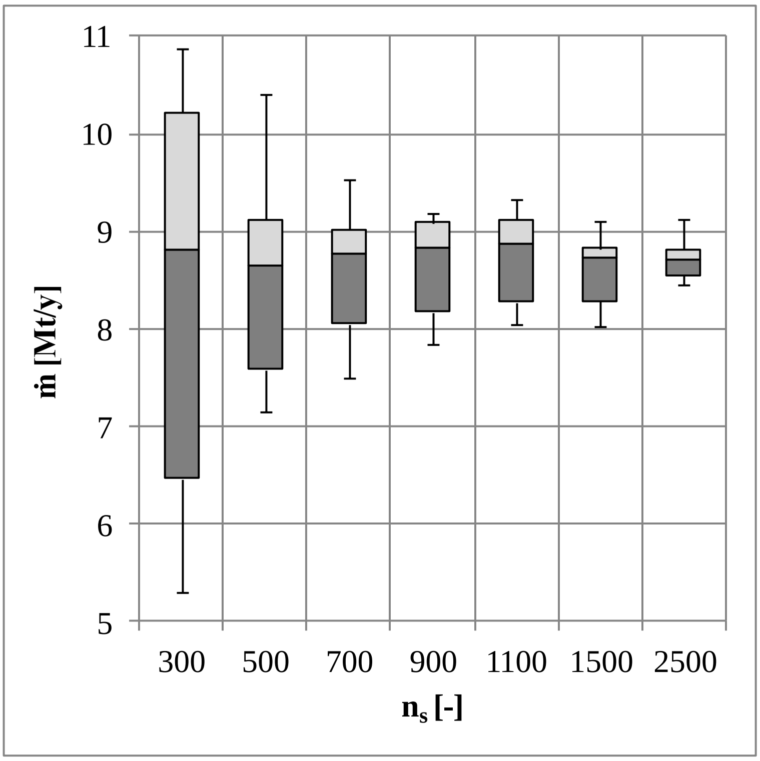

Figure 5.9: Boxplots that display the dispersion of annual throughputs for different number of ships for a stockyard size of 24 hectares

5.4.6 Validation

In this section the stockyard model will be validated by comparing the actual stockyard size of an import terminal (T2) with the outcome of the simulation model. The operational data of the year 2008 was used as input for the simulation model. Table 5.4 shows the input parameters where the annual throughputs for iron ore ($\dot{m}_{iron\ ore}$) and coal ($\dot{m}_{coal}$) represent the material that was supplied and stored at the stockyard. The total terminal's annual throughput exceeds the sum of those two because a relatively large amount of materials (~20%) was directly transferred to the hinterland without being stored.

Figure 5.10 shows the required stockyard size versus the annual throughput per bulk commodity obtained using the simulation model. To facilitate the storage of both bulk commodities, 99±2.5 hectares are required (for coal: 72±1.8 [ha] and for iron ore: 27±0.7 [ha]). When the stockpile's area is cleared for coal stockpiles directly when material is reclaimed (CPA) and when relocation (REL) is applied for coal stockpiles, the stockyard area can be reduced with 20 hectares to 79 hectares.

The stockyard area determined of 99 hectares (with an accuracy of ± 2.5 hectares) has a comparable order of magnitude compared to the actual stockyard size of 110 hectares. An explanation for the deviation is that in the simulation model all piles are stacked until the maximum pile's height and all piles are stacked over the entire lanes' width. In real operations, piles are not always stored over the entire lane's width and piles have different heights. Despite this deviation, the simulation model proves to be useful for stockyard dimensioning.

Table 5.4: Input parameters for the case study

Parameter	Description	Value	Unit
$\dot{m}_{iron\ ore}$	Annual throughput of iron ore	13	[Mt/y]
$\dot{m}_{coal}$	Annual throughput of coal	16	[Mt/y]
$\rho_{iron\ ore}$	Bulk density for iron ore	2.8	[t/m^3]
ρ_{coal}	Bulk density for iron ore	0.8	[t/m^3]
w	Pile's width	90	[m]
h	Pile's height	20	[m]
α	Angle of repose	38	[°]
IATDist	Interarrival time distribution	NED	-
SlDist	Shipload distribution	T2 (see Figure 3.21B)	
T_sDist	Storage time distribution	E2	-
T_s	Average storage time	0.2	[y]

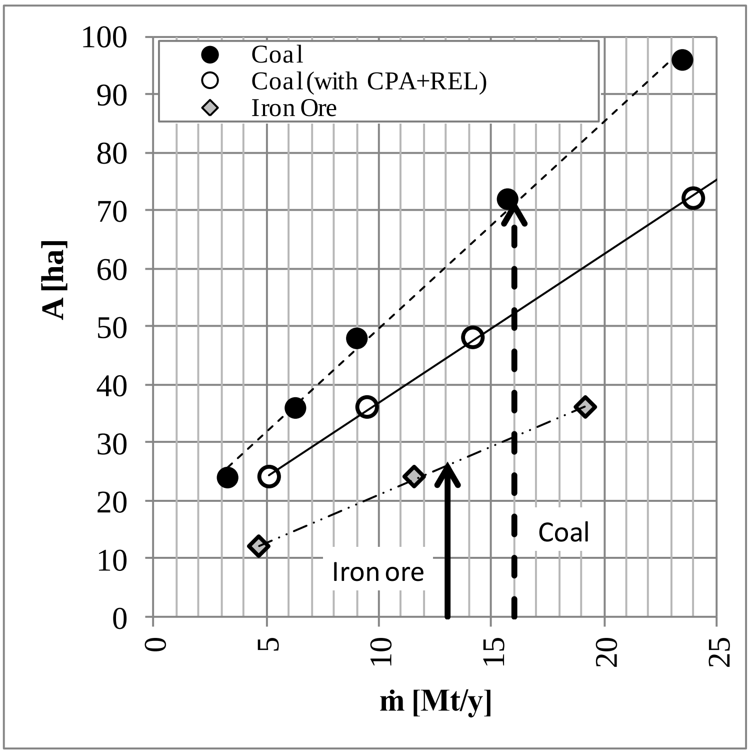

Figure 5.10: Stockyard area needed versus the annual throughput for both bulk commodities and specific operational procedures (CPA and REL)

5.5 Simulation experimental results

The impact of the stochastic processes and the operational procedures of section 5.4.2 were investigated using the stockyard model. The stockyard size required for several cases of stochastic distributions is presented in section 5.5.1 and in section 5.5.2 the reduction of the stockyard size required by applying several operational procedures is discussed. It was assumed that the ship unloading and the loading capacity was selected in such way that ships only have to wait when there is no area available to store the load. For both sections, a specific stockyard of four lanes was defined resulting that four jobs can be served simultaneously. The lane length was varied to achieve different stockyard sizes and the parameters of Table 5.1 were used.

5.5.1 Stochastic processes and stockyard size

Four cases were defined with different combinations for the interarrival times, shipload and storage time distributions. For example, for the series (*NED*, *T2*, *E2)* the ships interarrival times were generated using a negative exponential distribution, the shiploads were based on the empirical shipload distribution from terminal T2 (see Figure 3.21B) and an Erlang-2 distribution was used to represent the storage time distribution. With constant interarrival times, shiploads and storage times (that means no variations); the series is called (D, D, D) (D stands for Deterministic).

Figure 5.11 shows the stockyard area size in hectares versus the annual throughput for the different cases. Linear trend lines, with a coefficient of determination (R^2) of at least 0.99, were drawn between the results to achieve more generic results. As expected, the stockyard area has to be enlarged when the degree of stochastic increases to prevent that ships have to wait.

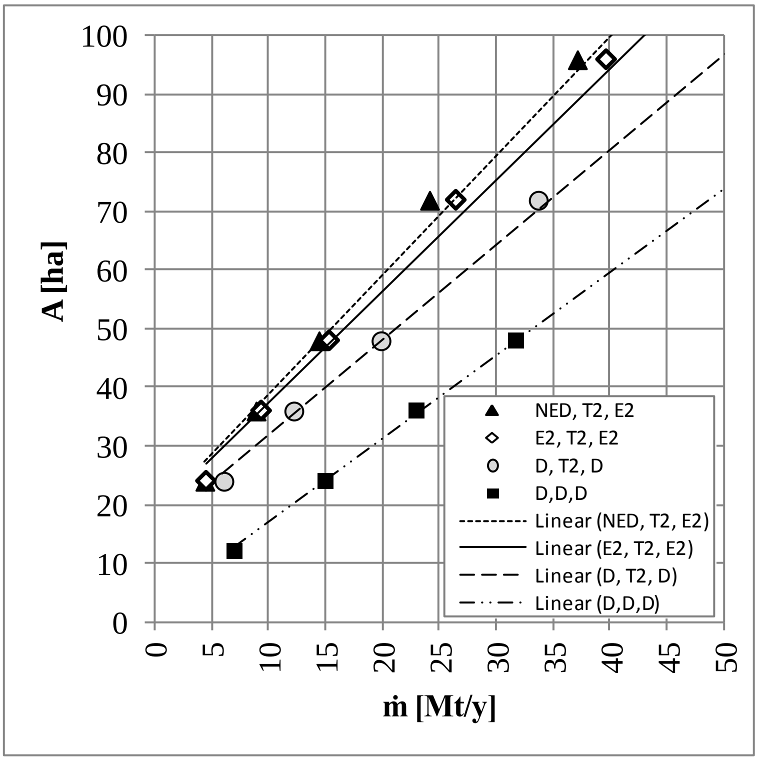

Figure 5.11: Stockyard area versus the annual throughput when no stochastics are involved (D,D,D) and for three different combinations of stochastic distributions (T_s was 0.11 [y])

5.5.2 Operational procedures and stockyard size

It is expected that the stockyard size required can be reduced by applying specific operational procedures like clearing the pile's area (CPA) and relocation (REL). For the CPA-method the pile's area is cleared directly when a portion of material is reclaimed from the pile, see section 5.4.2 for more details. For the REL-method, small piles are relocated in advance when newly arrived material cannot be stored. Figure 5.12 shows for a stockyard of four lanes and a specific combination of stochastic processes (NED, T2, E2), a considerable reduction when the operational procedures (CPA and REL) were used. For example, for an annual throughput of 30 [Mt/y] the stockyard size can be reduced from 80 hectares to 68 hectares 16% using the CPA-method and even to 55 hectares when both CPA-method and REL-method are used. Note that the values mentioned are the average values.

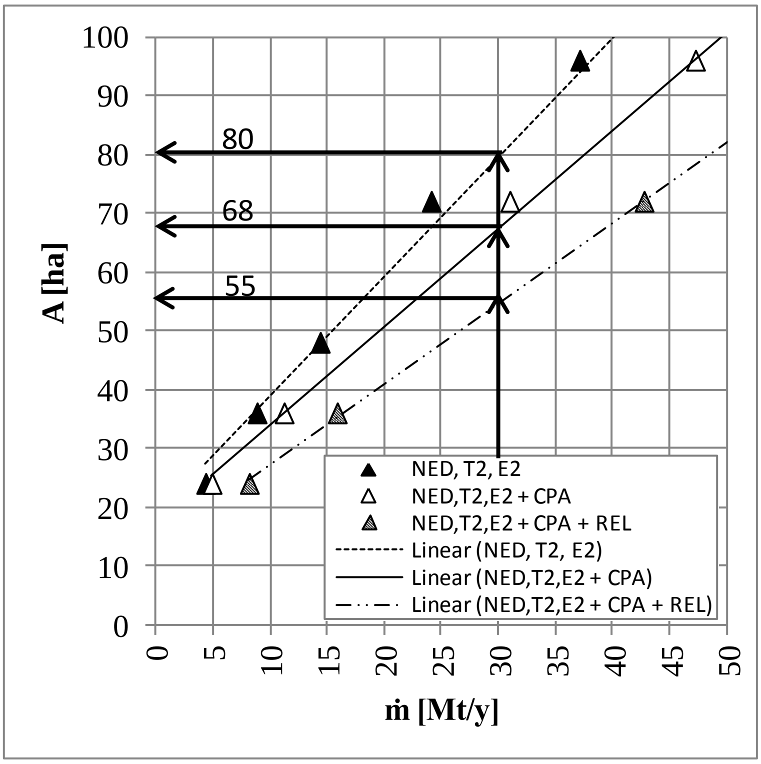

Figure 5.12: Stockyard area versus the annual throughput as function of the clearing pile's area method (CPA) and relocation (REL) for a specific case (NED, T2, E2)

5.6 Conclusions and recommendations

The storage factor was proposed by Ligteringen and Velsink (2012) for the determination of the stockyard size. The storage factor relates to the ratio mass per square meter and the number of replenishments per year. Suggested values do not correspond with values found in real-world applications and will lead to oversized stockyard areas when used as-is.

The stockyard size depends strongly on the stochastic variations for the material arrivals and piles' storage times. Using specific operational procedures like dividing incoming material over multiple piles, clearing the pile's area when material is reclaimed and relocation of small piles results in a significant reduction of the stockyard size needed. In the stockyard model, the developed simulation tool to support the stockyard sizing process, different stochastic distributions can be selected or real-world data can be used as input. Also different combinations of the stockyard operational procedures can be selected for assessment.

In this chapter, the stockyard size was determined with the precondition that ships should not wait for available stockyard area. This assumption may lead to oversized stockyard areas because it will not happen frequently that the stockyard area is fully occupied. Reducing the stockyard size and allowing paying a demurrage penalty to ship-owners may result in less annual costs. For future research, it is recommended to include a cost function that includes the demurrage and area investment costs.

Import terminals may benefit the most from the presented approach because of the larger number of piles stored at the stockyards, especially when the Identity Preserved storage policy is applied when piles need to be stored separately to prevent contamination.

For the expansion of the design methods concerning the terminal’s stockyard, the following additions are formulated based on the research performed in this chapter:

1. The storage factor is a usefull indicator for a quick estimate of the stockyard size required because it describes the relation between the annual throughput and the stockyard area needed. Furthermore, the parameters that determine this storage factor (the ratio mass per square meter and the number of replenishments per year) provide insights which critera have to be considered for stockyard sizing.
2. The stockyard size can be decreased significantly by applying several operational procedures like the relocation of small piles in advance before newly material has been arrived or by clearing the pile’s area when portions of piles have been reclaimed.
3. The degree of stochastics determine the stockyard size, the greater the variations in ship interarrival times, shiploads and storage times the greater the stockyard size required.
4. To take the stochastic variations and specific operational procedures into account, simulation proved to be a practicle tool.

6 Stockyard machine selection

This chapter is based on van Vianen et al. (2013 and 2014b).

In this chapter, stockyard machine characteristics are introduced and the selection of such machines is described. Three stockyard functions can be distinguished: storage, blending and homogenizing of dry bulk materials. When material must be blended and/or homogenized the correct stacking method and reclaiming machine must be selected. Generally, the better blending effect is realized when layers of different materials are spread over the pile's cross section and piles are reclaimed from the face side. The selection of stockyard machines was supported using simulation to take the conflicting objectives of servicing the water and landside demands into account. Experimental results using the transport network model have shown for a specific case that stacker-reclaimers require higher capacities compared to single machines to achieve a predefined terminal performance. However, the investment costs for single stackers and reclaimers are higher due to the larger number of belt conveyers needed. The terminal performance can be improved when stacker-reclaimers are redundant in the access to piles and when ship servicing can be interrupted temporarily in favor of train loading.

6.1 Introduction

In the previous chapter it was introduced that dry bulk materials are stored at stockyards to absorb unavoidable differences between the incoming and outgoing flows of bulk materials. Apart from storing at stockyards, bulk materials sometimes have to be blended and/or homogenized. Figure 6.1 shows the stockyard functions schematically. Batches of material are represented with arrows and stacked material with piles. Figure 6.1A shows the functions for an import terminal. Large batches are delivered to the stockyard and small batches are transported to industrial clients in the hinterland. At export terminals, small batches are railed to the stockyard and after consolidation large batches are loaded into bulk ships.

The blending process is schematically shown in Figure 6.1B. Blending is the process where at least two similar bulk materials with different properties are mixed to achieve a blend with a new average level of material properties (e.g., iron percentage, lump size, ash content or heating value). Blended bulk materials are used as base materials for coal-fired power plants or steel factories. Industrial clients who own these companies plan to guarantee coal and iron ore delivery from multiple sources. The delivered materials may have widely varying properties, which is undesirable and uneconomical for both combustion requirements and environmental considerations. The obvious solution is to blend various materials to create a product with desired characteristics. Blending is sometimes applied already at mine stockyards where raw materials from various mining faces are blended (Lieberwirth, 2012).

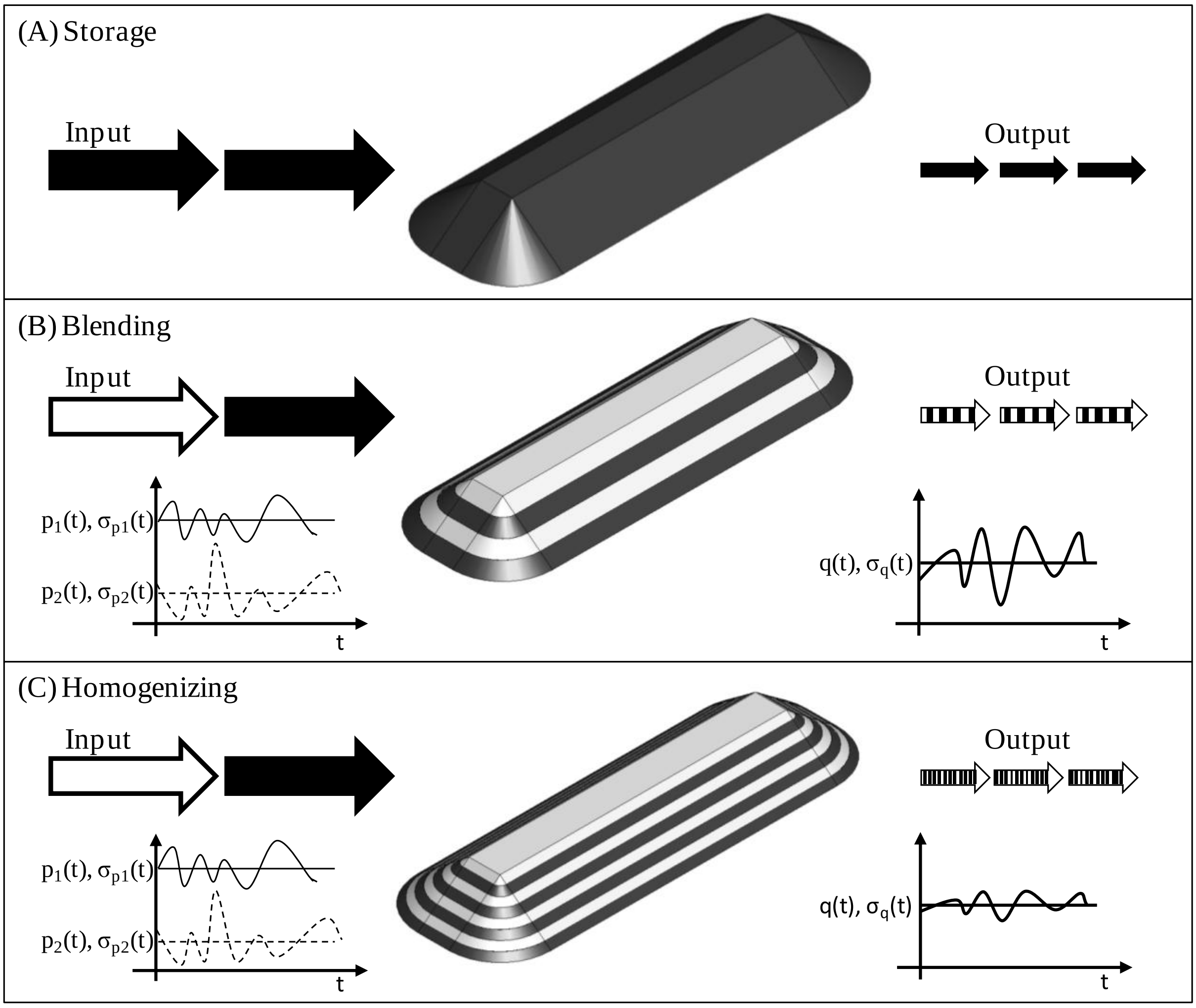

Figure 6.1: Schematic representation of the stockyard functions (derived from Lieberwirth, 2012), where p(t) represents average values for bulk properties during time, q(t) is the average property value after blending/homogenizing and σ(t) represents the standard deviation for the bulk properties

Homogenization is the process to form a homogenous, uniform product from a blend of at least two unique grades. During the homogenization process, represented in Figure 6.1C, the variation of bulk properties (such as their chemical composition or particle size) is reduced while the average value remains the same. The variation of the properties is expressed with the standard deviation. When appropriate stacking and reclaiming machines are selected, the input flow for a pile of material is transformed into an output flow where the fluctuations of the bulk properties are evened out. Homogenization is important for sintering plants or for coke making plants, but has less significance for power generating plants (Zador, 1991).

The stockyard layout design and operation is discussed in this chapter. In this chapter a design of the stockyard layout contains the selection of the machine type, the determination of the machine's capacity and the specification for the stockyard layout (e.g., small or wide lanes). In section 6.2, an overview of available stockyard machines is given and characteristics like the maximum capacity and effective utilization are listed. In section 6.3, the selection for blending/homogenizing machines is addressed. Simulation is used in section 6.4 for the selection of stacker-reclaimers or single stackers and reclaimers to take the dual functionality of stacking and reclaiming by the stacker-reclaimers into account. In section 6.5, methods to improve the stacker-reclaimers operation are introduced. A case study where a stacking and a reclaiming machine were selected to deliver blended coal to a power-plant is discussed in section 6.6. Finally, conclusions are presented in section 6.7.

6.2 Stockyard machine characteristics

For a proper machine selection the various stockyard machine characteristics are required. For relatively small terminals (e.g., terminals with an annual throughput less than 4 million tons), wheel loaders and mobile feeding bunkers are used. Such machines are shown in Figure 6.2. The mobile feeding bunker can also be used to transfer material onto belt conveyors.

Figure 6.2: Handling of dry bulk materials using wheel loaders and a mobile feeding bunker (Courtesy of N.M. Heilig BV)

At larger dry bulk terminals, rail-mounted stackers and reclaimers are installed. These machines stack material onto piles and reclaim material from these piles. Generally, stackers move in three directions; travelling alongside piles, luffing and slewing the boom to stack materials on both sides of the machine. Figure 6.3 shows a stacker that uses a tripper car to transfer material from the yard belt conveyor to the belt conveyor on the stacker's boom.

Circular storage systems are often installed near coal-fired power plants where radial stackers stack material by slewing their booms up to 360° and radial bridge scraper reclaimers reclaim the stockpile from the pile's face side (see Figure 6.4). Circular storage systems have advantages: a compact design, simultaneously endless stacking and reclaiming and well suited for roofed storage of bulk materials. Disadvantages are the higher investment costs, the limited storage capacity compared to longitudinal piles and the expandability only in large batches.

Reclaimers are used to continuously reclaim and discharge stored material from the stockyard. Reclaimers consist of a reclaiming mechanism and an intermediate belt conveyor to convey bulk materials to the yard belt conveyor. The reclaiming mechanism may be a moving chain with gathering scrapers (see Figure 6.5) or a revolving wheel on which buckets are attached (see Figure 6.6 and Figure 6.7).

Figure 6.3: Stacker with a tripper car (Courtesy of ThyssenKrupp)

Figure 6.4: A circular storage system with a radial stacker and a bridge scraper reclaimer installed near a coal-fired power plant in Amsterdam (Courtesy Kees Vlot)

Figure 6.5: Stacking of coal using an overhead conveyor with telescopic loading chute and a side scraper reclaimer (Courtesy of Taim Weser)

Stacker-reclaimers combine the two functions of stacking and reclaiming into one machine. Consequently, only one of the two functions can be fulfilled at a time. Figure 6.6 shows a bucket wheel stacker-reclaimer during stacking of coal. The belt conveyor on the machine's boom travels in the discharge direction, with the bucket wheel stationary, when discharging, and in the reverse direction with the bucket wheel in operation when reclaiming. Figure 6.7 shows a reclaiming bucket wheel in operation. A tripper car is needed to transfer the bulk material from the yard belt conveyor to the boom conveyor during the stacking mode. During reclaiming, the material is dumped through the center of the machine onto the yard conveyor.

Figure 6.6: A bucket wheel stacker-reclaimer during stacking (Courtesy of ThyssenKrupp)

Figure 6.7: A bucket wheel reclaims material from a pile (Courtesy ThyssenKrupp)

Table 6.1 lists values for stockyard machine characteristics mentioned by several authors together with values determined in this research. Not all machines were explained in this chapter but details can easily be found from manufactures websites or brochures. One of machine characteristics is the effective utilization. Due to all kinds of circumstances, like the variation in ship unloading capacity and the travelling times during operation, stockyard machines cannot always operate at maximum speed. The effective utilization expresses the ratio between the effective and installed capacity. For example, the maximum technical capacity for a machine is 1,000 [t/h] but due to luffing, slewing and travelling during operation the net capacity is 850 [t/h]. The effective utilization for this machine is 0.85.

Values for the effective utilization for stackers were not found. This utilization can be derived from machines which feed the stackers, the stackers' capacity must have at least the same value. If a stacker has to handle the unloaded materials from ships, the effective stacking utilization is determined by the ship unloader. In chapter 3 it was mentioned that ship unloading efficiencies vary between 0.5 (for grab cranes) and 0.65 (for continuous unloaders). If a stacker is fed by a railcar or barge unloader, comparable utilization values are expected (see the average landside equipment utilizations mentioned in section 2.4).

Several authors proposed values for the effective utilization of reclaimers. For bucket wheel reclaimers different values were proposed. Leech (2010) suggested values between 0.70 and 0.75 when the slewing reclaiming method is applied and for the long-travel reclaiming method values between 0.88 and 0.92. Knappe (1995) introduced values between 0.50 and 0.95 for the effective reclaiming utilization. Operational data of the net reclaiming capacity of bucket wheel stacker-reclaimers at a Dutch dry bulk terminal was investigated. This analysis has shown values for the effective utilization between 0.35 and 0.57. To explain the variation of these observed values and to explain the difference with values proposed by others, extra research was performed which parameters affect the utilization of bucket-wheel reclaimers.

In Appendix E, the effective reclaiming utilization for bucket wheel reclaimers is presented. It appeared that this utilization relates to the reclaiming method, the adjustment of the slewing speed and pile dimensions. Table 6.1 lists, among other things, values determined for the effective reclaiming utilization for bucket wheel reclaimers for a specific set of input parameters. These parameters are listed in Appendix E.

Table 6.1: Stockyard machine characteristics derived from Erasmus (2001), FAM (2010), Müller (2010) and Strien (2010) completed with own results

Machine type	Maximum technical capacity [kt/h]	Effective utilization [-]	Stockpile width [m]
Stacker	10	0.5 - 0.65	30-60
Radial stacker	8	0.5 - 0.65	Ø120
Side scraper reclaimer	1	0.75	10-25
Single boom portal scraper reclaimer	2. 2	0.75	15-60
Double boom portal scraper reclaimer	4.4	0.75	15-60
Bridge scraper reclaimer	1.8	0.95	15-60
Bridge bucket wheel reclaimer	10	0.95	30-60
Drum reclaimer	4.5	0.95	20-50
Bucket wheel reclaimer	12	0.4 - 0.8	30-60

6.3 Stockyard machine selection for blending and homogenization

In this section a stockyard machine selection is presented for blending and homogenizing dry bulk materials. By stacking different grades a blend is formed and the reclaiming operation determines if in the final product the grades are homogeneously distributed. In section 6.3.1, a brief literature review of bed blending is given. Section 6.3.2 describes four stacking methods to build up blending piles. In section 6.3.3, basic blending equations are introduced and in section 6.3.4 a ranking for the combinations of the stacking method and reclaiming machine is presented.

6.3.1 Bed blending theory: a literature review

In many papers the bed blending theory was applied to design blending stockpiles. The first pioneers of the blending and homogenizing theory were Gerstel (1979) and Gy (1981). The bed blending theory can be used to determine the variation which would occur if the geometry of stacking and reclaiming are perfect in the sense that each parcel of stacked material is equally represented in each parcel of reclaimed material (Robinson, 2004). The theory of bed blending assumed that each layer in the blending pile can be characterized by an average composition and a standard deviation corresponding to a random variation around this average (Petersen, 2004).

Many computer models (e.g., Zador (1991), Robinson (2004), Petersen (2004) and Kumral (2006)) were developed for computing three-dimensional geometries of blending piles, for assessing combinations of stacking methods and reclaiming machines, for predicting the blending performance and for evaluating coal purchasing programs. Schott (2004) focuses on the applicability of blending and homogenizing in mammoth silos. Others used simulation to optimize blending in longitudinal stockpiles (Pavloudakis and Agioutantis, 2003) or cone shell stockpiles (Duinkerken et al., 2011).

6.3.2 Stacking methods

Four stacking methods can be distinguished for the composition of blending piles: cone shell, chevron, strata and windrow stacking. Figure 6.8 shows schematically these blending piles built up out of two grades.

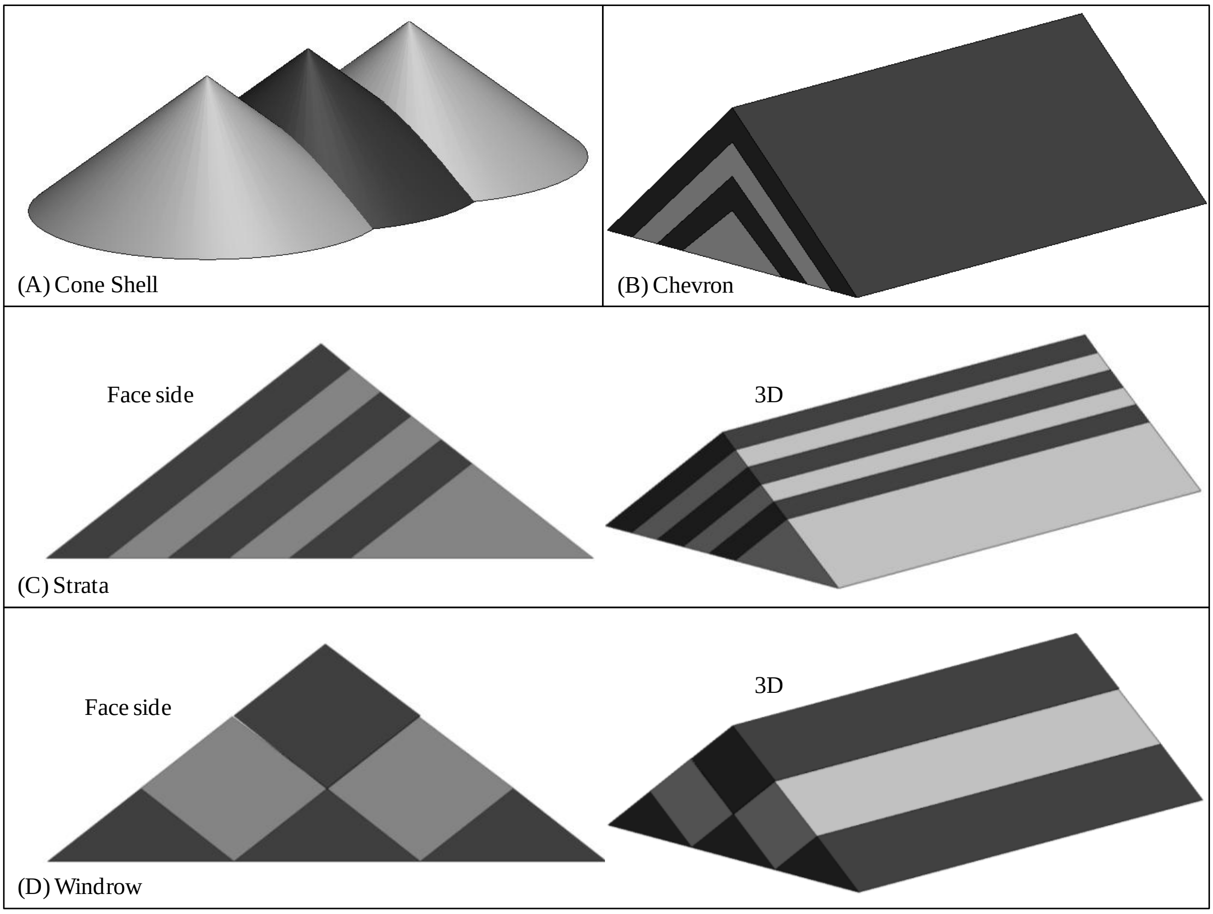

Figure 6.8: Schematically representation of blended piles when different stacking methods were applied; derived from Wolpers (1995), FAM (2010) and Müller (2010)

For the cone shell stacking method (Figure 6.8A) the material is discharged at a single point. The stacker's boom remains stationary until a cone of the required height is formed. The stacker moves a short distance and material is poured again connecting a new cone to the first one. Cone shell stacking is usually performed using a stacker with a luffing boom. Blending can be realized by extending the pile longitudinally along its length with interconnected cones of material with different grades.

Chevron stacking (Figure 6.8B) involves the creation of a longitudinal pile by stacking the material at the stockyard while the stacker moves slowly down the stockyard. The first layer is then created. At the end of the pile, the stacker boom is luffed to create room for the second layer and the stacker travels backwards. By running the stacker alongside the pile, triangular bands of different qualities of materials are stacked in thin layers over the whole pile length.

Strata stacking (Figure 6.8C) requires a stacker with a luffable and slewing boom. An initial small pile is created at one side of the storage area. After the creation of the first layer, the boom is slewed further and luffed. The stacker travels back and pours material behind the first layer to create the second one. By repeatedly slewing and luffing the boom at each layer end, layers of different material qualities are built up parallel.

Also windrow stacking (Figure 6.8D) requires a luffable and slewing stacker boom. This stacking method is a combination of chevron and strata stacking. Small separate piles are formed by travelling alongside the pile and the gaps between these piles are filled afterwards to build up the windrow. The material quality is therefore layered in blocks across the pile's cross section.

6.3.3 Basic blending equations

For the composition of blending piles the mass balance can be used to determine the mass fractions for different grades (Gerstel, 1999). Bulk properties, like the ash content, volatile matter or moisture content, are stochastic variables with an average value and a distribution. The distribution is normally expressed by the standard deviation. Samples are generally made from the different grades to determine the average values and standard deviations for several bulk properties. In the simplest case blending piles are built up out of two grades (as shown in Figure 6.8). The mass per grade can then be determined using the following equation.

$$p_1 m_1 + p_2 m_2 = qm \quad \forall\, p_1 < q < p_2 \tag{6.1}$$

Where p_1 and p_2 are the average values of a bulk property, q is the required average value after blending, m_1 and m_2 are the masses per grade and m is the required mass after blending.

When it is assumed that the sum of the individual masses equals the required mass after blending, equations (6.2) and (6.3) can be derived to determine the mass fractions.

$$m_1 = \left(\frac{p_2 - q}{p_2 - p_1} \right) m \tag{6.2}$$

$$m_2 = \left(\frac{q - p_1}{p_2 - p_1} \right) m \tag{6.3}$$

When it is assumed that each parcel of stacked grade is equally represented in each parcel of reclaimed material, the standard deviation of the reclaimed material can then, according to elementary statistics, be calculated as:

$$\sigma_q = \frac{\sqrt{\sum_{i=1}^{n_m} \left(\frac{m_i}{m} \right)^2 \sigma_{pi}^{\;2}}}{b\sqrt{N}} \tag{6.4}$$

Where σ_q is the standard deviation of a bulk property after blending and homogenization, n_m is the number of stacked grades, m_i is the mass per stacked grade [t], m is the total blended mass, σ_{pi} is the standard deviation of a bulk property per grade, N [-] is the number of layers in the stockpile and b [-] is an empirical factor that expresses the blending ratio achievable in practice. De Wet (1994) and FAM (2010) proposed values for the parameter b between 0.5 and 0.7. Note that each layer of the blended material represents the composition of the different blended grades.

6.3.4 The blending and homogenization effect

The combination of the stacking method and reclaiming machine determines the blending and homogenization effect. Reclaiming over the pile's cross-section increases the probability that each parcel of stacked grade is represented in the parcel of reclaimed material. The variations of the incoming grades are evened out. To express the effect of blending and homogenization the following references were consulted; Zador (1991), Müller (2010) and FAM (2010). These references show for several combinations of stacking methods and reclaiming machines values for the blending/homogenization effect. These values were determined during practical tests and represent the ratio between the variations before stacking and after reclaiming, or expressed algebraically:

$$\varepsilon = \frac{\sigma_{in}}{\sigma_q} \tag{6.5}$$

Where ε is the blending/homogenization effect [-], σ_{in} represents the standard deviation of a bulk property for the incoming grades and σ_q is the standard deviation of a bulk property after blending and homogenization. Table 6.2 shows values for the blending/homogenization effect. Note that the values for the blending/homogenization effects as listed in Table 6.2 are partly derived from commercial information of stockyard machine manufacturers and these suppliers do not present data to verify the proposed results.

Table 6.2: The blending/homogenization effect as function of several combinations for stacking methods and reclaiming machines (derived from Zador (1991), Müller (2010) and FAM (2010)

Reclaiming machine	Stacking method (see Figure 6.8)			
	Cone Shell	Chevron	Strata	Windrow
Single scraper reclaimer and Portal scraper reclaimer	2	2	3-4	4-6
Bridge scraper reclaimer	-	10	5-6	8-9
Bridge bucket wheel reclaimer	-	4-8	4-6	4-8
Drum reclaimer	-	9-10	4-6	7-8
Bucket wheel reclaimer	-	4-5	5-6	4-6

From Table 6.2 it can be learned that a chevron stacked pile together with a bridge scraper reclaimer (this machine is shown in Figure 6.4) or drum reclaimer realize the best blending and homogenization effect. Both reclaiming machines dig material away from the pile's face side. In section 6.6, a case study will be discussed to select the stacking method, the stacking machine and the reclaiming machine based on the information presented in this section.

6.4 Stacker-reclaimers or stackers and reclaimers

Currently, stacker-reclaimers or single stackers and reclaimers are both installed at stockyards. An advantage of stacker-reclaimers is the limited number of belt conveyors needed (the same belt conveyor is used for the transport of bulk material to and from the stacker-reclaimer). A disadvantage is the decrease of the terminal performance due to conflicting objectives for servicing ships and trains at the same time. In this section, an economical trade-off will be made based on investment costs for stockyard machines and belt conveyors and predefined average port times for ships and trains.

In section 6.4.1, a method to estimate the investment costs for stockyard machines and belt conveyors is described. To determine the average ship and train port times, simulation is needed to take the stochastic arrival processes, equipment disturbances and variation in piles storage times into account. Furthermore, by using simulation the conflicts for stacker-reclaimers for servicing ships or trains can be taken into account. The simulation model will be discussed in section 6.4.2. Specific details for using a discrete-event simulation model to represent a continuous flow of bulk materials are presented in section 6.4.3. The verification of the simulation model is mentioned in section 6.4.4 and simulation experimental results are presented in section 6.4.5.

6.4.1 Investment costs for stockyard machines and belt conveyors

Manufactures consider the selling prices for their stockyard machines and belt conveyors as confidential and do not want to share these prices easily. In this section, the machines investment costs (defined as costs when machines are fully installed at stockyards) will therefore be estimated based on the machines weight.

From 75 stockyard machines (stackers, bucket wheel reclaimers and bucket wheel stacker-reclaimers) the weight, the boom length and the stacking and/or reclaiming capacity were compiled from several sources like Wöhlbier (1977) and brochures from manufactures. In Appendix F, the method is explained that was used to formulate the relation between the machines' weight and machines' characteristics. Based on the results mentioned in Appendix F the following equation was derived:

$$w = e_1 l_b \left(Q_{sg} + Q_{rg} \right) + e_2 \tag{6.6}$$

Where w is the machine's weight [t], e_1 and e_2 are constants for the different machine types (values are listed in Table 6.3), l_b is the boom length [m], Q_{sg} and Q_{rg} [kt/h] are the gross stacking and reclaiming capacities respectively. The gross capacity is also called the machine's name plate capacity.

Table 6.3: Determined constant values per stockyard machine type

Stockyard machine	e_1 [-]	e_2 [-]
Stackers	1.61	61
Bucket wheel reclaimers	1.43	275
Bucket wheel stacker-reclaimers	1.38	238

For the belt conveyor investment costs, Roberts (1981) developed an economic cost model. A relation between the investment cost and the transportation capacity was proposed. However, even when the results determined were indexed to the year 2014, the investment cost per running meter is only a fraction compared to the limited number of quotations received from belt conveyor system suppliers. In Appendix F, prices for a running meter of belt conveyor systems based on the received quotations are shown. These prices include the drive unit, the belt, idler sets, stringers and tensioning unit but exclude the civil works, sidewalks, covers, etc. From Figure F.3 in Appendix F, it can be concluded that the belt conveyor investment costs vary significantly. Apparently these costs vary per country, per supplier or even per project. An upper and a lower limit were derived to limit the maximum and minimum price per running meter versus the transportation capacity. Note that these limits were not validated due to the lack of real-world data.

6.4.2 Transport network model

The stockyard model as presented in chapter 5 describes the stockyard operation with a simplified seaside and landside handling. That model has been extended with stockyard machines and belt conveyors. This further developed simulation model developed is called the 'Transport network model'. Details for this model are presented in Appendix D, section D.4. In this section, the main important algorithms for the transport network model are briefly described. In the transport network model the stockyard machine main functions (stacking and/or reclaiming), the machine's location at the stockyard, the routes to this machine and the machine capacities has been considered.

For the stockyard machines the following algorithms were implemented; S*electJob* to select the next appropriate job, *RouteSelection* to select available transportation routes and *StorageAllocation* to allocate the shipload to a lane that contains available storage area. In this section the algorithms will be explained for an import terminal but these algorithms can also be applied at export terminals. The time needed to stack or reclaim the job is determined by dividing the job's load by the machine's effective capacity. Activities to handle a certain bulk load are called jobs. A job can be a trainload or a (part of the) shipload.

Machine's algorithm *SelectJob*

When a new job is generated, each idle machine checks one after the other if this job can be handled. A ship will be accepted when the shipload can be stored and there is an available transportation route from the ship unloader to this machine. A train will be accepted when the requested material is stored at one of stockyard lanes in the machine's reach and material can be transported from this machine to a railcar loader.

Machine's algorithm *RouteSelection*

To each machine, transportation routes are assigned and listed in the machine's routes list. A route is formed by multiple belt conveyors in series. A belt conveyor can only be used in one route at the time. After finishing the transportation of a job, the selected route is put as last item in the machine's routes list. In this way a random selection of all routes will be realized.

Machine's algorithm *StorageAllocation*

The required pile length to store a (part of a) new arrived shipload is calculated based on the shipload, specific dimensions (lane width and stacking height) and material properties (angle of repose and bulk density) (as introduced in chapter 5). To allocate this pile to the stockyard, a certain length of the lane will be claimed. To prevent mixing between piles, an empty space of at least two meters will be created between piles. The pile's area will be made available as soon as all material is reclaimed.

The transport network model was used to evaluate stockyard layouts. Figure 6.9 shows for this case both investigated layouts. In the layout shown in Figure 6.9A, three stacker-reclaimers are installed and in Figure 6.9B three stackers and three reclaimers are used. Machines installed on the same track between two stockyard lanes can pass each other, which corresponds to real operations where the machines' booms have to be slewed parallel to the stockyard lanes before these machines can pass each other. In the simulation model, the time needed for slewing is not included. Figure 6.9 shows arbitrary situations where material is reclaimed from the first lane (L1) by a stacker-reclaimer or reclaimer to be loaded in a freight train. At the same time, two ship unloaders are used to unload a bulk ship. Material out of this ship is stacked in two different piles. Shipload splitting and storing across multiple piles was already introduced in chapter 5 and is applied here again.

Data of (historically served) ships was used as input for ships with specific arrival times and shiploads. For each pile the storage time (which is the load's time-in-system) is drawn from a distribution. After finishing the stacking operation, a specific train generator generates trains to pick up the pile's load within its storage time.

In the transport network model each piece of belt conveyor uses its own disturbance generator. Tewari et al., (1991) stated that for belt conveyors the mean time between failures (MTBF) and the mean time to repair (MTTR) can be retrieved by sampling values from negative exponential distributions (NED). In the first instance this assumption seems to be a strange one. Although this proposed distribution type does not correspond exactly with operational data of belt conveyors at an export terminal (as analyzed by Klaasen, 2007), there are some similarities. The historical data has shown that in most cases the time needed to repair is relatively short (solving a disturbance takes approximately 15 minutes) and only in a few situations the time between failures is very long. Furthermore, by using the NED-distribution for the generation of MTBF and MTTR-times the worst-case scenario will be investigated, resulting in a better performing real situation.

The historical operational data of the disturbance behavior of belt conveyors has values for the technical availability (η) between 0.9 and 0.97. In this research, a technical availability of 0.97 will be used for each belt conveyor. The relation between the technical availability and the MTBF and MTTR can be expressed with the following equation:

$$\eta = \frac{MTBF}{MTBF + MTTR} \tag{6.7}$$

Where η is the technical availability [-], MTBF is the Mean Time Between Failures [h] and MTTR is the Mean Time To Repair [h].

When a belt conveyor breaks down, the active job's handling time will be extended with the mean time to repair. This assumption does for many cases correspond with the real situation, especially when disturbances that take a relatively small time occur. However, when a belt conveyor breaks down a long-time, the remaining material that has to be transported will be performed using another route in real-operations. This transition to another transportation route when the transportation activitiy is not finished is not implemented in the transport network model; again the worst case scenario will be investigated.

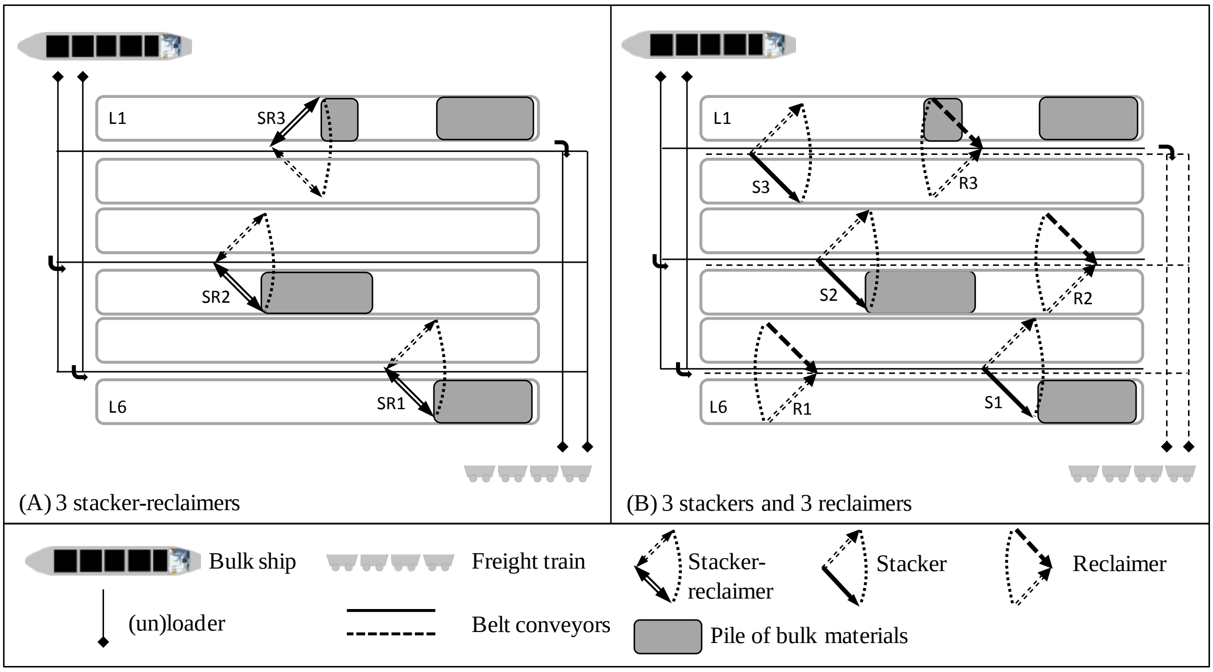

Figure 6.9: Investigated stockyard layouts with (A) three stacker-reclaimers and (B) three stackers and three reclaimers

6.4.3 Using discrete-event simulation for continuous flow transportation

In the transport network model, the continuous transport of dry bulk materials has been implemented in a discrete-event simulation. Fioroni et al., (2007) already applied the discretization of the continuous transportation for iron ore using belt conveyors for the case of a steel factory in Brazil by dividing the load onto the belt conveyor into portions. When a route could be selected to transport material between a predefined source and destination, each portion of material that departs from the source decreases the stockpile volume and arriving portions increase the volume at the destination. Unfortantely, the authors do not mention which portion size was selected to model the continuous behavior of the belt conveyors.

Contrary to the work of Fioroni et al., (2007) in the transport network model, the running time of material on the belt conveyors (the time needed to feed the material from the start to the end of a transportation route) was not taken into account. This approach was followed because the behavior of the continuous flow itself is less relevant compared to the complexity of route selection and the prioritization of transportation activities.

For each material transport, the maximum transportation rate (in tons per hour) was determined by the investigation of the capacities of the individual belt conveyors and the arrival rate of the material. For example, when two cranes are unloading with free-digging speed and both cranes dump their material onto one quay conveyor, the transportation rate of this conveyor may be less than the material arrival rate. However, when one crane feeds the conveyor system, the crane’s capacity may be less than the maximum transportation capacity. The time needed for transportation is then determined by dividing the amount of material with either the maximum transportation rate or the arrival rate. Times needed for starting up or stopping the transportation routes are not included in the transport network model because these times will only lower the maximum transportation capacities.

6.4.4 Verification

For the verification of the transport network model, the tracing function of the simulation software was used and simulation results of a simplified case were compared with analytical results. The average ship waiting time (W_t) as function of the inverse of the ship unloading rate (1/μ) was determined analytically for an M/M/n queuing model. Equations for this model were already introduced in chapter 3. For the simulation results a similar layout as shown in Figure 6.9B with an extra ship unloader and railcar loader was used. Moreover, the following preconditions were set to achieve a correct comparison; the ships interarrival times and shiploads were represented by negative exponential distributions, the shipload was stored in one pile and there was no variation in piles storage times.

Following the outcome of the verification study concerning the seaside model (as described in section 3.6.2) ten files that contain each 2,500 ships were used as input for the verification of the simulation model. In Figure 6.10 the average ship waiting time as function of the average ship service time is shown versus the average stackers utilization (ρ_s) [-] for the analytical solution (M/M/3) a well as the outcomes of the simulation model. The relatively large variation of the average values obtained using the simulation model can be explained by the fact that negative exponential distributions were used for the ships arrival times as wel as shiploads. Although, the average values and corresponding variations are in line with the analytical results, the transport network model can be considered as correct.

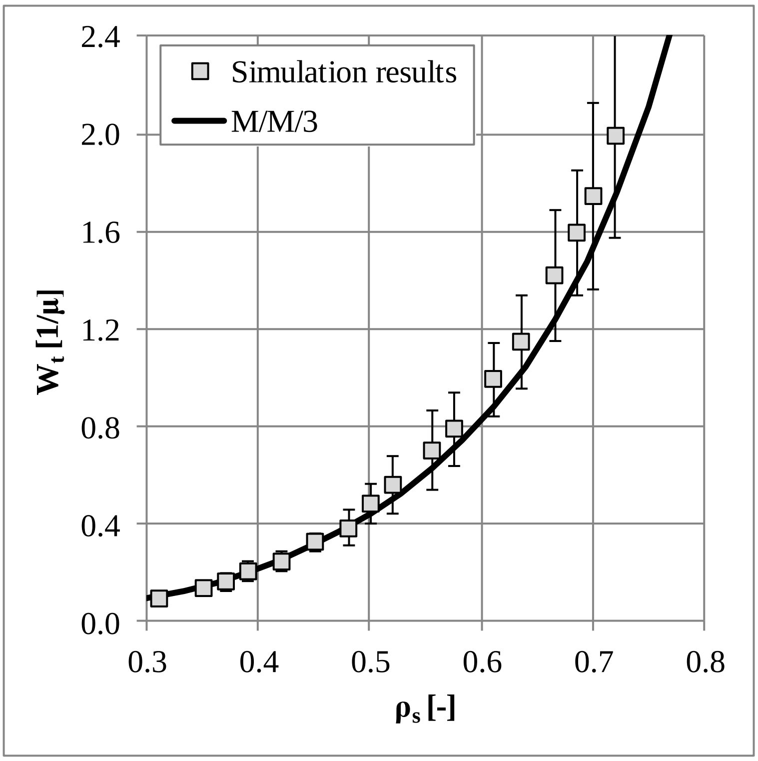

Figure 6.10: Verification of the simulation model by comparing analytical results with results obtained using the simulation model for ten replications

During the development of the transport network model the (provisional) results were discussed in close cooperation with different, independent terminal operators (expert validation). For example, for the route selection comparable approaches were followed as applied by terminal operations planners.

6.4.5 Simulation experimental results and run control

The transport network model was used to determine for both layouts of Figure 6.9 the average ship and the average train port times versus the net stacking and/or reclaiming capacities. Table 6.4 lists the input parameters used. The simulation run time was determined using the same method as described in section 3.7.1. However, based on the results from this section, input files that contained 2,500 ships were used because comparable stochastic distributions are applied for the ships interarrival times and shiploads. For the simulation experiments as discussed in this section, extra stochastic variations are introduced by the storage time distributions and the equipment technical availability distributions.

Table 6.4: Input parameters for the simulation experimental results

Parameter	Description	Value	Unit
$\dot{m}$	Annual throughput	15	[Mt/y]
IATDist	Interarrival time distribution	NED	
SlDist	Shipload distribution	See Figure 3.21B	
sl	Average shipload	101	[kt]
T_s	Average pile's storage time	500	[h]
STDist	Storage time distribution	NED	
Storage policy		Identity-preserved	
η	Equipment technical availability	0.97	[-]
Trainload		4	[kt]

For the experiments it was assumed that the terminal acts as an import terminal and the stockyard area was set large enough to prevent that ships have to wait before delivering their material. The jobs were selected according the First-Come-First-Served method. In Figure 6.11 a boxplot is shown composed from the variations of ten replications for the case with three stacker-reclaimers and a stacking capacity of 2.3 [kt/h]. The average value is listed in Figure 6.12 as a single result. The average value was 51.3 [h] with a standard deviation of 0.95 [h], which is 1.9%. This accuracy was assumed to be precise enough to perform the stockyard machine selection.

In Figure 6.12 results for the average ship and train port times are presented together with predefined limits for the assessment (W_{ship}: 60]h] and W_{train}: 12 [h]). The net capacities required to meet these maximum values can be read from Figure 6.12. The requirement for the high reclaiming capacity needed for stacker-reclaimers (as shown in Figure 6.12B) can be explained by the variations in load between ships and trains. When stacker-reclaimers are active with stacking (servicing the ship unloading activity) these machines are claimed a long time. That results in a limited time available for reclaiming material that is stored within its reach. A high reclaiming capacity should be installed to meet the predefined average train port time.

The gross stacking and gross reclaiming capacities were calculated by multiplying the net stacking and reclaiming capacities determined with an effective utilization value of 0.5. This value for the effective utilization was already listed in Table 6.1. The assessment between stacker-reclaimers and single stackers and reclaimers is presented in Table 6.5. From this table, it can be concluded that for the layout of Figure 6.9 stacker-reclaimers require less investment costs compared to single stackers and reclaimers to realize the predefined maximum average ship and train port times.

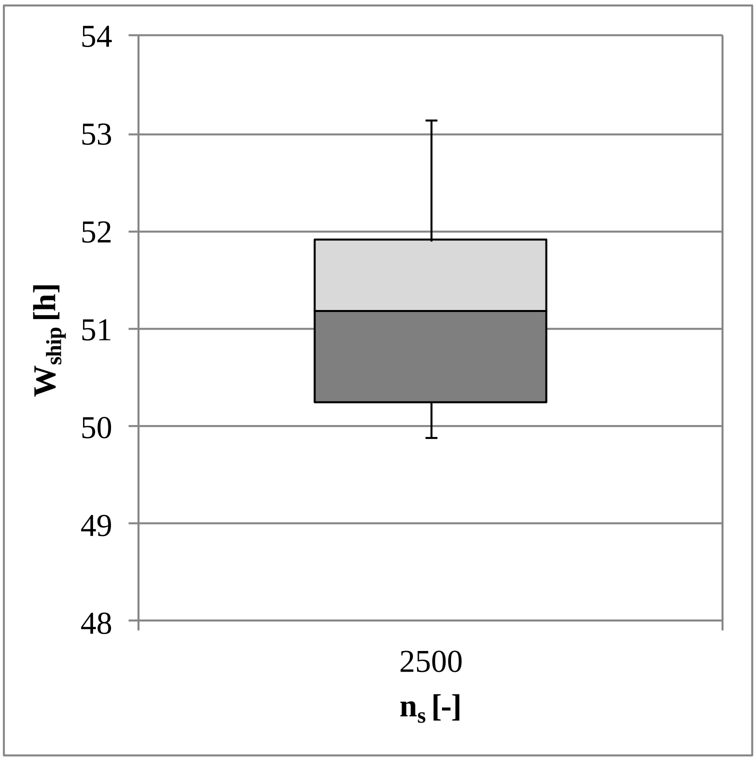

Figure 6.11: Boxplot that displays the variations for the average ship port time obtained using the transport network model for an input file of 2,500 ships for a single result as shown in Figure 6.12

Table 6.5: Assessment between stacker-reclaimers and single stackers and reclaimers

Layout	Machines	Q_{sg} [1] [kt/h]	Q_{rg} [1] [kt/h]	w [kt] [2]	C_{sm} [M€] [3]	C_{bc} [M€] [4]	C_{tot} [M€]
Figure 6.9A	3 stacker-reclaimers	4.2	5.4	900	21.6	8.1	29.7
Figure 6.9B	3 stackers	4	-	385	9.2	6	31.5
	3 reclaimers	-	3	490	11.8	4.5	

[1] Q_{sg} is the gross stacking capacity and Q_{rg} is the gross reclaiming capacity
[2] The machine's weight was determined using equation (6.6) and the constant values as listed in Table 6.3. For all machines a boom length of 50 meter was assumed.
[3] The investment cost for stockyard machines (C_{sm}) was calculated based on the assumption that each machine fully installed at the stockyard costs 8 times more than its weight in kilograms.
[4] The investment cost for belt conveyors (C_{bc}) was based on the lower limit of the cost per running meter versus the transportation capacity as shown in Figure F.3 (in Appendix F). For all yard belt conveyors a length of 1 kilometer was assumed. Only the yard belt conveyors were included in this analysis because both layouts in Figure 6.9 show a comparable configuration for the cross conveyors (the conveyors that connect the (un)loading machines with the yard belt conveyors).

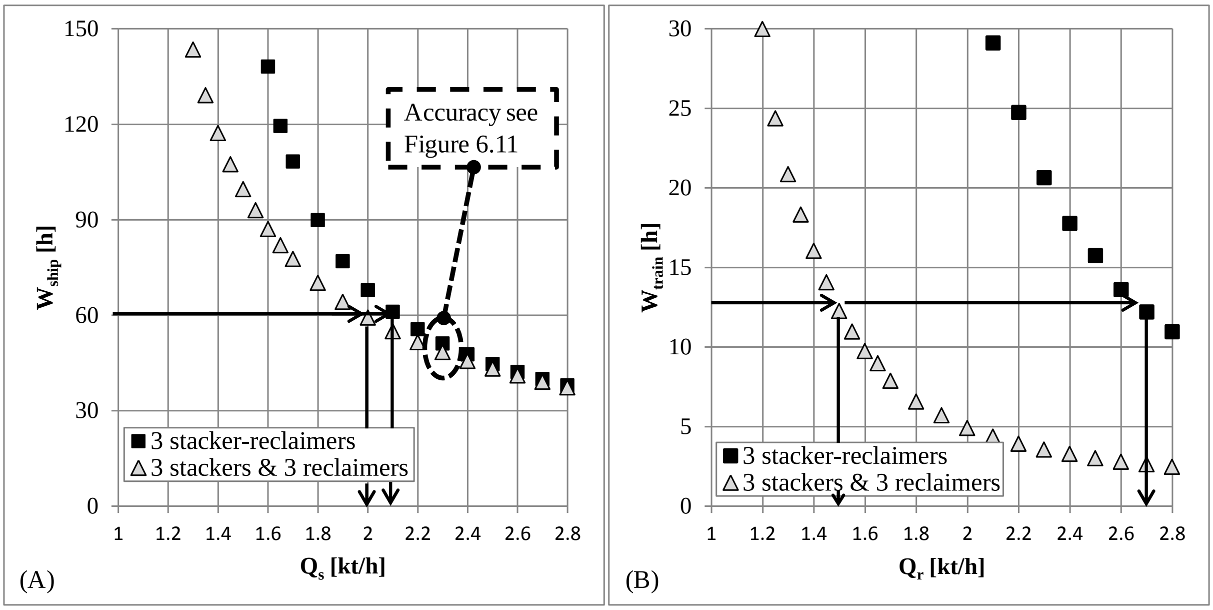

Figure 6.12: Simulation experimental results to assess layouts (as shown in Figure 6.9) that contain individual stockyard machines or combined stacker-reclaimers. The stacking capacity required is shown in (A) and the reclaiming capacity required in (B).

6.5 Reduction of the needed stacker-reclaimer reclaiming capacity

From the previous section it can be concluded that stacker-reclaimers require a relatively high reclaiming capacity to realize a predefined average train port time. In this section, two methods will be presented that will reduce the reclaiming capacity needed without exceeding a predefined average train port time. The first method, described in section 6.5.1, is the stacker-reclaimer redundancy. The second method is to interrupt ship servicing temporarily under certain conditions to load trains in between. This rescheduling procedure is presented in section 6.5.2 and was based on van Vianen et al. (2013) and van Vianen et al. (2014b).

6.5.1 Stacker-reclaimer redundancy

The stacker-reclaimer redundancy is defined as the accessibility of two machines to individual piles. Figure 6.13 shows a layout where piles stored at lanes (L2 and L3) can be reclaimed by two machines; at these lanes there is a stacker-reclaimer redundancy. When, for example, stacker-reclaimer SR2 is active with stacking at lane L3, SR1 is also able to reclaim material from piles which are stored at this lane. Piles at L2 and L3 have to be stacked by two stacker-reclaimers from both sides. Piles at lanes L1 and L4 remain accessible by one stacker-reclaimer. The reduction of the reclaiming capacity needed was investigated and the results are shown in Figure 6.14 with the series ‘*3 SRs with redundancy*’. From this figure, it can be concluded that the net reclaiming capacity (Q_r) can be reduced from 2.7 to 2.5 [kt/h].

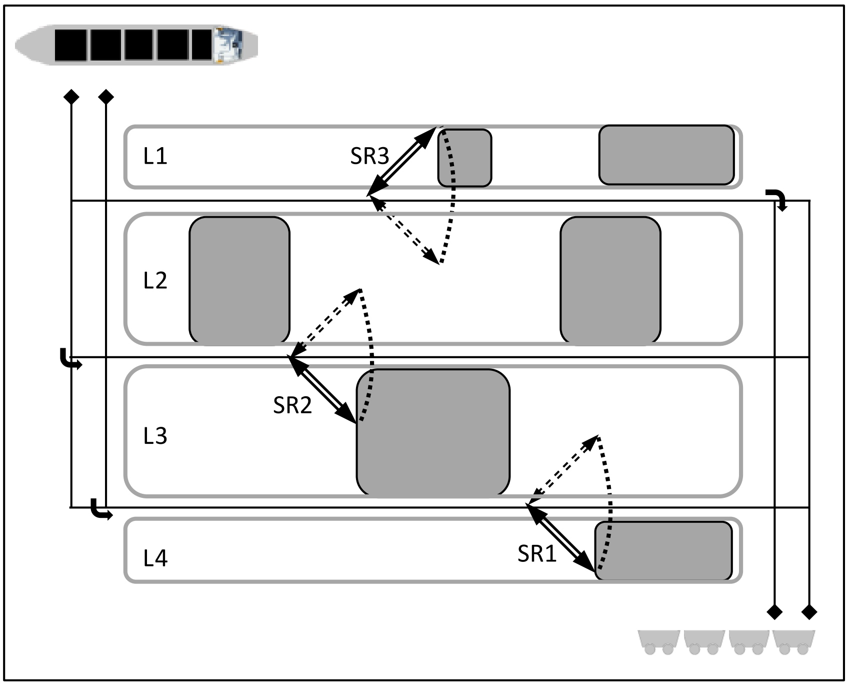

Figure 6.13: A stockyard layout with the stacker-reclaimer redundancy for piles stored at lanes L2 and L3

6.5.2 The rescheduling algorithm for stacker-reclaimers

Hu and Yao (2012) formulated the stacker-reclaimer scheduling problem as a mixed integer programming model with the objective of minimizing the makespan (which is the total time between the start of the first operation and the end of the last operation) for a given set of handling operations. The approach developed was based on genetic algorithms using two types of chromosome representations. In the greedy assignment procedure, operations were assigned to machines based on their availability, minimized completion time and minimized setup times. Computational experiments were performed for a specific case for a planning horizon of 8 hours. The authors assumed that the processing time per operation varies between the 60 and 150 minutes and that a stacker-reclaimer completes the operation without any interruption or shift.

At dry bulk terminals the jobs' operation time show much more variation than proposed by Hu and Yao (2012). In our approach the reduction of the needed reclaiming capacity was investigated when the stacking operation is interrupted temporarily in favor of train loading. The so-called rescheduling algorithm was developed and implemented in the transport network model. The interruption of the ship servicing can only be performed when certain conditions like the availability of transportation routes and expected disturbances are considered. When a train arrives to pick up materials, the rescheduling algorithm investigates if this train can be handled immediately. The following preconditions were implemented in the rescheduling algorithm:

- If a stacker-reclaimer is active with reclaiming the operation will not be rescheduled due to the limited operation time.
- There should be a transportation route to be formed from idle belt conveyors to transport the requested material to a railcar loader.

- There must be spare time left within the agreed ship port time after serving the train in between. The time needed to reposition stacker-reclaimers (assumed as maximum 15 minutes) must be taken into account as well.
- An interruption of the ship's operation is only acceptable when the maximum number of interruptions per ship is not reached.

The last precondition was introduced to prevent that ship unloading is interrupted too frequently. This may result in an extension of the ship end time due to unexpected breakdowns during the remaining operation. When requested material is stored in the reach of two stacker-reclaimers and both machines are active with stacking, the stacker-reclaimer with most spare time within the maximum ship port time is selected.

The question is how many times may the ship unloading be interrupted when the route availability and breakdowns are not known on beforehand? A fixed number of interruptions per ship will not be a useful parameter because shiploads vary considerably. Therefore, it was proposed that the number of interruptions per ship depends on the shipload and will be defined by dividing the shipload with a parameter that was called '*shipload distributer'*. For example, for a shipload distributer of 15 [kt] maximum four interruptions of the ship unloading is accepted for a shipload of 65 [kt].

The transportation route that was used during stacking remains claimed during the reclaiming operation. Consequently, the belt conveyors in this route cannot be assigned to other stacker-reclaimers and after finishing the train loading interruption, the stacker-reclaimer continues with the stacking operation.

For the layout as shown in Figure 6.13 simulation results were determined when the rescheduling algorithm was active. The parameters as listed in Table 6.4 were used together with two extra parameters. For the shipload distributer a value of 15 [kt] was used and the stacker-reclaimer repositioning time was assumed to be 15 minutes.

In Figure 6.14 the average ship and train port times determined are presented. From Figure 6.14B it can be concluded that rescheduling the stacker-reclaimer operation will decrease the required reclaiming capacity from 2.7 [kt/h] to 2.4 [kt/h] still guaranteeing the predefined average train port time of 12 hours. However, from Figure 6.14A it can be concluded that the average ship port time will increase from 60 to 80 [h] when the stacking capacity of 2.1 [kt/h] will remain the same. The effect can be explained by the fact that each interruption requires two times repositioning of the stacker-reclaimer, which takes half an hour. During repositioning, the machines are not able to handle material, ineffective machines hours are introduced. For the investigated case rescheduling the stacker-reclaimer operation is only beneficial if the average ship port time of 80 hours does still satisfy the required seaside performance, otherwise the required increase of the stacking capacity required neutralizes the reduction of the reclaiming capacity required.

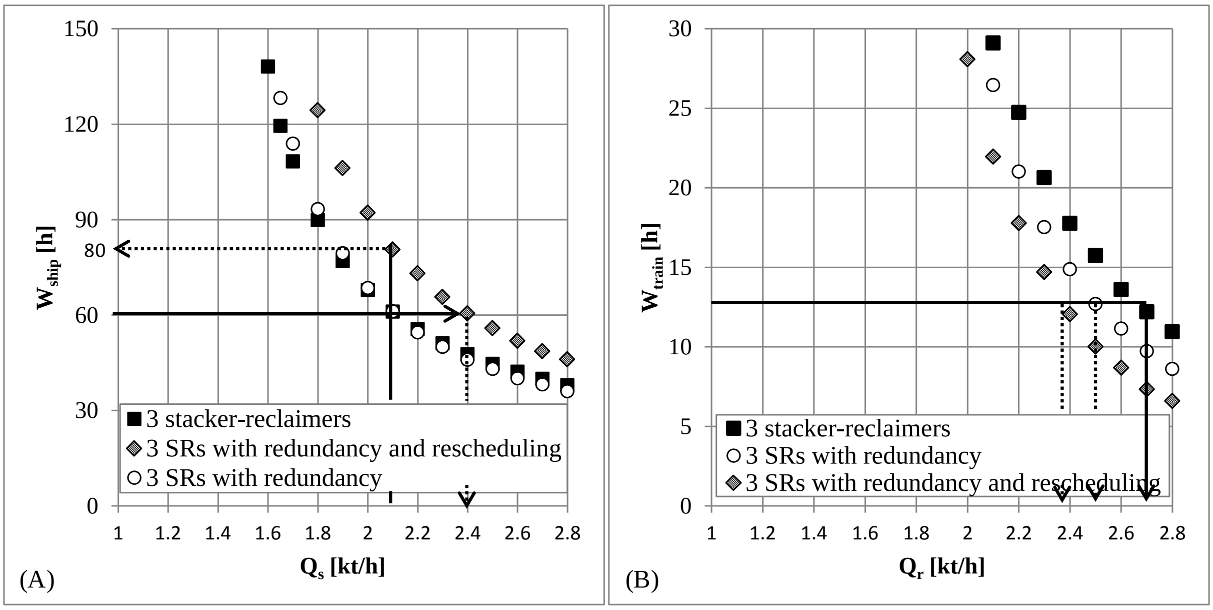

Figure 6.14: The average port times for ships (A) and trains (B) as function of the stacker-reclaimers' capacity with redundancy of piles at middle stockyard lanes (as shown in Figure 6.13) and the rescheduling procedure

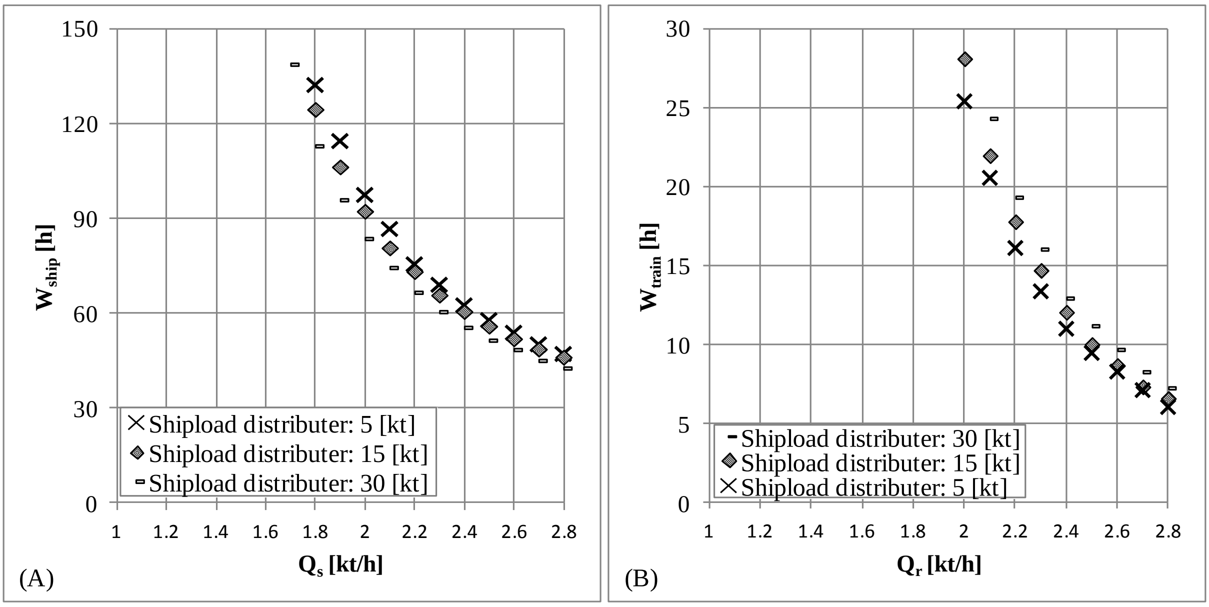

Figure 6.15: The average port times for ships (A) and trains (B) as function of different values for the shipload distributer (results for 15 [kt] were already shown in Figure 6.13)

The impact of the number of interruptions during ship unloading was investigated by varying the value for the shipload distributer. For two different values, 5 [kt] and 30 [kt], the average ship and train port times were determined and compared with the already presented results in Figure 6.14 (the series '*3SR with redundancy and rescheduling*'). Figure 6.15 shows the average port times determined as function of the shipload distributer and in Figure 6.16 the registered average numbers of interruptions per ship (n_i) [-] as function of the shipload distributer are shown. As expected, from Figure 6.15 and 6.16 it can be concluded that a reduction of the shipload distributer will increase the average number of interruptions per ship which will increase the average ship port time and will decrease the average train port time.

The transport network model can be used to determine the maximum acceptable number of interruptions per ship to realize predefined average ship and train port times.

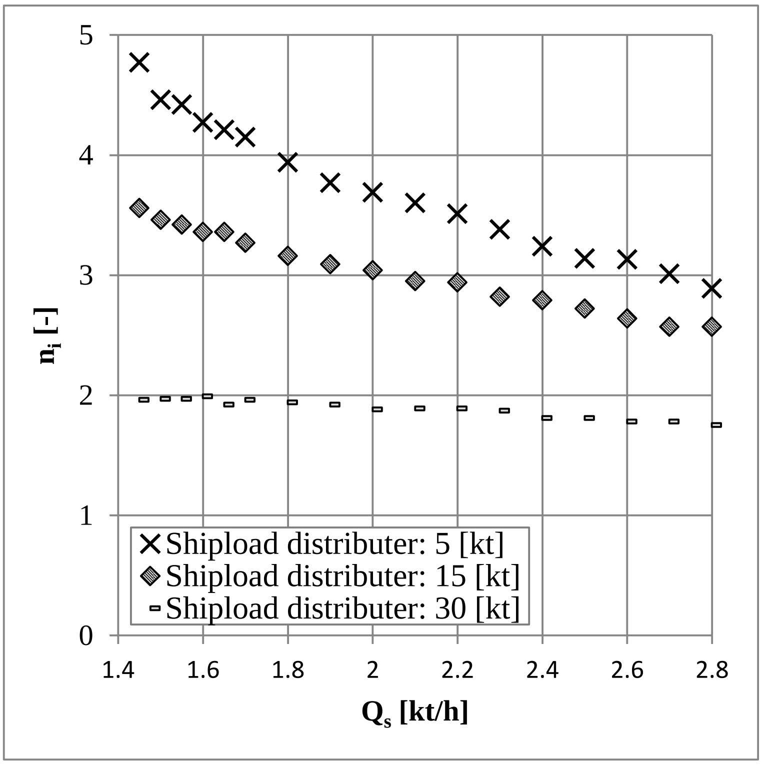

Figure 6.16: The average number of interruptions during ship unloading (n_i) as function of three different values for the shipload distributer

6.6 Case study: the selection of blending and homogenization machines

In this case study, preferred types of stockyard machines will be selected to deliver material with predefined characteristics to a coal-fired power plant. In Figure 6.17, a schematically representation of this case study is presented. From two different grades of coal a blending bed is formed and after reclaiming the final product is transported to the power plant. In this case study, the blending bed is composed out of two grades while in real operations blending beds are built up from a larger number of materials. Specific software is developed to support the terminal operations planner with the composition of blending beds.

Characteristics for both grades are listed in Table 6.6. These characteristics were derived from several references, which are listed in Table 6.6. The requirements for the final product that has to be delivered to the power plant are also listed in Table 6.6. Another requirement was the maximum weekly consumption of 200 [kt] of blended and homogenized material. This material has to comply with predefined requirements for the average value and standard deviation of the ash content to realize an efficient combustion process in the boiler.

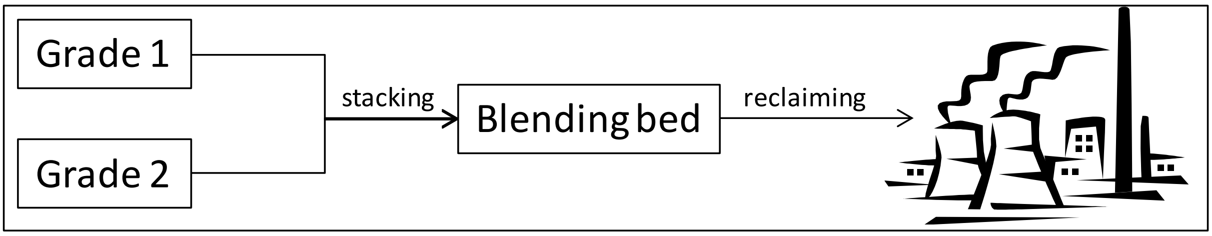

Figure 6.17: Schematically representation of delivering blended and homogenized material to a coal-fired power plant

Table 6.6: Characteristics for the base grades and the final product

Material property	Grade 1[1]	Grade 2[2]	Final product
Origin	Colombia	India	-
Mass [kt]	m_1= 149	m_2= 51	200
Heating value [MJ/kg]	31	18	27.7
Moisture [%]	4.6	12	6.5
Ash content [%]	4.4	45.6	15
σ_{ash} [%]	1.8[3]	3.4[3]	0.3

[1]derived from Tewalt et al. (2006) for the coal field with number IGM1237
[2]derived from Muthuraman et al. (2010)
[3]the standard deviations for the average ash content (σ_{ash} [%]) were derived from Dziunikowski and Stochalski (1983)

Equations (6.2) and (6.3) were used to determine the masses for the individual grades to realize the blending bed. The standard deviation for the average ash content of the blended bed can be determined using equation (6.8) by taken the individual mass fractions into account.

$$\sigma_{ash,BB} = \frac{m_1}{m}\sigma_{ash,G1} + \frac{m_2}{m}\sigma_{ash,G2} \tag{6.8}$$

Where $\sigma_{ash,BB}$, $\sigma_{ash,G1}$ and $\sigma_{ash,G2}$ [%] represent the standard deviation for the average ash content of the blending bed and the individual grades respectively, m_1 and m_2 [kt] represent the masses per grade, m is the mass of the blended bed.

In Figure 6.18 the variations for the ash contents are graphically presented as probability density functions for the grades, the blending bed and the final product. The standard deviation of the ash content of the blending bed (2.2%) does not comply with the predefined standard deviation for the final product (0.3%). To reduce the variability of the blending bed, the material must be homogenized by reclaiming the blended pile in such a way that multiple layers of materials are reclaimed at the same time.

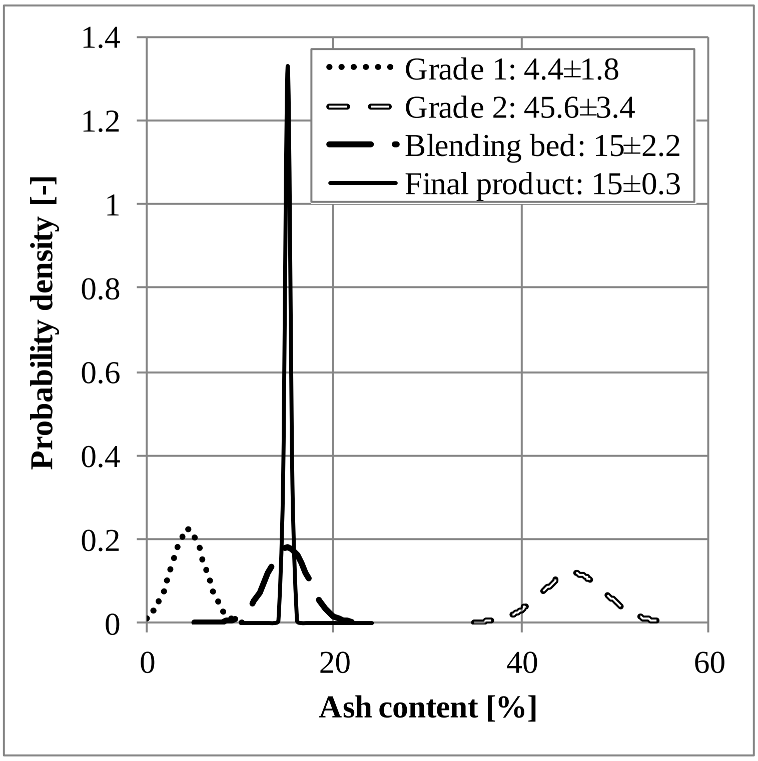

Figure 6.18: Probability density functions for the ash content for the grades from which the blending bed is composed and the final product

Equation (6.4) was used to determine the minimum required number of layers; the blending bed must be created by at least 113 different layers. Each layer must contain both grades distributed by their mass fractions. The blending/ homogenization effect was determined using equation (6.5) and becomes at least 7.3. After consulting Table 6.2, the combinations for the stacking method and reclaiming machine are listed in Table 6.7. In this table, the maximum attainable capacities for the reclaiming machines are also listed. These values are used to confirm that the selected machines are able to realize the reclaiming capacity needed. These maximum attainable capacities were determined by multiplying the values for the maximum capacity with the effective utilizations as listed in Table 6.1.

Table 6.7: Possible combinations for the stacking method, type of stacker and reclaimer to deliver blended and homogenized material to a coal-fired power plant

Stacking Method	Stacker	Possible reclaimer types	Maximum attainable reclaiming capacity [kt/h]
Chevron	Luffable boom	A) Bridge scraper reclaimer B) Bridge bucket wheel reclaimer C) Drum reclaimers	1.7 9.5 4.3
Windrow	Luffable boom Slewing boom		

In Table 6.7, the possible combinations for stacking and reclaiming are listed. The chevron as well as the windrow stacking method can be used. Building up a blending pile with the required large number of layers can best be realized using a stacker with a luffable boom. To deliver a mass of 200 [kt] within 7 days, the minimum required reclaiming capacity is 1.4 [kt/h] when assumed that the equipment is 20 hours per day in operation. For this case study, the combination of the chevron stacking method, a stacker with a luffable boom and a bridge scraper reclaimer satisfy the requirements. Bridge scraper reclaimers are built with a reclaiming capacity larger than 1.4 [kt/h] and the other machines as listed in Table 6.7 are technically more complex and therefore more expensive.

6.7 Conclusions

The characteristics determined for stockyard machines are necessary to realize an appropriate stockyard machine selection. The blending and/or homogenization effect for dry bulk materials relates to the stacking method used and the installed type of reclaiming machine. The selection for the stacking method, stacking and reclaiming machines was made for a case study where blended coal has to be delivered to a coal-fired power plant.

For the storage of material at stockyards, bucket-wheel stacker-reclaimers or individual stackers and bucket-wheel reclaimers are generally installed. For the selection of stacker-reclaimers or single stackers and reclaimers the stockyard model from Chapter 5 was extended with stockyard machines and the belt conveyors to transport the material. Simulation was needed for the machine type assessment to take the conflicting objectives for stacker-reclaimers for servicing ships or trains into account. As expected, simulation experiments have shown that stacker-reclaimers require higher capacities than individual machines to meet the predefined performance. However, based on the machines weight and by including the yard belt conveyors into the assessment, the investment costs for stacker-reclaimers are less compared to using individual stackers and reclaimers.

The reclaiming capacity for stacker-reclaimers can be reduced when piles, stacked on wide lanes, are accessible by two stacker-reclaimers or when ship servicing can be interrupted in favor of train loading.

For the expansion of the design methods concerning the stockyard machines, the following additions are formulated based on the research performed in this chapter:

1. At stockyards different functions have to be performed; buffering, blending and homogenizing of dry bulk materials. The blending effect required determines the stockyard machine selection. An overview of attainable blending effects for the combination of stacking method and reclaiming machine type is presented.
2. Individual stackers and reclaimers or dual-purpose stacker-reclaimers are generally installed at stockyards. The installation of stacker-reclaimer requires less investment costs but introduces limitations to simultaneously stacking and reclaiming from the same stockyard area. Using the transport network model enables a correct assessment of machine type by taking the conflicting objectives for stacking and reclaiming into account.
3. When stacker-reclaimers are installed, specific operational procedures like the redundancy of stacker-reclaimers (access of piles by two machines) and the interruption of ship servicing in favor of servicing trains will increase the terminal service demands.

7 Belt conveyor network design

This chapter is based on van Vianen et al. (2014c).

In this chapter the design and operation of belt conveyor networks are discussed. Belt conveyors are dynamically assigned to transportation routes to convey material from several sources to different destinations. Terminal operators strive for extended, flexible networks to perform multiple transportation activities simultaneously. Therefore, a large number of transfer points is installed to guide the streams of bulk materials between belt conveyors. However, these transfer points require extra power, maintenance and cleaning activities and are expensive. In this chapter the question is answered what the impact will be on the terminal performance when less connections are installed. Another design parameter is the type of the belt conveyor. At some terminals bi-way belt conveyors are installed but are these conveyors recommended to be applied at terminals? In this chapter, two case studies are described. In the first study, several network designs were formulated and assessed to be implemented in an existing terminal layout. In the second case study, two different route selection procedures were evaluated.

7.1 Introduction

Belt conveyors are widely used at terminals for the continuous transport of dry bulk materials. An advantage of continuous transport systems is the lower operational cost compared to discontinuous transport systems such as wheel loaders or dump trucks. Generally, discontinuous transport systems present lower capital costs but higher operational costs. Wheel loaders, dump trucks and mobile feeding bunkers are generally used at relatively small terminals (e.g., Dutch import terminals with an annual throughput less than 4 million tons). In this chapter transportation networks which consist of belt conveyors will be investigated.

All types of belt conveyors share the same components like the endless rubber belt, idlers to support the belt, a drive and tail pulley, a loading and discharge chute and a take-up system. Figure 7.1 shows schematically these main components.

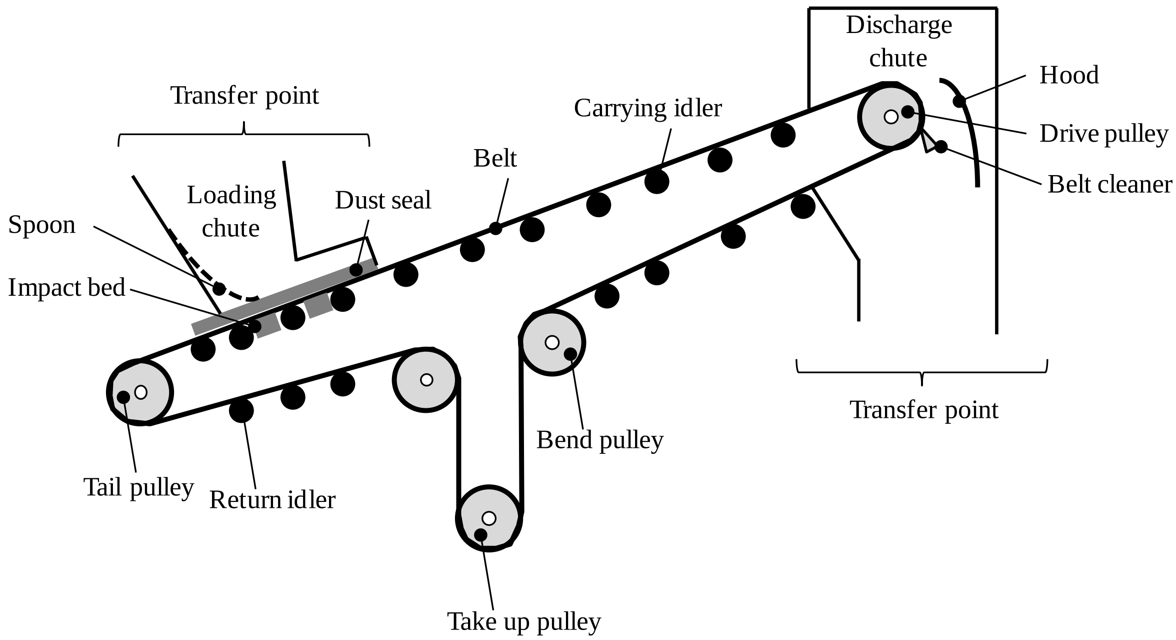

Figure 7.1: Simplified representation of a belt conveyor for the introduction of the main components

Improvement of the energy efficiency of belt conveyor systems can be achieved at equipment or operation level (Zhang and Xia, 2010). For the equipment improvement the idlers (e.g., Reicks, 2008), the belt material (e.g., Lodewijks, 2011) and the drive system (e.g., de Almeida et al., 2002) are the main targets to achieve a better efficiency. Switching control (e.g., Middelberg et al., 2009) and variable speed control (e.g., Hiltermann et al., 2011) are proposed to improve the energy efficiency of belt conveyor systems at the operational level.

At dry bulk terminals multiple belt conveyors are dynamically switched in series to connect several sources and destinations. Between different belt conveyors the material flow must be transferred in a so-called transfer point. The material is conveyed upwards by the first conveyor and dumped through a chute onto the receiving belt conveyor. The chute confines the material stream to reduce the dust creation. The '*hood*' in the discharge chute (see Figure 7.1) maintains a coherent stream of bulk materials and the '*spoon*' in the loading chute places the load on the receiving belt conveyor with proper speed, minimized dust creation and minimal material degradation. For the design of transfer points, many models were developed (Lodewijks, 2010). Examples are the "trajectory model" to describe the material stream from the belt onto the hood, the "impact model" and "chute flow model" to determine the hood and spoon geometry and the "free-fall model" to describe the falling of the material stream from the hood onto the spoon.

Thanks to extended belt conveyor networks at terminals the operation may continue by selecting another transportation route during a break down of a single belt conveyor. Most real-world belt conveyor networks are utilized with flexible connections between belt conveyors. Belt conveyors are then equipped with 'moving heads' where the drive pulleys can be put in different positions across multiple belt conveyors, see for a schematically representation Figure 7.2D. Disadvantages of these moving heads are the occurrence of extra disturbances during operation and the requirement for extra maintenance. In this chapter the reduction of the terminal performance will be investigated when the number of connections will be decreased.

At some dry bulk terminals bi-way belt conveyors (conveyors with two transportation directions) are installed instead of single-way belt conveyors. The transportation network becomes simpler but will this simplification result in a reduction of the terminal performance? This question will be answered in this chapter. Another research topic that will be discussed in this chapter is the operational control, and particularly the route selection within belt conveyor networks.

In conclusion, in this chapter the design of belt conveyor networks as function of the number of connections, the belt conveyor type (bi-way or single-way) and the operation of belt conveyor networks (route selection) will be investigated. This chapter is organized as follows: a literature review of the terminal integrated in the bulk supply chain, the belt conveyor network design and route scheduling is listed in section 7.2. Details of a route selection procedure based on routes' performances are presented in section 7.3. In section 7.4, experimental results which describe the effects of the network characteristics and routing flexibility on the network design, are presented. In section 7.5, the simulation model that was already developed in the previous chapter is used in a case study to assess two network designs and compare these designs with the existing layout. In a second case study, discussed in section 7.6, the belt conveyor network operation is investigated by evaluating two different route selection procedures. Finally, conclusions are presented in section 7.7.

7.2 Literature review

There is a surprising absence of research that investigates belt conveyor network design, possibly due to the protection of its substantial commercial value by industrial practitioners or consultancy companies. In chapter one it was mentioned that the most comprehensive design method for dry bulk terminals was already introduced by the United Nations Conference on Trade and Development in 1985 (UNCTAD, 1985). Unfortunately, this design method is not very specific and detailed and does not specify how the belt conveyor network should be designed.

Many references discussed models for freight transportation networks which might be applied to belt conveyor networks. These models are used to represent a wide range of planning and operations in transportation, telecommunications, logistics, and production-distribution systems. The objective of such models is to select links in existing networks in order to satisfy the demand for transportation at the lowest cost. Network models usually take the form of mixed-integer optimization problems for which no efficient, exact solutions exist, except for special variants. Heuristics are therefore proposed in most cases (Crainic, 2000). However, a model that can support the belt conveyor network design by taking stochastic processes into account was not found.

Research papers which address the integrated transport system in dry bulk supply chains are reviewed in section 7.2.1. A limited number of papers investigated the routing problem at dry bulk terminals, these papers are reviewed in section 7.2.2. In section 7.2.3, the routing problem for the continuous transport in Operations Research is discussed. The literature review is evaluated and the modeling approach selected is explained in section 7.2.4.

7.2.1 The terminal integrated in the bulk supply chain

Dry bulk terminals have to facilitate all transportation and storage needs imposed by bulk supply chains. Several operations within the bulk supply chains cannot easily be integrated for operational efficiency because of their complexity and the underlying stakeholder relationships by which they are structured. Due to the complexity of these supply chains the terminal operation can better be described as a combined push and pull scheduling problem than as a typical push or pull logistic system (Conradie et al., 2008). Many end users, traders and rail operators negotiate on prices, amounts and brands of dry bulk materials and particularly over the time window, in which the commodities should be available for shipping to and from the terminal (Kozan and Liu, 2012). These authors modeled an integrated train, ship and stockpile operation for a coal export terminal as a demand-responsive decision support system by extending train scheduling methodologies to deal with the real-world shipment problems.

Singh et al. (2010) proposed a large scale capacity planning model for a coal supply chain. A mixed-integer linear programming method was proposed to determine the handling capacity requirements through the supply chain. The needed dumping, stacking and reclaiming capacities could be determined but specific belt conveyor network details were missing.

7.2.2 The routing problem at dry bulk terminals

A limited number of papers discussed the routing problem at dry bulk terminals. In belt conveyor networks, conflicts may occur in deploying multiple routes simultaneously because these routes may share one or more belt conveyors. A simultaneous storage allocation and routing problem for a set of transportation requests was presented by Ago et al. (2007). This problem was also formulated as a mixed-integer linear programming problem. Langrangian decomposition and coordination approach were used to solve the problem. Transportation routes from three berths to several storage locations and from several stockpiles to the production facilities are proposed for a planning horizon of 45 hours. The authors acknowledged that actual stockyards operate under more complex situations than researched. Circumstances like machine accidents and weather conditions must be considered as well to create a more accurate tool.

Lodewijks et al. (2009) proposed several alternative belt conveyor networks for an export terminal. One of the proposed layouts showed a direct transshipment of material from arriving trains to ships. In another layout reversible (bi-way) belt conveyors were used instead of single-way belt conveyors. The material is transported in both directions when reversible belt conveyors are installed which will reduce the number of belt conveyors and transfer points. A further selection can be made for multiple shared or dedicated transportation routes. The authors proposed to apply discrete-event simulation to assess network designs based on the optimization of equipment and land use.

A research paper by Kim et al. (2011) described a heuristic approach for scheduling unloaded raw-material at a South Korean steelwork terminal. The solution covered the following decisions; assignment of berths to arriving ships, the allocation of unloading capacity to ships and the route selection. A two-fold decision making method was proposed that contains the berth-unloading process and the unloading-routing process. A tool was developed that is currently in use as a planning tool. The authors used a nondeterministic polynomial time approach for the selection of multiple routes. Routes which form a set in the route-independence graph were assigned to transportation needs.

A simulation-based decision support tool was introduced by van Vianen et al. (2012b) assisting a terminal operator to select the best transportation routes. The tool developed consists of two integrated simulation models. A primary simulation model, that simulates the terminal's operation and dynamics, and within this model, a secondary simulation model that simulates future scenarios and proposes route selections. Practical experiments have shown that the tool developed is useful for assisting terminal operations planners to select transportation routes or to present alternative routes if a conveyor or machine breaks down.

7.2.3 The routing problem in Operations Research

Numerous references were found which address route scheduling approaches for individual vehicles like automatic guided vehicles (AGV's) in automated container terminals or cars on highways. However, scheduling routes for the transport of material in a continuous mode has received significant less attention. Other related engineering applications such as the oil and food industry were investigated. Similar to the dry bulk industry products are transported in a continuous mode. A belt conveyor can be compared with a pipe and stockpiles with tanks. Promising references about pipeline network design (e.g., Mah and Shacham, 1978) formulated the optimal network design as a constrained minimization problem based on the number of pipe sections, the length and diameter of the pipe sections and cost coefficients which are directly related to investment costs. This problem corresponds with the determination of the required transport capacity of belt conveyors but did not give any suggestions for network layouts. Furthermore, a difference between dry bulk and tank terminals is that generally at tank terminals, product dedicated or customer dedicated pipelines are used between specific sources and destinations.

7.2.4 Evaluation and selection of the modeling approach

Models that can be implemented to support the design of belt conveyor networks were not found in literature. General network design models are used in freight transportation systems to assist the decision process concerning the construction or improvement of infrastructure and facilities, the selection of transportation services and the allocation of resources (Crainic, 2000). However, the network design models do hardly take the stochastic processes and varying material flows into account. Specific belt conveyor network characteristics (e.g., a transfer point can only be used by one route at the time) hindered the application of these models.

At dry bulk terminals several batches of materials must be transported simultaneously and on time while taking the stochastic arrival processes, equipment breakdown behavior and material flows into account. The transport network model as already introduced in chapter six will be used. The cyclic route selection procedure, as presented in section 6.4.2, is extended with the selection of preferred routes. By varying belt conveyor networks and by registering the terminal performances, relevant insight will be acquired to design such networks. Another application of the simulation model is to evaluate existing and planned networks.

7.3 Route selection based on routes performances

A selection of routes based on route performances can be made when multiple routes can perform a required transportation activity. In this research the objective of the selection procedure was to limit the energy required for transportation and to limit maintenance activities. For all transportation routes performance indicators were defined. It was assumed that these route performance indicators relate to the number of belt conveyors in the route, the total route length and the number of transfer points. Other objectives for the selection procedure like the selection of routes that hinder the least other routes are not investigated in this research.

The first term was defined as the number of belt conveyors in a route. An increase of this number will decrease the route reliability and will increase the required power to transport materials. A performance indicator that relates to number of belt conveyors is called (J_{cv}) [-] and is expressed algebraically in equation (7.1). This indicator relates to the route that contains most belt conveyors, the route with the highest number of belt conveyors gets the lowest value for this indicator.

$$J_{cv} = \left(1 - \frac{n_{cv} - n_{cv,\min}}{n_{cv,\max} - n_{cv,\min}}\right) \tag{7.1}$$

Where J_{cv} [-] is the performance indicator that relates to the number of belt conveyors, n_{cv} [-] is the number of belt conveyors in a route, $n_{cv,max}$ and $n_{cv,min}$ [-] are the maximum and minimum number of belt conveyors in a route respectively.

An increase of the route length will result in an increase of the required transportation power. This fact forms the basis for the second term of the performance indicator, J_{rl} [-] and is expressed in equation (7.2). The route with the maximum transportation length gets the lowest value.

$$J_{rl} = \left(1 - \frac{L_{r} - L_{r,\min}}{L_{r,\max} - L_{r,\min}}\right) \tag{7.2}$$

Where J_{rl} [-] is the performance indicator that relates to the route length, L_r [m] is the length of the route, $L_{r,max}$ [m] is the maximum route length number and $L_{r,min}$ [m] is the minimum route length.

The needed power to transport material depends also on the number of transfer points because the material must be conveyed up before it can be dumped onto another belt conveyor. Transfer points introduce additional costs due to the required maintenance (wear of the hood, spoon and the chute) and cleaning activities to remove (manually) the spillage around these transfer points. As third term an indicator was defined that relates to number of transfer point in a route, see equation (7.3). The route with the maximum number of transfer points gets the lowest value.

$$J_{tp} = \left(1 - \frac{n_{tp} - n_{tp,\min}}{n_{tp,\max} - n_{tp,\min}}\right) \tag{7.3}$$

Where J_{tp} [-] is the performance indicator that relates to the number of transfer points, n_{tp} [-] is the number of transfer points in a route, $n_{tp,max}$ [-]and $n_{tp,min}$ [-] are the maximum and minimum number of transfer points a route.

After a discussion with technicians at dry bulk terminals, it appeared that an increase of the number of transfer points resulted in higher additional costs than the increase of energy costs for longer routes. To consider the relevance for the different route attributes weighing factors (φ_1-φ_3) are introduced. Values for the weighing factors were determined in consultation with terminal operators. The following values can be applied; φ_1: 0.2, φ_2: 0.3 and φ_3: 0.5 respectively. These values will be used in this research but values for these weighing factors can be set individually. Finally, the route performance indicator was defined as the sum of the performance indicators multiplied with subjective weighing factors, or expressed algebraically:

$$J = \phi_1 J_{cv} + \phi_2 J_{rl} + \phi_3 J_{tp} \tag{7.4}$$

Where J [-] is the route performance, φ_1-φ_3 [-] are the weighing factors for the number of belt conveyors, route length and the number of transfer points respectively. J_{cv}, J_{rl} and J_{tp} [-] are the route performance indicators for the number of belt conveyors (see equation 7.1), the route length (see equation 7.2) and the number of transfer points (see equation 7.3) respectively. Note that the route with the minimum number of belt conveyors, minimum route length and minimum number of transfer points gets the highest route performance indicator of 1.

Two different route selection procedures will be investigated in a case study in section 7.6; the '*cyclic routes selection'* and the '*preferred routes selection*'. The cyclic routes selection procedure was already introduced in section 6.4.2 and assigns available routes in succession to transportation activities. Applying the cyclic route selection will result that all routes will be used during operation. For the preferred routes selection, routes are sorted based on their performance indicator. When multiple routes are possible, the route with the highest route performance indicator will be selected.

7.4 Simulation experimental results

Several experiments were performed using the transport network model that was already introduced in chapter 6, to investigate the consequences of the number of connections and belt conveyor type on the belt conveyor network design.

A new indicator was defined to express the measure of the network's robustness. This indicator, called τ [-], expresses the ratio between the number of installed and the maximum number of transfer points, or expressed algebraically:

$$\tau = \frac{n_{tp}}{n_{tp,\max}} \tag{7.5}$$

Where τ [-] represents the network's connectivity, n_{tp} [-] is the number of transfer points installed and $n_{tp,max}$ [-] is the maximum number of transfer point possible in the belt conveyor network.

The maximum value for the network's connectivity is 1 that represents a transportation network where all possible connections between belt conveyors can be realized, see for example the stockyard layout as shown in Figure 6.12. When the number of connections decreases, the network's connectivity decreases as well. For example, for the network as shown in Figure 7.2A the network's connectivity (τ) becomes $^{7}/_{12}$. This network is equipped with seven transfer points while the maximum number is twelve. Note that several network configurations can result in the same value for the network's connectivity.

In Figure 7.2D, a possible configuration to connect an overhead belt conveyor with either the first receiving belt conveyor or the second one is shown, the moving head. When the moving head is positioned in its rear position, the material is dumped onto the first receiving belt conveyor. When the moving head is moved forward, the overhead belt dumps the material onto the second receiving belt.

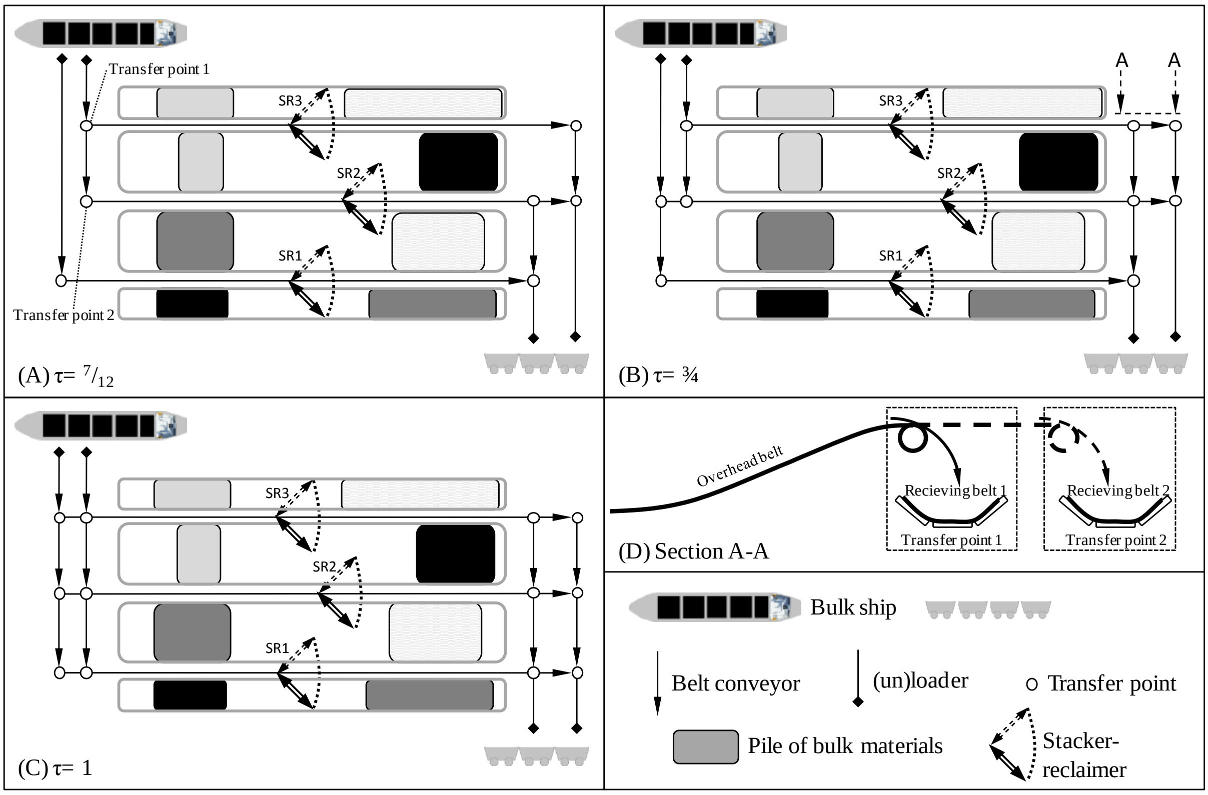

Figure 7.2: Evaluated belt conveyor networks with different values for the network's connectivity (τ)

Table 7.1 lists the input parameters used for the simulation experiments. The storage capacity was defined in such a way that bulk ships do not have to wait before delivering their material due to a lack of storage area. That explains the high value used for the stockyard lane length. Furthermore, it was assumed that the terminal acts as an import terminal. Material is delivered by bulk ships and at the terminal's landside only trains are used to transport material to the industrial clients. As performance indicators the average port times for ships and trains will be determined as well as the realized annual throughput in million tons per year [Mt/y].

The run control for the transport network model was already addressed in section 6.4.5 and because comparable distribution types are used, a simulation run time of servicing 2,500 ships is applied realizing an accuracy (expressed by the standard deviation of the average ship port time) of ±2%.

Figure 7.2 shows the investigated terminal layouts with different values for the network's connectivity. Figure 7.2A shows a limited connectivity ($\tau = {}^{7}/_{12}$) and Figure 7.2C shows a belt conveyor network where all belt conveyors can be connected with each other ($\tau = 1$). Each layout contains three stacker-reclaimers (SR1-SR3), two ship unloaders and two railcar loaders. It was assumed that ships can moor at any positions along the quay and trains can be loaded at both loaders.

Table 7.1: Input parameters for the simulation experiments and case studies

Parameter	Description	Value	Unit
IATDist	Interarrival time distribution of ships	NED	
SlDist	Shipload distribution	See Figure 3.21B	
sl	Average shipload	101	[kt]
T_s	Average storage time	500	[h]
STDist	Storage time distribution	NED	
η	Equipment technical availability	0.97	[-]
Trainload		4	[kt]
w	Lane width	50/90	[m]
L_l	Stockyard lane length	2000	[m]
α	Angle of repose	38	[°]
ρ	Bulk density	2.8	[t/m^3]
d	Separation distance	2	[m]
Q_s	Stacking capacity	2.5	[kt/h]
Q_r	Reclaiming capacity	2.5	[kt/h]

In Figure 7.3, the average port times for ships and for trains are presented versus the annual throughput for the investigated networks of Figure 7.2. As expected, the average ship port time decreases for increasing values of the network's connectivity. However, from Figure 7.3A it can determined that an increase of the network's connectivity from ¾ to 1 will not bring any significant improvement anymore for the investigated belt conveyor networks. From Figure 7.3B it can be seen that the average port time for trains increased slightly for increasing values of the network's connectivity. An explanation is that trains have to wait more often because the stockyard machines are more frequently occupied by servicing the ships.

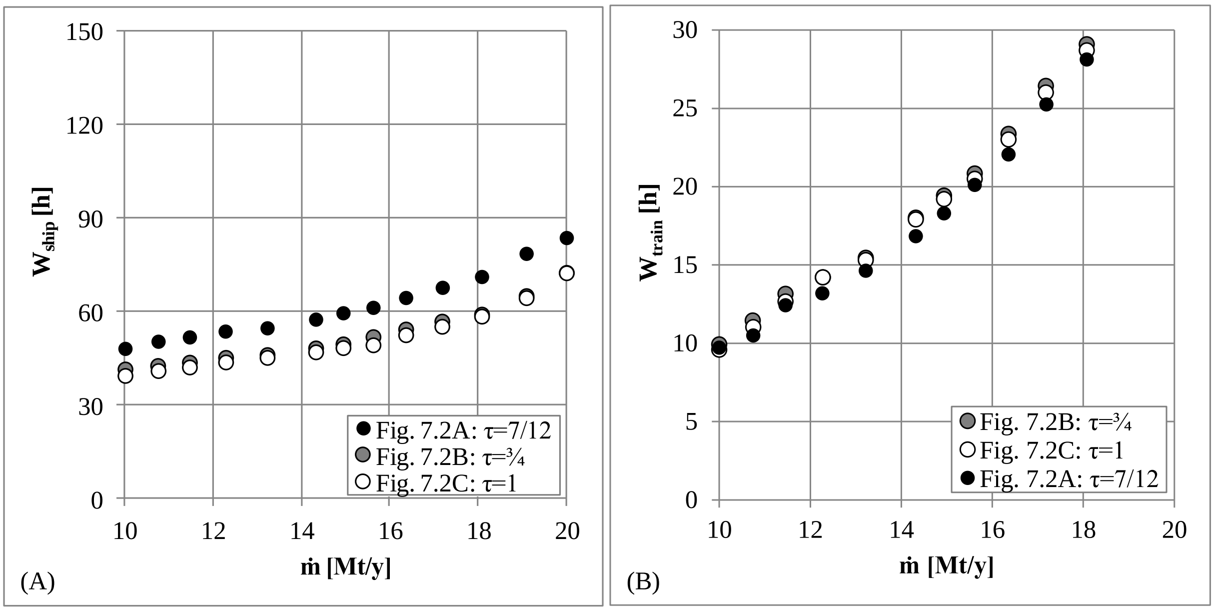

Figure 7.3: The average port times for ships (A) and trains (B) versus the annual throughput for the belt conveyor networks of Figure 7.2

The transport network model supports the design process of belt conveyor networks. The following steps must be taken to define an appropriate belt conveyor network. The first step is to formulate the most extended transport network. Such network connects all seaside and landside machine with the stockyard machines. The second step is to feed the transport network model with correct input data with a particular focus on correct stochastic distributions for the case under study. The third step is to determine the terminal performance using the transport network model. In the fourth step, the number of connections is reduced when the terminal performs initially better than required as long as the requirements are met. For example, a reduction of the connectivity between seaside and stockyard machines reduces the seaside performance. The assessment of alternative networks provides insight which layout still meets the predefined requirements.

When bi-way belt conveyors are used instead of single-way belt conveyors, the number of belt conveyors and transfer points can be reduced. Figure 7.4 shows a belt conveyor network with bi-way yard belt conveyors. Only six transfer points are needed to realize all connections. The network's connectivity (τ) becomes ½. The impact on the terminal performance was investigated and the results are shown in Figure 7.5.

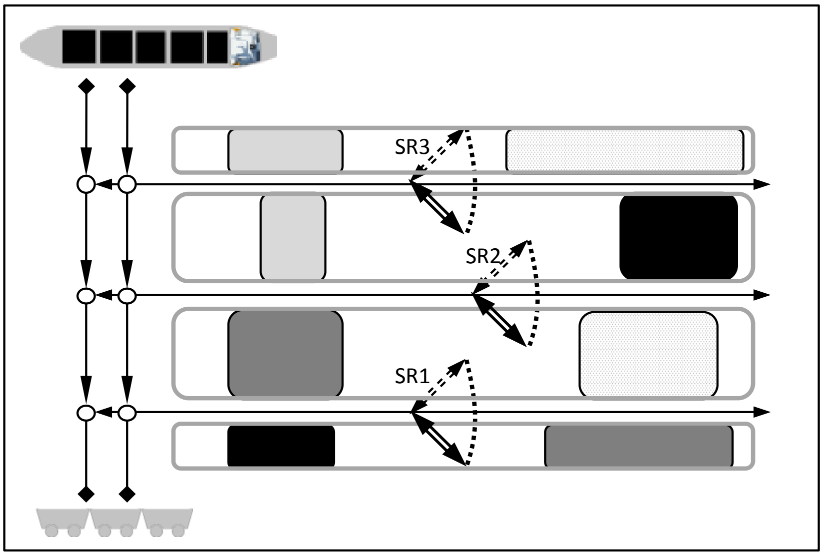

Figure 7.4: A belt conveyor network equipped with bi-way yard belt conveyors

From Figure 7.5B it can be concluded that a belt conveyor network with bi-way yard conveyors resulted in a significant increase of the average train port time. This increase can be explained by the higher utilization of the cross belt conveyors (conveyors to connect the (un)loaders with the yard conveyors) in the network of Figure 7.4. These conveyors have to transport the incoming as well as the outgoing streams of bulk materials. A possibility to increase the performance is to install a third line of cross conveyors next to the current two one. However, these cross conveyors need an extra unloader and loader; the network's connectivity (τ) will then be increased from ½ to ¾.

Installing bi-way belt conveyors as yard conveyors together with a limited number of belt conveyors (like in Figure 7.4) is not recommended due to the reduction of the terminal performance. Moreover, bi-way belt conveyors show a lower availability than one-way belt conveyors due to the fact that they are more complex (more mechanical components, tracking of the belt becomes more of an issue). Also the transfer points have to be designed more carefully due to the fact that more transfers have to be installed in a certain area (Lodewijks et al., 2009).

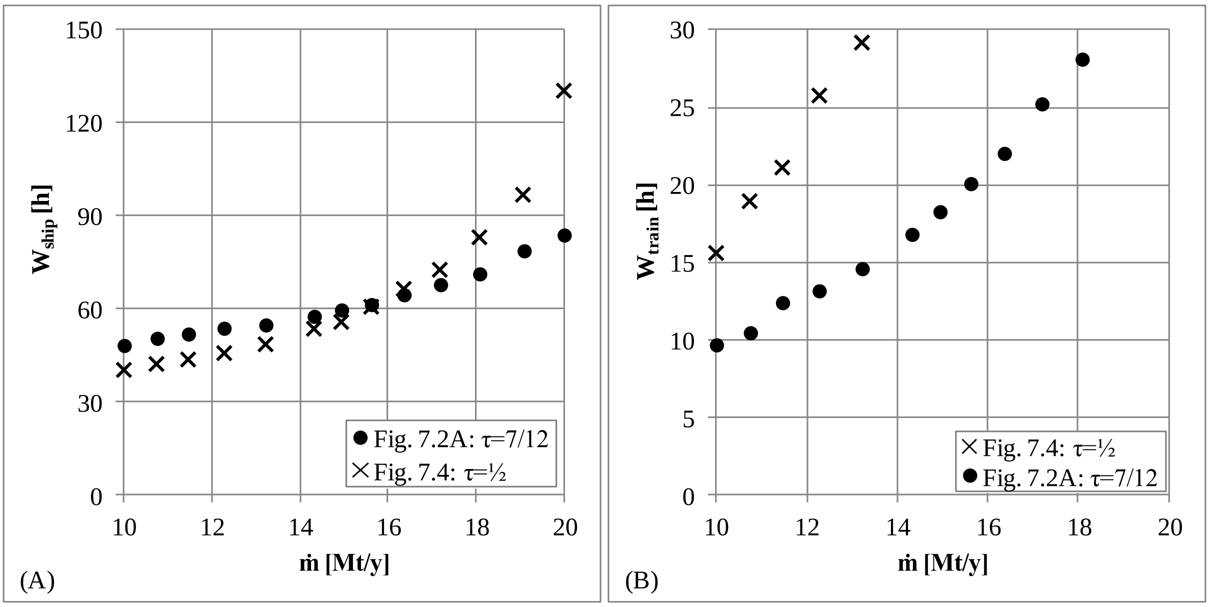

Figure 7.5: The average port times for ships (A) and trains (B) for a network with bi-way belt conveyors (Fig. 7.4) and a network with single-way belt conveyors (Fig. 7.2A)

7.5 Case study 1: belt conveyor network redesign

The simulation model as already explained in the previous chapter was used for a multi-user import terminal to redesign a specific part of an existing belt conveyor network. Figure 7.6 shows the terminal layout as it was in 2011. Six stacker-reclaimers (SR1-SR6) were installed and three quay belt conveyors (QCV1 – QCV3) were used to transport unloaded bulk materials from the quay to the stockyard. The stockyard consists of seven stockyard lanes (L1-L7) for which it was assumed that the outer lanes (L1 and L7) have a width of 50 meter and for the remaining lanes the width is 90 meter. Eight different loading machines are installed; two railcar loaders, a loader for coastal ships, three barge loaders, a belt conveyor that transports the material to a coal-fired power plant, and a belt conveyor that feeds material to one of the six blending silos. The transport activity of material out of the silos to the coal-fired power plant or a barge loader was not included in this research. It was assumed that this activity could be scheduled during the idle times of the required belt conveyors.

The terminal operator planned to revise the 'backbone' of its belt conveyor network. Within this part, shown with the hatch filled rectangle in Figure 7.6, many connections between different belt conveyors can be made. Figure 7.7 shows the existing backbone's belt conveyor network and two designs. For each network the network's connectivity (τ) [-] within the backbone was determined by dividing the number of transfer points installed with the maximum number of transfer points (52). This maximum number was determined as follows; the three quay conveyors need to be connected with three stacker-reclaimers (SR1-SR3) (resulting in 9 transfer points), six stacker-reclaimers (SR1-SR6) need to be connected with five loading machines (6x5 = 30 transfer points), to realize direct transshipment from the quay using the unloading cranes to barges the three quay conveyors need to be connected with three barge loaders (9 transfer points) and four transfer points are needed due to the geographical locations of barge loaders 1 and 2.

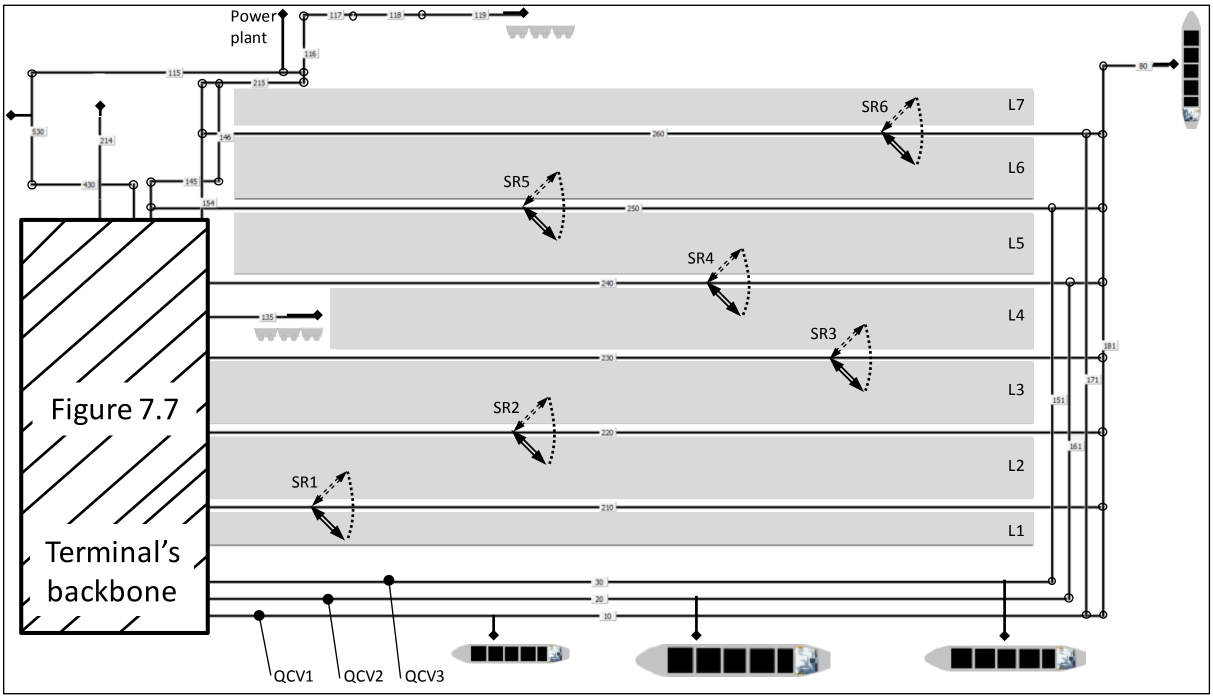

Figure 7.6: The investigated terminal layout with the specification of the network’s part (shows as the terminal’s backbone) that needs to be redesigned

For the formulation of the several designs the following procedure was followed. A source-destination matrix was composed for the existing layout that shows the possible connections between sources (quay conveyors or stacker-reclaimers) and destinations (stacker-reclaimers and loading machines). Subsequently, this matrix was used to define all connections needed for the two designs. For the first design (Figure 7.7B) it was defined that the same network’s connectivity needs to be realized as in the existing layout. Not even all connections should be the same as in the existing layout but even the simultaneity of the transportation activities should be remained. In Design 2 (Figure 7.8A) the network’s complexity was reduced by maintaining the same number of connections but allowing that some transportation activities cannot be performed simultaneously. Design 3 (Figure 7.8B) is a combination of Layout 2011 and Design 1; some transfer points remained intact while also dedicated belt conveyors to loading machines are proposed.

According the requirement of the terminal operator the yard belt conveyors and the belt conveyors to the loading machines should remain intact. In Design 1 (Figure 7.7B) dedicated belt conveyors (numbered with 100, 111, 121, 131) are proposed between the stacker-reclaimers (SR1: 210, SR2: 220 and SR3:230) to loading machines. Using dedicated belt conveyors decreased the number of belt conveyors in the network from 51 to 45 belt conveyors. Two extra transfer points are needed and the network’s connectivity (τ) becomes 0.94. Main advantages for this solution are the reduction of the total disturbance time, thanks to the decrease of the number of belt conveyors, and the decrease of the transportation power because the material does not need to be fed up as frequent as in the existing network.

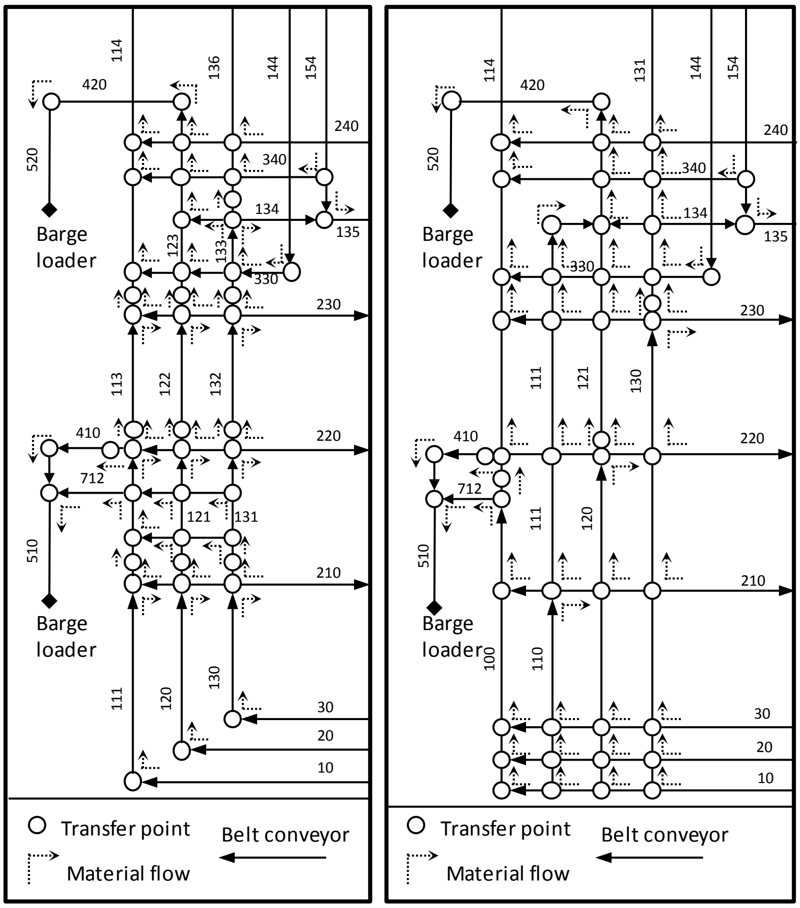

(A) Layout 2011 (τ: 0.9) (B) Design 1 (τ: 0.94)

Figure 7.7: Different configurations for the backbone's network; the existing layout (A) and (B) Design 1 with dedicated belt conveyors and an extra cross-conveyor (100)

Design 2 (Figure 7.8A) applies the fundamentals of the first design; the quay conveyors are equipped with moving heads and the same dedicated belt conveyors as in design 1 are proposed for the transport to the loading machines. However, a concession was made that the transport of materials to the second barge loader (represented with belt 520) cannot be performed at the same time when material is transported to the iron ore railcar loader (represented with belt 135) or to the blending silos (is belt 114). This concession was justified by the fact that at the terminal three barge loaders are installed so one of the other barge loaders can probably be used. Moreover, based on historical data a relatively small amount of material (only 11% of coal) is fed to the blending silos so the probability is limited that this conflicting situation will occur. Minor connections are then needed that results in a lower value for the network's connectivity, τ becomes 0.83.

In Design 3 (Figure 7.8B) some belt conveyors (113, 114, 120, 130, 131 and 132) and corresponding transfer points remained intact. Based on the judgment of the terminal operator these belt conveyors and transfer points are in good technical condition and can be re-used. In this design dedicated belt conveyors (111 and 121) and an extra cross conveyor (100) are also proposed. The advantage of Design 3 is that each stacker-reclaimer can be reached by at least two cross conveyors contrary to Design 1 and Design 2 where each stacker-reclaimer has it's specific cross conveyor. The number of transfer points increased significantly resulting in a network connectivity of 0.98. Note, that the maximum number of transfer points was determined for Layout 2011 but Designs 1 until 3 are equipped with extra cross conveyors (100 and 111) resulting that the network's connectivity (τ) can achieve higher values than 1.

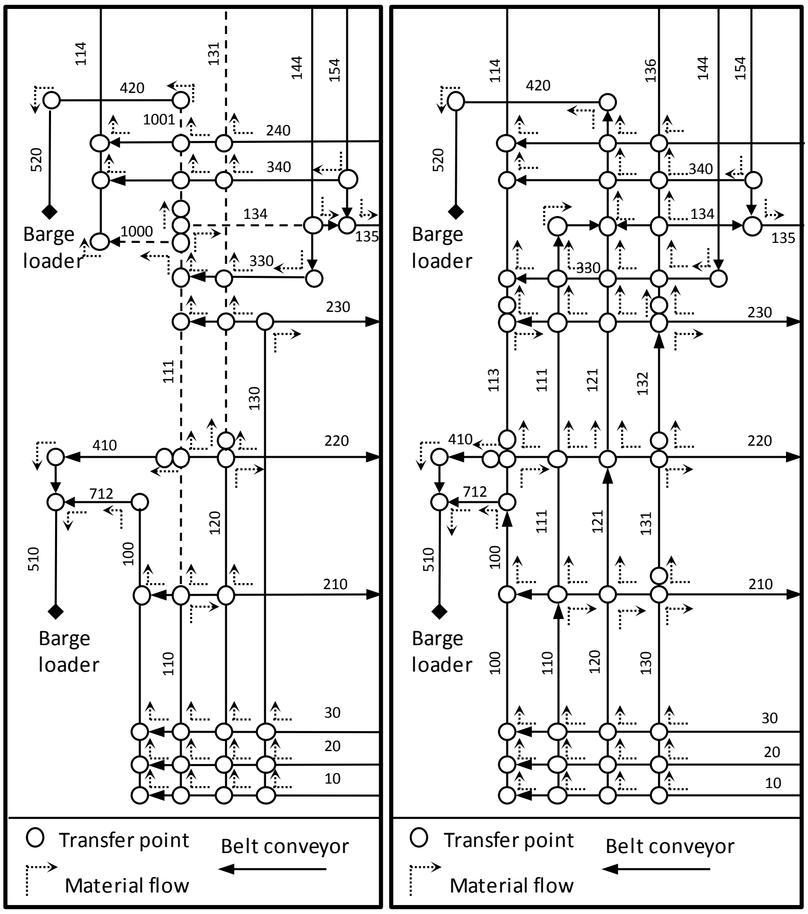

(A) Design 2 (τ: 0.83) (B) Design 3 (τ: 0.98)

Figure 7.8: Design 2 with a reduced number of transfer points (A) and B) Design 3 which is a combination of Layout 2011 and Design 1 (details are given in text)

Direct transshipment of materials is not included in the simulation model that implicates that all materials have to be stored onto the stockyard before being transferred. In this study, it was assumed that all landside jobs have the same size, i.e. 4 [kt]. To each stored pile a specific loading machine is assigned based on empirical data of the relative throughput per loading machine. After the expiry of the storage time, a landside job arrives at the predefined loading machine to be loaded. Contrary to train loading, the selection for one of the three barge loaders is made based on the availabilities of the stacker-reclaimers, barge loaders and the belt conveyors that feed these barge loaders. Routes were assigned to transportation activities cyclically (see for more details about this route selection procedure section 6.4.2).

For the terminal layout of Figure 7.6 together with the three network layouts as shown in Figure 7.7B and Figure 7.8, the average port times for ships and landside jobs (trains, barges, coastal ships and exports to the coal-fired power plant) were determined as function of the annual throughput. The average ship port times are shown in Figure 7.9A and the average port time for the landside jobs are presented in Figure 7.9B. From this figure two conclusions can be drawn. Firstly, the average port times is reduced for the three designs in comparison to the layout in 2011, and secondly, there is hardly any difference in performance for the three designs. In all the three designs, the average port times are reduced. Especially, the reductions of the average train port time are remarkable. These improvements are primarily determined by the implementation of moving heads in the quay conveyors realizing a higher availability to transport material to the stacker-reclaimers, the extra cross conveyor (belt 100) and less disturbances due the reduction of the number of belt conveyors.

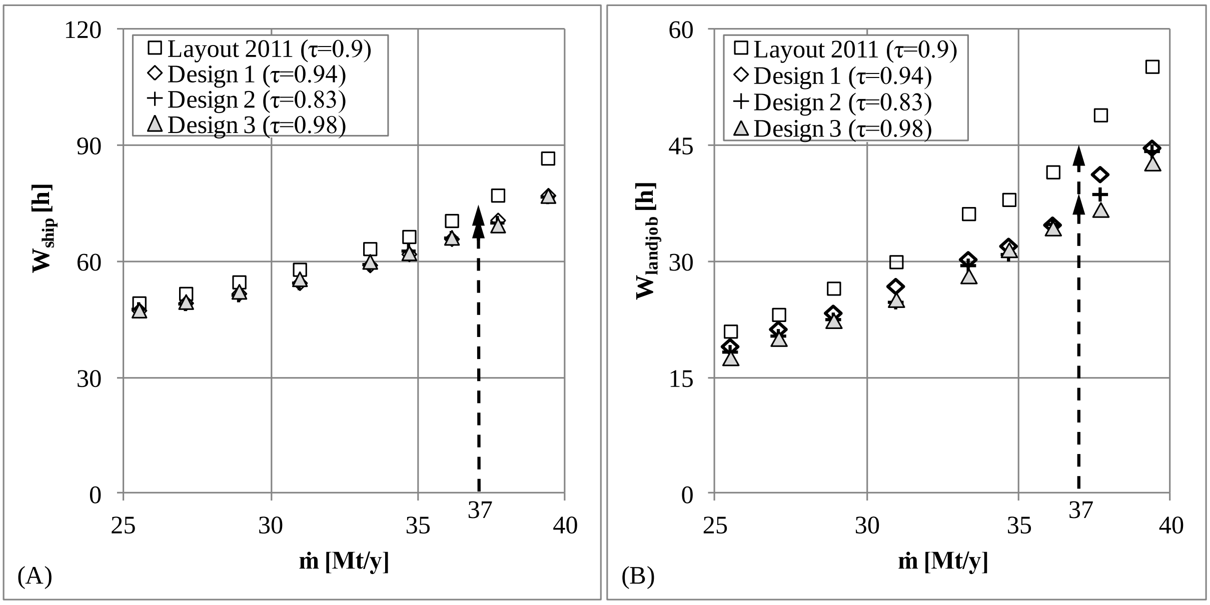

Figure 7.9: The average port times for ships (A) and landside jobs (B) versus the annual throughput for the terminal layout of Fig. 7.6 together with the layouts of Fig. 7.7

The minor difference in port times between the three designs is notable. Although the value for the network connectivity differs, the performance remains comparable. Especially, for Design 3 it was expected that this layout should perform better thanks to the high value for the network connectivity. Further analysis has shown that the time lost due to disturbances was higher for this layout due to the increased number of belt conveyors annulling the performance improvement thanks to the increased number of connections.

In Design 2, the network connectivity was reduced by eliminating belt conveyors and transfer points in such manner that some activities cannot be performed simultaneously anymore compared to Layout 2011. Apparently, these conflicting activities did not happen frequently during simulation which can be explained by the input parameters used. These parameters were based on historical data. However, if these activities will be required more frequently in future (the belt conveyor network is installed for the next thirty years), the proposed reduction of network connectivity will limit the terminal performance.

For a correct selection of the final layout, additional selection criteria like the investment costs and operational costs (e.g., maintenance, cleaning, personell and energy costs) must be considered as well. The transport network model can be applied to assess the terminal performance for several belt conveyor networks.

7.6 Case study 2: route selection in a belt conveyor network

In the second case study, the impact of two route selection procedures on the terminal performance will be determined. The first route selection procedure is called the '*cyclic routes selection*' (CRS). Using this procedure, already introduced in section 6.4.2, available routes are assigned one after the other to transportation activities. The second route selection procedure is called the ‘*preferred routes selection’ (PRS).* This procedure was explained in section 7.3. If there are multiple routes possible for a specific transportation need, the route with the highest value for the route performance indicator will be selected.

The terminal layout (Figures 7.6 with 7.7A) discussed in the previous section as it was in 2011, was used in this case study. The average port times for ships and land jobs are determined when both route selection procedures were applied. These results are shown in Figure 7.10.

An extra parameter was defined to express the average performance of the selected routes. This parameter, called J(avg) [-], was determined after each simulation run by dividing the sum of the performances of the selected routes with the number of routes. A higher value for the average route performance indicates that better performing routes were more frequently selected and will result in a reduction of the power required to transport materials. Furthermore, less maintenance and cleaning is required because less transfer points are used. For both route selection procedures, values for the average route performance are listed in the legends of Figure 7.10.

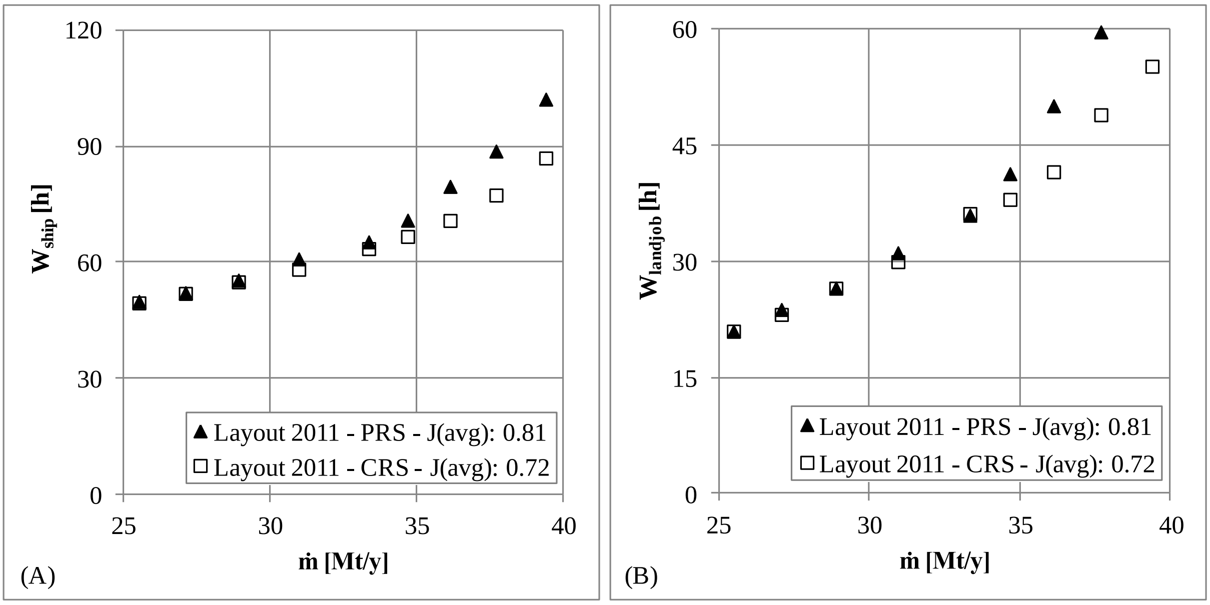

Figure 7.10: Evaluation of two route selection procedures for the terminal layout as shown in Fig. 7.6 combined with Fig. 7.7A

As expected the average route performance gets a higher value when the *preferred routes selection* is selected. However, the average port times for both ships and landside jobs increased, especially when the annual throughput exceeds the 34 [Mt/y]. This increase can be explained by the following reasons. Firstly, when the *cyclic routes selection* is applied the exports to barges is equally distributed over the three barge loaders. However, when the PRS is used one of the barge loaders (with belt conveyor 520) is significantly fewer times used because routes to this barge loader are relatively long and contain many transfer points. The second reason is that when PRS is applied, preferred routes are as first selected but some routes hinder the use of other routes at the same time. Another disadvantage of using the PRS is that a limited number of belt conveyors is used more frequently which will result in more wear and tear of these preferred belt conveyors.

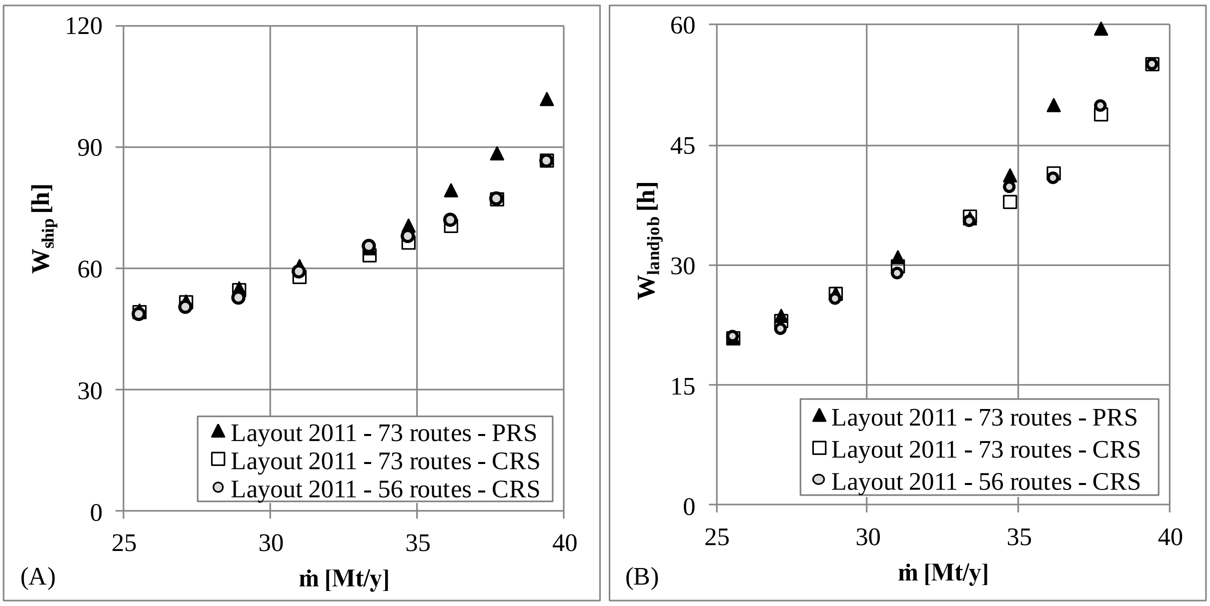

Figure 7.11: The average port times for ships (A) and landside jobs (B) versus the annual throughput for different numbers of routes

The simulation model was used for the determination of the routes that are hardly used when the preferred route selection procedure was applied. These routes must only be available to be selected when major break downs of belt conveyors occur or long maintenance activities are planned. Simulation results showed that seventeen routes were never or hardly used. Originally, the layout 2011 contained 73 routes and this number was reduced to 56. Subsequently, simulation runs were performed by assigning the 56 routes cyclically to the transportation activities. Results for these experiments are presented in Figure 7.11 (’*Layout 2011 - 56 routes – CRS’).* The remaining series in this figure were already shown in Figure 7.10. From Figure 7.11 it can be concluded that a reduction of the number of routes will hardly increase the average port times for ships and landside jobs. The proposed reduction of the number of routes will benefit terminal operators to select appropriate routes from a small list.

7.7 Conclusions

Terminal operators strive for extended belt conveyor networks to perform multiple transportation activities at the same time. Flexible connections, mostly carried out with moving heads between belt conveyors, are widely accepted. Disadvantages for such flexible connections are that these connections require extra power because material must be fed up to be dumped on other belts and extra maintenance and cleaning is required due to spillage of bulk materials. Furthermore, the flexible connections require extra investments compared to fixed connections.

Simulation results have shown that an increase of the number of connections in a belt conveyor network decreased the average port times for ships and for landside transportation modalities. However, from a certain level of connectivity (in the investigated network at about 75% of the maximum number of connections) a further increase of the network’s connectivity did hardly bring a significant improvement of the terminal performance. Another finding was that a network that contained bi-way belt conveyors performed worse than a network with single-way belt conveyors due to the higher occupation of the cross belt conveyors that connect the (un)loaders with the stockyard machines.

Simulation proved to be a tool to support the design process of belt conveyor networks. For a case study, three designs were formulated for the replacement of a part of an existing belt conveyor network. Simulation results have shown that the newly formulated designs perform better than the existing layout thanks to the implementation of moving heads in the quay belt conveyors, an extra cross conveyor and reduced disturbances as a result of the reduction of the number of belt conveyors. Another finding was that the designs formulated perform comparable even with different values for the network connectivity.

Route selection is an important procedure in the network's operation because several routes require the same belt conveyors. Two route selection procedures were evaluated; the cyclic routes selection (all routes are assigned in succession) and the preferred routes selection (better performing routes are selected as first). Simulation results have shown that when the preferred routes selection is applied the average port times will slightly be increased. The reason for this increase was that the use of preferred routes hindered the number of transportation activities that can be performed simultaneously.

For the expansion of the design methods concerning the belt conveyor network design, the following additions are formulated based on the research performed in this chapter:

1. Despite the tendency to install maximum flexible belt conveyor networks, where many transportation routes can be realized at the same time, the need for flexibility required must be investigated carefully. Moving heads between belt conveyors are commonly used to realize flexible connections. Such flexible connections require extra power to feed up the material, extra maintenance and cleaning activities and are expensive to realize.
2. Several belt conveyor networks were analyzed using the transport network model. This analysis has shown that installing the maximum number of connections does not always bring a performance improvement anymore.
3. Installing bi-way belt conveyors is not recommended when there is a limited number of (un)loaders and cross-conveyors preventing the use of multiple routes at the same time.
4. Route selection within belt conveyor networks will reduce the total power required by selecting 'better performing' routes in advance. However, simulation studies have shown that better performing routes may also hinder the use of other routes, which may result in a reduction of the terminal service performance.

8 Total terminal design

The total terminal design covers the various subsystems and the dependencies between these subsystems. Designing subsystems assisted by individual simulation models realize local solutions. However, some subsystems relate to each other and have to be designed together. In this chapter the total terminal model is introduced. This model is composed out of the seaside and landside model, the stockyard model and the transport network model. The total terminal model was validated using real-world operational data. Simulation results proved that this model provides realistic outcomes. The total terminal model was used to formulate and assess terminal designs. The necessity for an integrated design approach was demonstrated in a case study where a distribution center for dry bulk materials for a dedicated client needs to be integrated into an existing terminal. Furthermore, the total terminal model was used to assess designs and to evaluate if predefined requirements were met.

8.1 Introduction

In the previous chapters the dry bulk terminal was decomposed into subsystems. Each subsystem was investigated individually by assuming that it was not influenced by others. However, this assumption does not comply with the daily operation where the coherence of the subsystems determines the overall terminal performance. For example, the ship unloading operation can be retarded either due to the unavailability of unloading cranes, stacker-reclaimers or transportation routes or due to the lack of storage area. To obtain an accurate representation of the entire terminal operation the subsystems have to be merged into one model.

The chapter's objectives are to introduce the total terminal model that includes all subsystems, to validate this simulation model, to apply this model during the terminal design process, and to present features of the model. This chapter is organized as follows; details for the total terminal model are presented in section 8.2. Features for the total terminal model are mentioned in section 8.3. Results for the validation study are shown in section 8.4. In section 8.5, a previously defined terminal layout is evaluated using the total terminal model and an alternative layout is determined. In section 8.6, a design is formulated and assessed to implement a '*dry bulk distribution center*' into an existing terminal. Finally, conclusions are presented in section 8.7.

8.2 Total terminal model

For the realization of a simulation model that covers all terminal operations two possibilities were investigated. The first option was to develop a distributed model and the second option was to develop one single, large simulation model. In a distributed model, a server mechanism (the 'TomasServer' has specifically been developed for this functionality) realizes the synchronization of separately designed simulation models. The individual models can be considered as clients who ask permission to the server for each event. Reasons to use distributed modeling instead of stand-alone modeling are inter alia, individual sub models can be expanded or detailed without changing other models and distributed model can be runned real-time as a virtual environment for testing real resources and control functions (Ottjes and Veek, 2003). A disadvantage of using distributed models is that the simulation time will increase significantly due to the relatively slow communication between the individual models and the server (Duinkerken et al., 2002).

In this research, the second option to develop a large simulation model was followed. The reasons are the increase of the simulation time when distributed simulation will be applied and the fact that the total terminal model could be built relatively easy. The transport network model already includes the stockyard operation, stockyard machines and belt conveyors; only the seaside operation has to be included.

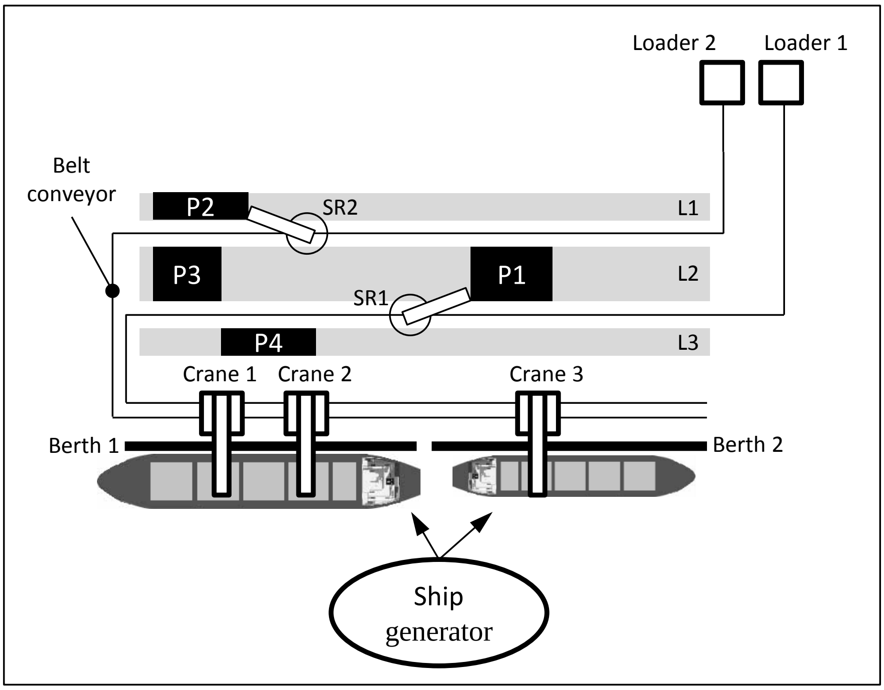

Figure 8.1: Schematic representation of the total terminal model for an arbitrary terminal layout

In Figure 8.1, the main elements from the total terminal model are shown for an arbitrary layout of a quay where two ships can moor at the same time, three cranes, two stacker-reclaimers and two loading machines. Stacker-reclaimers have to facilitate operations at the terminal's seaside and landside. Element classes that represent these machines own the main processes in the simulation model. For import terminals, a stacker-reclaimer accepts ship unloading when material out of this ship can be stored within its reach and a route is available to transport material from the quay to itself. A landside job is accepted when the requested material is stored within its reach and material can be transported to the correct loading machine. By merging the simulation models, some algorithms that cover the seaside or stockyard operation are added to the operation of the stacker-reclaimers. Details for these extra stacker-reclaimer's algorithms are listed in Appendix D, section D.5.

8.3 Features of the total terminal model

The total terminal model realizes a 'virtual' dry bulk terminal. This virtual terminal enables the investigation of operational procedures for berth allocation, crane assignment, storage allocation and route selection on beforehand before implementation in real operation. Another feature is to perform what-if scenarios. Future scenarios, like the impact on the terminal performance when ship sizes will increase, or what to do when one of the quay cranes will be unavailable for a longer period of time due to maintenance, can be investigated. Furthermore, planned modifications for the terminal layout or extra terminal functions (like the dry bulk distribution center functionality as mentioned in the previous section) can be assessed to support the design process. The visual representation of this model enables terminal designers to show their proposals to clients and users.

8.4 Validation of the total terminal model

For the validation of the total terminal model, there is operational data available that covers the terminal activities during three years of operations. Unfortanetely, real-world operational data does not provide specific insight how much stockyard area is used during the three years of operation. The terminal operator owns 110 hectares of storage area from which only 66 hectares is in direct stacker-reclaimers reach. Based on the terminal operator's judgement the total stockyard area was not completely occupied during the years under research. Another difficulty is that the terminal operator applied partially the stockyard operational procedures clearing pile's area (CPA) and relocation (REL). These procedures were already explained in section 5.4.2.

To tackle this deficiency the following method was followed. The stockyard area required will be determined for two extreme scenarios. For the first scenario, the stockyard operational procedures are fully applied and in the second scenario these procedures were not used at all. Per scenario the stockyard area required will be determined by aligning the simulation outcomes with the terminal's KPI's. The extent to which the determined stockyard sizes correspond with real values indicates whether the total terminal model provides realistic outcomes. In Table 8.1 the terminal's KPI's were listed. Note that the average annual throughput only indicates the unloaded tons that are stored at the stockyard.

A screenshot of the total terminal model (at an arbitrary moment during simulation) is shown in Figure 8.2. The stockyard size will gradually be increased from 66 hectares to 110 hectares by extending the length of the lanes. It was assumed that the stacker-reclaimers can also operate at these longer lanes.

Table 8.1: Terminal's KPI's used for validation based on average values during the real operations in 2008, 2009 and 2010

Parameter	Description	Value	Unit
$\dot{m}$	Annual throughput	24	[Mt/y]
W_{ship}	Average ship port time	70	[h]
A	Stockyard area	66-110	[ha]
m_{rel}	Mass of relocated tons	0.9	[Mt/y]

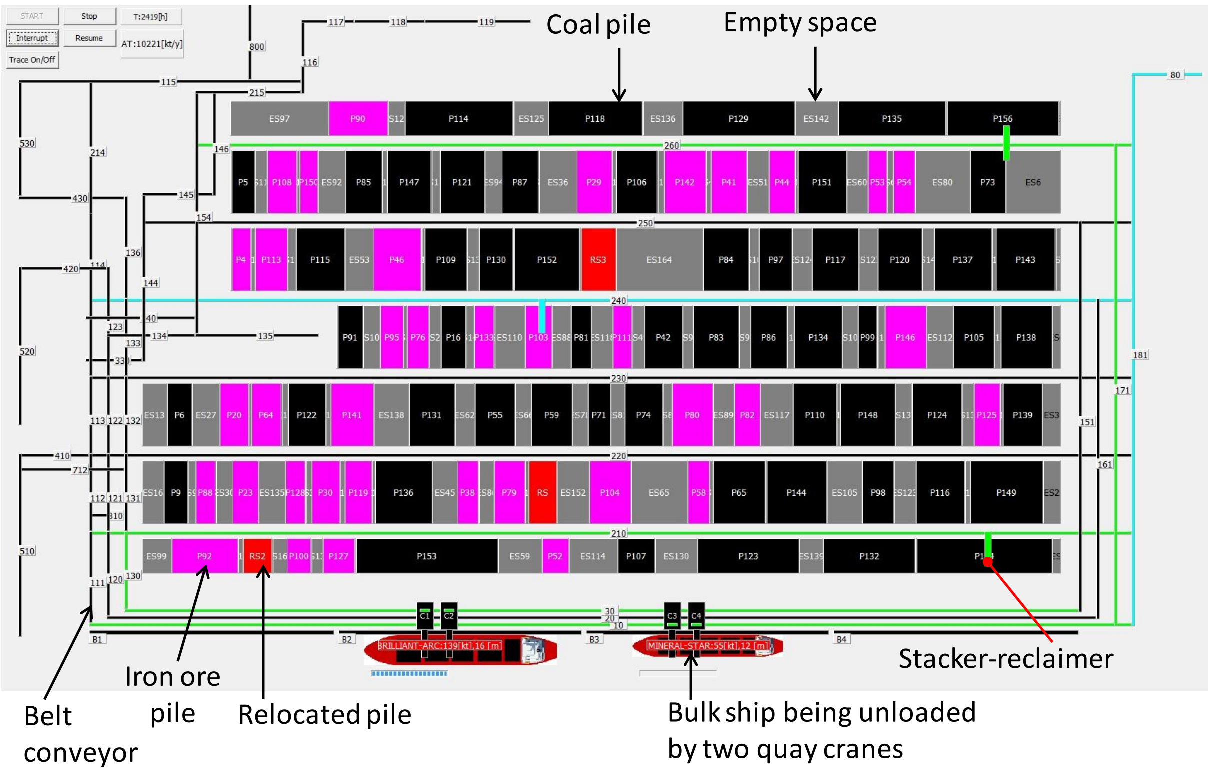

Figure 8.2: Screenshot of the terminal layout used during the validation study

For the input of the simulation model, historical data covering 897 ship arrivals was given by the terminal operator. Each ship contains its arrival time, shipload, material type (coal or iron ore) and the total storage time this material was stored at the stockyard. In Appendix G, this input file is listed. The terminal layout as it was in 2011 was used as terminal configuration. In Table 8.2, additional parameters for the simulation model are listed.

Despite receiving very detailed operational data from the terminal operator, there are still some parameters left that have to be generated using stochastic distributions. For example, the distributions for assigning material to specific landside transportation modalities and the breakdown behavior of machines and belt conveyors. Furthermore, the simulation starts empty which was not the case for the real-world operations data. That's why the run control for the total terminal model was investigated as well. The same method as mentioned for the run control of the individual simulation models was followed. Ten replications were performed with different seed values for the MTBF, MTTR distributions and the table-type distributions for material allocations to different landside machines. Also the simulation run time was varied by using the input data one, twice or even three times in a single file. The spread of the measured ship port times are presented in boxplots in Figure 8.3 and other results are listed in Table 8.3.

Table 8.2: Additional parameters used as input for the total terminal model

Seaside					
Parameter	Value	Unit	Parameter	Value	Unit
Number of berths	4	[-]	Maximum ship's draft per berth	3x17[1], 1x23	[m]
Number of cranes	4	[-]	Cranes free-digging capacity	2x2.5 2x4	[kt/h]
Ship interarrival time distribution	Figure 3.8B		Crane unloading efficiencies	Figure 3.21A	
Average shipload	103	[kt]	Shipload distribution	Figure 3.21B	
Breakdown behavior	See info stockyard machines		[1] reduced from 18 [m] to 17 [m] to compensate the draft reduction due to the elimination of the bypassed tons		
Landside					
Coal exports (0.64 of total)			Iron ore exports (0.36 of total)		
Transportation modality	Frequency	Load [kt]	Transportation modality	Frequency	Load [kt]
Barges	0.49	1.9	Barges	0.41	2.1
Trains	0.36	2.3	Trains	0.44	3.3
Coastal ships	0.04	7.3	Coastal ships	0.15	16.2
Mixing silo's	0.11	12.1			
Stockyard					
Parameter	Value	Unit	Parameter	Value	Unit
Stockyard area	66 - 110	[ha]	Width of outer lanes	50	[m]
Number of lanes	7	[-]	Width of middle lanes	90	[m]
Stockyard layout	see Figure 7.6		Maximum relocated tons	30	[kt]
Trapezoidal pile	see Figure 5.2		Relocation (REL)	Yes/No	
Shipload splitting		Yes	Clearing pile area (CPA)	Yes/No	
Stockyard machines					
Parameter	Value	Unit	Parameter	Value	Unit
Nr. of stacker-reclaimers	6	[-]	Mean time between failures (MTBF)	16	[h]
Stacking capacity	6x4	[kt/h]	Mean time to repair (MTTR)	0.5	[h]
Net reclaiming capacity	6x2.5	[kt/h]	MTBF and MTTR distributions	NED	
Belt conveyor network					
Parameter	Value	Unit	Parameter	Value	Unit
Network layout	Fig. 7.6 and 7.7A		Belt conveyors break down behavior	See info stockyard machines	
Route selection procedure	Cyclic route selection				
Number of loading machines	7	[-]	Maximum transportation capacity	4	[kt/h]
Number of belt conveyors	51	[-]	Number of transportation routes	73	[-]

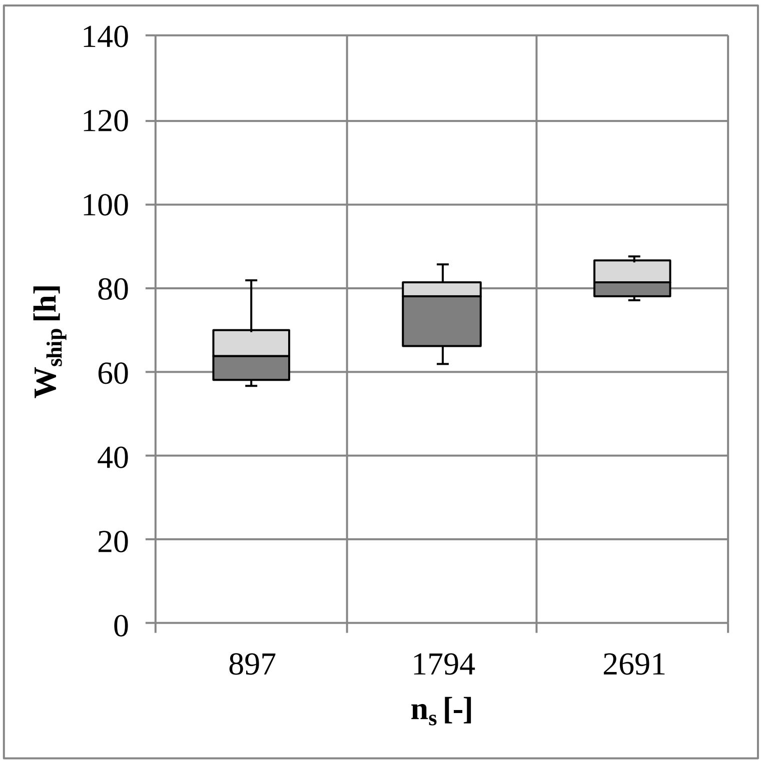

Figure 8.3: Boxplots that displays the variations for the average ship port time for different numbers of ships for a single result as shown in Figure 8.4

Table 8.3: Accuracy of the average ship port time for different number of ships with ten replications

n_s [-]	W_{ship} [h]	$W_{ship,min}$ [h]	$W_{ship,max}$ [h]	StDev [h]	StDev in [%] of W_{ship}
897	65.5	58.2	82	7.7	11.8
1794	76.6	66.3	86.1	7.3	9.5
2691	82.5	78.2	86.4	3.9	4.7

From Table 8.3 it can be concluded that when inputfiles that contain almost 2,700 ships were used (three times the historical data in a single file) the standard deviation of the average value is within the 5%, which is assumed to be precise enough also considering the simulation run time. The simulation run time was for one replication 4:50 minutes (using a pc with the following characteristics: Intel® Core ™ i5-2310 CPU @2.90GHz with 4 GB RAM). The spread of the measured ship port times shows a larger variation than in the previous sections for a comparable number of ships. This can be explained by the fact that in the total terminal model all processes are involved and the simulation starts empty.

Besides to the parameters listed in Table 8.2, the following assumptions were made; the repositioning times for stacker-reclaimers and quay cranes were not included (it was assumed that these machines were already repositioned before starting a new activity), relocation of piles did not take time (it was assumed that piles have already been relocated before a ship arrives) and the transport of material from the mixing silo's to the coal-fired power plant was not included (it was assumed that these transports were planned during the idle times of the transportation routes required).

Figure 8.4 shows the simulation results, represented by the average ship port time (A) and the average amount of annual relocated tons (B) versus the annual throughput. Also two historical KPI's, shown with the series "*T2's performance*", are shown. From Figure 8.4A it can be concluded that for scenario 1, with the stockyard operational procedures CPA and REL, a stockyard size of 77 hectares is needed to realize a comparable performance than in real-world. For the second scenario, a stockyard that contains 95 hectares is required when these operational procedures were not applied. The minimum stockyard size of 77 hectares corresponds with the fact that a stockyard of 66 hectares was inadequate and the maximum size of 95 hectares is less than the maximum stockyard size of 110 hectares.

From Figure 8.4B it can be concluded that the average amount of relocated tons does not correspond exactly with the determined value for scenario 1. This deviation can be explained by the fact that during real operations there are additional reasons to relocate material. For example, material is relocated on beforehand to enable a faster train loading. In conclusion, the order of magnitude of the determined stockyard sizes and the determined relocated mass of bulk material per year are in line with historical data of the real operations.

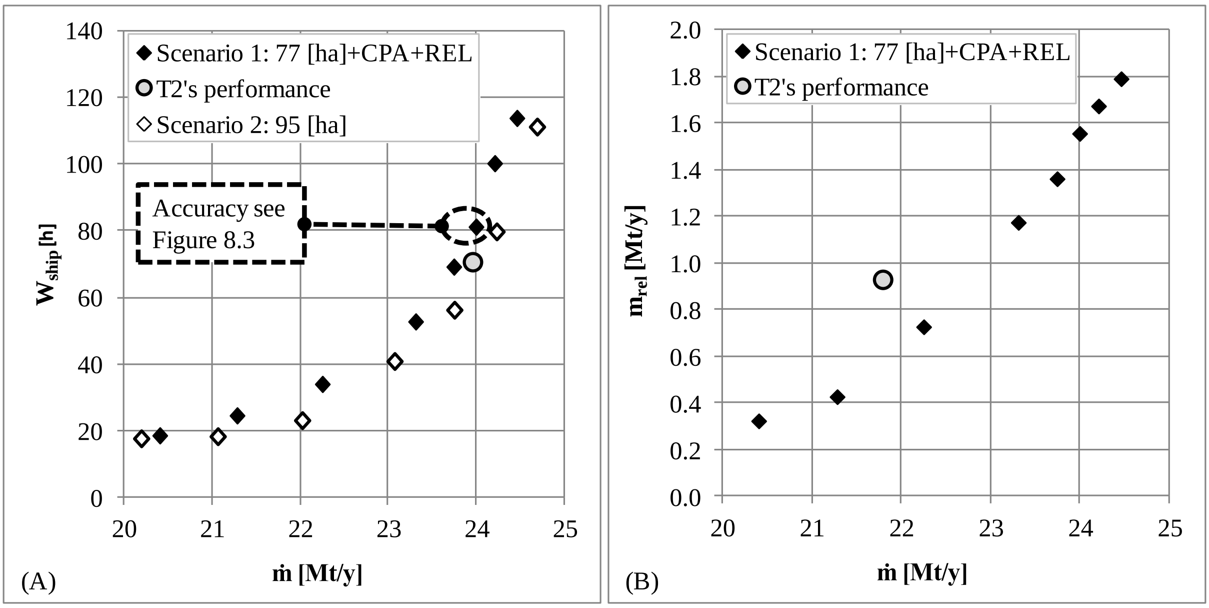

Figure 8.4: The average ship port time (A) and the average amount of relocated tons per year (B) for both scenarios and historical data

8.5 Case study 1: Evaluation of the terminal design from section 2.5

In section 2.5, a terminal design was formulated based on rules-of-thumb and practical experiences. In Figure 8.5A this design is shown, which is a copy of Figure 2.7. The total terminal model was used to evaluate this design and to determine an alternative layout. Before formulating the alternative layout, several steps have been completed. In Table 8.4, these steps are summarized with the values determined for average ship and train port times. A short explanation of the activities per design step is given below in text.

Table 8.4: Design steps using simulation and corresponding KPI's determined

Design step	Layout	Applied characteristic(s)	$W_{s\text{-ship}}$[1] [h]	$W_{s\text{-train}}$[1] [h]
1	Fig. 8.4A	no stochastic	44	7
2	Fig. 8.4A	with stochastic processes as shown in Table 8.4 (sp)	316	6
3	Fig. 8.4A	sp – continuous quay layout (see section 3.7.2) (cql)	242	5
4	Fig. 8.4A	sp – cql – SR's redundancy (see section 6.5.1)	42	3.5
5	Fig. 8.4B	increased reclaiming and train loading capacity	59	3

[1]accuracy of the average ship port time can be expressed by the standard deviation of ±5% and for trains a standard deviation of the average train port time of ±3.5% is valid.

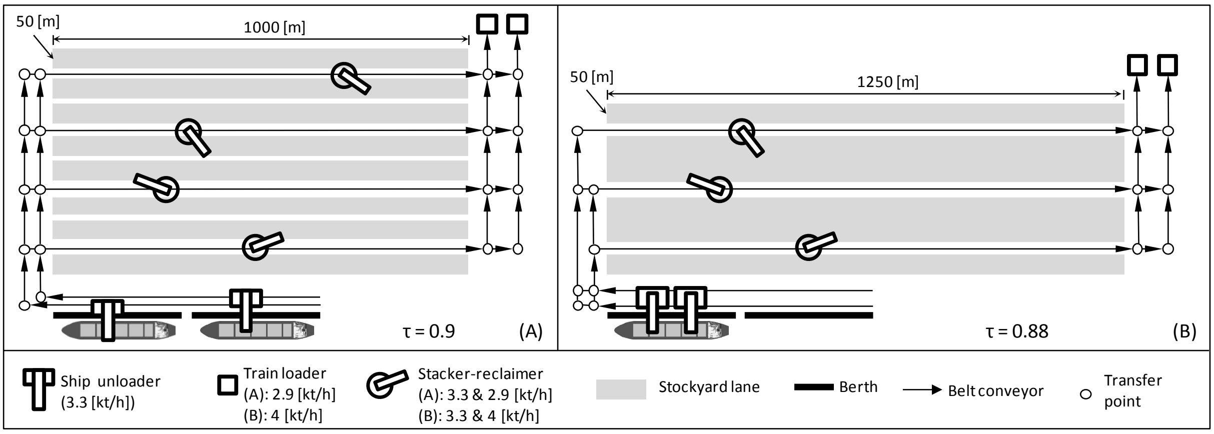

Figure 8.5: Evaluation of the terminal design as formulated in section 2.5 (A) and (B) presents an alternative terminal layout

In step 1 the terminal layout of Figure 8.5A was assessed without taken into account the stochastic variations for the ship interarrival times, shiploads and material storage times. Simulation results has shown that the average ship and train port times do not exceed the predefined times of 60 and 3 hours respectively. The belt conveyor network's connectivity of the original layout is 0.9; only the two connections for the quay conveyors to the cross conveyors could be added. However, a terminal that operates with constant interarrival times and shiploads does not exist in the real world.

In the second step, stochastic variation was included for the ship arrival process, storage process and the equipment break down behavior. Details for the added stochastic processes are listed in Table 8.5. When the stochastic processes are included, ships and trains spend significantly more time in the port than allowed (see for the values in Table 8.4).

Table 8.5: Included stochastic processes

Stochastic process	Distribution type
Ship interarrival times	NED
Shipload	Uniformly distributed between 30 – 170 [kt]
Storage times	Uniformly distributed between 0.1 – 0.3 [y]
Equipment disturbances	See Table 8.2

In step 3, the continuous quay operation was applied. Both unloaders can move alongside the quay and ships can be unloaded by two cranes simultaneously. Applying this functionality resulted in a remarkable reduction of the average port times. However, the predefined port times were not met.

In step 4, the stacker-reclaimer's redundancy was introduced. Piles stored at the middle lanes are now accessible by two stacker-reclaimers. The reduction of the average port times is sensational, especially for ship unloading. For stacking, the material from ships is distributed across two stacker-reclaimers that resulted in faster servicing. Besides, the machines are shorter occupied per operation which increases the availability for a new operation. Furthermore, the material is accessible by two machines for reclaiming that resulted in less waiting time of trains. Actually, the terminal layout performs better than needed and gives a reason to investigate alternative terminal layouts.

In step 5, this alternative terminal layout that contains three stacker-reclaimers was formulated. Figure 8.5B shows this design. The stockyard size was reduced from 40 to 37.5 hectares. Simulation experiments have shown that a further reduction lead to excessive ship waiting times. During the definition of this alternative layout, the network's connectivity was investigated starting from a fully utilized network ($\tau = 1$). Experiments have shown that for the transport of the incoming materials to the stacker-reclaimers, two connections could be removed without reducing the average ship port time significantly. The removed transfer points connected previously the cross conveyors with both outer stacker-reclaimers because these machines have a limited number of piles stored in their reach. Simulation experiments proved also that the maximum connectivity to the train loaders should be maintained; all yard belt conveyors should be connected to both train loaders.

To realize an average train port time of 3 hours, the gross train loading capacity (and thus also the reclaiming and transportation capacity) must be increased to 4 [kt/h]. The reason was that due to conflicting activities for stacking and reclaiming the predefined requirements could not be met.

The original layout (as shown in Figure 8.5A) does not present a feasible solution when the stochastic variations are taken into account. The total terminal model was used to support the formulation of an alternative design. Several steps were taken to come up with a new layout. This layout (as shown in Figure 8.5B) satisfies the requirements (as listed in Table 2.1) with less equipment needed. Especially applying terminal procedures like the continuous quay operation and the stacker-reclaimer redundancy are the major causes for this improvement.

In the alternative terminal layout, only three stacker-reclaimers have to be installed and a limited number of belt conveyors and transfer points are needed. Also the stockyard size can be reduced with 2.5 hectares. It is expected that additional stockyard management procedures like relocation and clearing pile's area will result in a further reduction of the stockyard size.

A summary for the design approach followed to realize a dry bulk terminal design is listed in Table 8.6. After the initialization stage (where design requirements for the new terminal were collected), a first design was formulated by using the existing design methods (more details for this stage are presented in section 2.5). The thesis' contribution starts with the integration of this design into the total terminal model. Subsequently, stochastic variations were included and specific terminal operational procedures (e.g., continuous quay layout, clearing the pile's area directly after reclaiming, relocation of small piles and stockyard machines redundancy) were applied. Not implemented in this section but included in Table 8.6 is step 11, when stockyard machines need to be specified for blending and homogenizing of dry bulk materials. In the last step it was investigated if the belt conveyor network could be simplified (by eliminating connections) still meeting the predefined service demands. Table 8.6 presents an overview of the additions to existing design methods as defined in this thesis.

Table 8.6: Summary of the design approach followed

	Step	Aspect	Procedure/Result
Initiali-zation	0	Collect terminal requirements	Specify the seaside and landside service demands, annual throughput, distribution types, average shipload, average storage time, landside transportation modalities, etc.
Existing design methods	1	Seaside design	Determine the number of berths and the number and capacity of ship (un)loading machines
	2	Landside design	Determine the number and capacity of landside machines
	3	Stockyard sizing	Calculate the stockyard size
	4	Stockyard machine selection	Determine the number and capacity of stockyard machines
	5	Belt conveyor network design	Define a transportation network with all possible connections
Thesis' contribution	6	Simulation-integrated design	Integrate the design (the results from steps 1-5) in the total terminal model
	7	Include stochastic variations	Verify if predefined service demands are met
	8	Apply the continuous quay layout	Redefine the quay length required and capacity ship (un)loading machines
	9	Apply stockyard operational procedures	Redefine the stockyard size
	10	Apply stockyard machines redundancy	Redefine the number and capacity of stockyard machine to meet the service demands
	11	Specify (if needed) machines for blending and homogenizing	Determine type and capacity of stacking and reclaiming machines and design blending beds
	12	Reduce the network's connectivity	Simplify a belt conveyor network while still guaranteeing the predefined service demands

8.6 Case study 2: 'Dry bulk distribution center'

A case study was defined to demonstrate the use of a simulation model that covers all the terminal's subsystems. In this case study a distribution center for bulk materials must be integrated in an existing import terminal. The changes in cargo flows for coal and iron ore worldwide are the background for this case study. More and more bulk materials are needed in Asia while in Western Europe the demand for these materials will slow down resulting that existing terminals can develop additional activities. In section 8.6.1, the feasibility of a distribution center in Western-Europe is described in more detail and in section 8.6.2 the fundamentals for the design are presented.

8.6.1 Feasibility of a distribution center

The following reasons justify the feasibility of a 'Dry bulk distribution center' in Western-Europe. The first one, as already mentioned, is the increasing demand for coal and iron ore in Asia while in Europe the demand will remain the same or will even decrease. The second one is that the limited water depth in export terminals in Russia and Canada prevents that large bulk ships can be loaded. The total cost per ton, including the transportation costs, will be higher when relatively small ships sail directly to Asia, especially with the high fuel prices nowadays, then when an extra transshipment into large Capesize ships is realized.

Possible seaborne trade flows to a distribution center located somewhere in Western-Europe are presented in Figure 8.6. Small bulk ships sail from export terminals located in, for example, Canada, Greenland, Russia, Poland, Sweden and Norway to a distribution center in Western Europe. From where the material can be transshipped in large Capesize ships and sailed via the Suez Canal to Asia.

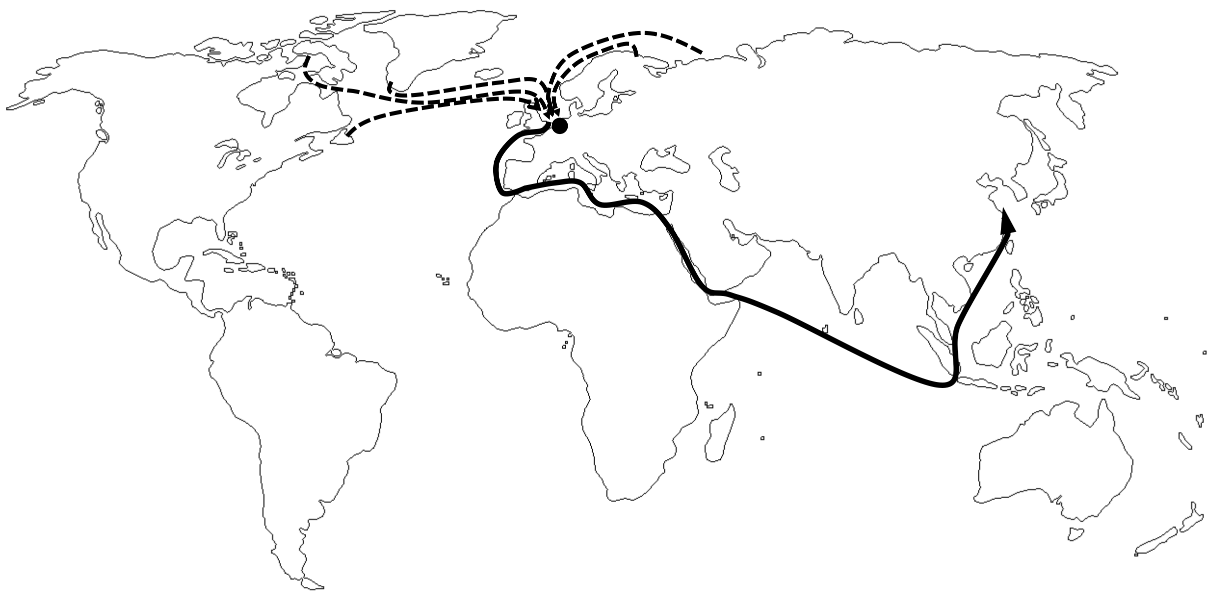

Figure 8.6: Possible seaborne trade flows for a 'Dry bulk distribution center' in Western-Europe

An alternative is to use a floating hub somewhere at the North Sea. Such hub is formed by a large bulk ship that is equipped with unloading cranes and loading machines for the direct transshipment of dry bulk materials (ABHR, 2013). However, the storage capacity is limited to the ship's size and the incoming and outgoing streams of dry bulk materials cannot be uncoupled. Furthermore, additional functionalities like blending and/or homogenizing cannot be performed. In this section the alternative of the implementation of a distribution center at an existing terminal is investigated. Advantages are that existing equipment can be used and material can be stored at the terminal's stockyard to uncouple the incoming and outgoing streams that makes the supply chain simpler.

For this case study the layout of terminal T2 will be used. The distribution center is particularly feasible for iron ore due to the expected decrease of the steel demand in Western-Europe. For the expected cargo flows to and from the distribution center the following assumptions were made: (the assumptions are summarized in Table 8.7).

- The first indication is an annual throughput of 3.5 million tons with an option that the volume can grow further.
- Bulk ships belonging to the Handymax class are selected to deliver iron ore to the distribution center due to the reduced water depths in the export terminals.
- The proposed ships to sail material to Asia are based on the maximum ship size that can pass the Suez Canal.
- The ships interarrival times for the incoming flow as well as the outgoing flow can be quite constant as a result of the scheduled, regular service needed for the distribution center concept. Although there is always some variation, normal distributions are proposed. The incoming flow has to sail a smaller distance resulting in a lower value for the standard deviation then the outgoing flow. To realize a supply chain with a constant flow, the maximum time that ships may spend in the port is limited. Values for the average ship port times are listed in Table 8.7.

Table 8.7: Characteristics for the expected cargo flows to and from the distribution center

Parameter	Description	Value for the incoming flow	Value for the outgoing flow	Unit
$\dot{m}$	Annual throughput	3.5	3.5	[Mt/y]
-	Ship's class	Handymax	Large Capesize	-
SlDist	Shipload distribution	Uniformly distributed (35 – 55 [kt])	Uniformly distributed (185 – 195 [kt])	-
IATDist	Interarrival time distribution	Normal	Normal	-
StDev IAT	Standard deviation of the interarrival time	5	10	[h]
W_{ship}	Average ship port time	36	48	[h]

8.6.2 Fundamentals for the design

In this section, the fundamentals for the additions to the existing terminal layout are presented. Per subsystem several questions have to be answered to come up with an adequate design.

- **Seaside:** Are the current berths and installed quay cranes able to handle the extra 3.5 million tons of iron ore without compromising on the ship service performance?
- **Landside:** Is the existing coastal ship loader able to load large Capesize ships within the predefined time?
- **Stockyard machines:** Do the stacker-reclaimers have sufficient capacity and can these machines meet the required blending effect?
- **Storage area:** How much extra area is required and which storage policy should be applied?
- **Belt conveyor network:** How to integrate the shiploader(s) into the belt conveyor network?

The following design steps were followed and the total terminal model was used to assess alternative designs for the terminal layout.

1. Specification of the shiploader(s) for the Capesize bulk ships
2. Integration of the shiploader(s) in the existing belt conveyor network
3. Realization of blending and homogenizing of iron ore
4. Determine the additional stockyard area in combination with the predefined ship unloading performance

Step 1: Shiploader(s) specification
The currently installed shiploader is able to load Panamax ships. Loading Capesize bulk ships cannot be performed because the outreach of 25 meter is inadequate (Capesize ships require an outreach of at least 30 meter). A larger shiploader is needed to load Capesize ships.

For the determination of the required number and capacity of the shiploader(s) the net reclaiming capacity of the stacker-reclaimers must be taken into account. According Table 8.2, the net reclaiming capacity is 2.5 [kt/h]. Loading a Capesize ship with 195 [kt] of iron ore with one shiploader will last at least 76 hours, which exceeds abundantly the predefined ship port time. Installing an extra ship loader will realize a loading time of 38 hours. However, each shiploader requires a stacker-reclaimer to reclaim the material from the stockyard. The total terminal model will be used to verify if the average port time for loading will be met.

Step 2: Integration of two ship loaders into the belt conveyor network
It is proposed to locate the ship loaders at a separate berth which is in line with the existing quay wall, which makes it easier to realize and to maintain the extra water depth, up to 18 [m]. To connect the stacker-reclaimers with the ship loaders, two belt conveyors are needed (one is a replacement of the belt conveyor that transports material to the existing Panamax shiploader). The moving heads of the yard conveyors have to be extended with an extra position to connect the stacker-reclaimers with the new belt conveyors. In Figure 8.7, the proposed modifications to the terminal layout are shown.

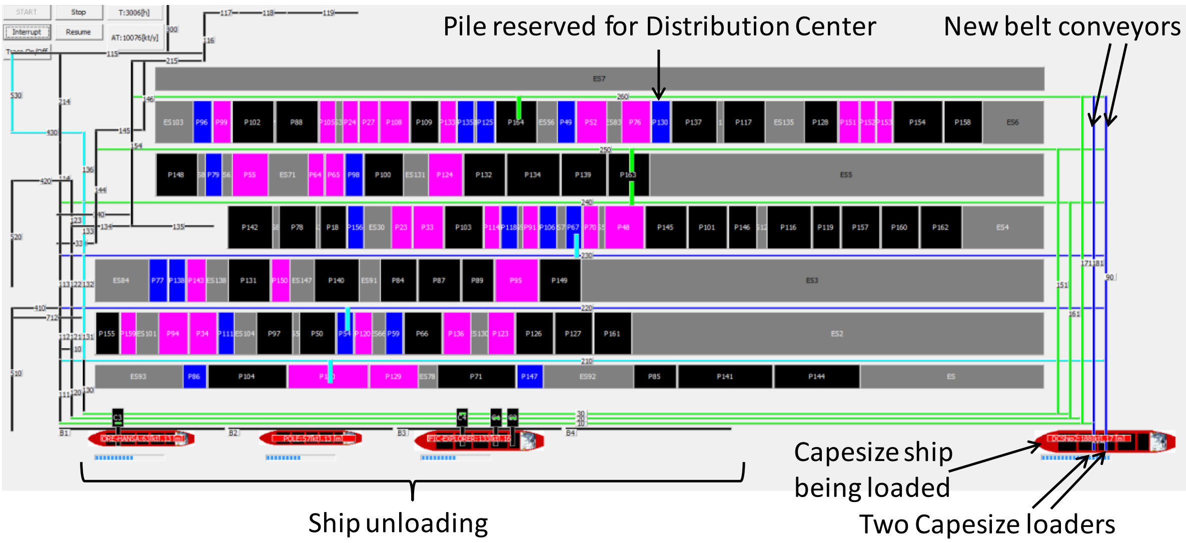

Figure 8.7: The integration of a distribution center for iron ore at an existing terminal

Step 3: Blending and homogenizing of iron ore
Currently, bucket wheel stacker-reclaimers are installed. According to Table 6.2, the blending/homogenization effect using these machines is limited. For the best blending effect, maximum 6 on a scale of 10 is possible for a bucket wheel reclaimer together with the strata stacking method. At this moment, specifications for delivered and requested iron ore are unknown. If these characteristics are given, the method as presented in section 6.6 can be used to determine if these stacker-reclaimers fulfill. Note that there is no need to realize a high value for the blending effect. The blended materials are stored in ship holds for a couple of weeks during the sea journey and are afterwards unloaded, transported and stored before being delivered to industrial clients. For this case study, it was assumed that the installed bucket wheel stacker-reclaimers are applicable.

Step 4: Determination of the stockyard size and quay side performance
Two stacker-reclaimers are needed to reclaim material that is loaded simultaneously into a Capesize ship. That's why it is proposed to spread materials dedicated for the distribution center across the stockyard, see Figure 8.7, resulting in the highest probability of having two stacker-reclaimers available. For ships that must be unloaded or loaded for the distribution function, specific input files were defined. In the total terminal model, these ships are added to the other ships.

The quay side performance, expressed in average ship port time, relates to the stockyard size. If there is no area available ships have to wait. The extra storage area was determined by increasing the stockyard size gradually and by measuring the average ship port times without extending the historical ship port time. Note that the average ship port time belongs to existing ships; the Handymax ships that deliver materials for the distribution center were not included due to the limited shiploads.

The total terminal model was used to determine the new stockyard size. As starting point the second scenario from section 8.4 was used. In Figure 8.8, the simulation results are presented. When the distribution center needs to be integrated in the existing terminal, a total stockyard of 103 hectares is required to realize an average ship port time comparable to the average ship port time valid for the current situation. The total annual throughput will be 27.5 [Mt/y], which is the 24 million tons currently handled plus the 3.5 [Mt/y] that needs to be handled for the distribution center.

The average ship port times for the DC-ships were measured using the total terminal model and compared with predefined times. Results for this comparison are listed in Table 8.8. For the Handymax ships the measured average ship port time exceeds the predefined time. Especially, the large variation (expressed by the standard deviation (StDev)) is remarkable. This can be explained by the fact that ships are served based on the First-Come-First-Served principle and DC-ships have to wait their turn. Prioritizing serving DC-ships is required but will influence the average port times of other ships. It is suggested to develop new planning rules to determine the best serving order when a DC-ship needs to be unloaded.

From Table 8.8, it can be concluded that the average ship port time for loading the Capesize ships is not exceeded. The low variation of the average ship port time is due to the distribution of the piles dedicated for the distribution center across the entire stockyard.

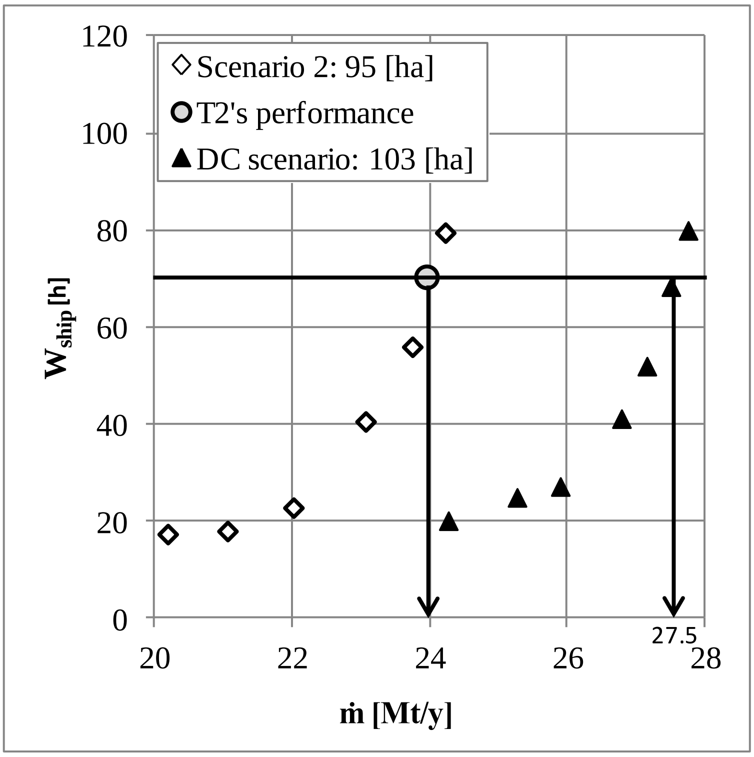

Figure 8.8: Determination of the total stockyard size in relation to the predefined average ship port time

Table 8.8: Predefined and measured average ship port times for DC ships

Shipclass	Operation	$W_{ship,predefined}$ [h][1]	$W_{ship,measured}$ [h]	StDev [h]
Handymax	Unloading	36	43.6	11.4
Capesize	Loading	48	41.3	1.6

[1] The predefined average ship port times are taken from Table 8.7.

8.7 Conclusions

To assess designs for dry bulk terminals that cover all subsystems, the total terminal model is introduced. This model is developed as a single large simulation model that is composed out of the seaside model, the stockyard model and the transport network model. The main reasons for developing a single model is the expected simulation run time when a distributed simulation model is developed for the several individual models. Moreover, the integration of the three above mentioned individual models could be realized relatively easy.

The total terminal model creates a virtual environment to determine essential design parameters (e.g., the stockyard size, the number and capacity of machines and the belt conveyor network), to assess predefined designs and to examine new operational procedures. Simulation results have shown that the model provides comparable outcomes as the real operation. The total terminal model is applicable to formulate and assess terminal designs. The assessment of terminal designs was demonstrated by evaluating the terminal layout that was originally based on rules-of-thumb and practical experiences. When the stochastic variations were taken into account the service demands were not met for the original design. The total terminal model was used to formulate an alternative design that meets the terminal requirements. Besides, the proposed alternative layout turned out to require less equipment to be installed.

The added value of an integrated terminal design was demonstrated by determining the design parameters to implement a ‘*dry bulk distribution center*’ at an existing import terminal. The total terminal model was applied afterwards to investigate if predefined requirements were met.

For the expansion of the design methods, the following additions are formulated based on the research performed in this chapter:

1. Developing dry bulk terminal designs based on existing known rules-of-thumb and practical experiences fail, especially when stochastic variations have been taken into account.
2. The developed total terminal model enables the modeling of the entire terminal operation. The conflicting objectives for storage and seaside and landside service demands are investigated at the same time.
3. The total terminal model is applicable for the formulation of terminal designs and for the evaluation of layouts proposed. Empirical data can be used as input or generalized distribution types can be selected. The accuracy of the simulation results as function of the stochastic variations and when the simulation is started using an empty stockyard should be investigated on beforehand.
4. Additional cargo flows can be added to the terminal operation for representing extra dedicated flows of dry bulk materials.
5. The additions to existing design methods are summarized in Table 8.6.

9 Conclusions and recommendations

To meet the expected global increase of seaborne trade flows for coal and iron ore many existing dry bulk terminals need to improve their daily operations or need to be expanded. Other developments like the shortage of port area, the lack of skilled personnel and stricter environmental requirements enforce terminal operators to develop plans to utilize their area more efficiently and redcue the energy consumption. A comprehensive design method for dry bulk terminals is missing. Nowadays, terminal designers base their proposals on rules-of-thumb and practical experience. However, suggested values for some rules-of-thumb match poorly with derived terminal characteristics. Besides, when rules-of-thumb and practical experiences are used there are still many questions and uncertainties left. In section 9.1 the main conclusions are presented and recommendations for future research are given in section 9.2.

9.1 Conclusions

In this thesis, the following main research question needs to be answered: How to design dry bulk terminals? The thesis objective is to expand existing design methods instead of developing a new one. Modeling the terminal as a whole is complicated due to dependencies between terminal functions. For example, the quay performance relate to the number of installed machines at the quay, the machine handling capacities, the stockyard size and the number of connections in the belt conveyor network. In this thesis the following approach was followed: the terminal was decomposed into subsystems, each subsystem was investigated individually and at the end the subsystems were combined.

Simulation is a must to take the stochastic variations of main sequential processes (like the arrivals of ships and trains) into account to realize adequate terminal designs. Simulation tools were developed to assess the sensitivity of design parameters on the subsystems and to evaluate if formulated designs meet the requirements predefined. In this chapter the main conclusions will be presented for the research questions as formulated in the first chapter. Note that generalized conclusions are presented instead of exact values because for most conclusions simulation experimental results were performed for cases using specific input parameters. The simulation models developed are applicable to determine exact values for other cases.

1. Can characteristics of existing dry bulk terminals be used as design guidelines?

No. Suggested values for potential factors like the quay length factor and the storage factor do not correspond with derived characteristics from 49 terminals. Using the suggested values will lead to undersized quay lengths and oversized stockyards. Also the equipment installation factors, which were determined by dividing the installed capacity with the capacity needed when machines operate for 100%, show a large variation. These factors cannot be used for a correct specification of equipment capacity required.

2. How should the terminal's seaside and landside be designed taking into account the stochastic arrival processes and load patterns?

Measured interarrival time and service time distributions show hardly a fit with the by other authors proposed analytical distributions. This prevents the use of analytical models (like queuing-theory) to model the terminal's seaside and landside accurately. A simulation model was developed to cover the seaside operation. Using this *seaside model*, empirical data can be used as input to represent ship interarrival times and shiploads. When there is no historical data available, it is recommended to apply one of the most suggested distribution types (e.g., NED, Erlang-2, Weibull or Gamma) and determine the sensitity of these distributions.

The continuous quay layout, when cranes can move alongside the quay to service multiple ships, is preferred to the discrete quay layout. The continuous quay operation will result in reduced quay length required and higher cranes utilizations. The selection for the water depth alongside the quay should be made carefully. Increased water depths are expensive to realize and maintain but may hinder the seaside operation when the probability increases that a number of deep (large) ships will call at the same time. Another finding is that the number and transportation rate of the quay conveyors needs to be determined precisely to prevent a hindrance of crane operations when multiple cranes unload ships simultaneously.

3. How to size the required stockyard?

The analytical derivation of the storage factor specifies which parameters affect stockyard sizing. The most important parameters are the ratio mass per square meter and the number of replenishments per year. Using these parameters, scenario's to size the stockyard can easily be evaluated. For example, the storage of iron ore leads to higher storage factors than the storage of coal (due to the higher bulk density) and will result in less stockyard required. Another example is that wider piles result in higher values for the storage factor. However, due to the imbalance between the incoming and outgoing streams of bulk materials, the amount of cargo that is stored at the stockyard varies during time. An analytical determination is not longer sufficient.

By using simulation, stochastic variations in arrivals, departures and storage times can be considered. As expected, results from experiments with the *stockyard model* developed confirmed that the degree of stochastics determine the stockyard size; the greater the variations the more stockyard area is required. Specific stockyard operational procedures are included in the stockyard model developed. Examples are the distribution of material across multiple piles, clearing the pile’s area when material is reclaimed and relocation of small piles to have area available for newly arrived material.

4. Which type and capacity of the stockyard machines are required to stack, reclaim and blend dry bulk materials?

To obtain a correct machine selection, machine characteristics were determined. When dry bulk materials need to be blended, the blending effect that can be achieved relates to the stacking method and the installed reclaimer type. In a case study, the selection of the stacking method and the stockyard machine type was demonstrated to deliver blended coal to a power plant.

Generally, at stockyards bucket-wheel stacker-reclaimers or individual stackers and bucket-wheel reclaimers are used. The stockyard model was expanded with stockyard machines and belt conveyors; this model is called the *transport network model*. Results from experiments with the transport network model have shown that stacker-reclaimers require higher capacities than individual machines to meet the predefined performance. However, based on the machines weight and the corresponding belt conveyor capacities the total investments for stacker-reclaimers are less compared to the investments for individual stackers and reclaimers. Moreover, it was investigated that the reclaiming capacity for stacker-reclaimers can be reduced when piles are stored in the reach of two stacker-reclaimers or when ship servicing is interrupted in favor of train loading.

5. How should the belt conveyor network be designed to connect all machines achieving sufficient connectivity, flexibility and operational predictability?

Flexible connections between belt conveyors, mostly carried out with moving heads, are widely accepted at dry bulk terminals. Disadvantages of these transfer points are the extra power, maintenance and cleaning needed. As expected, an increase of the number of connections in a belt conveyor network increases the terminal performance. However, results from experiments with the *transport network model* have shown for a specific case that installing more than 75% of the maximum number of connections will not bring a notable performance improvement anymore. Another finding was that a network that contained bi-way belt conveyors performed significantly worse than a network equipped with single-way belt conveyors due to the reduced number of transportation routes that can be performed at the same time.

In belt conveyor networks, appropriate route selection allows the use of multiple routes at the same time. In a case study, different route selection procedures were assessed; the cyclic routes selection (all routes are assigned in succession) and the preferred routes selection (better performing routes are selected as first). Simulation results have shown that the selection of preferred routes increased the average ship port times but also resulted in less power required and will result in a reduction of maintenance and cleaning activities.

6. How to integrate the subsystems into the overall design of dry bulk terminals?

For a total terminal design an integrated approach was proposed because using individual simulation models will only realize local solutions. For an overall design the subsystems depend on each other and will influence each other. A single, large simulation model was developed; this model is called the *total terminal model*. In this model the conflicting objectives for storage, seaside and landside service demands can be investigated at the same time. This model was used to verify the design that was originally formulated by applying currently known rules-of-thumb and practical experiences. Results from experiments have shown that this design fails, especially when stochastic variations have to be taken into account. The total terminal model proved to be applicable for the formulation of terminal designs and to confirm that predefined requirements are met.

The additions developed in this thesis to existing design methods were demonstrated during (re)design studies. A formulation of a design starts with the initialization stage in which design requirements (like service demands and annual throughput) have to be collected. Afterwards existing designs methods have to be applied to formulate a first design. Subsequently, this design should be integrated into the total terminal model to include stochastic variations and apply specific terminal operational procedures for the seaside, stockyard and stockyard machine operations. The number and capacities for machines and stockyard size have to be verified and (if necessary) be redefined to meet the service demands. Finally, a simplification of the belt conveyor network has to be investigated, by eliminating connections, still meeting predefined service demands.

9.2 Recommendations

During the design of subsystems, economical assessments are hardly made due to the unavailability of required investments for the various terminal components and operational costs. Because of the competition among equipment manufactures, they are not willing to share selling prices easily. Only an economic assessment was made for the stockyard machine type selection. By further including economical data the solutions can be assessed on economical feasibility as well. For example, by sizing the stockyard it was assumed that there was always storage area available when ships arrive. By allowing that terminal operators will pay some demurrage penalties to ship-owners the stockyard size can be reduced which may result in a reduction of the annual costs.

The following recommendations are formulated for the simulation models developed:

1. Include direct transshipment. In some cases the material that is transferred directly from seagoing ships to inland ships is handled by pontoon-mounted cranes. However, in many cases quay-mounted cranes are also used for direct transshipment, resulting in higher utilizations.
2. Load the stockyard with material on beforehand, for example by defining piles that are already been stored at the stockyard. Currently, the stockyard starts empty in the simulation model, which results in a relatively large simulation run time (~5 minutes for the total terminal model) to compensate the empty initial start.
3. Assign a larger part of material to idle stockyard machines when a pile must be built using two stockyard machines when the second machine is already in operation.
4. Include a hauling function (movement of ships alongside the quay using tug boats) to move ships from deep water berths when new ships arrive that need these deep water berths.

References

ABB (2008) ABB solutions for the world's first unmanned bulk cargo terminal, [http://www.abb.com] cited 15/01/2014.

Abdekhodaee, A., S. Dunstall, A.T. Ernst, L. Lam (2004) Integration of stockyard and rail network: a scheduling case study, in: *Proceedings of the Fifth Asia Pacific Industrial Engineering and Management Systems Conference*, Gold Coast, Australia.

ABHR (2013) Second floating hub for Vale iron ore transshipment, in: *Australian Bulk Handling Review*, May-June, pp.76-78.

Adan, I., J. Resing (2002) *Queueing Theory - lecture notes*, Eindhoven University of Technology, The Netherlands.

Ago, M., T. Nishi, M. Konishi (2007) Simultaneous optimization of storage allocation and routing problems for belt conveyor transportation, in: *Journal of advanced mechanical design, systems and manufacturing*, 1, pp. 250-261.

Almeida de, A.T., P. Fonseca, P. Bertoldi (2003) Energy-efficient motor systems in the industrial and in the services sectors in the European Union: characterisation, potentials, barriers and policies, in: *Energy*, 28, pp.673-90.

Altiok, T. (2000) Tandem queues in bulk operations, in: *Annals of Operations Research*, 93, pp. 1–14.

Asperen van, E., R. Dekker, M. Polman, H. Swaan Arons de (2003) Modeling ship arrivals in ports, In: *Proceedings of the 2003 Winter Simulation Conference*, New Orleans, United States.

Ayu, M.A., M. Cardew-Hall (2002) An Application of IPA approach on the optimization of a mining port stockyard system, in: *Proceedings of the 6th International Workshop on Discrete Event Systems*, Zaragoza, Spain.

Babcock and Brown Infrastructure (BBI) (2007) Dalrymple Bay Coal Terminal – Master Plan 2007, [www.primeinfrastructure.com] cited: 25/08/2010.

Barros, V.H., T. Souza Costa, A.C.M. Oliveira, L.A.N. Lorena (2011) Model and heuristic for berth allocation in tidal bulk ports with stock level constraints, in: *Computer and Industrial Engineering*, 60 (4), pp. 606-613.

Baunach, G.R., E.S. Wibberley, B.R. Wood (1985) Simulation of a coal transshipment terminal: Batam Island, Indonesia, in: *Mathematics and computers in simulation*, 27, pp. 115-120.

Bierwirth, C., F. Meisel (2010) A survey of berth allocation and quay crane scheduling problems in container terminals, in: *European Journal of Operational Research*, 202, pp. 615-627.

Binkowski, M., B.J. McCarragher (1999) A Queueing Model for the design and analysis of a mining stockyard, in: *Discrete Event Dynamics Systems: Theory and Applications*, 9, pp. 75-98.

Boland, N., D. Gulcynski, M.P. Jackson, M.W.P. Savelsberg, M.K. Tam (2011) Improved stockyard management strategies for coal export terminals at Newcastle, in: *Proceedings of the 19th International Congress of Modeling and Simulation*, Perth, Australia.

Bontekoning, Y.M., C. Macharis, J.J. Trip (2004) Is a new applied transportation research field emerging? A review of intermodal rail–truck freight transport literature, in: *Transportation Research Part A*, 38, pp. 1-34.

Botter, R.C., A.S. Siqueira, L.R. Castro Neto, W.R.A. Ceciliano (2005) Economic operational study of the stockyard and shipment of Ubu port, in: *Proceedings of the 11th International Congress of the International Maritime Association of the Mediterranean*, Lisbon, Portugal.

Boschert, S., T. Hellmuth (2010) Simulation in bulk material handling, in: *Proceedings of the BulkSolids Europe conference*, Glasgow, Scotland.

Boxma, O.J., J.W. Cohen, N. Huffels (1979) Approximations of the mean waiting time in an M/G/s queueing system, in: *Operations Research*, 27 (6), pp. 1115-1127.

Bradly, C.E., S.G. Taylor, W.I. Gray (1985) Sizing storage facilities for open pit coal mines, in: *IIE Transactions*, 17 (4), pp. 320-326.

Bugaric, U.S., P.B. Petrovic (2007) Increasing the capacity of terminal for bulk cargo unloading, in: *Simulation Modelling Practice and Theory*, 15, pp. 1366-1381.

Bugaric, U.S., P.B. Petrovic, Z.V. Jeli, D.V. Petrovic (2012) Optimal utilization of the terminal for bulk cargo unloading, in: *Simulation*, 88 (12), pp. 1508–1521

Burkolter, M., (2005) Capacity of railways in station areas using petri nets, PhD thesis submitted to the Swiss Federal Institute Of Technology, Zurich, Swiss.

Canonaco, P., P. Legato, R.M. Mazza, R. Musmanno (2008) A queuing network model for the management of berth crane operations, in: *Computers and Operations Research*, 35, pp. 2432-2446.

Cassettari, L., R. Mosca, R., Revetria, F. Rolando (2011) Sizing of a 3,000,000t bulk cargo port through discrete and stochastic simulation integrated with response surface methodology techniques, in: *Proceedings of the 11th WSEAS International conference on Signal processing, Computational Geometry and Artificial Vision*, Florence, Italy, pp. 211–216.

Chu, J., H. Ermolowich (1980) Determining the optimum size of a coal silo, in: *Simulation*, 35, pp. 191-197.

Chirwa, R. (2010) RBCT – 91 Mtpa terminal & beyond – Meeting India's rising demand, in: *Proceedings of the McCloskey's Coal Export Conference*, Cape Town, South Africa.

Conradie, D.G., L.E. Morison, J.W. Joubert (2008) Scheduling at coal handling facilities using simulated annealing, in: *Mathematical Methods of Operations Research*, 68, pp. 277-293.

Crainic, T.G. (2000) Service network design in freight transportation, in: *European Journal of Operational Research*, 122, pp. 272-288.

Daganzo, C.F. (1989) The crane scheduling problem, in: *Transportation Research Part B*, 23 (3), pp. 159-175.

Dahal, K.P., S.J. Galloway, G.M. Burt, J.R. McDonald, I. Hopkins (2003) A port system simulation facility with an optimization capability, in: *International Journal of Computational Intelligence and Applications*, 3, pp. 395-410.

Demirci, E. (2003) Simulation modeling and analysis of port investment, in: *Simulation*, 79 (2), pp. 94-105.

Dipsar, S., T. Altiok (1998) Control policies for material flow in bulk-port marine terminals, in: *Proceedings of the IEEE International Conference on Systems, Man, and Cybernetics*, San Diego, USA.

Douma, A., M. Schutten, P. Schuur (2009) Waiting profiles: An efficient protocol for enabling distributed planning of container barge rotations along terminals in the port of Rotterdam, in: *Transportation Research Part C* , 17, pp. 133-148.

Douma, A., P. Schuur, R. Jagerman (2011) Degrees of terminal cooperativeness and the efficiency of the barge handling process, in: *Expert Systems with Applications*, 38, pp. 3580-3589.

Dragovic, B., N.K. Park, Z. Radmilovic (2006) Ship-berth link performance evaluation: simulation and analytical approaches, in: *Maritime Policy and Management*, 33 (3), pp. 281-299.

Dry Cargo International (DCI) (2013) Keeping Europe's light burning, in: *Dry Cargo International Magazine*, 158, pp. 8-9.

Duinkerken, M., J.A. Ottjes, G. Lodewijks (2002) The application of distributed simulation in TOMAS: redesigning a complex transportation model, in: *Proceedings of the 2002 Winter Simulation Conference (WSC2002)*, San Diego, United States.

Duinkerken, M., D.L. Schott, J.T. van der Geest, P. Stoop, G. Lodewijks (2011) Simulation as tool to estimate the homogenization efficiency of bulk material handling, in: *Proceedings of the 25th European Simulation and Modelling Conference- ESM'2011*, Guimaraes, Portugal.

Dziunikowski, B., A. Stochalski (1983) Rapid determination of coal ash content by means of x-ray fluorescence and scattering, in: *Journal of Radioanalytical Chemistry*, 77, pp. 159-165.

El Sheikh, A.A.R, R.J. Paul, A.S. Harding, D.W. Balmer (1987) A microcomputer-based simulation study of a port, in: *Journal of the Operational Research Society*, 38, pp. 673-681.

Erasmus, J.H. (2001) Bulk raw materials storage selection, in: *Proceedings of Beltcon 11 conference*, Johannesburg, South Africa.

FAM (2010) Bulk materials handling, manual based on engineering know-how of FAM Förderanlagen Magdeburg, www.fam.de.

Fioroni, M.M., L.A.G. Franzese, C.E. Zanin, J.Furia, L. De Toledo Perfetti, D. Leonardo, N.L. Da Silva (2007) Simulation of continuous behavior using discrete tools: ore conveyor transport, in: *Proceedings of the 2007 Winter Simulation Conference*, Washington DC, United States.

Fishmann, G.S. (2001) *Discrete event simulation. Modeling, programming, and analysis*, Springer-Verlag, New York.

Gerstel, A.W. (1979) The homogenization of bulk material in blending piles, PhD thesis, Delft University of Technology.

Gerstel, A.W. (1999) Werktuigen en stortgoed (in Dutch), lecture notes for course wb3412, Delft University of Technology.

GHD (2003) Dalrymple Bay Coal Terminal - Infrastructure Valuations, [www.qca.org.au] cited 02/08/2010.

Gross, D., J.F. Shortle, J.M. Thompson, C.M. Harris (2008) *Fundamentals of queueing theory*, John Wiley and Sons Inc., Hoboken, United States.

Grubor, N., S. Milinkovic, S. Veskovic, P. Márton (2013) Simulation analysis of the regional railways in south banat region, in: *Scientific – technical journal for railway transport and carriage, logistics and management*, 9 (3), pp. 30-36.

Gu, J., M. Goetschalckx, L.F. McGinnis (2010) Research on warehouse design and performance evaluation: A comprehensive review, in: *European Journal of Operational Research*, 203, pp. 539-549.

Gy P.M. (1981) A new theory of bed-blending derived from the theory of sampling – development and full-scale experimental check, in: *International Journal of mineral processing*, 8, pp. 201-238.

Haftendorn, C., F. Holz, C.V. Hirschhausen (2012) The end of cheap coal? A techno-economic analysis until 2030 using the COALMOD-World model, in: *Fuel*, 102, pp. 305-325.

Han, M., P. Li, J. Sun (2006) The algorithm for berth scheduling problem by hybrid optimization strategy GASA, In: *Proceedings of the ninth International Conference on Control, Automation, Robotics and Vision (ICARCV'06)*, Washington DC, United States.

Han, X., Z. Lu, L. Xi (2010) A Proactive approach for simultaneous berth and quay crane scheduling problem with stochastic handling time, in: *European Journal of Operational Research*, 207 (3), pp. 1327-1340.

Han, N.N. (2013) Global Steel Industry and China: Future Outlook, in: *Proceedings of Mining on Top Conference*, Stockholm, Sweden.

Hartmann, S., J. Pohlmann, A. Schönknecht (2011) Simulation of container ship arrivals and quay occupation. In: Jürgen W. Böse (ed) Handbook of Terminal Planning, Springer, Berlin.

Henesey, L., P. Davidsson, J.A. Persson (2004) Using simulation in evaluating berth allocation at a container terminal, in: *Proceedings at 3rd International Conference on Computer Applications and Information Technology in the Maritime Industries (COMPIT'04)*, Siguënza, Spain.

Hillier, FS, G.J. Lieberman (2010) *Introduction to Operations Research,* McGraw-Hill Publishing Company, New York.

Hiltermann, J., G. Lodewijks, D.L. Schott, J.C. Rijsenbrij, J.A.J.M. Dekkers, Y. Pang (2011) A methodology to predict power savings of troughed belt conveyors by speed control, in: *Particulate Science and Technology,* 29 (1), pp. 14-27.

Hu, D., Z., Yao (2012) Stacker-reclaimer scheduling in a dry bulk terminal, in: *International Journal of computer integrated manufacturing*, 25, pp. 1047-1058.

Huang W.C., S.C. Wu (2005) The estimation of the initial number of berths in a port system based on cost function, in: *Journal of Marine Science and Technology,* 13 (1), pp. 34-45.

Imai, A., X. Sun, E. Nishimura, S. Papadimitriou (2005) Berth allocation in a container port: using a continuous location space approach, in: *Transportation Research Part B,* 39 (3), pp. 199-221.

Imai, A., H.C. Chen, E. Nishimura, S. Papadimitriou (2008) The simultaneous berth and quay crane allocation problem, in: *Transportation Research Part E,* 44 (5), pp. 900-920.

International Energy Agency (IEA) (2011) World energy outlook 2011, [www.worldenergyoutlook.org] cited 30/12/2013.

International Energy Agency (IEA) (2013) World energy outlook 2013 – Executive summary, [www.worldenergyoutlook.org] cited 30/12/2013.

iSAM (2010) iSAM AG helps the Port of Hamburg to become 'operatorless', in: *Dry Cargo International*, 129, pp. 29.

Jagerman, D.L., T. Altiok (2003) Vessel arrival process and queuing in marine ports handling bulk materials, in: *Queueing Systems,* 45, pp. 223-243.

Jagerman, D.L., B. Balcioğlu, T. Altiok, B. Melamed (2004) Mean waiting time approximations in the G/G/1 queue, in: *Queuing Systems,* 46, pp. 481-506.

Kia, M., E. Shayan, F. Ghotb (2002) Investigation of port capacity under a new approach by computer simulation, in: *Computers and Industrial Engineering,* 42, pp. 533-540.

Kim, B, S.Y. Chang, J. Chang, Y. Han, J. Koo, K. Lim, J. Shin, S. Jeong, W. Kwak (2011) Scheduling of raw-materials unloading from ships at a steelworks, in: *Production Planning & Control,* 22 (4), pp. 389-402.

King D.H., B.A. Radomske, G.S. Manocha (1993) Recent advances in simulation models for bulk terminal design, in: *Bulk Solids Handling*, 13, pp. 23-27.

Klaassen, M.J.A. (2007) Data analysis of an export bulk terminal in South-Africa, report no. 2007.TEL.7116, Delft University of Technology, The Netherlands.

Kleijn, M.J., R. Dekker (1999) An overview of inventory systems with several demand classes, in: *New Trends in Distribution Logistics*, Springer Berlin, Germany.

Kleijnen, J.P.C. (1995) Verification and validation of simulation models, in: *European Journal of Operational Research*, 82, pp. 145-162.

Knappe, W. (1995) Performance of bucket wheel reclaimers, in: *Proceedings of Beltcon 8 conference*, Johannesburg, South Africa.

Kondratowicz, L.J. (1990) Simulation methodology for intermodal freight transportation terminals, in: *Simulation*, 55, pp. 49-57.

Kozan, E. (1997) Comparison of analytical and simulation planning models of seaport container terminals, in: *Transportation Planning and Technology*, 20 (3), pp. 235-248.

Kozan, E., S.Q. Liu (2012) A demand-responsive decision support system for coal transportation, in: *Decision Support Systems,* 54, pp. 665-680.

Kraaijeveld van Hemert, J. (1984) Coal receiving terminals in relation to electricity generation in developing countries, in: *Natural Resources Forum*, 8 (1), pp. 37–49.

Kumral, M. (2006) Bed blending design incorporating multiple regression modeling and genetic algorithms, in: *Journal of the South African Institute of Mining and Metallurgy*, 106, pp. 229-236.

Kuo, T.C., W.C. Huang, S.C. Wu, P.L. Cheng (2006) A case study of interarrival time distributions of container ships, in: *Journal of Marine Science and Technology*, 14 (3), pp. 155-164.

Lai, K.K., K. Shih (1992) A study of container berth allocation, in: *Journal of Advanced Transportation,* 26 (1), pp. 45-60.

Langen de, P.W., J. van Meijeren, L.A. Tavasszy (2012) Combining models and commodity chain research for making long-term projections of port throughput: an application to the Hamburg – Le Havre range, in: *European Journal of Transport and Infrastructure Research*, 12 (3), pp. 310-331.

Laugharne, A. (2012) Iron ore market outlook, in: *Proceedings of the Scotia Capital Commodities Conference*, Toronto, Canada.

Leech, J. (2010) Design of an efficient coal export terminal, in: *Proceedings of the Queensland Mining and Engineering exhibition,* Mackay, Australia.

Leech, J. (2012) Optimising a bulk minerals export chain, in: *Mining Magazine*, pp. 42-48.

Legato, P., R.M. Mazza (2001) Berth planning and resources optimization at a container terminal via discrete event simulation, in: *European Journal of Operational Research,* 133 (3), pp. 537-547.

Legato, P., R.M. Mazza (2013) Addressing robust berth planning under uncertainty via simulation based optimization, in: *Proceedings of the International Conference on Modeling and Applied Simulation,* Athens, Greece.

Lieberwirth, H. (2012) Bed blending efficiency – adding value with stockyard systems, in: *Proceedings of the BulkSolids Europe 2012 conference*, Berlin, Germany.

Ligteringen, H., H. Velsink (2012) *Port and terminals*, VSSD, Delft.

Little, J.D.C. (1961) A Proof for the queuing formula: L = λW, in: *Operations Research*, 9, pp. 383 – 387.

Lloyd's Register (2013) Global Marine Trends 2030, [www.lr.org] cited 31/12/2013.

Lodewijks, G., D.L. Schott, J.A. Ottjes (2009) Dry bulk terminal expansion or redesign?, in: *Port Technology International*, 43, pp. 87-94.

Lodewijks, G. (2010) Interaction between bulk solids and transport equipment – lecture notes, Delft University of Technology, The Netherlands.

Lodewijks, G. (2011) The next generation low loss conveyor belts, in: *Proceedings of the Beltcon 16 conference,* Johannesburg, South-Africa.

Lodi, A., S. Martello, M. Monaci (2002) Two-dimensional packing problems: a survey, in: *European Journal of Operational Research,* 141 (2), pp. 241-252.

Mah, R.S., M. Shacham (1978) Pipeline network design and synthesis, in: *Advances in Chemical Engineering*, Thomas B. Drew (ed), Academic Press, London, pp 142-226.

McCartney, R.H. (1996) Coal and Limestone Handling. In: *Power Plant Engineering*, Chapman and Hall, New York.

Meisel, F., C. Bierwirth (2006) Integration of berth allocation and crane assignment to improve the resource utilization at seaport container terminals. In: Haasis, H.D., Kopfer, H, Schönberger J. (Eds.), *Operations Research Proceedings 2005*. Springer, Berlin.

Meisel, F., C. Bierwirth (2009) Heuristics for the integration of crane productivity in the berth allocation problem, in: *Transportation Research Part E*, 45 (1), pp. 196-209.

Memos, C.D. (2004) Port Planning, in: *Port engineering: planning, construction, maintenance, and security*, John Wiley & Sons, New Jersey, pp. 7-64.

Meng, C., S.S. Nageshwaraniyer, A. Maghsoudi, Y.J. Son, S. Dessureault (2013) Data-driven modeling and simulation framework for materials handling systems in coal mines, in: *Computers & Industrial Engineering*, 64, pp. 766-779.

Middelberg, A., J. Zhang, X. Xia (2009) An optimal control model for load shifting – with application in the energy management of a colliery, in: *Applied Energy*, 86, pp. 1266–1273.

Molck, P., R. Goncalves, T. Caldas, J. Valentim, L. Lima, E. Newton, M. França, R. Mendes, F. Gomide (2001) Intelligent stockpile building in iron ore shipping yard, in: *Proceedings of* *the third international conference on intelligent processing and manufacturing of materials (IPMM 2001)*, Richmond, Canada.

Morrison, R. (2009) Robotic wagon vibrator discharges sticky coal, in: *Bulk Solids Handling*, 29 (4), pp. 224-226.

Muthuraman, M., T. Namioka, K. Yoshikawa (2010) Characteristics of co-combustion and kinetic study on hydrthermally treated municipal solid waste with different rank coals: A thermogravimetric analysis, in: *Applied Energy*, 87, pp. 141-148.

Müller K.P. (2010) Stacking, reclaiming and blending effects, in: *Mechanical Technology*, Crown publications, South-Africa, pp. 14-17.

Narayanaswami, S., N. Rangaraj (2011) Scheduling and rescheduling of railway operations: a review and expository analysis, in: *Technology Operation Management*, 2 (2), pp. 102-122.

O'Brien, G.G., R.R. Crane (1959) The scheduling of a barge line, in: *Operations Research*, 7 (5), pp. 561-570.

Oğuz, C., J. Błażewicz, T.C.E. Cheng, M. Machowiak (2004) Berth allocation as a moldable task scheduling problem, in: *Proceedings of the 9th International Workshop on Project Management and Scheduling (PMS 2004)*, Nancy, France.

Orbán-Mihályko, E., B.G. Lakatos (2004) Intermediate storage in batch/continuous processing systems under stochastic operation conditions, in: *Computer and Chemical Engineering*, 28, 2493-2508.

Ottjes, J.A., H.P.M. Veeke (2002) Prototyping in process oriented modeling and simulation, in: *Proceedings of the 16th European Simulation Multi Conference (ESM 2002)*, Darmstadt, Germany.

Ottjes, J.A., H.P.M. Veeke (2003) Transparent distributed discrete event modeling, in: *Proceedings of the 2003 European Simulation and Modelling Conference (ESM2003)*, Naples, Italy.

Ottjes, J.A., G. Lodewijks (2004) Reliability of large scale conveyor systems, in: *Proceedings of the Industrial Simulation Conference (ISC 2004)*, Malaga, Spain.

Ottjes, J.A., G. Lodewijks, D.L. Schott (2007) Bulk terminal modelling and simulation, in: *Proceedings of the Industrial Simulation Conference (ISC 2007)*, Delft, The Netherlands.

Pachakis, D., A.S. Kiremidjian (2003) Ship traffic modeling methodology for ports, in: *Journal of Waterway, Port, Coastal and Ocean Engineering*, 129 (5), pp. 193-202.

Park, C.S, Y.D. Noh (1987) A port simulation model for bulk cargo operations, in: *Simulation*, 48 (6), pp. 236-246.

Park, Y.M., K.H. Kim (2003) A scheduling method for berth and quay cranes, in: *OR Spectrum*, 25 (1), pp. 1-23.

Pavloudakis, F.F., Z. Agioutantis (2010) Simulation of bulk solids blending in longitudinal stockpiles, in: *International journal of surface mining, reclamation and environment*, 17 (2), pp. 98-112.

Peterkofsky, R.I., C.F. Daganzo (1990) A branch and bound solution method for the crane scheduling problem, in: *Transportation Research Part B*, 24 (3), pp. 159-172.

Petersen, I.F. (2004) Blending in circular and longitudinal mixing piles, in: *Chemometrics and intelligent laboratory systems*, 74, pp. 135-141.

Pidgeon, A. (2007) Dampier Port Upgrade, in: *Bulk Solids Handling*, 27, pp. 540-547.

Plumlee, C.H. (1966) Optimum size seaport, in: *Journal of Waterway, Port, Coastal and Ocean Engineering*, 92 (3), pp. 1-24.

Radmilovich, Z.R. (1992) Ship-berth link as bulk queuing system in ports, in: *Journal of Waterway, Port, Coastal and Ocean Engineering*, 118 (5), pp. 474-495.

Reicks, A.V. (2008) Belt conveyor idler roll behaviours, in: *Bulk material handling by conveyor belt*, M.A. Alspaugh (ed.), pp. 35–40.

Robenek, T., N. Umang, M. Bierlaire, S. Ropke (2013) A branch-and-price algorithm to solve the integrated berth allocation and yard assignment problem in bulk ports, in: *European Journal of Operational Research*, 235 (2), pp. 399-411.

Roberts, A.W. (1981) Economic analysis in the optimization of belt conveyor systems, in: *Proceedings of Beltcon 1 conference*, Johannesburg, South Africa.

Robinson, G.K. (2004) How much would a blending stockpile reduce variation?, in: *Chemometrics and intelligent laboratory systems*, 74, pp. 121-133.

Saanen, Y.A. (2004) An approach for designing robotized marine container terminals, PhD thesis, Delft University of Technology.

Sanchez, C, R. Uribe, J.C. Espinal (2005) Port simulation model for the discharge and delivery of imported coal for a thermal power plant located in Lazaro Cardenas Port, Mexican Pacific Coast, in: *Proceedings of 2nd International Conference on Maritime Heritage*, Barcelona, Spain, pp. 339–349.

Sarkar, R.A., E.A. Gunn (1994) Coal bank scheduling using a mathematical programming model, in: *Applied Mathematical Modelling*, 18, pp. 672-678.

Schmidt, M., W. Hartmann, P. Nyhuis (2012) Simulation based comparison of safety-stock calculation methods, in: *Manufacturing Technology*, 61, pp. 403-406.

Schonfeld, P., S. Frank (1984) Optimizing the use of a containership berth, in: *Transportation Research Record*, 984, pp. 56-62.

Schott, D.L. (2004) Large-scale homogenization of bulk materials in mammoth silos, PhD thesis, Delft University of Technology.

Shabayek, A.A., W.W. Yeung (2002) A simulation model for the Kwai Chung container terminals in Hong-Kong, in: *European Journal of Operational Research*, 140, pp. 1-11.

Singh, G., D. Sier, A. T. Ernst, O. Gavriliouk, R. Oysten, T. Giles, P. Welgama (2010) A mixed integer programming model for long term capacity expansion planning: a case from the Hunter Valley Coal Chain, in: *European Journal of Operational Research*, 222 (1), pp. 210-224.

Soros, P. (1991) The linear shiploader – an overview, in: *Bulk Solids Handling*, 11, pp. 293-298.

Soros, P. (1993) Dual-Linear Loader, cost breakthrough in shiploading, in: *Bulk Solids Handling*, 13, pp. 13-19.

Stahlbock, R., S. Voß (2008) Operations research at container terminals: a literature update, in: *OR Spectrum*, 30 (1), pp. 1-52.

Strien J.N. (2010) Details of stacker, reclaimers and stacker-reclaimers for the use at terminal stockyards, report no. 2010.TEL.7510, Delft University of Technology, The Netherlands.

Sultoon, J. (2013) Global coal markets and their impacts on the US, [www.stb.dot.gov] cited 30/12/2013.

Swedish, J.A. (1998) Simulation of an inland waterway barge fleet distribution network, in: *Proceedings of the 1998 Winter Simulation Conference*, Washington, United States.

Tahar, M.R., K. Hussain (2000) Simulation and analysis for the Kelang Container Terminal operations, in: *Logistics Information Management*, 13 (1), pp. 14-20.

Taylor, G.D., T.C. Whyte, G.W. DePuy, D.J. Drosos (2005) A simulation-based software system for barge dispatching and boat assignment in inland waterways, in: *Simulation Modelling Practice and Theory*, 13, pp. 550-565

Tengku-Adnan, T. D. Sier, R.N. Ibrahim (2009) Performance of Ship Queuing Rules at Coal Export Terminals, in: *Proceedings of the IEEE International Conference on Industrial Engineering and Engineering Management*, Hong-Kong, China.

Tewalt, S.J., R.B. Finkelman, I.E. Torres, F. Simoni (2006) World Coal Quality Inventory: Colombia, in: *World Coal Quality Inventory: South America*, (Eds.) A.W. Karlsen, S.J. Tewalt, L.J. Bragg, R.B. Finkelman, U.S. Geological Survey Open File Report 2006-1241.

Tewari, P.C., I.P. Singh, M.K. Khare (1991) Reliability analysis of a conveyor belt system, with only one server, subject to failures and idleness after repair, in: *Microelectronic Reliability*, 31 (5), pp. 823-826.

Theis, C. (2009) The Russian Transport Infrastructure, in: *Proceedings of the 4th CoalTrans Conference*, Moskow, Russia.

Tijms, H.C., E.M.F. Kalvelagen (1994) *Modelbouw in de operations research,* Academic Service, Schoonhoven.

Umang, N., M. Bierlaire, I. Vacca (2013) Exact and heuristic methods to solve the berth allocation problem in bulk ports, in: *Transportation Research Part E,* 54, pp. 14-31.

United Nations Conference on Trade and Developments (UNCTAD) (1985) *Port Development - a handbook for planners in developing countries*, United Nations, New York.

Veeke, H.P.M., J.A. Ottjes (1999) TOMAS: Tool for Object Oriented Modeling and Simulation, in: *Proceedings of the Business and Industry Simulation Symposium ASTC*, Washington D.C., United States.

Verschoof, J. (2002) *Cranes, Design, Practice and Maintenance*, Professional Engineering Publishing Limited, London.

Vianen van, T.A., J.A. Ottjes, G. Lodewijks (2011a) Dry bulk terminal characteristics, in: *Proceedings of Bulk Solids Handling 2011*, Mumbai, India.

Vianen van, T.A., J.A. Ottjes, G. Lodewijks (2011b) Dry bulk terminal characteristics, [http://www.bulk-solids-handling.com/dry-bulk-terminal-characteristics-v-17205-9336] cited 12/01/2014.

Vianen van, T.A., J.A. Ottjes, G. Lodewijks (2012a) Modeling the arrival process at dry bulk terminals, in: *Proceedings of the Bulk ports, terminals and logistics 2012 conference*, Amsterdam, The Netherlands.

Vianen van, T.A., D.L. Mooijman, J.A. Ottjes, R.R. Negenborn, G. Lodewijks (2012b) Simulation-based operational control of a dry bulk terminal, in: *Proceedings of the 2012 IEEE International Conference on Networking, Sensing and Control (ICNSC 2012),* Beijing, China.

Vianen van, T.A., J.A. Ottjes, G. Lodewijks (2013) Operational control for stacker-reclaimers, in: *Proceedings of the 15th International conference on harbor, maritime and multimodal logistics modeling and simulation,* Athens, Greece.

Vianen van, T.A., J.A. Ottjes, G. Lodewijks (2014a) Simulation based determination of the required stockyard size for dry bulk terminals, in: *Simulation Modelling Practice and Theory*, 42, pp. 119-128.

Vianen van, T.A., J.A. Ottjes, G. Lodewijks (2014b) Simulation based rescheduling of the stacker-reclaimers operation, in: *Journal of Computational Science*, DOI: 10.1016/j.jocs.2014.06.004 (available online 12 June 2014).

Vianen van, T.A., J.A. Ottjes, G. Lodewijks (2014c) Belt conveyor network design using simulation, in: *Journal of Simulation,* advance online publication, doi:10.1057/jos.2014.38.

Vikram, K., P.K. Sarkar (2008) Installation of a material handling system for multipurpose berths, in: *Port Technology International*, 39, pp. 96-100.

Vis, I.F.A., R. De Koster (2003) Transshipment of containers at a container terminal: an overview, in: *European Journal of Operational Research,* 147 (1), pp. 1-16.

Vukadinović, K., D. Teodorović (1994) A fuzzy approach to vessel dispatching problem, in: *European Journal of Operational Research*, 76, pp. 155-164.

Walker, T., B. Miller (2004) Precision unit-train loading systems, in: *CoalAge Magazine*, pp. 22-28.

Weiss, M., M. Thomet, F. Mostoufi (1999) Interactive simulation model for bulk shipping terminals, in: *Bulk Solids Handling*, 19 (1), pp. 95-98.

Wet de, N. (1994) Homogenizing/blending in South Africa – an update, in: *Bulk Solids Handling*, 14 (1).

Willekes, M.J. (1999) Dry bulk terminals in seaports - lecture notes, Delft University of Technology, The Netherlands.

Wöhlbier, R.H. (1977) *Stacking, blending, reclaiming*, Trans Tech Publications, Clausthal-Zellerfeld, Germany.

Wolpers, F.M. (1995) Homogenization of bulk materials in longitudinal and circular stockpile arrangements, in: *Proceedings of Beltcon 8 conference*, Johannesburg, South Africa.

Ye, W, (2004) Development of modern continuous ship unloaders, in: *Proceedings of Port Handling Systems 2004*, Mumbai, India.

Zador, A.T. (1991) Technology and economy of blending and mixing, in: *Bulk Solids Handling*, 11 (1), pp. 1-11.

Zeigler, B.P., H. Praehofer, T.G. Kim (2000) *Theory of modeling and simulation*, 2nd Edition, Academic Press, San Diego.

Zhang, S., X. Xia (2010) Optimal control of operation efficiency of belt conveyor systems, in: *Applied Energy*, 87, pp. 1929-1937.

Zhou, P., H. Kang, L. Lin (2006) A dynamic berth allocation model based on stochastic consideration, In: *Proceedings of the sixth World Congress on Intelligent Control and Automation (WCICA'06)*, Washington DC, United States.

A. Consulted dry bulk terminals

From 49 terminals that handle coal and/or iron ore detailed information was gathered. To cover the expected range of different terminal characteristics, import as well as export terminals from different sizes and different annual throughputs located all over the world, were investigated. Table A.1 lists the names, locations and consulted references for import terminals and in Table A.2 detailed information for export terminals is listed.

Table A.1: Names, locations and consulted references for investigated import terminals

Name	City	Country	References
OBA Bulk Terminal	Amsterdam	the Netherlands	www.oba-bulk.nl, www.portofamsterdam.nl and interview
Tata Steel Bulk Terminal	IJmuiden	the Netherlands	www.portofamsterdam.nl and interview
Europees Massagoed Overslagbedrijf	Rotterdam	the Netherlands	www.emo.nl and interview
Ertsoverslagbedrijf Europoort C.V.	Rotterdam	the Netherlands	www.eecv.nl and interview
European Bulk Services Laurenshaven	Rotterdam	the Netherlands	www.ebsbulk.com and interview
Delwaidedok	Antwerp	Belgium	www.portofantwerp.com and www.sea-invest.be
Kanaaldok	Antwerp	Belgium	www.portofantwerp.com and www.sea-invest.be
Western Bulk Terminal	Dunkirk	France	www.sea-invest.be and www.dunkerque-port.fr

Name	City	Country	References
ArcelorMittal Dunkirk	Dunkirk	France	www.dunkerque-port.fr, www.arcelormittal.com and interview
Ports Le Havre	Le Havre	France	www.havre-port.fr
Hansaport	Hamburg	Germany	www.hansaport.de and interview
Immingham Bulk Terminal	Immingham	United Kingdom	www.abports.co.uk, www.worldportsource.com (GBR_Port_of_Immingham)
Bulk Terminal 2A	Bourgas	Bulgaria	www.port-burgas.com (Terminal 2A) and www.mtc.government.bg (Port of Bourgas)
Luojing Terminal	Shanghai	China	www.portshanghai.com.cn/en/subcompany/lj.html , www.sipgl.com and interview
BaoShan Port	Shanghai	China	www.baosteel.com and interview
Muroran Port	Muroran	Japan	www.hkd.mlit.go.jp/zigyoka/z_kowan/bayport/profile/muroran.html
Kashima Steelworks	Kashima	Japan	www.ihi.co.jp and www.steelguru.com
Nippon Steel Bulk Terminal	Kitakyushu	Japan	www.kitaqport.or.jp and www.nsc.co.jp
Oita Works	Oita	Japan	www.nsc.co.jp/en/oita
Kaohsiung Port	Kaohsiung	Taiwan	www.worldportsource.com and www.khb.gov.tw
Posco Bulk Terminal	Pohang	South Korea	www.poscoterminal.co.kr
Gwangyang Works	Gwangyang	South Korea	www.posco.com
Vale Praia Mole Terminal	Tubarao	Brazil	www.vale.com

Table A.2: Names, locations and consulted references for investigated export terminals

Name	City	Country	References
Ports BHP Billiton	Hedland	Australia	www.phpa.com.au , www.bhpbilliton.com, www.laingorourke.com.au and interview
Port Fortescue Metal Group	Hedland	Australia	www.phpa.com.au , www.fmgl.com.au, www.metsominerals.com (Twin cell rotary train unloader) and www.epa.wa.gov.au
Carrington Coal Terminal	Newcastle	Australia	www.pwcs.com.au (Carrington)
Kooragang Coal Terminal	Newcastle	Australia	www.pwcs.com.au (Kooragang)

Name	City	Country	References
Parker Point	Dampier	Australia	www.riotintoironore.com, www.dpa.wa.gov.au , www.eimco.co.uk, www.miningandconstruction.sandvik.com and (Pidgeon, 2007)
East Intercourse Island	Dampier	Australia	www.riotintoironore.com and www.dpa.wa.gov.au
Rio Tinto Iron Ore Port	Cape Lambert	Australia	www.riotintoironore.com , www.bulk-solids-handling.com (Pilbara Capacity Extension) and www.smc.sandvik.com
Port of Kembla Coal Terminal	Kembla	Australia	www.pkct.com.au and www.bhpbilliton.com
Dalrymple Bay Coal Terminal	Hay Point	Australia	www.dbct.com.au , www.nqbp.com.au, GHD (2003) , BBI (2007) and www.dnv.az
Hay Point Coal Terminal	Hay Point	Australia	www.nqbp.com.au and www.bhpbilliton.com
Richard Bay Coal Terminal	Richard Bay	South Africa	www.rbct.co.za, Chirwa (2010) and interview
Saldanha Iron Ore Terminal	Saldanha	South Africa	http://ports.co.za/saldanha-bay.php
Port of Qinhuangdao	Qinhuangdao	China	www.portqhd.com , www.cosco.com and www.metso.com (Qinhuangdao Port)
Port of Chennai (Ore handling facility)	Chennai	India	www.chennaiport.gov.in and Lodewijks et al. (2009)
Vizag Seaport	Visakhapatnam	India	www.vizagport.com and Vikram and Sarkar (2008)
Mormugao Port (Ore berth E9)	Goa	India	www.mptgoa.com, www.krupprobins.com and www.asiatradehub.com
Port of Paradip	Paradip	India	www.paradipport.gov.in and www.mcnallybharat.com
Vale Tubarao	Tubarao	Brazil	www.vale.com
Ponta da Madeira	Sao Luis	Brazil	www.vale.com and www.bulk-online.com
Lamberts Point Coal Terminal	Norfolk	USA	www.globalsecurity.org/military/facility/lamberts-point.htm and www.reuters.com/article/idUSN0659969120080206
Westshore Terminals	Vancouver	Canada	www.westshore.com and interview
Ridley Terminals	Prince Rupert	Canada	www.rti.ca
Puerto Bolívar	Bolívar	Colombia	www.cerrejoncoal.com, www.xstratacoal.com
Pulau Laut Coal Terminal	Kota Baru	Indonesia	www.indonesiabulkterminal.com
Bontang Coal Terminal	Bontang	Indonesia	www.itmg.co.id and www.banpu.co.th
Port of Murmansk	Murmansk	Russia	www.suek.ru and www.portmurmansk.ru

B. Bulk ships

In this Appendix details of bulk ships are presented. Several ship registers classifies bulk ships in several classes. To give an idea about the sizes of the bulk ships per class, for each class a picture of a bulk ship is presented.

For the seaside design, dimensions of visited ships determine the berth length needed, the water depth required alongside the quay and the cranes' outreach required. From 289 bulk ships carrying coal and iron ore, values for the length, draft and beam were determined using the database of Sea-web (http://www.sea-web.com). These details are listed in Table B.1. Note that the actual draft can differ from the maximum draft, depending on the actual shipload. Detailed information about the ship unloading process was provided by a multi-user import terminal. This dataset contains information about the number of material grades loaded in the ships, the number of hatches per ship, the material type unloaded and the needed unloading time. Table B.2 lists this data. This dataset was used to determine the histogram of the number of materials per ship (Figure 3.3) and the relation for the ship unloading rate as function of several parameters (see section 3.5.3).

Figure B.1: An Handysize bulk ship; Rodopi (dwt: 23 [kt], L_s: 181 [m], B: 23 [m] and D: 10.4 [m]) (Courtesy of M. Guney @Marinetraffic.com)

Figure B.2: An Handymax bulk ship; Hemus (dwt: 43 [kt], L_s: 186 [m], B: 30 [m] and D: 11.7 [m]) (Courtesy of Marinetraffic.com)

Figure B.3: A Panamax bulk ship; Yarrawonga (dwt: 82 [kt], L_s: 229 [m], B: 32 [m] and D: 14.6 [m]) (Courtesy of P. Jakobsen @Marinetraffic.com)

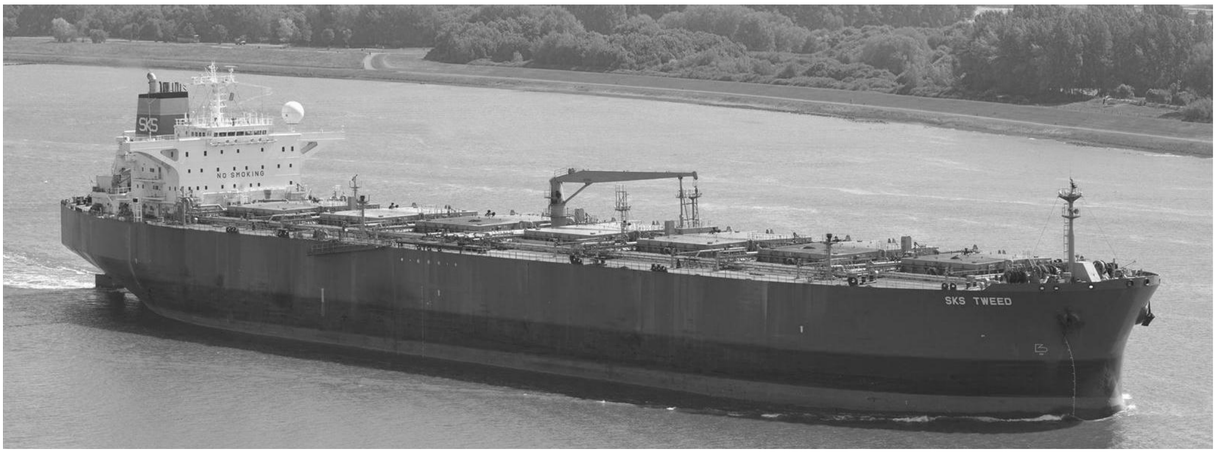

Figure B.4: A small Capesize bulk ship; SKS-Tweed (dwt: 110 [kt], L_s: 243 [m], B: 42 [m] and D: 15.7 [m]) (Courtesy R.Maat @Marinetraffic.com)

Figure B.5: A large Capesize bulk ship: Vale Rio de Janeiro (dwt: 400 [kt], L_s: 365 [m], B: 65 [m] and D: 23 [m]) (Courtesy Aerolin Photo BV @Marinetraffic.com)

Table B.1: Names and details of the investigated bulk ships

Bulk ship	Deadweight (dwt) [kt]	Length (L_s) [m]	Beam (B) [m]	Max. draft (D) [m]
C ATLAS	180	292	45	17.1
YARRAWONGA	82	229	32	14.1
CAPE HARRIER	177	289	45	17.1
ALPHA ERA	170	289	45	17.6
MINERAL CAPEASIA	175	289	45	17.6
TIANRONGHAI	172	299	45	17.5
KING ROBERT	173	290	45	17.3
HANJIN SINES	173	291	45	17.3
RENATE N	286	327	55	20.5
CHINA FORTUNE	152	270	43	16.7
ATLANTIC LEGEND	80	229	32	14.2
MARIA A.ANGELICOU	170	289	45	17
IVAN SUSANIN	20	181	23	9.7
KING SAIL	178	289	45	17.3
ALEXANDRA	82	229	32	14.1
CAPE UNITY	178	289	45	17.7
CAPE LOTUS	171	289	45	16.9
FORMOSABULK BRAVE	170	289	45	17.3
MARGOT N	277	322	56	19.6
NSS BONANZA	171	289	47	16.7
COAL AGE	73	225	32	14.1
TRITON CONDOR	180	289	45	16.9
CAPE DOVER	186	290	48	17
ALFRED N	260	325	54	20.1
ANGELINA	75	225	32	14.2
CAPE TAVOR	173	289	45	17.4
ERICA	82	229	32	14.7
CAST. DE VALVERDE	173	289	45	17.7
AQUACHARM	171	289	45	17.7
MARIPERLA	180	292	45	18
PACIFIC FORTUNE	172	289	45	17.3

Bulk ship	Deadweight (dwt) [kt]	Length (L_s) [m]	Beam (B) [m]	Max. draft (D) [m]
HAI XIANG	165	282	45	17.4
GRAND DIVA	77	225	32	13.8
LONDON COURAGE	203	300	50	16.2
MEYNELL	186	292	48	17.4
ABIGAIL N	300	327	55	21
ASIA GRAECA	74	225	32	13.8
HEMUS	43	186	30	11.7
MACIEJ RATAJ	34	195	26	10.5
CAPE OCEANIA	149	270	43	17.2
WU ZHU HAI	75	225	32	11.9
EMPRESS	152	274	45	16.5
INNOVATOR	149	269	43	16.8
CHINA FORTUNE	152	270	43	16
MAHA ANOSHA	170	288	50	17.1
MINERAL BELGIUM	174	288	45	17.5
ARIADNE	180	291	44	17.8
BATTERSEA	174	288	45	17.4
AVOCA	77	218	32	13.8
CHIN SHAN	176	289	45	17
PARADISE N	322	332	58	21.5
HEMUS	43	186	30	11.7
MINERAL WATER	170	289	45	17.4
MACIEJ RATAJ	34	195	26	10.5
CAPE FRONTIER	180	289	45	17.9
CAST. DE SAN JUAN	173	290	46	17.1
CSK ENTERPRISE	168	283	45	17.5
G.B. CORRADO	76	225	32	14
THALIA	75	224	32	11.6
FAITH N	261	325	54	20.2
A DUCKLING	171	289	45	16.9
OCEAN CREATION	203	300	50	16.1
MANGARELLA	82	229	32	14.1
OCEAN ROAD	180	292	45	17.9
MACIEJ RATAJ	34	195	26	10.8
XINWANG HAI	175	289	45	17.4
CAST. DE CATOIRA	174	289	45	17.4
OCEAN LADY	173	295	46	17.6
KAMISU MARU	151	268	43	13.6
ELEGANT STAR	177	289	45	17.6
ETERNAL SALUTE	87	228	38	13.8
BATALIONY CHLOPSK	37	195	26	10.9
RODOPI	23	181	23	10.4
CAPE AWOBA	171	289	45	17.4
SKS TRENT	110	243	42	12.3
PONTONIKIS	74	225	32	13.3
MAHA ANOSHA	170	288	50	17
ORE GUAIBA	169	288	45	17.8
AM EXPRESS	75	222	32	14.4
VOGERUNNER	177	289	45	17.6
FLECHA	170	289	45	16.9
DONG-A SATURN	150	264	43	16.7
CHENEBOURG	150	270	40	17
REDONDO	75	225	38	14.1
CAPE ORCHID	173	289	45	17.1
ALPHA MILLENNIUM	170	289	44	17.1
ALIKI	180	287	46	17.5
MONA PEGASUS	173	289	45	17.8
UNITED STARS	44	190	31	10.9
REBEKKA N	255	332	56	20
LOWLANDS ORCHID	176	284	45	18.3
LADY GIOVI	75	226	32	11.7
PARADISE N	322	332	58	22.6
CHIN SHAN	176	289	45	14.7
PIONEER ATLANTIC	70	225	32	11.7
CAST. DE GORMAZ	154	289	45	16.1
BET FIGHTER	173	298	46	17.7
BIANCO ID	71	224	32	13.3
PARTAGAS	174	289	45	15.2
JULIAN N	149	270	43	17.1
PACIFIC EAGLE	74	224	31	14.1

Bulk ship	Deadweight (dwt) [kt]	Length (L_s) [m]	Beam (B) [m]	Max. draft (D) [m]
DIONE	180	292	45	17.5
CAST. DE CATOIRA	174	289	45	17
RUBENA N	203	300	50	18.1
CAPE GARLAND	180	292	45	17
GREAT NAVIGATOR	176	289	45	17.4
PETKA	75	225	32	12.8
SAGA PIONEER	47	199	30	11.8
FAITH N	261	325	54	20.6
MAGANARI	76	225	33	14.3
BERGE FJORD	311	332	57	21.5
MIHO PRACAT	81	229	32	12.1
TRITON CONDOR	177	289	45	18.1
MARCHEROKEE	21	153	23	9.8
CHENEBOURG	150	270	40	17.3
PACIFIC FORTUNE	172	289	45	17
KOHJU	172	289	45	17.8
GOONYELLA TRADER	171	288	45	17.2
ITALIC G	87	229	38	14.2
KING ROBERT	173	290	45	15
IRON FUZEYYA	82	229	32	13.8
NORD NAVIGATOR	82	229	32	11.7
PARADISE N	322	332	58	22.5
ARTHUR N	261	325	54	20.5
AQUAGLORY	171	289	45	17
FOUR EARTH	77	249	32	13.7
ROBUSTO	177	289	45	18.1
NORD MERCURY	76	225	32	14.2
ALEKSANDR SUVOROV	23	181	23	10
KOHFUKUSAN	173	293	45	16.2
AGIOS EFRAIM	73	224	32	13.7
MONA RIVER	171	287	45	17.8
BRUNHILDE SALAMON	76	225	32	14
BW ARCTIC	174	292	48	17.1
MIKHAIL KUTUZOV	23	181	23	9.8
NSS BONANZA	171	289	47	16.8
GRACEFUL MADONNA	171	288	45	14.8
BANZAI	74	225	33	14
MINERAL STAR	76	224	32	13.5
ROYAL CHORALE	178	289	45	17.3
ALFRED N	260	325	54	20.7
STORRINGTON	12	138	19	7.6
ROYAL ACCORD	173	290	45	17.3
CHENEBOURG	150	270	40	17.3
CAPE LOTUS	171	289	45	14.6
TRITON CONDOR	177	289	45	17.2
BULK HONG KONG	180	289	45	17.7
PACIFIC FORTUNE	172	289	45	16.1
MARGOT N	277	322	56	19.9
CAPE RIVIERA	186	280	47	17.9
AQUAGEM	167	283	45	15.6
GIUSEPPE LEMBO	173	295	46	17
OCEAN DUKE	173	295	46	18.5
SKS TWEED	110	243	42	15.7
BENITA	7	107	18	6.7
BERGE BONDE	206	300	50	18.1
GIUSEPPE RIZZO	78	225	32	14.1
CHINA ST. RESPONS	176	289	45	17.9
ANANGEL INNOVATIO	172	289	46	17.8
CAPE AWOBA	171	289	45	17
STRIGGLA	75	225	32	14.2
MARIPERLA	180	292	45	17.2
ARIADNE	180	291	44	17.9
CAST. DE GORMAZ	154	289	45	17.1
LEGIONY POLSKIE	74	229	32	14.2
MANASOTA	171	288	45	17.1
ORLETA LWOWSKIE	74	228	32	14.2
MILAGRO	75	225	32	14
E.R. BAYONNE	180	292	45	17
AMY N	322	332	58	17.5
FIRST EAGLE	177	289	45	18.2

Bulk ship	Deadweight (dwt) [kt]	Length (L_s) [m]	Beam (B) [m]	Max. draft (D) [m]
AMITY	173	295	46	17.5
BERGE FJORD	311	332	57	15.2
YARRAWONGA	82	229	32	14.6
ANANGEL VISION	172	280	45	17.2
RUBIN ARTEMIS	152	273	44	17.6
BING N	323	339	55	21.5
OCEAN CREATION	206	300	50	18.2
ALFRED N	260	325	54	20.5
KING ROBERT	173	290	45	16.5
CAPE YAMABUKI	180	292	46	17
SAMJOHN AMITY	75	225	32	13.8
CAST. DE SAN JORG	173	289	46	17.6
AQUAGLORY	171	289	45	18
SUCCESSOR	174	289	45	17.7
CAPE RIVIERA	186	280	47	17.9
OKOLTCHITZA	26	185	23	9.9
VINALINES FORTUNA	27	165	26	9.5
MIHO PRACAT	81	229	32	12
MANASOTA	171	288	45	16.7
BRISBANE	151	273	43	17.6
CAPE GARLAND	180	292	45	17.1
KEY ACTION	81	229	32	14.1
AMAPOLA	77	225	33	14.2
LEGIONY POLSKIE	74	229	32	13.8
BIC IRINI	103	243	42	12.5
CAPE AWOBA	171	289	45	14.8
EMPRESS	152	274	45	17
MIKHAIL STREKALOV	19	181	23	9.9
BERLIN	77	217	31	12.8
CHRISTINE	177	289	45	17.9
AMITY	173	295	46	17.2
NORD DORADO	110	250	43	11.6
CHIN SHAN	176	289	45	17.2
LINDA DREAM	177	289	45	18.1
LONDON COURAGE	206	300	50	16.2
STELLA	180	292	45	18.5
CHINA STEEL TEAM	203	299	50	18.1
LOWLANDS QUEEN	75	225	32	14.1
LEGIONY POLSKIE	74	229	32	14.2
C.LAUREL	151	272	42	17.1
VINALINES FORTUNA	27	165	26	9.4
GAURI PREM	75	225	32	14.2
ATHENIAN PHOENIX	180	292	45	17.5
KAMISU MARU	151	268	43	17.7
HANJIN CAPETOWN	152	274	45	12.8
AQUAGLORY	171	289	45	17.8
AMAGISAN	160	280	43	17.2
PACIFIC FORTUNE	172	289	45	17.6
CAST. DE VALVERDE	173	289	45	16.8
MARINICKI	77	218	32	11.8
NYON	73	225	32	14.1
ZENITH EXPLORER	27	169	28	9.8
CAPE MARIA	170	289	45	16.9
GOLDEN CROWN	177	289	46	17.9
LEGIONY POLSKIE	74	229	32	13.7
ALPHA FLAME	75	225	32	14
IRON FUZEYYA	82	229	32	13.6
AQUABREEZE	171	289	45	17.9
KWK GENESIS	168	283	45	16.9
CAPE FRONTIER	180	289	45	18.1
CAPE AWOBA	171	289	45	17
ARTHUR N	261	325	54	20.5
ORANGE TRIDENT	78	225	32	13.5
ORIENT VENUS	165	281	45	17.6
SARAJI TRADER	170	289	45	17.3
LOWLANDS BEILUN	170	289	45	17.3
YUE SHAN	180	292	45	17.4
OCEAN VANGUARD	206	311	50	16.1
BET SCOUTER	172	296	46	17.4
GOLDEN ECLIPSE	81	230	33	14.2

Bulk ship	Deadweight (dwt) [kt]	Length (L_s) [m]	Beam (B) [m]	Max. draft (D) [m]
PARADISE N	322	332	58	18.9
GLORIUS	171	289	45	16.9
CAST. DE SAN JUAN	173	290	46	17.6
GOLDEN FUTURE	180	292	45	17.4
PARTAGAS	174	289	45	17.7
SANKO POWER	180	292	45	17.2
TAIJU	173	289	45	17.4
TASMAN ID	22	157	32	9.3
E.R. BORNEO	180	292	45	17.1
BERGE FJORD	311	332	57	21.1
CAPE TAVOR	173	289	45	17
LEGIONY POLSKIE	74	229	32	13.8
RODON AMARANDON	74	225	32	13.6
FORTUNE MIRACLE	82	190	32	14
TORM PACIFIC	77	225	32	14.1
IVS CABERNET	177	289	45	17.5
ALPHA ERA	170	289	45	16.1
AMAGISAN	143	280	43	17.3
ORLETA LWOWSKIE	74	228	32	13.9
IDSHIP BULKER	28	169	28	9.7
ALFRED N	260	325	54	20.9
ANGELINA	74	225	32	13.4
AQUACHARM	171	289	45	17.7
LEGIONY POLSKIE	74	229	32	13.9
GREAT NAVIGATOR	176	268	45	17.3
HYUNDAI CONT.	200	309	50	16.2
FD.VITTORIORAIOLA	77	218	32	13.9
ARTHUR N	260	325	54	20.3
GENCO CONSTANTINE	180	289	45	17.3
NSS BONANZA	170	289	47	14.9
LENE SELMER	175	292	45	16.0
IRON BARON	170	289	45	16.5
CAST. DE CATOIRA	174	289	45	17.8
CAPE TAVOR	173	289	45	17.1
NAVIOS ESPERANZA	75	225	32	11.8
LOWLANDS BEILUN	170	289	45	16.8
HANJIN SINES	179	291	45	17.6
CAPE UNITY	180	289	45	17.8
HANJIN FOS	179	292	45	17.2
NAVIOS MAGELLAN	74	225	32	13.6
BERGE FJORD	310	332	57	21.3
SHIBUMI	178	292	45	17.9
CAPE CARMEL	180	290	46	17.4
SOUTHERN WISDOM	177	289	45	17.6
VALE RIO DE JANEIRO	400	365	65	23

Table B.2: Investigated characteristics of 791 unloaded bulk ship at the seaside of terminal T2, dwt is the ship's deadweight [kt], n_m is the number of materials in the ship [-], n_h is the number of unloaded holds [-], sl is the shipload [kt], W_s is the registered service time [h] and three different materials were unloaded (IO: iron ore, CC: coking coal and SC: steam coal)

Ship nr.	dwt [kt]	n_m [-]	n_h [-]	sl [kt]	W_s [h]	Mat.	Ship nr.	dwt [kt]	n_m [-]	n_h [-]	sl [kt]	W_s [h]	Mat.
1	23	1	7	22	63	SC	397	110	1	7	100	114	SC
2	176	2	8	41	92	IO	398	23	1	7	18	20	SC
3	171	2	1	16	34	CC	399	14	1	4	13	15	SC
4	170	2	4	39	77	SC	400	81	2	7	78	87	CC
5	23	1	7	21	41	SC	401	23	1	7	21	24	SC
6	22	1	4	19	37	SC	402	171	2	8	45	50	SC
7	179	1	4	32	59	IO	403	76	1	6	74	82	CC
8	170	1	4	19	32	SC	404	75	1	7	72	79	SC
9	58	2	4	37	61	CC	405	93	1	7	77	81	CC
10	174	2	3	44	71	IO	406	82	1	7	79	82	SC
11	174	1	3	37	59	IO	407	170	1	4	51	52	SC
12	8	1	2	7	11	IO	408	182	3	4	95	97	CC

Ship nr.	dwt [kt]	n_m [-]	n_h [-]	sl [kt]	W_s [h]	Mat.	Ship nr.	dwt [kt]	n_m [-]	n_h [-]	sl [kt]	W_s [h]	Mat.
13	23	1	7	22	34	SC	409	77	2	6	74	75	CC
14	23	2	6	22	34	SC	410	176	1	4	69	70	IO
15	7	1	3	7	10	IO	411	171	2	9	132	131	SC
16	171	2	2	39	57	CC	412	76	2	7	73	72	SC
17	8	1	3	7	11	IO	413	174	2	4	76	75	CC
18	22	1	5	19	27	SC	414	180	2	8	164	159	SC
19	154	1	4	65	90	IO	415	17	1	4	16	15	IO
20	77	1	2	22	29	CC	416	80	1	7	60	58	CC
21	180	3	9	47	63	SC	417	80	2	5	25	24	SC
22	200	1	2	16	21	SC	418	83	1	4	47	45	IO
23	110	2	7	77	101	CC	419	170	1	2	31	30	CC
24	152	1	5	50	64	SC	420	23	3	6	31	29	SC
25	12	1	3	10	13	IO	421	74	2	7	64	60	SC
26	23	1	7	22	27	SC	422	75	1	7	72	69	CC
27	76	3	7	71	87	CC	423	180	1	4	51	48	IO
28	177	1	5	88	108	IO	424	48	1	5	44	41	IO
29	73	1	6	69	82	SC	425	82	2	7	76	71	SC
30	21	1	5	20	24	SC	426	87	2	6	78	72	SC
31	83	2	7	78	92	SC	427	75	2	7	59	54	SC
32	73	2	7	70	81	SC	428	80	1	7	56	51	SC
33	181	3	3	69	79	CC	429	80	4	7	75	68	CC
34	180	3	4	55	63	SC	430	26	2	7	24	22	SC
35	177	2	4	98	112	IO	431	180	1	8	175	155	IO
36	34	3	5	32	28	SC	432	179	1	2	37	32	CC
37	75	1	7	73	64	SC	433	26	1	5	25	22	SC
38	174	2	2	37	33	CC	434	179	2	9	165	144	SC
39	149	1	5	30	26	SC	435	115	1	4	32	28	SC
40	180	5	9	165	145	SC	436	73	2	7	68	59	SC
41	73	2	7	68	59	SC	437	183	4	8	170	117	IO
42	74	1	7	72	62	CC	438	174	3	9	151	104	SC
43	41	2	5	39	34	SC	439	83	3	6	77	53	SC
44	179	1	2	38	33	IO	440	74	1	7	70	48	CC
45	30	2	6	26	22	SC	441	110	1	7	105	72	IO
46	34	1	5	32	27	SC	442	179	1	9	176	120	IO
47	38	1	3	31	26	IO	443	183	3	9	166	113	SC
48	207	4	9	186	156	SC	444	179	3	4	77	52	CC
49	77	1	7	75	63	IO	445	34	1	5	32	22	SC
50	81	1	7	77	64	SC	446	87	1	7	77	52	CC
51	93	2	6	63	52	SC	447	178	4	9	95	65	SC
52	74	1	7	58	49	SC	448	82	1	7	77	52	CC
53	171	1	2	35	29	SC	449	180	1	2	38	25	CC
54	26	1	5	24	20	SC	450	28	1	5	26	18	SC
55	173	3	9	171	142	IO	451	180	2	9	112	76	SC
56	151	3	3	46	38	CC	452	77	1	7	73	49	IO
57	76	2	6	75	61	SC	453	73	2	6	70	47	CC
58	150	4	9	52	43	SC	454	83	1	7	78	52	SC
59	77	2	7	74	61	SC	455	177	1	3	44	29	IO
60	75	2	6	70	57	SC	456	171	2	4	77	51	CC
61	311	4	5	166	136	IO	457	170	2	9	45	30	SC
62	178	3	3	53	43	CC	458	180	4	3	78	52	CC
63	43	1	5	39	32	SC	459	170	2	5	76	50	IO
64	75	2	6	71	58	CC	460	177	4	4	92	60	CC
65	174	4	8	160	131	SC	461	172	4	9	158	104	SC
66	178	3	9	162	132	SC	462	84	2	7	74	49	CC
67	82	3	6	57	46	SC	463	77	2	6	73	48	CC
68	172	8	9	160	129	CC	464	175	2	9	50	33	SC
69	73	1	7	64	52	SC	465	176	1	3	58	38	SC
70	180	2	3	44	35	SC	466	76	3	6	72	47	CC
71	180	2	4	85	68	IO	467	47	1	5	35	23	IO
72	24	1	7	22	17	SC	468	93	1	7	82	54	IO
73	82	1	7	61	49	CC	469	181	1	9	163	106	SC
74	176	1	4	53	42	SC	470	77	2	6	73	48	SC
75	249	1	9	241	190	IO	471	74	3	6	69	45	CC
76	83	5	7	77	61	CC	472	170	1	9	151	98	IO
77	181	7	9	191	149	SC	473	162	1	4	55	35	SC
78	76	3	6	72	56	SC	474	180	3	8	173	112	SC
79	96	2	7	82	64	SC	475	180	1	4	71	46	SC
80	173	4	7	110	85	SC	476	180	2	8	58	37	SC
81	118	1	7	77	59	CC	477	179	2	3	56	36	SC

Ship nr.	dwt [kt]	n_m [-]	n_h [-]	sl [kt]	W_s [h]	Mat.	Ship nr.	dwt [kt]	n_m [-]	n_h [-]	sl [kt]	W_s [h]	Mat.
82	74	5	9	71	55	SC	478	92	2	6	79	51	SC
83	74	3	8	70	54	SC	479	93	1	7	83	53	SC
84	76	2	6	69	52	CC	480	74	2	6	71	45	SC
85	174	2	3	51	39	SC	481	110	2	7	108	69	SC
86	76	1	7	69	53	CC	482	170	2	9	156	99	IO
87	114	2	6	107	81	SC	483	70	1	7	58	37	SC
88	180	1	4	77	58	CC	484	174	2	9	154	97	CC
89	182	2	8	55	42	SC	485	82	2	7	81	51	SC
90	83	1	7	78	59	SC	486	76	2	7	71	45	SC
91	171	8	8	163	123	SC	487	34	1	5	32	20	IO
92	171	1	2	40	30	IO	488	81	1	7	75	47	SC
93	83	2	7	79	59	IO	489	173	2	9	118	74	SC
94	170	1	3	44	33	SC	490	180	1	4	48	30	IO
95	180	5	9	169	127	SC	491	82	2	6	77	48	SC
96	173	3	9	168	126	SC	492	73	2	7	66	41	SC
97	170	2	9	46	34	SC	493	169	2	9	158	98	SC
98	178	2	5	51	38	SC	494	77	2	7	74	46	SC
99	205	4	7	197	145	SC	495	84	4	6	77	48	CC
100	26	1	7	22	16	SC	496	179	6	9	165	102	SC
101	77	1	7	53	39	SC	497	81	3	6	77	47	SC
102	171	1	4	41	30	IO	498	74	1	7	72	45	CC
103	76	1	6	67	49	IO	499	80	3	6	75	46	SC
104	170	1	4	37	27	IO	500	69	2	7	66	41	SC
105	179	3	2	51	37	CC	501	180	2	2	45	28	SC
106	114	2	4	42	31	CC	502	93	3	4	77	48	CC
107	82	1	7	78	57	SC	503	180	2	1	37	22	CC
108	115	2	7	107	78	IO	504	177	2	9	46	28	IO
109	170	1	5	25	18	SC	505	180	2	4	78	47	IO
110	75	1	7	69	50	CC	506	76	2	7	74	45	SC
111	44	1	5	35	26	IO	507	82	1	6	79	48	SC
112	180	4	8	168	121	SC	508	180	1	9	59	36	SC
113	74	2	9	70	50	SC	509	83	2	7	77	47	CC
114	171	2	3	50	36	SC	510	84	3	7	77	47	CC
115	179	7	9	171	123	CC	511	183	2	3	55	33	SC
116	77	1	7	75	54	SC	512	171	3	9	55	33	SC
117	170	1	4	47	33	SC	513	180	1	9	42	25	IO
118	179	4	9	111	79	SC	514	76	2	7	74	45	SC
119	171	3	6	110	78	CC	515	150	2	8	142	85	SC
120	93	4	7	91	64	SC	516	180	1	9	44	27	SC
121	74	1	7	71	51	CC	517	174	1	4	35	21	IO
122	180	1	4	25	18	SC	518	74	2	7	71	43	SC
123	83	2	7	79	56	SC	519	172	4	9	109	65	SC
124	47	1	5	44	31	IO	520	76	4	4	32	19	SC
125	77	1	7	75	53	CC	521	178	1	9	166	99	SC
126	180	2	5	90	64	CC	522	171	3	9	159	95	SC
127	80	1	7	43	30	SC	523	75	2	7	70	42	CC
128	83	2	7	74	52	CC	524	174	3	8	165	98	SC
129	170	2	2	37	26	CC	525	179	1	9	175	104	IO
130	180	3	4	74	52	CC	526	151	2	3	42	25	SC
131	82	1	7	75	52	SC	527	77	1	7	75	44	IO
132	174	1	4	50	35	SC	528	82	1	7	78	46	SC
133	180	2	9	135	94	SC	529	171	2	3	43	26	SC
134	176	2	3	60	42	SC	530	179	3	9	172	101	SC
135	73	1	7	69	48	CC	531	180	1	5	69	41	SC
136	182	2	9	164	113	SC	532	180	5	4	76	45	CC
137	56	1	5	55	38	SC	533	74	4	9	71	42	SC
138	76	1	7	57	34	IO	534	179	4	9	173	88	IO
139	84	1	7	80	47	IO	535	75	1	7	74	37	SC
140	110	2	7	77	45	CC	536	180	7	9	165	84	SC
141	172	2	9	91	54	IO	537	96	1	6	88	45	SC
142	149	3	4	65	38	CC	538	114	2	6	108	55	IO
143	74	2	7	72	42	SC	539	174	1	4	45	23	IO
144	151	2	8	146	85	SC	540	74	4	9	73	37	SC
145	181	3	6	45	26	SC	541	170	4	8	136	69	SC
146	170	3	5	80	46	SC	542	182	3	8	176	89	IO
147	179	3	9	174	101	SC	543	82	1	5	77	39	CC
148	81	1	7	78	45	SC	544	79	1	7	72	36	SC
149	77	1	7	74	43	CC	545	176	2	3	48	24	SC
150	180	5	4	73	42	CC	546	150	3	9	143	72	SC

Ship nr.	dwt [kt]	n_m [-]	n_h [-]	sl [kt]	W_s [h]	Mat.	Ship nr.	dwt [kt]	n_m [-]	n_h [-]	sl [kt]	W_s [h]	Mat.
151	83	1	7	68	40	IO	547	170	1	5	51	26	SC
152	149	1	4	37	21	SC	548	186	1	4	39	20	SC
153	174	2	8	89	51	IO	549	172	4	4	116	58	SC
154	176	5	9	168	97	IO	550	206	4	8	176	88	IO
155	180	2	9	162	93	SC	551	171	3	4	75	38	CC
156	77	2	6	70	40	SC	552	75	2	7	70	35	SC
157	178	1	4	44	25	IO	553	261	3	6	257	129	IO
158	180	2	4	65	38	SC	554	171	3	4	76	38	IO
159	151	4	9	145	83	SC	555	87	1	7	82	41	SC
160	179	5	8	161	92	SC	556	203	5	9	187	93	IO
161	83	2	6	81	46	SC	557	80	1	7	56	28	SC
162	208	1	9	176	101	SC	558	249	1	6	165	82	IO
163	47	1	8	42	24	IO	559	180	4	9	177	88	IO
164	170	1	9	163	93	SC	560	74	1	9	71	35	SC
165	173	2	2	39	22	CC	561	94	1	7	82	41	IO
166	172	2	6	54	31	SC	562	173	2	9	158	78	SC
167	178	1	2	38	22	SC	563	203	2	8	39	19	SC
168	77	1	7	72	41	SC	564	177	1	9	170	84	IO
169	77	1	7	75	43	IO	565	180	2	8	180	89	IO
170	80	1	7	76	43	SC	566	176	5	8	163	81	SC
171	93	3	7	83	46	SC	567	93	1	7	83	41	SC
172	87	3	6	77	43	CC	568	149	2	8	135	67	SC
173	82	1	7	34	19	SC	569	151	3	8	145	71	SC
174	72	2	6	69	39	SC	570	103	1	7	83	41	IO
175	87	1	7	83	47	SC	571	180	1	9	175	86	IO
176	84	3	7	77	43	SC	572	174	2	2	52	26	IO
177	170	2	3	55	30	CC	573	179	3	9	167	82	SC
178	77	2	4	73	41	IO	574	205	4	8	204	100	IO
179	255	3	8	124	69	IO	575	172	1	9	151	74	IO
180	115	2	6	82	46	SC	576	178	1	4	73	36	SC
181	75	2	7	65	36	SC	577	115	2	7	113	55	IO
182	76	2	7	72	40	SC	578	170	1	2	40	20	IO
183	174	1	3	50	28	IO	579	152	1	9	150	73	IO
184	72	2	6	69	39	SC	580	76	1	7	72	35	IO
185	180	2	9	39	22	CC	581	277	1	9	266	130	IO
186	176	3	8	163	91	CC	582	180	1	9	176	86	IO
187	183	2	8	138	76	SC	583	178	1	5	47	23	IO
188	183	1	9	154	86	SC	584	176	3	9	165	80	SC
189	93	1	6	77	43	IO	585	178	1	9	159	78	SC
190	152	2	3	69	38	CC	586	180	1	9	162	79	SC
191	77	1	7	75	42	IO	587	180	3	8	165	80	SC
192	93	1	6	78	43	IO	588	177	5	8	170	82	SC
193	152	2	5	81	45	CC	589	149	2	9	157	76	SC
194	170	3	3	57	31	SC	590	176	2	5	93	45	CC
195	181	2	4	55	30	SC	591	178	1	9	171	83	IO
196	179	3	9	171	93	SC	592	83	2	7	77	37	SC
197	83	1	4	79	43	IO	593	170	4	8	166	80	SC
198	82	2	7	80	44	SC	594	74	1	9	72	35	SC
199	152	2	9	144	79	IO	595	180	1	9	173	84	IO
200	172	2	4	89	48	SC	596	180	3	3	57	27	CC
201	174	1	4	44	24	IO	597	167	1	9	135	65	SC
202	75	4	6	72	39	SC	598	80	3	6	75	36	SC
203	178	5	8	159	86	SC	599	261	2	3	139	67	IO
204	180	3	8	164	89	SC	600	180	1	5	51	25	SC
205	81	2	6	77	41	SC	601	80	1	7	77	37	CC
206	82	2	7	78	42	SC	602	110	1	7	84	40	SC
207	173	2	9	161	87	SC	603	110	1	4	83	40	IO
208	77	1	7	72	39	SC	604	82	2	6	69	33	SC
209	170	1	9	151	81	IO	605	178	3	8	135	65	SC
210	169	2	4	52	28	SC	606	176	2	3	47	23	IO
211	81	3	6	65	35	SC	607	93	1	7	77	37	IO
212	110	2	7	103	55	SC	608	205	2	9	204	97	IO
213	175	2	6	112	60	SC	609	178	1	9	170	81	IO
214	255	3	9	245	132	IO	610	180	2	8	163	78	IO
215	175	2	4	48	26	SC	611	180	1	9	171	81	IO
216	93	2	6	77	41	SC	612	180	2	5	75	36	SC
217	181	2	9	54	29	SC	613	171	4	9	159	76	SC
218	77	1	7	74	40	CC	614	75	1	7	55	26	SC
219	76	2	6	74	40	SC	615	82	1	7	61	29	IO

Ship nr.	dwt [kt]	n_m [-]	n_h [-]	sl [kt]	W_s [h]	Mat.	Ship nr.	dwt [kt]	n_m [-]	n_h [-]	sl [kt]	W_s [h]	Mat.
220	77	2	6	73	39	SC	616	69	1	7	55	26	SC
221	174	1	5	33	18	IO	617	76	1	7	67	32	SC
222	180	2	8	76	41	SC	618	75	2	6	78	37	SC
223	161	2	3	38	21	SC	619	181	6	8	176	83	SC
224	179	1	2	42	23	IO	620	179	2	9	167	79	SC
225	77	2	6	74	40	SC	621	177	2	3	58	27	IO
226	172	3	9	163	87	SC	622	286	1	4	122	58	IO
227	176	3	9	161	86	SC	623	57	1	5	50	24	IO
228	181	2	9	63	33	SC	624	172	1	9	165	78	IO
229	170	3	4	57	30	SC	625	149	2	5	44	21	SC
230	169	1	9	165	87	SC	626	175	2	9	140	66	IO
231	176	1	9	52	28	SC	627	177	1	4	75	35	SC
232	171	1	3	36	19	SC	628	174	1	7	44	21	IO
233	176	2	8	174	92	IO	629	208	2	9	202	95	IO
234	180	1	9	165	87	SC	630	154	1	5	50	24	SC
235	173	2	9	162	85	SC	631	220	1	7	211	99	IO
236	180	4	9	168	88	SC	632	186	3	9	174	82	SC
237	180	1	5	43	22	IO	633	179	2	9	161	76	SC
238	178	1	9	164	86	SC	634	175	1	9	164	76	SC
239	170	2	6	51	27	IO	635	180	1	9	74	34	IO
240	180	3	9	55	29	SC	636	176	5	8	165	77	SC
241	170	2	9	160	83	IO	637	180	3	9	173	80	SC
242	74	1	7	72	37	CC	638	186	2	4	86	40	IO
243	170	2	1	38	20	CC	639	170	2	2	37	17	CC
244	161	5	8	151	79	SC	640	181	3	4	60	28	SC
245	177	2	9	172	89	IO	641	179	1	9	173	80	IO
246	181	3	9	112	58	SC	642	178	1	4	54	25	SC
247	173	1	6	55	29	SC	643	180	5	9	55	26	SC
248	73	1	7	70	36	IO	644	178	1	9	163	75	SC
249	76	1	7	75	39	SC	645	73	1	7	69	32	SC
250	180	2	8	165	85	SC	646	82	1	7	77	35	IO
251	92	1	7	80	42	IO	647	180	2	8	34	15	SC
252	180	2	4	44	23	SC	648	170	4	5	57	26	SC
253	180	2	9	59	30	SC	649	161	5	9	150	69	SC
254	170	2	3	72	37	SC	650	171	1	2	37	17	CC
255	179	2	8	45	23	SC	651	176	2	8	169	78	SC
256	79	2	6	77	40	SC	652	75	1	7	60	27	IO
257	177	2	3	49	25	IO	653	71	1	7	34	16	IO
258	178	2	4	56	29	SC	654	76	1	7	73	33	IO
259	178	1	4	34	18	SC	655	178	1	2	38	18	CC
260	149	3	9	135	69	SC	656	83	3	6	80	36	SC
261	82	3	7	81	42	SC	657	80	2	7	77	35	SC
262	177	1	3	55	28	SC	658	79	2	6	76	35	SC
263	178	2	5	50	25	IO	659	74	1	4	39	18	SC
264	80	2	7	60	31	SC	660	177	2	8	163	74	SC
265	181	3	5	57	29	SC	661	251	1	8	241	110	IO
266	176	3	9	170	87	IO	662	87	1	7	83	38	IO
267	110	2	6	82	42	SC	663	176	1	9	163	74	SC
268	171	1	2	43	22	IO	664	181	1	4	77	35	CC
269	173	3	8	163	74	SC	665	179	2	9	171	67	IO
270	171	4	9	159	72	SC	666	297	2	2	147	57	IO
271	176	1	9	52	24	SC	667	178	1	9	175	68	IO
272	180	1	9	163	74	SC	668	298	4	5	161	63	IO
273	180	1	3	45	20	SC	669	323	2	1	90	35	IO
274	261	1	7	259	117	IO	670	170	2	5	70	27	IO
275	167	2	9	174	79	IO	671	170	2	4	67	26	SC
276	151	1	9	134	60	IO	672	84	2	7	80	31	IO
277	77	1	7	74	33	SC	673	311	3	6	157	61	IO
278	180	1	3	50	22	IO	674	173	1	9	166	64	IO
279	170	2	8	128	58	IO	675	179	7	9	165	64	SC
280	177	2	8	169	76	SC	676	99	2	7	94	36	SC
281	77	1	7	75	34	SC	677	178	7	8	164	63	SC
282	182	1	9	165	74	SC	678	177	1	9	166	63	IO
283	74	5	8	77	34	SC	679	205	4	8	204	78	IO
284	180	1	9	173	78	IO	680	173	1	9	45	17	IO
285	173	2	8	168	75	IO	681	176	1	9	169	64	IO
286	174	3	9	174	78	SC	682	388	1	8	363	138	IO
287	83	1	7	71	32	SC	683	175	6	9	165	62	SC
288	170	1	9	163	73	SC	684	186	4	8	169	64	SC

Ship nr.	dwt [kt]	n_m [-]	n_h [-]	sl [kt]	W_s [h]	Mat.	Ship nr.	dwt [kt]	n_m [-]	n_h [-]	sl [kt]	W_s [h]	Mat.
289	180	2	9	174	78	SC	685	182	5	8	165	62	SC
290	75	1	7	69	31	SC	686	322	1	7	220	83	IO
291	180	2	9	178	79	IO	687	311	1	6	89	33	IO
292	171	1	4	61	27	SC	688	183	3	2	39	15	CC
293	176	1	3	49	22	IO	689	171	3	9	165	62	SC
294	180	4	8	170	75	SC	690	180	1	9	172	65	IO
295	171	1	6	101	45	SC	691	181	1	4	58	22	SC
296	169	2	8	151	67	SC	692	173	3	9	160	60	SC
297	170	1	4	57	25	IO	693	176	6	8	170	63	CC
298	175	3	9	165	73	SC	694	178	2	9	174	65	IO
299	172	2	5	63	28	SC	695	322	1	7	275	102	IO
300	261	1	7	252	111	IO	696	84	1	7	81	30	IO
301	171	3	3	65	29	CC	697	183	3	4	57	21	SC
302	178	5	8	165	73	SC	698	103	1	7	78	29	SC
303	76	1	7	68	30	IO	699	203	2	6	126	47	IO
304	169	2	9	162	71	SC	700	311	1	4	70	26	IO
305	180	3	9	167	73	SC	701	169	4	9	161	59	SC
306	182	1	9	178	78	IO	702	261	3	4	188	69	IO
307	207	1	2	37	16	CC	703	311	3	8	160	58	IO
308	180	3	8	177	77	IO	704	180	4	9	177	65	IO
309	180	2	8	172	75	IO	705	180	2	8	160	59	SC
310	83	3	7	79	34	SC	706	177	4	8	169	61	SC
311	180	3	9	168	73	SC	707	173	4	8	151	55	CC
312	180	4	8	74	32	CC	708	177	5	8	164	60	SC
313	174	1	2	49	21	IO	709	179	3	9	173	63	SC
314	152	2	9	146	63	IO	710	149	4	8	146	53	SC
315	171	1	2	44	19	IO	711	161	2	8	104	38	SC
316	143	1	9	152	66	IO	712	170	5	5	90	33	CC
317	180	2	9	164	71	IO	713	149	1	2	30	11	IO
318	182	4	9	165	71	SC	714	169	1	9	166	60	IO
319	171	4	9	162	70	SC	715	171	1	2	38	14	IO
320	164	1	6	58	25	SC	716	261	1	7	252	91	IO
321	180	1	5	71	31	SC	717	176	3	5	85	31	SC
322	178	1	9	50	21	SC	718	178	1	9	186	67	SC
323	75	2	7	71	30	SC	719	171	3	8	165	59	SC
324	180	4	6	107	46	CC	720	169	5	8	166	60	SC
325	205	2	9	197	84	IO	721	169	1	4	55	20	SC
326	169	2	8	162	69	IO	722	169	3	9	164	59	SC
327	83	1	9	77	33	IO	723	174	1	9	172	61	IO
328	171	2	9	159	68	SC	724	172	1	8	56	20	SC
329	161	5	9	154	65	SC	725	206	3	9	178	63	SC
330	179	1	9	170	73	SC	726	317	2	4	167	59	IO
331	179	2	9	162	69	SC	727	179	4	8	165	59	SC
332	76	1	7	71	30	IO	728	298	2	6	165	58	IO
333	170	4	8	112	48	SC	729	169	4	8	158	56	SC
334	181	1	9	174	73	IO	730	93	1	7	86	30	SC
335	178	5	4	76	32	CC	731	176	2	3	52	18	SC
336	180	3	8	161	68	SC	732	176	1	9	162	57	SC
337	177	1	8	169	71	IO	733	261	1	7	253	89	IO
338	181	5	9	81	34	CC	734	83	2	7	78	27	SC
339	180	1	9	174	73	IO	735	178	2	8	165	58	SC
340	177	2	9	86	36	IO	736	170	4	9	108	37	SC
341	82	2	7	79	33	IO	737	206	5	9	187	65	SC
342	169	4	9	172	72	IO	738	170	1	9	149	52	IO
343	171	1	9	169	70	IO	739	249	2	9	240	83	IO
344	115	1	7	109	46	IO	740	176	2	7	132	46	IO
345	78	1	7	74	31	SC	741	297	3	6	177	61	IO
346	180	2	9	178	74	IO	742	186	1	9	183	63	IO
347	176	2	4	56	23	SC	743	150	3	9	145	49	SC
348	82	1	3	35	15	IO	744	174	4	5	84	28	CC
349	179	5	9	165	68	SC	745	176	1	9	174	59	IO
350	179	1	9	172	71	IO	746	261	1	7	258	87	IO
351	79	1	6	77	32	SC	747	175	1	9	170	57	IO
352	178	3	9	168	69	SC	748	169	2	4	48	16	SC
353	298	3	5	153	63	IO	749	168	4	9	151	51	SC
354	180	2	9	161	66	SC	750	311	2	6	156	52	IO
355	261	3	7	258	106	IO	751	317	3	6	310	103	IO
356	180	2	9	162	67	SC	752	180	4	5	90	30	CC
357	178	2	9	160	65	IO	753	311	2	5	162	54	IO

Ship nr.	dwt [kt]	n_m [-]	n_h [-]	sl [kt]	W_s [h]	Mat.	Ship nr.	dwt [kt]	n_m [-]	n_h [-]	sl [kt]	W_s [h]	Mat.
358	180	4	9	167	68	SC	754	203	2	9	200	67	IO
359	76	1	7	72	29	SC	755	186	2	9	176	59	IO
360	77	3	6	63	26	SC	756	180	1	9	59	19	SC
361	297	4	5	286	116	IO	757	178	5	8	166	55	SC
362	171	2	7	118	48	SC	758	169	2	8	162	54	SC
363	178	4	8	175	71	IO	759	180	2	2	48	16	SC
364	161	1	2	30	12	IO	760	298	2	4	198	65	IO
365	176	6	6	165	66	SC	761	154	3	8	142	46	IO
366	177	1	9	170	68	IO	762	172	2	9	160	52	IO
367	179	3	9	168	67	SC	763	180	5	9	174	57	SC
368	180	2	8	52	21	SC	764	180	3	5	58	19	SC
369	176	3	3	76	30	CC	765	181	2	9	168	54	SC
370	297	1	3	140	56	IO	766	261	1	7	251	81	IO
371	143	2	2	35	14	CC	767	261	2	3	103	33	IO
372	83	1	4	77	31	IO	768	176	2	9	163	52	SC
373	179	2	9	164	66	SC	769	207	1	9	203	64	IO
374	170	1	6	80	32	SC	770	154	1	2	37	12	IO
375	177	1	9	164	65	IO	771	204	1	9	200	62	IO
376	176	2	3	43	17	IO	772	261	2	4	131	41	IO
377	177	2	9	154	61	CC	773	176	3	8	164	51	SC
378	179	1	9	172	68	IO	774	173	2	3	57	18	SC
379	122	1	9	121	48	IO	775	180	1	5	65	20	SC
380	174	1	4	43	17	IO	776	176	2	9	173	53	IO
381	149	3	9	137	54	IO	777	298	3	4	152	46	IO
382	269	2	2	86	34	IO	778	311	2	4	108	33	IO
383	180	2	9	165	65	IO	779	206	2	8	177	53	SC
384	261	4	6	251	74	IO	780	177	3	9	56	15	SC
385	206	2	8	199	58	IO	781	176	1	9	168	44	IO
386	171	1	3	44	13	IO	782	317	2	7	312	82	IO
387	180	5	8	142	41	IO	783	181	1	9	176	44	IO
388	172	3	8	166	48	SC	784	178	1	9	57	14	SC
389	261	3	7	257	74	IO	785	169	1	9	167	41	IO
390	206	3	8	182	52	SC	786	180	1	9	176	43	IO
391	172	3	9	168	48	SC	787	180	1	9	172	39	SC
392	178	1	9	159	45	IO	788	205	2	8	203	41	IO
393	180	4	9	176	49	SC	789	400	1	6	365	74	IO
394	317	4	6	248	68	IO	790	176	1	9	173	34	IO
395	180	4	9	162	44	SC	791	181	1	9	176	35	IO
396	151	3	9	148	40	SC							

C. Measured stochastic distributions

In this appendix details for measured distributions are listed. Five terminal operators provided operational data that was measured during daily operation. From these datasets interarrival times, service times and shipload distributions were determined. Table C.1 until Table C.3 shows details for these measured distributions. Due to confidential circumstances the terminals are anonymized and called from now T1 until T5. Note that the intervals mentioned in tables are defined as follows; e.g., 0-5 means larger or equal to 0 but smaller than 5.

Table C.1: Shipload distributions for five dry bulk terminals (the shipload ranges as in the bulk ship classification were used (see Table 3.1); an extra range (150-200 [kt]) was introduced to distinguish different ship sizes in the 'Large Capesize' range)

Shipload [kt]	T1	T2	T3	T4[1]	T5
10-35	0.16	0.01	0.00	0.11	0.71
35-55	0.18	0.08	0.00	0.13	0.18
55-90	0.40	0.17	0.03	0.47	0.12
90-150	0.10	0.29	0.17	0.10	0.00
150-200	0.15	0.14	0.24	0.18	0.00
200-350	0.00	0.25	0.47	0.00	0.00

[1] only the ships loaded with coal were considered

Table C.2: Ship interarrival time distributions for five terminals (histograms for these distributions are shown in Figures 3.10 – 3.12)

IAT [h]	Frequency number of ships [-]					IAT [h]	Frequency number of ships [-]				
	T1	T2	T3	T4	T5		T1	T2	T3	T4	T5
0-5	0.01	0.17	0.03	0.03	0.08	85-90	0.02	0.01	0.00	0.05	0.01
5-10	0.03	0.15	0.05	0.05	0.07	90-95	0.01	0.00	0.02	0.01	0.02
10-15	0.06	0.11	0.03	0.08	0.12	95-100	0.02	0.01	0.01	0.00	0.02
15-20	0.03	0.09	0.08	0.08	0.09	100-105	0.01	0.01	0.00	0.03	0.01
20-25	0.07	0.07	0.03	0.03	0.10	105-110	0.02	0.00	0.01	0.02	0.01
25-30	0.07	0.05	0.03	0.03	0.07	110-115	0.01	0.01	0.00	0.01	0.01
30-35	0.06	0.05	0.11	0.04	0.06	115-120	0.01	0.00	0.01	0.02	0.03
35-40	0.09	0.05	0.15	0.03	0.06	120-125	0.01	0.00	0.02	0.02	0.01
40-45	0.07	0.03	0.11	0.03	0.04	125-130	0.01	0.00	0.00	0.00	0.01
45-50	0.07	0.03	0.06	0.05	0.05	130-135	0.01	0.00	0.00	0.00	0.02
50-55	0.05	0.03	0.03	0.06	0.05	135-140	0.00	0.00	0.01	0.01	0.00
55-60	0.04	0.04	0.05	0.03	0.02	140-145	0.00	0.00	0.00	0.02	0.01
60-65	0.05	0.02	0.07	0.03	0.03	145-150	0.01	0.00	0.01	0.01	0.01
65-70	0.03	0.02	0.04	0.03	0.02	150-155	0.00	0.00	0.00	0.01	0.01
70-75	0.03	0.01	0.02	0.00	0.02	155-160	0.01	0.00	0.00	0.02	0.00
75-80	0.02	0.01	0.02	0.03	0.03	>160	0.04	0.01	0.01	0.13	0.00
80-85	0.02	0.01	0.01	0.01	0.00						

Table C.3: Ship service time distributions for three terminals (histograms for these distributions are shown in Figure 3.13 and Figure 3.14)

W_s [h]	Frequency number of ships [-]			W_s [h]	Frequency number of ships [-]		
	T2	T4	T5		T2	T4	T5
0-10	0.00	0.00	0.15	130-140	0.01	0.04	0.01
10-20	0.06	0.04	0.20	140-150	0.01	0.00	0.00
20-30	0.14	0.05	0.21	150-160	0.01	0.03	0.00
30-40	0.16	0.09	0.09	160-170	0.00	0.01	0.00
40-50	0.14	0.13	0.08	170-180	0.00	0.03	0.00
50-60	0.11	0.11	0.07	180-190	0.00	0.03	0.00
60-70	0.12	0.09	0.05	190-210	0.00	0.02	0.00
70-80	0.10	0.05	0.04	210-230	0.00	0.02	0.00
80-90	0.07	0.06	0.03	230-250	0.00	0.03	0.00
90-100	0.03	0.06	0.04	250-270	0.00	0.01	0.00
100-110	0.02	0.03	0.02	270-290	0.00	0.01	0.01
110-120	0.01	0.03	0.01	290-310	0.00	0.02	0.00

Three terminal operators (T2, T3 and T4) provided operational data of their landside operation. From these datasets interarrival and service times distributions were determined. At these terminals multiple landside transportation modalities can be served; trains, inland ships (barges), coastal ships and belt conveyors to feed material to coal-fired power stations.

Table C.4: Train interarrival time distributions for three terminals (histograms for these distributions are shown in Figure 4.6 and Figure 4.7)

IAT [h]	Frequency number of trains [-]			IAT [h]	Frequency number of trains [-]		
	T2	T3	T4		T2	T3	T4
0-1	0.24	0.01	0.01	13-14	0.00	0.01	0.02
1-2	0.21	0.04	0.01	14-15	0.00	0.00	0.02
2-3	0.22	0.07	0.10	15-16	0.00	0.00	0.03
3-4	0.13	0.15	0.17	16-17	0.00	0.00	0.02
4-5	0.06	0.35	0.14	17-18	0.00	0.00	0.01
5-6	0.03	0.17	0.08	18-19	0.00	0.00	0.00
6-7	0.02	0.08	0.05	19-20	0.00	0.00	0.02
7-8	0.02	0.04	0.06	20-21	0.00	0.00	0.02
8-9	0.01	0.02	0.05	21-22	0.00	0.00	0.02
9-10	0.01	0.02	0.04	22-23	0.00	0.00	0.01
10-11	0.01	0.01	0.02	23-24	0.00	0.00	0.01
11-12	0.01	0.01	0.04	24-25	0.00	0.00	0.01
12-13	0.01	0.01	0.04				

Table C.5: Train service time distribution for three terminals (histograms for these distributions are shown in Figure 4.8 and Figure 4.9)

W_s [h]	Frequency number of trains [-]			W_s [h]	Frequency number of trains [-]		
	T2	T3	T4		T2	T3	T4
0-0.5	0.00	0.00	0.00	5-5.5	0.01	0.15	0.00
0.5-1	0.03	0.00	0.02	5.5-6	0.01	0.10	0.00
1-1.5	0.12	0.01	0.10	6-6.5	0.00	0.07	0.00
1.5-2	0.25	0.02	0.29	6.5-7	0.00	0.04	0.00
2-2.5	0.25	0.04	0.32	7-7.5	0.00	0.02	0.00
2.5-3	0.16	0.04	0.16	7.5-8	0.00	0.01	0.00
3-3.5	0.08	0.03	0.07	8-8.5	0.00	0.01	0.00
3.5-4	0.05	0.06	0.01	8.5-9	0.00	0.00	0.00
4-4.5	0.02	0.19	0.02	9-9.5	0.00	0.00	0.00
4.5-5	0.01	0.19	0.00	9.5-10	0.00	0.00	0.00

For the inlands ships, coastal ships and export of bulk materials from the terminals via belt conveyors distributions were determined for the interarrival times and service times. These distributions are shown in the Figures C.1 until C.6. The values for the frequency per range are also listed in these figures. Results for the distribution fit of these measured distributions with analytical distributions are shown for the interarrival time distributions in Table 4.2 and for the service time distributions in Table 4.3.

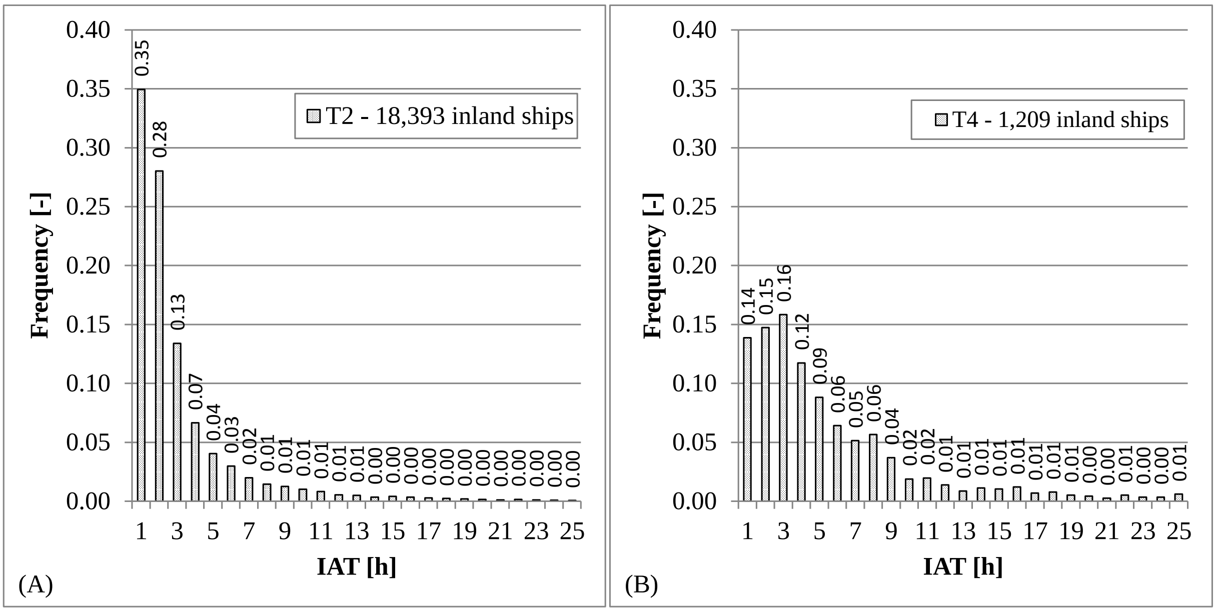

Figure C.1: Inland ships' interarrival time distributions for terminal T2 (A) and T4 (B)

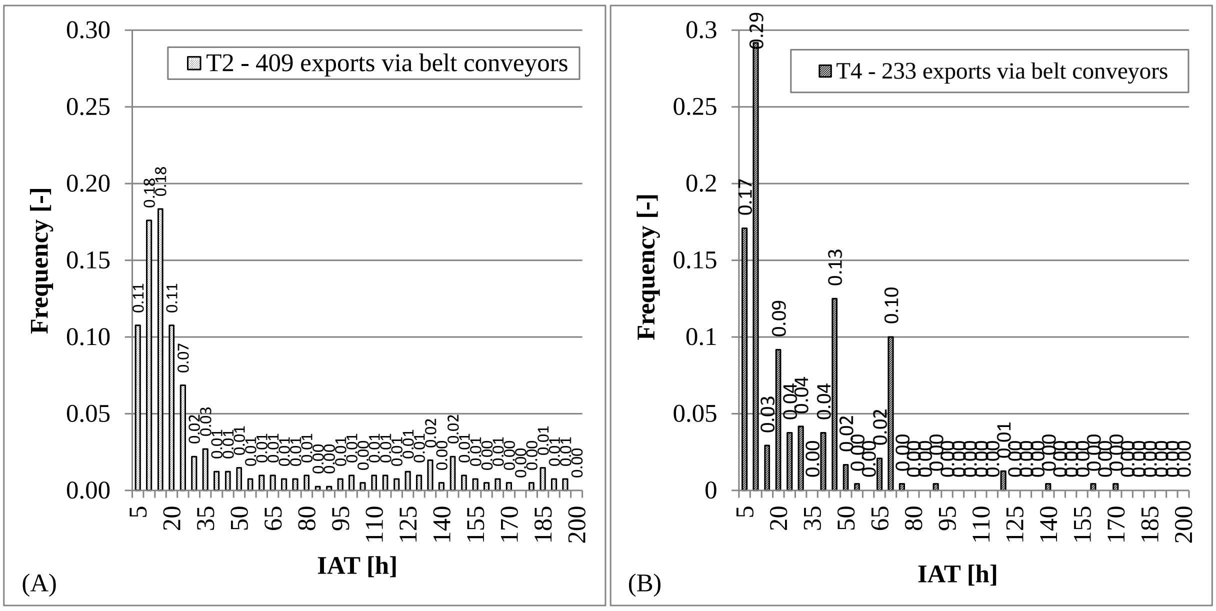

Figure C.2: Interarrival time distributions for material export via belt conveyors to coal-fired power stations near terminals T2 (A) and T4 (B)

From Figure C.2B it can be seen that at terminal T4 there are some regular times when material is transported using belt conveyors to the coal-fired power plant of 630 MW. The export from terminal T2 to the coal-fired power plant (1040 MW) shows a larger variation.

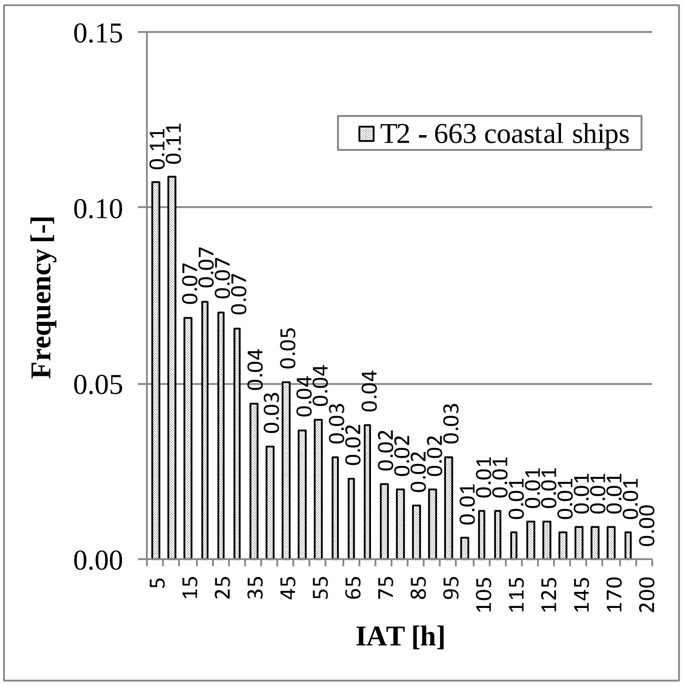

Figure C.3: Interarrival time distribution determined for coastal ships at terminal T2

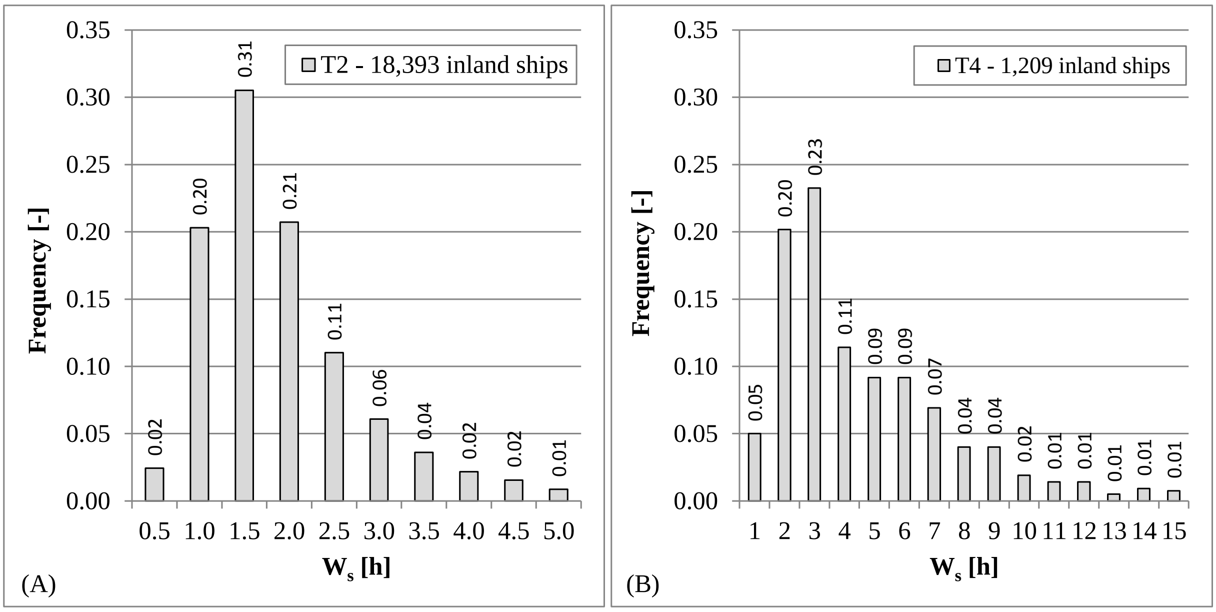

Figure C.4: Inland ships' service time distributions at terminal T2 (A) and T4 (B)

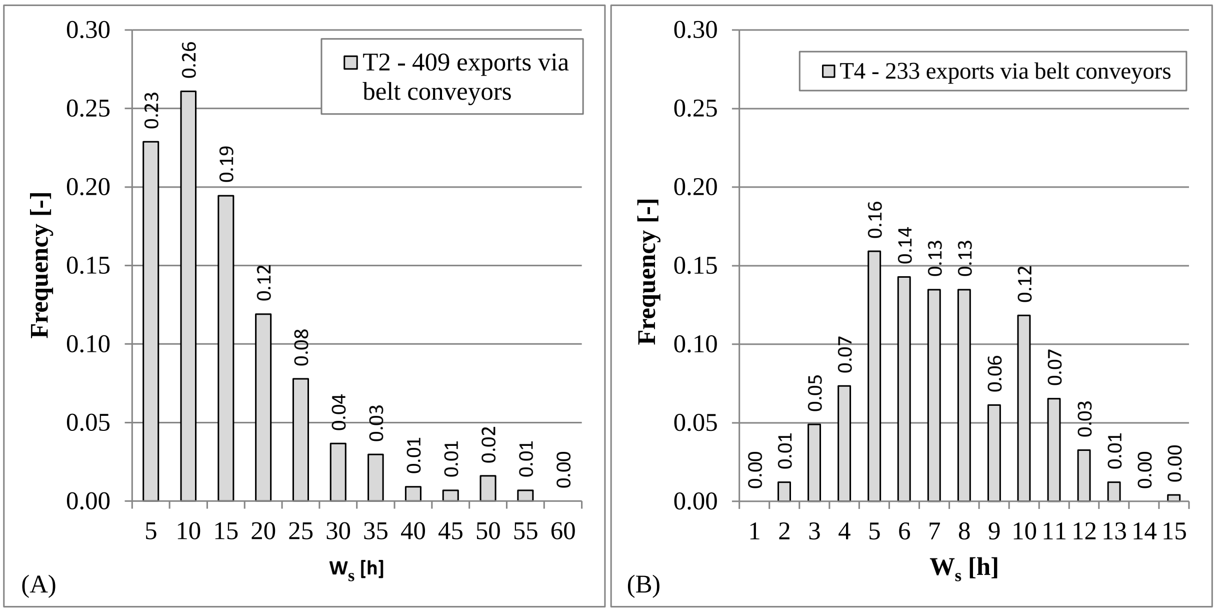

Figure C.5: Service time distributions determined for material export via belt conveyors to coal-fired power plants near terminals T2 (A) and T4 (B)

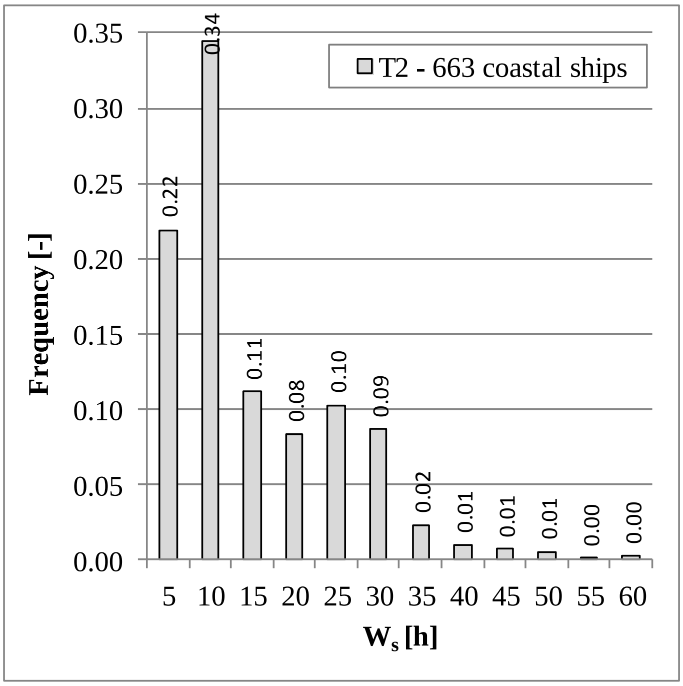

Figure C.6: Service time distribution for coastal ships at terminal T2

D. Simulation models

For modeling and simulation the process-interaction approach was followed. This approach can be summarized by three steps (derived from Zeigler et al., 2000):

- Decompose the system into relevant element classes, preferably patterned on the real-world elements.
- Identify the attributes of each element class
- Provide for the 'living' element classes process descriptions that govern the dynamic behavior of these elements including interactions with other elements.

The descriptions for the processes and functions of the simulation elements will be presented in a pseudo language, as previously introduced by Ottjes and Veeke (2002) and Ottjes and Lodewijks (2004). From the descriptions, the simulation model can further be derived and coded.

Some terms used in the pseudo language need a further explanation.

- **Queue**: a queue is a collection of simulation elements. Each queue owns its attributes and methods (e.g., Enter, Add, AddSortedOn, Leave, Remove, FirstElement, LastElement, Successor, Predecessor, Length, MeanTime, Clear). Queues are useful in the control part of a model. Control decisions often come down by selecting the right element in a queue.
- **Hold(t)**: time scheduled interval, the process continuous after time ***t*** has elapsed
- **Standby(while** condition**)**: is a state scheduled interval, the process proceeds as soon as the condition becomes false.
- **Repeat:** repeat the process indefinitely
- **Repeat(n):** repeat the process n-times
- **Repeat(condition):** repeat while the condition is true

- **Read:** a value to be read from a data file
- **Write:** a value to be written to some destination file
- **Sample(Distribution):** gives a sample from a distribution
- **Now:** indicates the current time in the model.

For qualifying attributes of elements the “dot” notation is used. For example: Job.load means the load of the Job. In the pseudo language blocks will be used and can be distinguished by intended lines. The function of blocks enables a structuring of the code and treats a group of statements as if these statements are one statement.

In Figure D.1 an overview of the simulation models developed is shown. The Input model, discussed in section D.1, was developed to generate input files representing the material flow through the terminal. Terminal characteristics are predefined in the configuration file and are used at the start of a simulation run to configure the (part of the) terminal to be tested. Simulation models developed for the seaside, the stockyard and the transport network model are presented in section D.2, D.3 and D.4 respectively. The *total terminal model* is composed out of these three models and is described in section D.5.

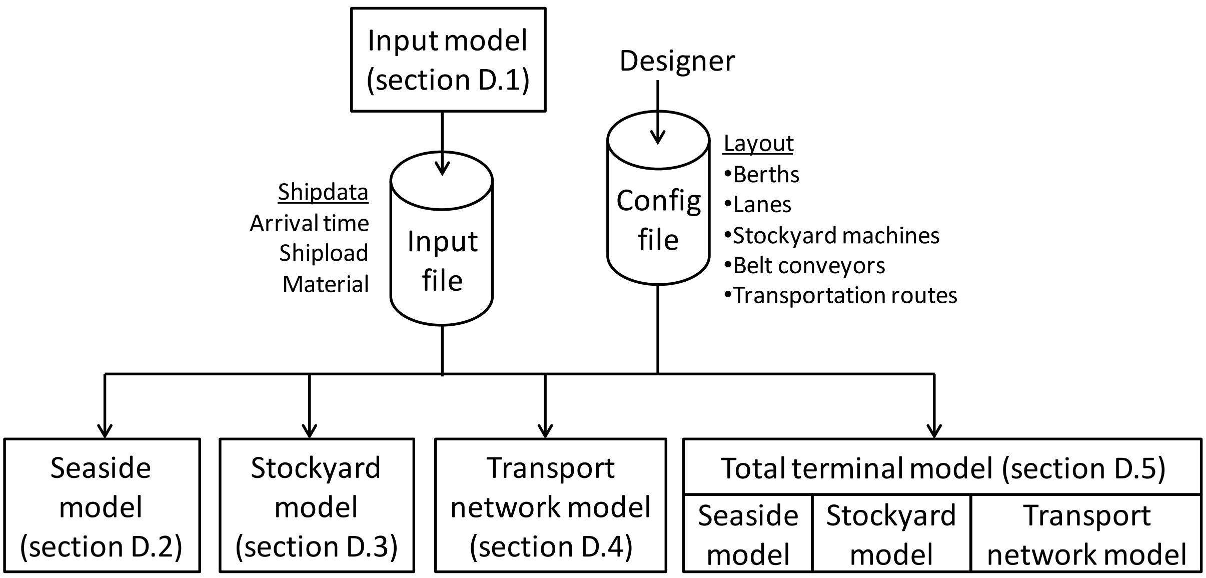

Figure D.1: Overview of the simulation models

D.1 Input model

A separate simulation model was developed to create files that are used as input for other models. Input files can also be composed from real-world operational data, so both generated input and real-world input can be used for the simulation models. An input file contains arrival times and job loads. A job can be a ship but also trains. Using the process interaction method the input model can be described as follows:

- Element classes: job and generator.
- Attributes: the attributes for the job class are listed in Table D.1 and for the generator class in Table D.2.
- Process descriptions: only the generator class owns a process, which is also discussed in Table D.2.

Table D.1: Element class: Job

Attributes of job class	Description
Arrivaltime	Time of arrival
Load	Load size

Table D.2: Element class: Generator

Attributes of generator class	Description
InputFile	Generated file that contains jobs' arrival times and loads
NrJobs	The number of jobs
NewJob	Reference to Job
Loaddistribution	Different load distributions were included; generalized NED, Erlang-2 and Normal distribution, but also a distribution with values uniformly distributed between a minimum and maximum value and a table input.
IATdistribution	Different interarrival time distributions were included; NED, Erlang-2 or Deterministic (=constant values)
Process	Create jobs with attributes and write data to InputFile
Process of Generator class	

Repeat (NrJobs)
Create a new job
Job.load = Sample(Loaddistribution) //draw the load from predefined Loaddistribution type
Job.Arrivaltime = Sample(IATdistribution) //draw arrival time from prefined IAT distribution type
Hold(Job.Arrivaltime) //to realize the interarrival time
Write Now and Job.Load to InputFile //write arrivaltime and load in InputFile	

D.2 Seaside model

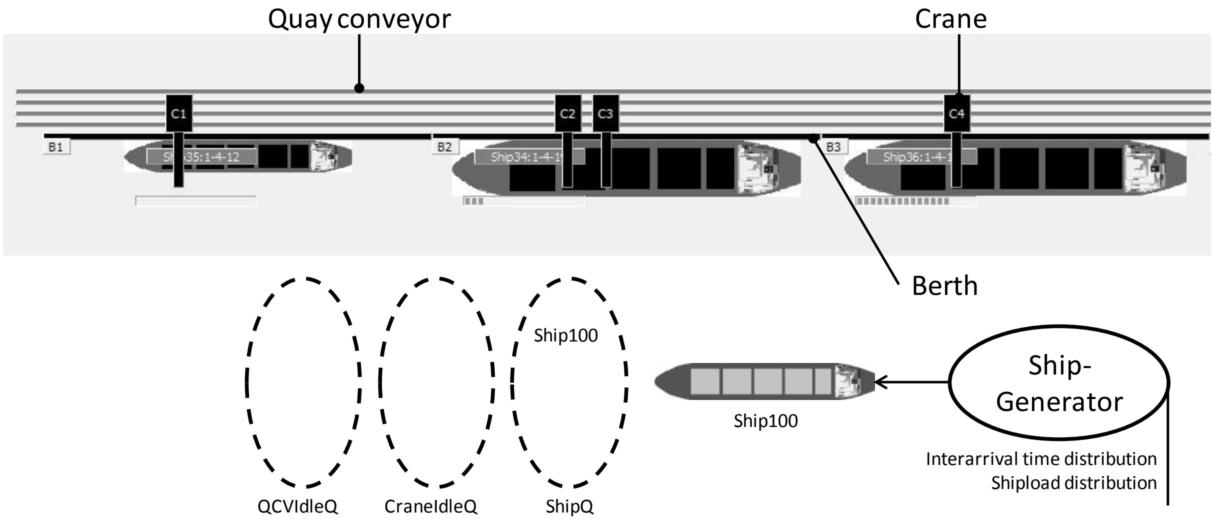

Figure D.2: The conceptual model for the seaside simulation model for an arbitrary layout where three ships are served simultaneously

The seaside model is explained already in section 3.6.1. In this section more details are presented. The shipgenerator generates ships (using distributions for the interarrival times and shiploads), moves generated ships into the ShipQ from where the ships are selected by idle berths to be moored. After the ship is berthed, the cranes are distributed over the ships to service these ships. In the arbitrary layout as shown in Figure D.2, the quay contains 3 berths, 4 quay conveyors and 4 cranes.

According the process interaction method the following descriptions can be distinguished:

- Element classes: terminal, ship generator, ship, berth, crane and quay conveyor
- Attributes: the attributes are listed in Table D.3 until Table D.8.
- Process descriptions: the element classes ship generator, crane and berth contain processes. These processes will be presented in Table D.6, Table D.7 and Table D.8 respectively.

Table D.3: Element class: Terminal (global attributes)

Attributes of terminal class	Description
ShipQ	Queue containing arrived ships
CraneIdleQ	Queue containing idle cranes
QCVIdleQ	Queue containing idle quay conveyors

Table D.4: Element class: Ship

Attributes of ship class	Description
MyCQ	Queue containing cranes that are assigned to the ship
MyQCVQ	Queue containing quay conveyors assigned to the ship
MaxNrCranes	Maximum number of cranes possible
Arrivaltime	Time of arrival
Shipload	Shipload
Length	Ship's length
Beam	Ship's beam
Draft	Ship's draft

Table D.5: Element class: Quay conveyor

Attributes of quay conveyor class	Description
Capacity	Transportation capacity

Table D.6: Element class: ShipGenerator

Attributes of ship generator class	Description
InputFile	Contains ships arrival times and loads
NewShip	Reference to Ship
NrGradesDistribution	TableDistribution of the number of grades per ship (the values used in this thesis are based on Figure 3.3 but can be adapted)
Process	Create ships with attributes and put these ships in ShipQ
Process of Ship generator class	

Repeat (NrJobs as defined in InputFile)
Read arrival time and load from InputFile
Hold(arrival time – t_{prev}) //to realize the Interarrival time between successive arrivals
t_{prev} = arrival time
Create a NewShip
NewShip.Shipload = load //assign load (out of InputFile to the newly generated ship)
Determine NewShip.Length, NewShip.Beam and NewShip.Draft based on eqs. (3.1 - 3.3)
Sample(NrGradesDistribution) //draw number of grades from a predefined table-type distribution
Determine NewShip.MaxNrCranes[1]
Add NewShip to tail of ShipQ //put newly generated ship as latest element in ShipQ to be serviced	

[1] The maximum number of cranes operating at the same time on a ship depends on the quay layout used and the ship size. When the discrete quay layout is used the maximum number is

one. For the continuous quay layout multiple cranes can be assigned and the maximum number of cranes per ship relates to the ship's length.

Table D.7: Element class: Crane

Attributes of crane class	Description
MyShip	Reference to Ship
MyCrane	Reference to crane
MyQCV	Reference to quay conveyor
Order	Sorting parameter to maintain the right positional order
FDCap	Free-digging capacity
C_{cranes}	Total free-digging capacity of cranes in MyShip.MyCQ
$C_{conveyors}$	Total transportation capacity of quay conveyors in MyShip.MyQCVQ
SetupTime	Time needed to shift from other berths
IsMoved	To indicate that crane is moved from other berth (True or False)
Δt	Time-interval for the crane handling
Process	Serve the ship
Process of Crane class	

```
Repeat
   Standby(while MyShip is not assigned)      //there is no ship to be serviced
   If IsMoved = True then Hold(SetupTime)  //when crane comes from another quay location wait driving time
   IsMoved = False                             //reset IsMoved Boolean to consider next crane movements

   C_cranes = 0, C_conveyors = 0               //determine the bottleneck capacity; cranes of quay conveyors
   MyCrane = MyShip.MyCQ.FirstElement   //determine C_cranes operating at MyShip
   Repeat(MyShip.MyCQ.Length)
      C_cranes = C_cranes + MyCrane.FDCap
      MyCrane = MyCrane.Successor(MyShip.MyCQ)
   MyQCV = MyShip.MyQCVQ.FirstElement             //determine C_conveyors operating at MyShip
   Repeat(MyShip.MyQCVQ.Length)
      C_conveyors = C_conveyors + MyQCV.Capacity
      MyQCV = MyQCV.Successor(MyShip.MyQCVQ)

   Repeat(while MyShip.Shipload > 0)                    //service the ship until the shipload is processed
      Determine the service capacity during Δt based on the ship's service stage[1], C_cranes and C_conveyors
      Hold(Δt)[2]
      MyShip. Shipload = MyShip.Shipload -[3] (service capacity* Δt) / MyShip.MyCQ.Length
  Remove MyShip. MyCQ                                          //ship is serviced completely
  AddSortedOn Order in CraneIdleQ or in another ship.MyCQ[4]  //put cranes in IdleQ or assign to other ship(s)
  Remove quay conveyor(s) from MyShip. MyQCVQ
  Add quay conveyor(s) to tail in QCVIdleQ                     //make quay conveyor available again
```

[1] Values for the ship's service stage (as introduced for ship unloading by Verschoof (2002) and shown in Figure 3.19) can be predefined. The actual service rate is determined by multiplying the total cranes' free-digging capacity (C_{cranes}) with the stage's capacity factor.
[2] The time interval for Δt was set to 1 hour that results that the shipload can reach a negative value. For example, before the time interval the shipload was 300 tons and after Δt the shipload was reduced with 1000 tons. Research has shown that using smaller time steps only increases the simulation time without improving the simulation accuracy.
[3] The shipload decreases for unloading and increases for ship loading
[4] When the discrete quay layout is applied, cranes are set as idle when the ship is ready. For the continuous quay layout, cranes can probably be moved to support the (un)loading operation of another ship. When cranes are moved, the right positional order of the cranes must be maintained. The crane's attribute IsMoved is set true to distinguish the crane's setup time for shifting to another berth.

Table D.8: Element class: Berth

Attributes of berth class	Description
MyDraft	Maximum allowable ship's draft at this berth
MyShip	Reference to Ship
NextShip	Reference to Ship
MyQCV	Reference to Quay conveyor
MyCrane	Reference to Crane
NrCranes	The number of the cranes that are assigned to the berthed ship
MyShipQ	Queue containing berthed ships
Process	Let a ship moor
SelectShip	Select a ship from ShipQ and assign quay conveyor(s); possible results are nil (no ship can be selected) or MyShip
AssignCranes	Assign crane(s) to the berthed ship

Process of berth class

```
Repeat
  Standby(while result of "SelectShip" is nil)     //standby while there is no ship calling
  Remove MyShip from ShipQ                         //remove the ship to be moored from the arrival queue
  Add MyShip to tail of MyShipQ                    //put this ship in MyShip queue from this berth
  Call "AssignCranes"                              //start the AssignCranes algorithm
  Standby(while MyShip.Shipload > 0)               //standby when the ship is serviced
```

SelectShip, a function of Berth class

```
Standby(while ShipQ.Length = 0)                    //standby while there is no ship in arrival queue
MyShip = ShipQ.FirstElement                        //select the first ship in arrival queue
Repeat(while MyShip is not nil)                    //continue until a ship is assigned to this berth
  if MyShip.Draft =< MyDraft then     //when the selected ship's draft is smaller or equal to the berth's draft
    if QCVIdleQ.Length > 0 then       //continue assigning when there is a quay conveyor available
      MyQCV = QCVIdleQ.FirstElement               //select the first quay conveyor
      Add(MyQCV) to MyShip.MyQCVQ                 //assign this quay conveyor to ship
      Remove MyQCV from QCVIdleQ     //remove assigned quay conveyor from idle quay conveyor queue
    else                                           //when there is no idle quay conveyor
      Select NextShip from which MyQCVQ.Length > 1  //select ship which more than one qcv
      MyQCV = NextShip.MyQCVQ.FirstElement          //select the first quay conveyor of this ship
      Remove MyQCV from NextShip.MyQCVQ    //unassign the selected qcv from ship with multiple qcv's
      Add MyQCV to tail of MyShip.MyQCVQ    //assign qcv to newly arrived ship
    Result = MyShip                     //newly arrived ship can be moored and a qcv is assigned
    Exit                                           //leave function
  MyShip = MyShip.Successor(ShipQ)                 //select next ship in ship arrival queue
Result = nil                                       //there is no ship to be moored
```

AssignCranes, a procedure of Berth class

```
If CraneIdleQ.Length > 0                                //when there are cranes available
  If MyShip.MaxNrCranes > CraneIdleQ.Length then NrCranes = CraneIdleQ.Length else
  NrCranes = MyShip.MaxNrCranes                         //determine number of cranes to assign
  MyCrane=CraneIdleQ.FirstElement                       //selects the first idle crane
  Repeat(NrCranes)
    Remove MyCrane from CraneIdleQ                      //moves crane out of idle cranes queue
    MyCrane AddSortedOn Order to MyShip.MyCQ            //assigns this to newly arrived ship
If CraneIdleQ.Length = 0                                //when there are no cranes idle
  Select NextShip[1] from which its MyCQ.Length > 1     //selects ship with multiple cranes assigned
  MyCrane = NextShip.MyCQ.FirstElement or NextShip.MyCQ.LastElement[1]
  Remove MyCrane from NextShip.MyCQ        //unassign a crane from ship with multiple cranes assigned
  MyCrane AddSortedOn Order to MyShip.MyCQ              //assigns to newly arrived ship
  MyCrane.MyShip = MyShip
```

[1] For the selection of NextShip and the crane to be moved (MyCrane), the positional order of cranes has to be maintained. See for an example of this repositioning algorithm Figure 3.18.

D.3 Stockyard model

The objective of the stockyard model is to model the stockyard operation enabling the specification for the stockyard size required. A schematic representation for the stockyard model has already been shown in Figure 5.4. In Figure D.3, a screenshot of model is shown for an arbitrary layout that consists of eight different stockyard lanes. The different colors of the rectangles at the lanes represent different types of strips; empty strips which do not contain stored materials are grey-colored and the color for the full strips (strips where material is stored) is determined by the material's grade. Red colored strips represent relocated piles; piles that are previously stored somewhere else but repositioned to realize free empty space for new piles.

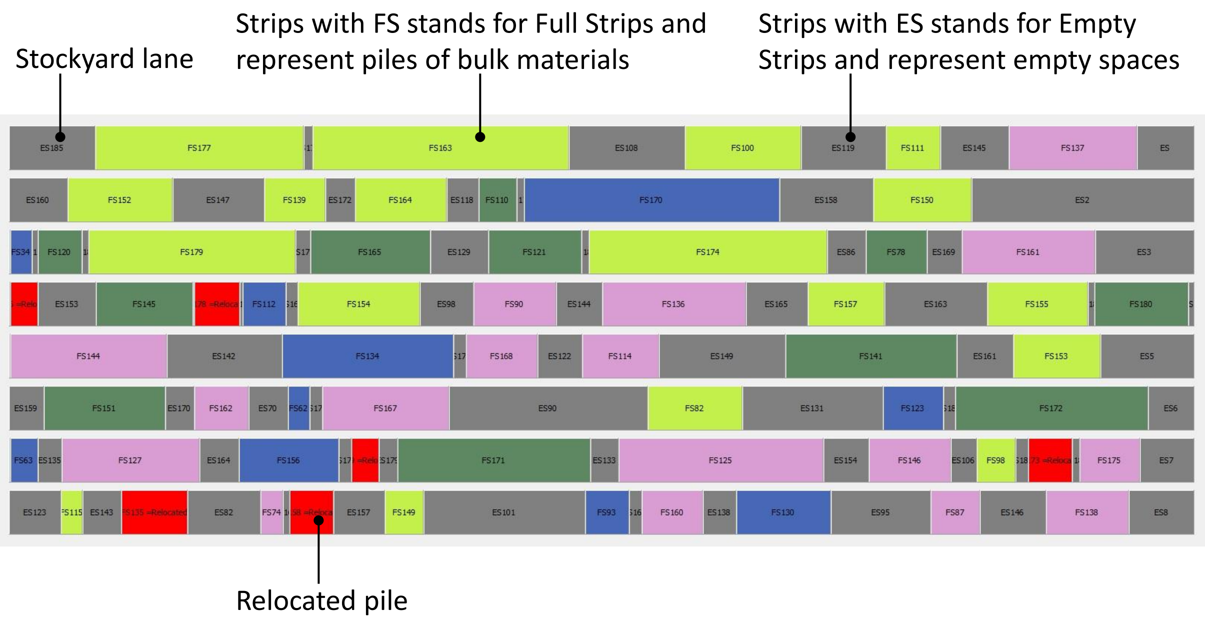

Figure D.3: Screenshot of the stockyard model for an arbitrary stockyard layout with 8 lanes and different sizes piles stored

According the process interaction method the following descriptions per step can be distinguished for the stockyard model:

- Element classes: terminal, ship generator, train generator, job, lane, pile, strip and grade
- Attributes: the attributes for the element classes are listed in Table D.9 until Table D.15. The element classes pile and grade do not have any attributes and are therefore not listed in specific tables.
- Process descriptions: the element classes ship generator, train generator and lane contain processes. The terminal class owns the function "Relocate", which is discussed in Table D.9. This function can be activated by the ship generator class as well as the lane class. The Job class owns a specific function to determine the length required to store the job's load at the stockyard. A description for the DetermineLength-function is presented in Table D.14.

Table D.9: Element class: Terminal (with global attributes and relocate-algorithm)

The relocation algorithm is defined as a global algorithm because this algorithm is used by the Lane class and Ship generator class.

Attributes of terminal class	Description
JobQ	Queue containing jobs that can be served
JobWQ	Queue containing waiting jobs due to the lack of storage area available
ShipQ	Queue containing ships to register average ship port time
TrainQ	Queue containing trains to register average train port time
GradesQ	Queue containing grades stored at stockyard
StoredGradesQ	Queue containing grades that are stored somewhere at the stockyard
LanesQ	Queue containing lanes
StoragePolicy	Global attribute to distinguish the ID-preserved storage policy (1) or the CAM storage policy (2) (details for these storage policies see section 5.2.2)
D	Separation distance between piles
MyJob	Reference to Job
MyLane	Reference to Lane
MyFS, FirstFS, PrevES, NextES, MyES	Reference to Strip (Full strip represents area where material is stored, empty strip does not contain material)
RelocateStripsQ	Queue containing full strips that can be relocated
MaxRelTons	Maximum to be relocated tons that is an input parameter
RelocatedJob	Reference to Job

Relocate, a function of Terminal class

```
MyJob = JobWQ.FirstElement                          //selects the first waiting job
RelocateStripsQ.Clear                               //removes all strips from this queue
MyLane = LanesQ.FirstElement                        //selects the first lane
Repeat(LanesQ.Length)                               //repeats for number of lanes
  MyFS = MyLane.MyFSQ.FirstElement                  //My FullStrip is first FullStrip of selected lane
  Repeat(MyLane.MyFSQ.Length)                       //repeats number of full strips for the selected lane
    PrevES = MyFS.Predecessor(MyLane.MyFSQ)         //determines empty strip left from MyFullStrip
    NextES = MyFS.Successor(MyLane.MyFSQ)           //determines empty strip right from MyFullStrip
MyFS.FreeLength = PrevES.Length + MyFS.Length + NextES.Length
                                                    //determines freecoming length when the selected fullstrip is moved
    If (MyFS.FreeLength – D > MyJob.Length) and (MyFS.MyTons < MaxRelTons)
      MyFS AddSortedOn MyTons to RelocateStripsQ   //This Full Strip can be relocated
    MyFS = MyFS.Successor(MyLane.MyFSQ)             //selects the next full strip of selected lane
  MyLane = MyLane.Successor(LanesQ)                 //selects next lane
  FirstFS = RelocateStripsQ.FirstElement            //Selects the first candidate Full strip to be relocated
  Find MyES where MyES.Length +2*D >= FirstFS.Length      //Find an empty strip with sufficient length
  Remove FirstFS from FirstFS.MyLane.MySQ and FirstFS.MyLane.MyFSQ     //removes relocated strip
  Create RelocatedJob                               //create a job of relocated tons
  RelocatedJob.MyTons = FirstFS.MyTons              //takes over the jobs from strip that will be relocated
  RelocatedJob.Length = FirstFS.Length              //takes over length
  RelocatedJob.MyGrade = FirstFS.MyGrade            //takes over grade
  If StoragePolicy = 1 then                         //if Identity Preserved re-assign full strip's pile
    Remove FirstFS.MyPile from FirstFS.MyLane.MyPilesQ
    RelocatedJob.MyPile = FirstFS.MyPile
  FirstFS.MyLane.CombineEmptyStrips                 //starts algorithm to combine the remaining empty strips
  Add RelocatedJob as first element in JobQ         //relocated job must be as first handled
  Remove MyJob from JobWQ
  Add MyJob to JobQ
```

Table D.10: Element class: Strip

Attributes of strip class	Description
MyLane	Reference to Lane
x1, x2	Start and end location of strip
Length, FreeLength	Strip's length, free coming length at stockyard if this strip is relocated
MyTons	Actual tons stored
Name	To distinguish a full strip or an empty strip (ES)

Table D.11: Element class: Ship

Attributes of ship class	Description
Shipload	Ship's load
Length	Ship's length
Beam	Ship's beam
Draft	Ship's draft

Table D.12: Element class: Train generator

Attributes of train generator class	Description
STNedDist	NED-Storage time distribution
STE_2Dist	Erlang-2 Storage time distribution
STDistType	Storage time distribution type (1=NED, 2= Erlang-2)
TST	Total storage time of pile
ST	Storage time between train jobs
NrTrains	Number of trains to reclaim pileload
TrainLoad	Amount of tons per train
NewTrain	Reference to Job
Process	Create trains with attributes and put these trains in TrainQ and JobQ

Process of Train generator class

```
If STDistType = 1 then TST=Sample(STNedDist) else TST =Sample(STE2Dist)      //determine total Ts
NrTrains = RoundUp(MyTons / TrainLoad)      //determines nr trains to export entire pile
ST = TST / NrTrains                         //determines interarrival time between trains (see Fig.5.4C)
Repeat(NrTrains)
   Create NewTrain
   NewTrain.MyTons = MyTons / NrTrains
   NewTrain.Length = NewTrain.DetermineLength          //calculates job's length based on it's tons
   If StoragePolicy = 1 then NewTrain.MyPile=MyPile    //If Identity Preserved assign pile
   NewTrain.MyGrade=MyGrade
   Hold(ST)                                            //waits train interarrival time
   Add NewTrain to JobQ and TrainQ                     //move newly generated to right queues
```

Table D.13: Element class: Ship generator

Attributes of ship generator class	Description
InputFile	Contains ships arrival times and loads
NewShip	Reference to Ship
NewJob	Reference to Job
MaxPileTons	The maximum load to be stored in a single pile
NrShipJobs	Number of jobs stored in a ship
MyEmptyStrip, MyFullStrip	Reference to Strip
AreaAvailable	Check the allocation of a new job to the stockyard
Process	Create ships with attributes and put these ships in ShipQ and JobQ or JobWQ

Process of Ship generator class

```
Repeat (NrJobs as defined in InputFile)
  Read arrival time, load and grade from InputFile
  Hold(arrival time – t_prev)
  t_prev = arrival time
  Create a NewShip
  NewShip.Shipload = load

  MyGrade = GradesQ.FirstElement                    //assigns grade to newly generated ship
  Repeat(GradesQ.Length)
    If MyGrade.Name = grade then NewShip.MyGrade = MyGrade
    MyGrade = MyGrade.Successor(GradesQ)

  Determine NewShip.Length, NewShip.Beam and NewShip.Draft based on eqs. (3.1 - 3.3)
  NrShipJobs = RoundUp(NewShip.Shipload / MaxPileTons)   //distributes shipload over multiple piles
  Repeat(NrShipJobs)
    Create a NewJob
    If StoragePolicy = 1 then Create NewJob.MyPile           //If Identity preserved creates separate pile
    NewJob.MyGrade = NewShip.MyGrade                         //assigns grade to new job
    NewJob.MyTons = NewShip.Shipload / NrShipJobs            //determines tons for new job
    NewJob.Length = NewJob.DetermineLength                   //calculates job's length based on its tons
    NewJob.MyShip = NewShip                                  //defines relation with ship
    Create NewJob.MyTrainGen                                 //creates traingenerator to generate exports for new job
    If StoragePolicy = 1 then NewJob.MyTrainGen.MyPile = NewJob.MyPile  //if ID assign pile to traingen.
    NewJob.MyTrainGen.MyTons = NewJob.MyTons                 //determines tons to be exported
    NewJob.MyTrainGen.MyGrade = NewJob.MyGrade               //assigns grade to traingen.
    If AreaAvailable = True then Add NewJob to JobQ          //starts AreaAvailable algorithm
    else Add NewJob to JobWQ and call "Relocate"             //if true job to JobQ else to JobWQ and starts Relocate
  Add NewShip to tail of ShipQ                               //ship can be moored
```

AreaAvailable, a function of Ship generator

```
If StoragePolicy = 1                                         //if Identity Preserved (section 5.2.2)
  MyLane = LanesQ.FirstElement
  Repeat(LanesQ.Length)
    MyEmptyStrip = MyLane.MyESQ.FirstElement
    Repeat(MyLane.MyESQ.Length)
      If MyEmptyStrip.Length > NewJob.Length + D
        Result = True
        Exit                                    //leave this function
      MyEmptyStrip = MyEmptyStrip.Successor(MyLane.MyESQ)
    MyLane = MyLane.Successor(LanesQ)
  Result = False
```

Find an emptystrip somewhere at stockyard lanes with sufficient length to store new job.

```
If StoragePolicy = 2                                         //if Cargo Assembly Mode (section 5.2.2)
  If NewJob.MyGrade is in StoredGradesQ
    Result = True
    Exit                     //leave this function
```

If grade is already stored somewhere at stockyard lanes, no need for search empty strip.

```
  If NewJob.MyGrade is not in StoredGradesQ
    Find MyFullStrip at MyLane that owns MyGrade
    MyEmptyStrip = MyFullStrip.Successor(MyLane.MySQ)
    If MyEmptyStrip.Length > NewJob.Length + D
        Result = True
        Exit                 //leave this function
    else
    Find Next FullStrip that owns MyGrade
  Result = False
```

If grade is nowhere stored find empty strip with sufficient length to store new job.

Table D.14: Element class: Job

Attributes of job class	**Description**
SeaJob	To indicate if this job is a seaside job (True) or landside job (False)
MyTons	Job's load
MyPile	Reference to Pile
MyGrade	Reference to Grade
MyShip	Reference to Ship
Length	Job's length required to store at a lane
MyTrainGen	Reference to Train generator to create trains to export jobload
DetermineLength	Determine Job's length
Volume	Pile's volume
BulkDensity	Bulk density of material stacked in pile
H_{max}	Maximum pile's height
PileWidth	Pile's width the same value as lane's width
PileHeight	Actual pile's height (input parameter)
Tan_aor	Tangent of the angle of repose
L_X, L_{table}	Length of sloping face, in Figure 5.2 (l_t – l) /2 and Length of the table-shaped middle part of the pile
V_X, V_{cone}	Volume for 2 times sloping face and Volume cone (4 times ¼ cone)
V_{table}	Volume for the table-shaped part of the pile
A_{table}	Area for the table-shaped part of the pile
DetermineLength, a function of Job class	

Volume = MyTons / BulkDensity //application of equation (5.5) to determine length required for tons
H_{max} = 0.5 * PileWidth * Tan_aor
L_X = PileHeight / Tan_aor
V_X = PileHeight * (PileHeight / Tan_aor) * (PileWidth – 2*L_X)
V_{cone} = (3.14159 * (PileHeight / Tan_aor) * (PileHeight / Tan_aor) * PileHeight) / 3
V_{table} = Volume – (V_X + V_{cone})
A_{table} = (PileHeight / H_{max}) * (2 – (PileHeight / H_{max})) * (0.5*PileWidth*H_{max})
L_{table} = V_{table} / A_{table}
Length = L_{table} + 2*L_X	

In lane's class several algorithms are included. The first one is the algorithm SelectJob to accept a job based on the following conditions:

- Storage Policy: Identity preserved (see section 5.2.2)
    - Job is from a ship and there is an empty strip available with sufficient length
    - Job is from a train and requested pile is stored at lane
- Storage Policy: Cargo Assembly Mode (see section 5.2.2)
    - Job is from ship and job's grade is stored at lane (complement existing pile)
    - Job is from train and requested grade is stored at lane

Another algorithm is CombineEmptyStrips. This algorithm is developed to remove empty strips to prevent that two empty strips are located next to each other. This happens when the full strip between two empty strips was removed because the pile's load was exported or due to the fact that this full strip (and thus the pile) was relocated to realize sufficient free length to store newly arrived material.

Details concerning the procedure Process are listed after two diagonal fraction bars (//).

Table D.15: Element class: Lane

Attributes of ship generator class	Description
MyPilesQ	Queue containing piles stored at lane
MyGradesQ	Queue containing grades stored at lane
MyFSQ, MyESQ, MySQ	Queues containing Full, Empty and All Strips stored at lane
MyEmptyStrip, MyES, NewES	Local elements belonging to strip class to represent empty strips
NewFS, MyFS	Local elements belonging to strip class to represent full strips
ReclaimMethod	To indicate the clearing pile's area (1=CPA) see Chapter 5
DummyJob	Reference to Job
StackCapacity, ReclaimCapacity	Stacking capacity and Reclaiming capacity
SelectJob	Algorithm to select a Job from JobQ
Process	Serve selected job
CombineEmptyStrips	See explanation above table

SelectJob, a function of Lane class

```
If (StoragePolicy = 1) and (MyJob=Ship)            //If Identity preserved and new job is from a ship
  MyEmptyStrip = MyESQ.FirstElement                //Find Empty Strip with sufficient length
  Repeat(MyESQ.Length)
    If MyEmptyStrip.Length >= MyJob.Length +D
      Result = MyJob                               //An EmptyStrip is found
      Exit                                         //leaves this function
    MyEmptyStrip=MyEmptyStrip.Successor(MyESQ)
  Result = False

If (StoragePolicy = 2) and (MyJob=Ship) and (MyJob.MyGrade is in StoredGradesQ)
and (MyJob.MyGrade is in MyGradesQ)
  Result = MyJob                                   //MyJob.MyGrade is stored on lane
  Exit

If (StoragePolicy = 2) and (MyJob=Ship) and (MyJob.MyGrade is NOT in StoredGradesQ)
  Find Empty Strip with sufficient length; see above

If (StoragePolicy = 1) and (MyJob=Train) and (MyJob.MyPile is in MyPilesQ) OR (StoragePolicy = 2) and
(MyJob=Train) and (MyJob.MyGrade is in MyGradesQ)
  Result = MyJob
```

Process of Lane class

```
Repeat
  Standby(while MyJob is not assigned)
  Remove MyJob from JobQ
  If (StoragePolicy=1) and (MyJob=Ship) OR (StoragePolicy=2) and (MyJob=Ship) and
  (MyJob.MyGrade is not in StoredGradesQ)
    MyEmptyStrip = MyESQ.FirstElement              //Finds Empty Strip with sufficient length
    Repeat(MyESQ.Length)
      If MyEmptyStrip.Length >= MyJob.Length +D then
        MyES = MyEmptyStrip                        //selects empty strip with sufficient length
        Remove MyES from MySQ and MyESQ
      Else MyEmptyStrip=MyEmptyStrip.Successor(MyESQ)

    Create NewFS                                   //creates new full strip
    Create NewES                                   //creates new empty strip
    NewES.Name = "ES"                              //New empty strip left from full strip
    NewES.x1 = MyES.x1                             //takes over start location
    NewES.x2 = NewES.x1 + D                        //determines end location (=start + separation distance)
    NewFS.MyLane = self
    NewES.Length = D                               //determines length
    NewFS.x1 = NewES.x2                            //determines start location full strip
    NewFS.x2 = NewFS.x1 + MyJob.Length             //determines end location
    NewFS.Length = MyJob.Length                    //determines length
```

```
    If StoragePolicy = 1 then NewFS.MyPile = MyJob.MyPile        //if ID assigns pile to full strip
    NewFS.MyGrade = MyJob.MyGrade                                //assigns grade to full strip
    NewFS.MyTons = MyJob.MyTons                                  //assigns tons to full strip
    MyES.x1 = NewFS.x2        //determines new start location MyES (MyES will be right from pull strip)
    MyES AddSortedOn x1 to MySQ and MyESQ  //removes strips in right positional order to right queues
    NewES AddSortedOn x1 to MySQ and MyESQ
    NewFS AddSortedOn x1 to MySQ and MyFSQ
    Add NewFS.MyGrade to MyGradesQ               //assigns full strip's grade to lane's grades queue
    If NewFS.MyGrade is not in StoredGradesQ then Add NewFS.MyGrade to
    StoredGradesQ
    If StoragePolicy = 1 then Add NewFS.MyPile to MyPilesQ
    Hold(MyJob.MyTons / StackCapacity)                               //time needed for stacking
    If MyJob.MyShip is in ShipQ then Remove MyJob.MyShip from ShipQ      //ship is serviced

    If MyJob=Train
      If StoragePolicy = 1                  //if storagepolicy is Identity preserved a job represents train
        MyFS=MyFSQ.FirstElement
        Repeat(MyFSQ.Length)
          If MyFS.MyPile = MyJob.MyPile
            MyFS.MyTons = MyFS.MyTons – MyJob.MyTons     //bookkeeping tons
            If ReclaimMethod = 1                         //is clearing pile's area see section 5.4.2
              Create DummyJob                            //to calculate new length
              DummyJob.MyTons = MyFS.MyTons
              MyFS.Length = DummyJob.DetermineLength
              MyFS.x2 = MyFS.x1 + MyFS.Length              //updates dimensions
              NextES = MyFS.Successor(MySQ)
              NextES.x1 = MyFS.x2                        //updates dimensions
              NextES.Length = NextES.x2 – NextES.x1    //updates dimensions
            Hold(MyJob.MyTons / ReclaimCapacity)         //time needed for reclaiming
            If MyFS.MyTons = 0                           //if all material is reclaimed
              Remove MyFS.MyPile from MyPilesQ        //removes full strip from corresponding queues
              Remove MyFS.MyGrade from MyGradesQ
              Remove MyFS from MySQ and MyFSQ
              Remove MyJob from TrainQ                   //train is serviced
              Call "CombineEmptryStrip"                  //starts algorithm CombineEmptyStrips
              If JobWQ.Length > 0 Call "Relocate"        //starts algorithm Relocate
```

CombineEmptyStrip, a function of Lane class

```
MyStrip = MySQ.FirstElement
Repeat(MySQ.Length)
  NextStrip=MyStrip.Successor(MySQ)
  If (NextStrip.Name = ES) and (MyStrip.Name = ES)
    NextStrip.x1 = MyStrip.x1
    NextStrip.Length = NextStrip.x2 – NextStrip.x1
    Remove MyStrip from MySQ and MyESQ
  Else MyStrip = MyStrip.Successor(MySQ)
```

Find the empty strips when two empty strips are next to each other in the strips queue. Update dimensions and destroy one of the empty strips.

D.4 Transport network model

The transport network model is an extension of the stockyard model with stockyard machines and belt conveyors to model the handling and transportation of bulk materials. Figure D.4 shows a screenshot of an arbitrary terminal network. Many element classes as already presented in the previous section were used and some of these algorithms were extended. The main difference between the transport network model and the stockyard model is that for the processes of the stockyard machines 'control' the transport network model contrary to the lane class processes for the stockyard model.

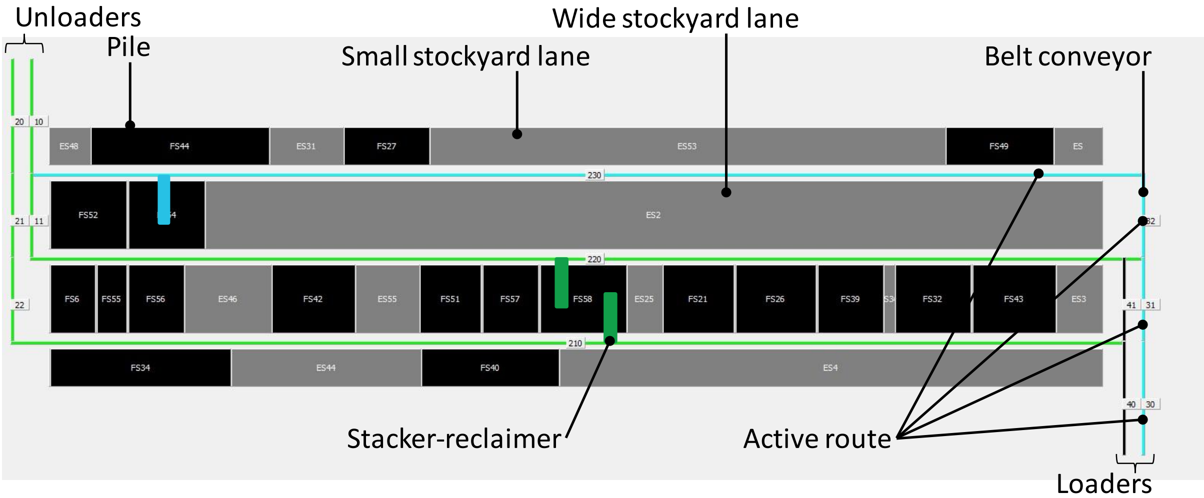

Figure D.4: Screenshot of the transport network model for an arbitrary layout with 4 lanes, 3 stacker-reclaimers, 3 yard belt conveyors and several conveyors to connect the (un)loaders with the stacker-reclaimers

Note that the (un)loaders are not modeled explicitly, only the belt conveyors connected to the (un)loading machines were considered.

For this model the steps for the process interaction method can be formulated as follows:

- Element classes: terminal, ship generator, train generator, disturbance generator, machine, route, conveyor, job, lane, pile and strip.
- Attributes: for many element classes attributes were already introduced in the previous section. Extra attributes are listed or attributes for new element classes are listed in Table D.16 until Table D.24.
- Process descriptions: due to the fact that some algorithms for the elements' processes were based on previously presented processes in section D.3, the modifications and additions are presented in this section. The functions and processes for the new developed machine class are listed in Table D.23.

Table D.16: Element class: Terminal with global attributes

Extra attributes of terminal class	Description
CVLQ	Queue containing landside conveyors
CVIdleQ	Queue containing conveyors that are idle

Table D.17: Element class: Job

Extra attributes of job class	Description
MyCVLQ[1]	Queue containing landside conveyors that can export this job
NrCVLs[1]	Number of landside conveyors to export job
MyRoute	Reference to route; selected route to transport this job
MyES	Reference to strip; selected to store job's load on
SeaJob	To distinguish seaside jobs (True) and landside jobs (False)
DisturbedTime	Extra time needed for job handling due to conveyor disturbances
SecondStacker	Reference to Machine indicating that this machine is needed to stack a job at a wide lane

[1] Extra attributes to Job are the number and predefined landside conveyors. At dry bulk terminals sometimes material cannot be transported from all stockyard locations to all (un)loaders due to limitations in the transportation network.

Table D.18: Element class: Ship

Extra attributes of ship class	Description
MyCVLQ	Queue containing landside conveyors that can export this job
NrCVLs	Number of landside conveyors to export jobs from ship

Table D.19: Element class: Lane

Extra attributes of lane class	Description
MyStackersQ	Queue containing stockyard machines that can stack at lane
Width	Different widths four outer or middle stockyard lanes

Table D.20: Element class: Ship generator

Extra attributes of ship generator class	Description
CVLString	Name of the landside conveyor
MyCVL	Reference to Conveyor
Process	Create Ships and put in JobQ, generally based on Table D.13

Additions to Process of Ship generator class

```
Read NewShip.NrCVLs from InputFile     //number of possible landside conveyors to export ship's material
Repeat(NewShip.NrCVLs)
   Read CVLString from InputFile        //read the name of landside conveyor
   MyCVL = CVLQ.FirstElement            //selects the first landside conveyor in CVLQ
   Repeat(CVLQ.Length)
      If MyCVL.Name = CVLString         //if name of landside conveyor corresponds
         Add MyCVL to NewShip.MyCVLQ //then assign this conveyor to new ship
      MyCVL = MyCVL.Successor(CVLQ) //else select the next conveyor in CVLQ
```

Landside conveyors from NewShip.MyCVLQ are also moved to NewJob.MyCVLQ and NewJob.MyTrainGen.MyCVLQ with similar algorithm

Table D.21: Element class: Route

Attributes of route class	Description
MyCVQ	Queue containing conveyors in this route

Table D.22: Element class: Conveyor

Attributes of conveyor class	Description
MyDistGen	Reference to Disturbance generator
MyJob	Reference to Job

Table D.23: Element class: Machine

Attributes of machine class	Description
MyCVLQ	Queue containing landside conveyors to which this machine can be connected
JobsToDoQ	Queue containing a part of a seaside job (is called PartialJob) that must be handled due to wide stockyard lanes. Piles must be stacked from both sides using two stackers.
MyRoutesQ, MySRoutesQ, MyLRoutesQ	Queue containing all routes, SRoutes represent transportation routes between the seaside and the stockyard and LRoutes represent the routes between the stockyard and the landside
MyLanesQ	Queue containing lanes within the machine's reach
JobHandling	Is set True if one of the predefined job's landside conveyor is in MyCVLQ
PartialJob	Reference to Job, if seaside job will be stored on a wide lane this job is created to model the stacking of piles using two stockyard machines
DistOnOff	Take disturbance of belt conveyors into account (0 = Off, 1 = On)
TwoStackingMachines	To determine if seaside job can be stacked by 2 stockyard machines
MyLane	Reference to lane
MyCV, MyCVL	Reference to conveyor
MyES	Reference to strip
SelectJob	Select Job from JobsToDoQ or JobQ
Process	Serve the selected Job, based on lane's process as described in Table D.15
EmptyStripAvailable	Check if seaside job's load can be stored on a lane (based on AreaAvailable algorithm of ship generator in Table D.13 with additions)
RouteAvailable	Check if there are routes available to transport the Job (Result = MyJob or nil)
CombineEmptyStrips	Remove empty strip to prevent that two empty strips are located next to each other, comparable to the algorithm as mentioned in Table D.15

Additions to Process of Machine class

```
MyCV = MyJob.MyRoute.MyCVQ.FirstElement      //removes conveyors from selected route from CVIdleQ
Repeat(MyJob.MyRoute.MyCVQ.Length)           //repeats for all conveyors in route
   Remove MyCV from CVIdleQ                  //removes conveyor out of conveyor idle queue
   If DistOnOff = 1 MyCV.MyDistGen.Resume    //activates disturbance generator
   MyCV = MyCV.Successor(MyJob.MyRoute.MyCVQ)   //selects the next conveyor in route

Hold(MyJob.MyTons / Capacity)                //represents the transportation and job's handling time
If MyJob.DisturbedTime > 0 then Hold(MyJob.DisturbedTime)   //wait the time that job was disturbed

MyCV = MyJob.MyRoute.MyCVQ.FirstElement      //Add conveyors after finishing to CVIdleQ
Repeat(MyJob.MyRoute.MyCVQ.Length)           //repeat for all conveyors in route
  Add MyCV to CVIdleQ                        //put conveyor back in conveyor idle queue
  If DistOnOff = 1 MyCV.MyDistGen.Pause      //pauses disturbance generator
  MyCV = MyCV.Successor(MyJob.MyRoute.MyCVQ)    //selects the next conveyor in route
```

SelectJob, a function of Machine class

```
If JobsToDoQ.Length > 0                //there is a partial job that must be handled due to wide lanes
   If (RouteAvailable = MyJob)         //starts algorithm RouteAvailable and continues when there is one
      Result = MyJob
      Exit
MyJob = JobQ.FirstElement
Repeat(while MyJob is not nil)
   JobHandling = False                 //set false before checking
   MyCVL = MyJob.MyCVLQ.FirstElement   //selects first landside conveyor for this job
   Repeat(MyJob.MyCVLQ.Length)         //repeats for number of possible landside conveyors
      If MyCVL is in MyCVLQ then JobHandling = True
```

```
    MyCVL = MyCVL.Successor(MyJob.MyCVLQ)

  If (MyJob.SeaJob = True) and (JobHandling = True) and (EmptyStripAvailable <> nil) and
  (RouteAvailable    <> nil)
    Result = MyJob
    If MyJob.SecondStacker <> nil //create a partial job that must be handled by the 2nd stockyard machine
      Create PartialJob
      PartialJob.MyPile = MyJob.MyPile
      PartialJob.MyTons = MyJob.MyTons / 2                //divides Job's load over 2 jobs
      MyJob.MyTons = PartialJob.MyTons
      Add PartialJob to MyJob.SecondMachine.JobsToDoQ

  If (MyJob.SeaJob = False) and (MyJob.MyPile is in MyPilesQ)
    MyRoute = MyLRoutesQ.FirstElement
    Repeat(MyLRoutesQ.Length)
      MyCV = MyRoute.MyCVQ.FirstElement
      If (MyCV is in CVIdleQ) and (MyCV is NOT MyRoute.MyCVQ.LastElement)
        MyCV = MyCV.Successor(MyRoute.MyCVQ)       //check availability of next conveyor
        If (MyCV is in CVIdleQ) and (MyCV is MyRoute.MyCVQ.LastElement) and
        (MyCV is in MyCVLQ)[1]
           Result = MyJob
           MyJob.MyRoute = MyRoute
           Exit
        If (MyCV is in CVIdleQ) and (MyCV is MyRoute.MyCVQ.LastElement) and (MyCV is
        NOT in MyCVLQ)
          MyRoute = MyRoute.Successor(MyLRoutesQ)

  If MyJob is not JobQ.LastElement then MyJob = MyJob.Successor(JobQ)
  Result = nil                                          //job cannot be handled by this machine
```

EmptyStripAvailable, a function of Machine class

```
MyLane = MyLanesQ.FirstElement
Repeat(MyLanesQ.Length)
  MyJob.Length=MyJob.DetermineLength with MyLane.Width        //different lengths for different widths
  MyES = MyLane.MyESQ.FirstElement                            //selects first empty strip
  Repeat(MyLane.MyESQ.Length)
    If (MyES.Length> MyJob.Length + D) and (MyLane.MyStackersQ.Length > 1) //stack pile by 2 machines
      MyMachine = MyLane.MyStackersQ.FirstElement              //selects first stacking machine
      TwoStackingMachines = False                        //is set True when pile must be stacked by 2 machines
      MyCVL = MyJob.MyCVLQ.FirstElement                       //selects first landside conveyor
      Repeat(MyJob.MyCVLQ.Length)
        If MyCVL is in MyCVLQ then TwoStackingMachines = True //2nd machine can be connected to
                                                                            a predefined Job's CVL
        MyCVL=MyCVL.Successor(MyJob.MyCVLQ)
      If TwoStackingMachines = True                     //if pile can be stacked by two stacking machines
        MyJob.SecondStacker = MyMachine                 //assigns stacking machine to job
        Result = MyJob
        MyJob.MyES = MyES                              //assigns empty strip to job
        MyJob.MyES.MyLane = MyLane
        Exit
      Else
        Result = nil                                   //no empty strip available
        Exit                                           //leaves this algorithm
    If (MyES.Length > MyJob.Length + D) and (MyLane.MyStackersQ.Length = 1) //stack pile by 1 machine
      Result = MyJob
      MyJob.MyES = MyES
      MyJob.MyES.MyLane = MyLane
      Exit
    MyES = MyES.Successor(MyLane.MyESQ)
  MyLane=MyLane.Successor(MyLanesQ)
Result = nil                                           //no empty strip available
```

RouteAvailable, a function of Machine class (Find a route from which all conveyors are available)

if (MyJob.SeaJob = True) then MyRoutesQ = MySRoutesQ else MyRoutesQ = MyLRoutesQ
MyRoute = MyRoutesQ.FirstElement
Repeat(MyRoutesQ.Length)
  MyCV=MyRoute.MyCVQ.FirstElement
  Repeat(MyRoute.MyCVQ.Length)
    If (MyCV is NOT in CVIdleQ) and (MyRoute is NOT MyRoutesQ.LastElement) //MyRoute not available
      MyRoute = MyRoute.Successor(MyRoutesQ
      MyCV = MyRoute.MyCVQ.FirstElement
    If (MyCV is NOT in CVIdleQ) and (MyRoute is MyRoutesQ.LastElement)
      Result = nil //No available route found
      Exit
    If (MyCV is in CVIdleQ) and (MyCV is NOT MyRoute.MyCVQ.LastElement) //Check next conveyor
      MyCV = MyCV.Successor(MyRoute.MyCVQ)
    If (MyCV is in CVIdleQ) and (MyCV = MyRoute.MyCVQ.LastElement) //all routes in MyRoute are idle
      Result = MyJob //job can be selected
      MyJob.MyRoute = MyRoute //route assigned to job
      Exit //leaves this algorithm

[1] Define the landside routes, during the initialization of the simulation model, in such a way that the landside conveyors, that represent the loading machines, are the last conveyors in the landside route.

Table D.24: Element class: Disturbance generator

Attributes of disturbance generator class	Description
MTBF	MeanTimeBetweenFailure
MTTR	MeanTimeToRepair
MTBFDistribution	Distribution to sample values for the MTBF
MTTRDistribution	Distribution to sample values for the MTTR
MyCV	Reference to conveyor[1]
Process of Disturbance generator class	

Repeat
  MTBF = Sample(MTBFDistribution) //draws MTBF time from predefined distribution
  Hold(MTBF) //waits the mean time between failures
  MTTR = Sample(MTTRDistribution) //draws MTTR time from predefined distribution
  MyCV.MyJob.DisturbedTime = MyCV.MyJob.DisturbedTime + MTTR //adds MTTR to disturbance time
  Hold(MTTR) //waits the mean time to repair	

[1] During the initialization stage each conveyor gets its own Disturbance generator, an attribute of this generator is MyCV to add the MTTR to the right job's DisturbedTime

D.5 Total terminal model

In the total terminal model (introduced in section 8.2) the transport network model of section D.4 is extended with berths and cranes. The algorithms for the berths and cranes are based on processes that were already presented in section D.3. In Figure D.5, a screenshot from the total terminal model is shown.

Although this model can be used for import as well as export terminals, in this section the description for import terminals will be given. Only the additions to the transport network model will be discussed. Extra element classes are berths and cranes. The berth class owns a process that represents the ship's mooring process and a function for the selection of bulk ships. Descriptions for these functions are listed in Table D.27.

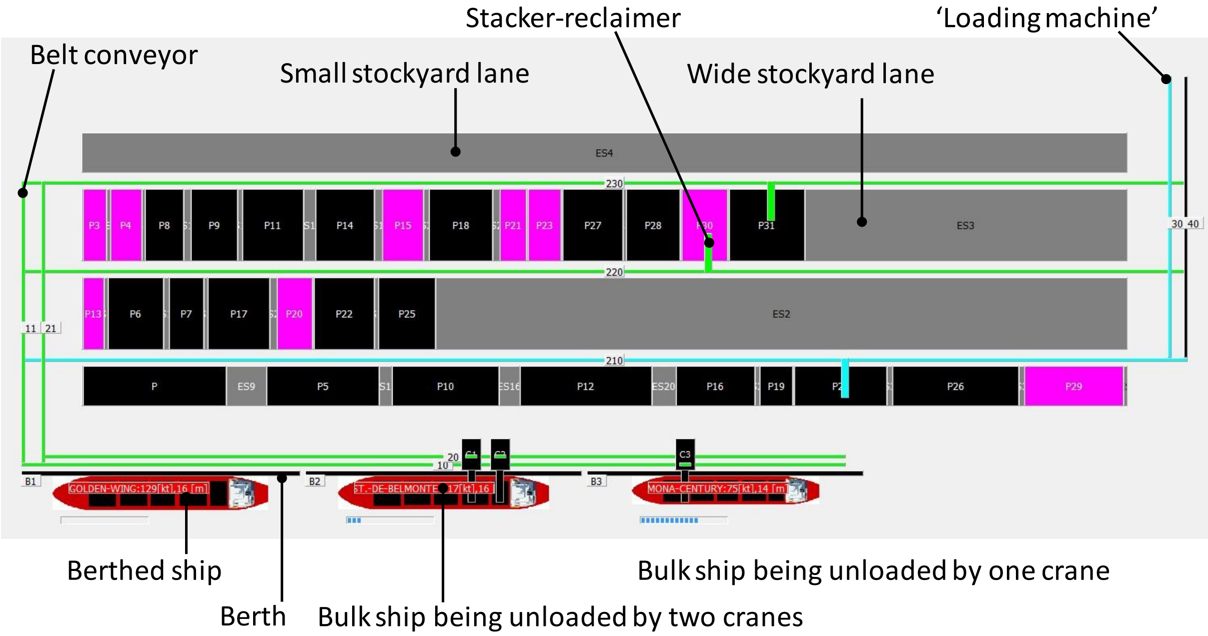

Figure D.5: Screenshot of the total terminal model for an arbitrary layout containing three berths, 3 cranes, four lanes, three stacker-reclaimers and several belt conveyors

Table D.25: Element class: Terminal with global attributes

Attributes of terminal class	Description
CranesQ	Queue containing cranes sorted on Order
ActiveJobQ	Queue containing active seaside jobs

Table D.26: Element class: Job

Attributes of job class	Description
MyCQ	Queue containing cranes assigned to job
PosX	X-coordinate of Job
MaxNrCranes	Maximum number of cranes operating at job

Table D.27: Element class: Berth

Attributes of berth class	Description
MyShip	Reference to Ship
MyJob	Reference to Job
Draft	Maximum ship's draft to accept ship at berth
PosX	Mid position of Berth

Process of Berth class

```
Repeat
   Standby(while MyShip is not assigned)          //wait for the result from SelectShip-algorithm
   Remove MyShip from ShipQ                        //ship can be serviced thus remove from ShipQ
   MyJob = MyShip.JobQ.FirstElement                //select first job from MyShip.JobQ to JobQ
   Repeat(MyShip.JobQ.Length)
      MyJob.PosX = PosX            //to align Job's position with Berth position to assign cranes on order
      Add MyJob to JobQ                            //moves selected Job into general JobQ
   MyJob = MyJob.Successor(MyShip.JobQ)            //selects next job in ship's JobQ
```

SelectShip, a function of Berth class

```
Repeat                                  }  Ship can be selected when
   MyShip = ShipQ.FirstElement          }  berth's draft exceeds the draft
   Repeat(while MyShip is not nil)      }  needed for newly arrived ship
```

If MyShip.Draft <= Draft Result = MyShip Exit MyShip = MyShip.Successor(ShipQ) Result = nil	Ship can be selected when berth's draft exceeds the draft needed for newly arrived ship

Table D.28: Element class: Machine

An extra function was developed for the machine element class; AssignCranes. In this algorithm cranes are assigned to berthed ships that enables the determination of the needed time for ship serving and thus for transporting and stacking. In Table D.28, the AssignCranes algorithm is described.

Extra attributes of machine class	**Description**
MyJob, AssignJob	Reference to Job
JobsToAssignQ	Queue containing jobs that need a crane, sorted on PosX
NrCranesToJob	The number of cranes to be assigned to Job
CranesToAssignQ	Queue containing cranes to be assigned, sorted on Order
UnloadingProgress	Function to serve ships by determining the capacity per time interval Δt. The capacity depends on the sum of the crane(s) capacity, the sum of the transport routes and the unloading stage. This is comparable to the process of the crane class which was already introduced in Table D.7. (Result = True when MyJob.MyTons <= 0)
Addition to Process of Machine class	
In stead of Hold(MyJob.MyTons / Capacity) for seaside jobs in Transport network model: Standby(while (UnloadingProgress = False) and (MyJob.SeaJob = True)) //when ship is empty UnloadingProgress is set True	
AssignCranes, a function of Machine class	

```
MyJob = ActiveJobsQ.FirstElement //jobs that are serviced are in this queue to spread cranes over the ships
Repeat(ActiveJobsQ.Length)                    //repeats for number of active jobs
  MyCrane = MyJob.MyCQ.FirstElement           //selects first job's it's first assigned crane
  Repeat(MyJob.MyCQ.Length)                   //repeats for number of cranes assigned to job
    Remove MyCrane from MyJob.MyCQ            //remove active cranes from active job to be sorted again
    If MyJob.MyCQ.Length > 0                  //if there is another r crane assigned to job
      MyCrane = MyJob.MyCQ.FirstElement       //selects the first crane
    MyJob AddSortedOn MyJob.PosX to JobsToAssignQ //put job sorted on geog.position in JobsToAssignQ
  MyJob = MyJob.Successor(ActiveJobsQ)        //selects next job in ActiveJobsQ

MyCrane = CranesQ.FirstElement                //selects first crane in cranes queue
Repeat(CranesQ.Length)                        //repeat for number of cranes
  Add MyCrane to CranesToAssignQ              //places cranes in CranesToAssignQ
  MyCrane = MyCrane.Successor(CranesQ)        //selects next crane in cranes queue


Repeat(while JobsToAssignQ.Length >0)         //repeats for number of jobs to assign
  AssignJob = JobsToAssignQ.FirstElement      //selects the first job in this queue
  NrCranesToJob = (CranesToAssignQ.Length + 1) – JobsToAssignQ.Length  //distribute cranes over jobs
  If NrCranesToJob > AssignJob.MaxNrCranes
    NrCranesToJob = AssignJob.MaxNrCranes     //do not assign more cranes than max. per ship
  Repeat(NrCranesToJob)
    MyCrane = CranesToAssignQ.FirstElement    //selects first crane
    MyCrane AddSortedOn MyCrane.Order to AssignJob.MyCQ   //puts crane in JobsToAssignQ
    MyCrane.PosX = AssignJob.PosX             //determines x-coordinate crane
    Remove MyCrane from CranesToAssignQ       //crane is re-assigned
  Remove AssignJob from JobsToAssignQ         //job gets crane(s)
```

The interactions between the several activities are realized with commands (e.g., standby, hold, suspend, resume and proceed), which are mentioned on several places in the tables in this section. In Figure D.6, an example of the trace function from TOMAS is displayed. The hold command is used. During the hold-time, which represents the ship servicing for one hour, other processes from different simulation elements become active.

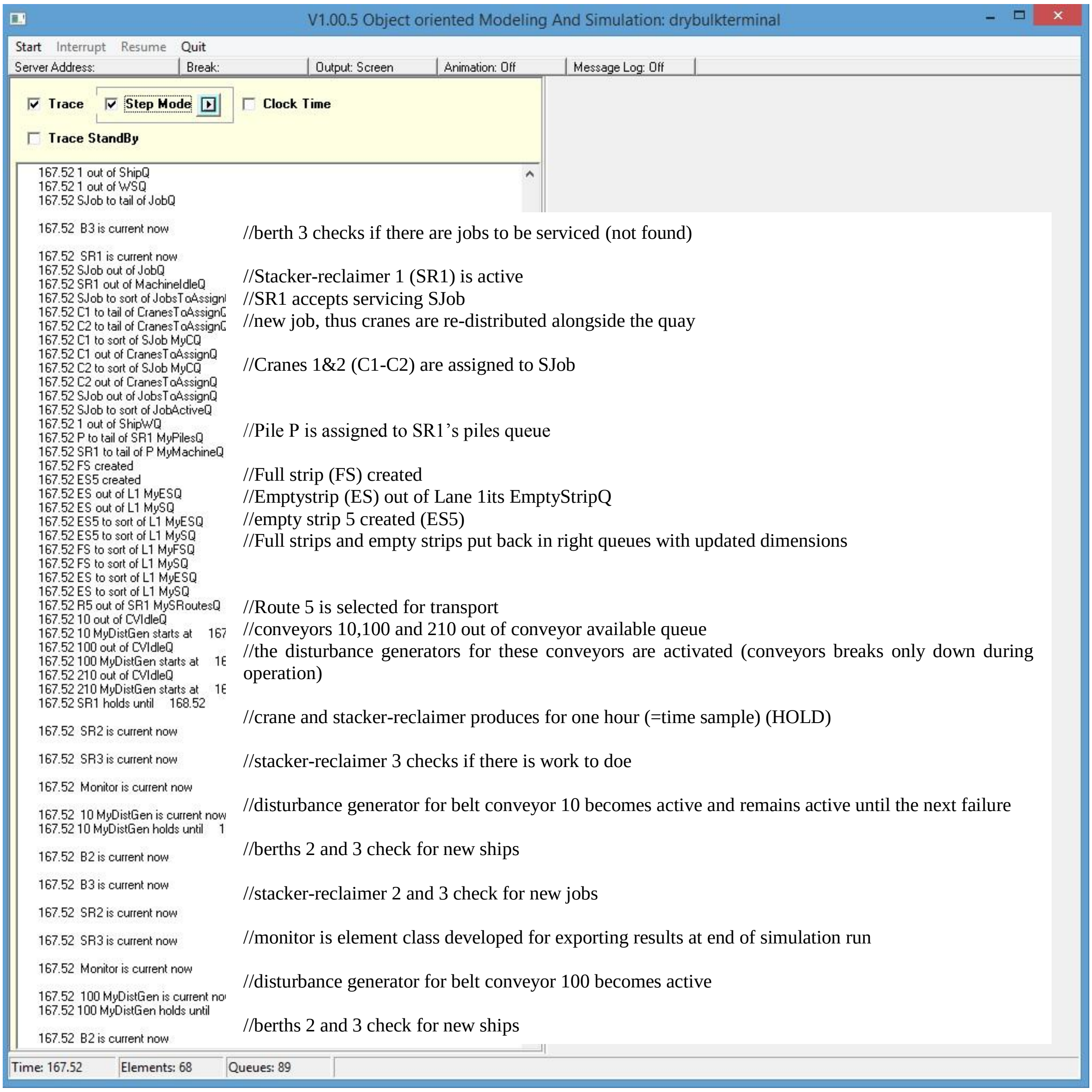

Figure D.6: Screenshot of the trace function of TOMAS for an arbitrary time of 167.52 hour

E. The effective reclaiming utilization

Due to the fact that different values were proposed for the effective reclaiming utilization (see section 6.2), this utilization will be determined analytically. The effective reclaiming utilization relates to many parameters such as the reclaiming method, the sloping face of the pile, the acceleration and deceleration of slewing and travelling motions, the time needed to luff the boom to reclaim the next layer, the bulk material properties, etc. In this appendix two generally applied reclaiming methods will be investigated (section E.1), followed by the calculation of the reclaiming capacity per slewing motion (section E.2) and ends with the determination of the effective reclaiming utilization for both reclaiming methods (section E.3).

E.1 Long-travel and slewing bench reclaiming method

The long-travel reclaiming method is based on the travelling motion of the bucket wheel reclaimer. Figure E.1 shows schematically the long-travel reclaiming method during two stages. The bucket wheel is brought into the pile and the machine travels alongside the pile with a rotating bucket wheel. At the end of the pile, the position of the bucket wheel is adjusted and the machine travels back.

The average reclaiming capacity during the long-travel reclaiming method depends largely on the travelling speed of the reclaimer and the maximum digging capacity of the bucket wheel. At the beginning of the pile, the machine accelerates and realizes a more or less constant reclaiming capacity until the machine decelerates at the end of the pile.

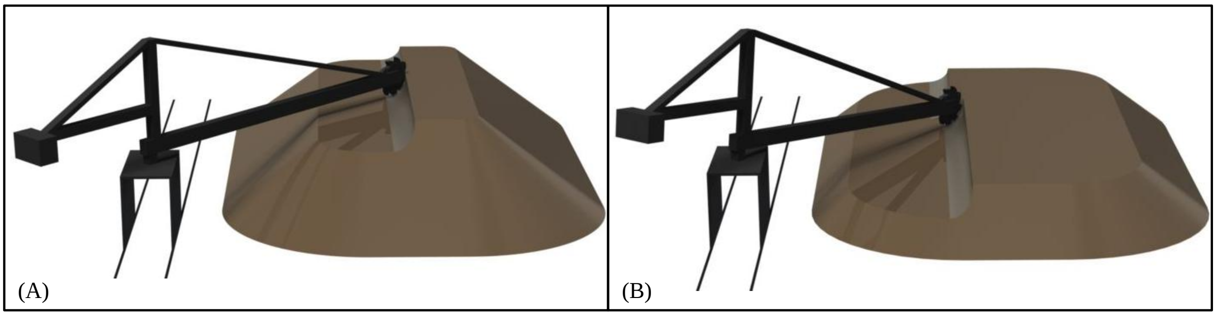

Figure E.1: Two stages during reclaiming for the long-travel reclaiming method

Another reclaiming method is the slewing bench reclaiming method, shown for two stages in Figure E.2. The boom of the reclaimer performs periodical crescent-type slewing motions and the machine steps forward at the end of the slewing motion. The pile is divided in vertical benches and bench for bench the pile is reclaimed. When a bench is reclaimed completely, the machine travels back and starts reclaiming the next bench. The net reclaiming capacity varies significantly for this reclaiming method. For each slewing movement the boom has to be accelerated and decelerated. The slewing radius relates to pile dimensions and the reclaiming stage.

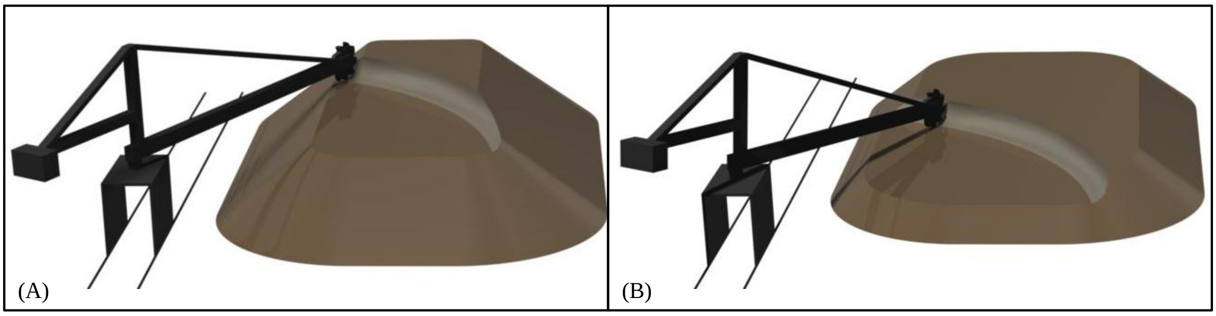

Figure E.2: Two stages during reclaiming for the slewing bench reclaiming method

E.2 Determination of the reclaiming capacity per slewing motion

To determine the effective reclaiming utilization, the reclaiming capacity for a single crescent-type slewing motion must be investigated. Due to the bucket wheel rotational motion, a cutting line with a radius (r_{bw}) [m] develops (see Figure E.3B). After setting the new chip thickness (Δx [m]), a second cutting line emerges so that a crescent-shaped area develops between these cutting lines. This slice cross-sectional area can be replaced by a rectangle (Schneidersmann, 1977). Equation (E.1) shows this assumption algebraically.

$$A_s(\theta) = h_s \Delta r(\theta) \tag{E.1}$$

Where $A_s(\theta)$ [m^2] is the slice cross-sectional area, h_s [m] is the slice height and $\Delta r(\theta)$ [m] is the chip thickness as function of the boom's slewing angle θ [rad].

The chip volume is further created by the rotary motion of the bucket wheel (ω_r) [rad/min] overlapping the boom's slewing motion (ω_s) [rad/min]. In the top view (see Figure E.3A) the chip volume is developed between the intersection circles around the slewing midpoints M and M'.

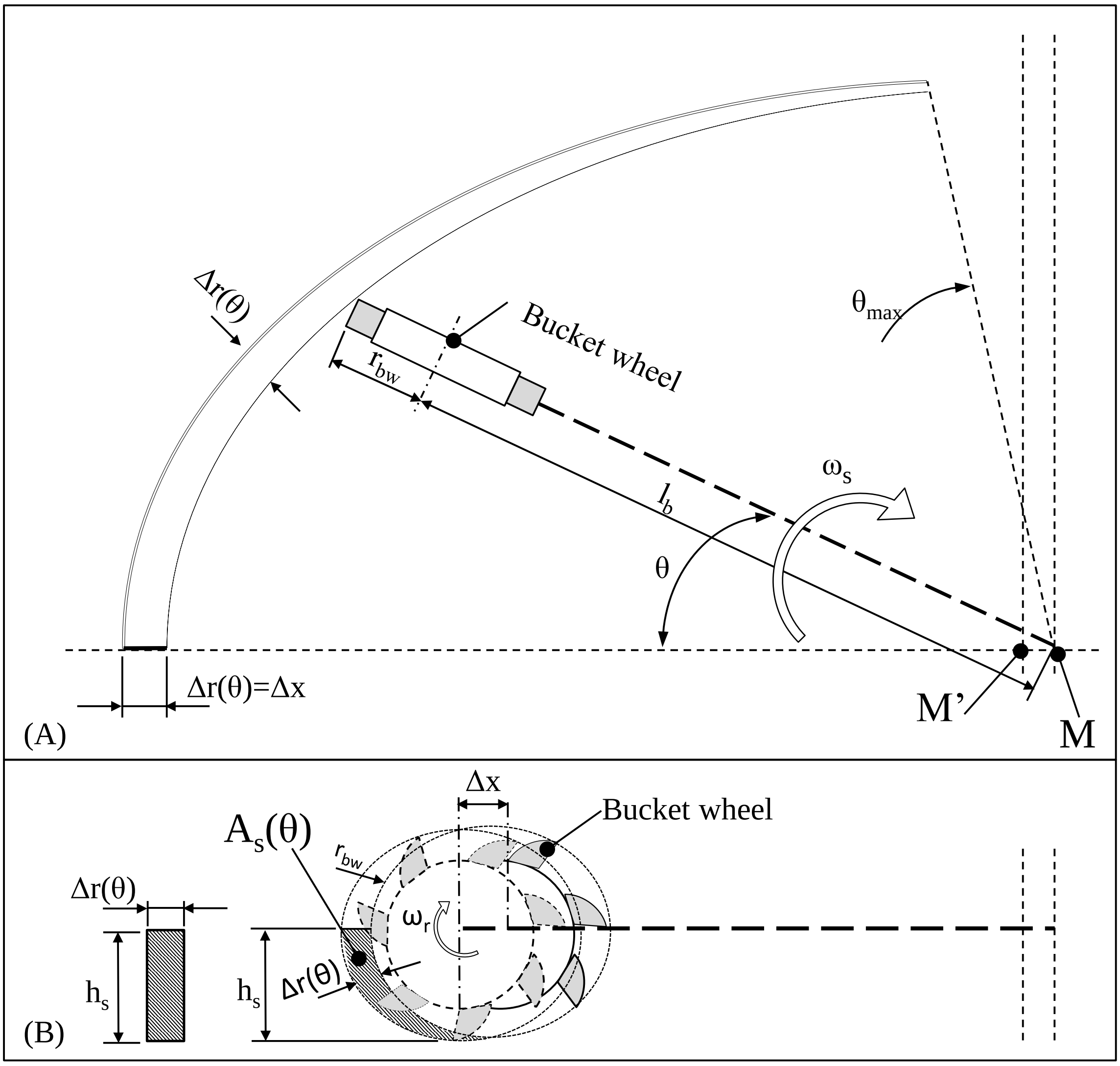

Figure E.3: Determination of the slice cross-sectional area ($A_s(\theta)$) in the top view (A) and in the view perpendicular to the bucket wheel (B)

From Figure E.3A can be derived that the maximum value for the chip thickness is reached at θ = 0° and that the chip thickness decreases almost to zero when the slewing angle reaches its maximum value. Oyler (1977) and Knappe (1995) mentioned that in practice it is customary to limit the slewing angle to about 75°. The following equation describes the chip thickness as function of the slewing angle.

$$\Delta r(\theta) = \Delta x \cos(\theta) \tag{E.2}$$

Where Δr(θ) [m] is the chip thickness as function of the boom's slewing angle (θ) [rad] and Δx [m] is the maximum chip thickness introduced by the machine's movement alongside the pile.

The reclaiming capacity can now be determined by multiplying the slice cross-sectional area with the slewing speed (both related to the slewing angle) and the bulk density. Equation (E.3) shows this relation algebraically:

$$Q_r = A_s(\theta)v(\theta)\rho_m \tag{E.3}$$

Where Q_r is the reclaiming capacity [t/h], $A_s(\theta)$ [m^2] is the slice cross-sectional area as function of the slewing angle (θ) [rad], $v(\theta)$ [m/s] is the slewing speed as function of the slewing angle and (ρ_m) is the material's bulk density [t/m^3].

The slice cross-sectional area reduces when the slewing angle increases. To compensate the reduction in reclaiming capacity, the slewing speed can be increased for increasing values of the slewing angle. The slewing speed at a specific slewing angle relates to the start slewing speed and can be determined using equation (E.4):

$$v(\theta) = \frac{v_s}{\cos(\theta)} \quad \forall\, v(\theta) \le v_{\max} \tag{E.4}$$

Where $v(\theta)$ [m/s] is the slewing speed as function of the slewing angle and v_s [m/s] is the start slewing speed after acceleration. Equation (E.4) is only valid when the slewing speed does not exceed the maximum slewing speed v_{max} [m/s], which is in practice limited by the slewing drive system.

The slewing speed relates to the slewing rotational speed ω_s [rad/min], the machine's boom length and the bucket wheel radius. Values for the minimum and maximum slewing rotational speeds are listed in technical specifications of bucket wheel reclaimers. The relation for the slewing rotational speed as function of the slewing angle can be expressed with the following equation:

$$v(\theta) = \frac{\omega_{ss}(\theta)}{\cos(\theta)}\left(l_b + r_{bw}\right) \quad \forall\, \varpi_s \le \varpi_{sm} \tag{E.5}$$

Where $v(\theta)$ [m/s] is the slewing speed as function of the slewing angle, ω_{ss} [rad/min] is the minimum slewing rotational speed, l_b [m] is the boom length and r_{bw} [m] is the radius of the bucket wheel. The actual slewing rotational speed cannot exceed the machine's maximum slewing rotational speed (ω_{sm}) [rad/min]. Finally, for the reclaiming capacity without slewing speed adjustment equation (E.6) was derived and equation (E.7) shows the relation for the reclaiming capacity with slewing speed adjustment.

$$Q_r = \left(h_s \Delta x \cos(\theta)\right)\omega_{ss}\left(l_b + r_{bw}\right)\rho_m \tag{E.6}$$

$$Q_r = \left(h_s \Delta x\right)\omega_{ss}\left(l_b + r_{bw}\right)\rho_m \quad \forall\, \varpi_s \le \varpi_{sm} \tag{E.7}$$

Oyler (1977) proposed that most common dry bulk materials a slice height (h_s) of about 45% of the bucket wheel diameter can be reached for. Liyimin, (1988) proposed that the maximum chip thickness (Δx) relates to material properties and varies generally between 0.3 and 1 meter.

For a case, the reclaiming capacity per slewing motion is determined as function of slewing speed adjustment. Table E.1 lists the used input parameters for this case.

Table E.1: Input parameters to determine the reclaiming capacity for one slewing motion

Parameter	Value	Unit	Parameter	Value	Unit
h_s	4.5	[m]	r_{bw}	4.5	[m]
Δx	1	[m]	ω_{ss}	0.145	[rad/min]
ρ_m	0.8	[t/m^3]	ω_{sm}	0.58	[rad/min]
l_b	60	[m]	a_s[1]	0.5	[rad/min^2]

[1]was defined as the maximum acceleration and deceleration of the slewing motion

The reclaiming capacities determined versus the slewing angles are shown in Figure E.4. For an easier understanding the slewing angle is shown in this figure in degrees. For this case, the slewing angle was varied between 0° and 90°. The machine's boom accelerates and decelerates with the maximum slewing acceleration and deceleration respectively. It was assumed that the slewing rotational speed increases and decreases linearly during acceleration and deceleration. The reclaiming capacity reaches its maximum value when the boom is accelerated. When the slewing rotational speed is kept constant during slewing the reclaiming capacity decreases for increasing values of the slewing angle (see Figure E.4A). When the slewing rotational speed is increased a constant reclaiming capacity can be realized (see Figure E.4B).

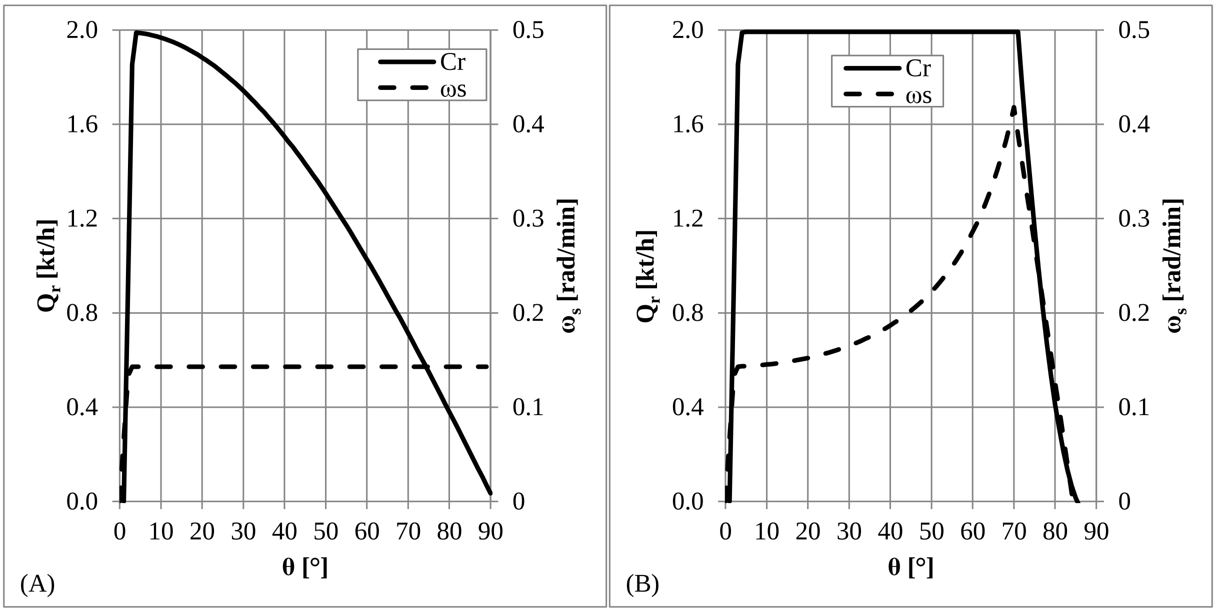

Figure E.4: Reclaiming capacities and slewing rotational speeds versus the slewing angle for a case without slewing speed adjustment (A) and a case with slewing speed adjustment (B)

E.3 Determination of the effective reclaiming utilization

For both presented reclaiming methods the effective reclaiming utilization will be determined by registering the needed reclaiming time for a specific pile. The input parameters of Table E.1 are used and in Table E.2 the extra parameters used are listed. These extra parameters define the pile geometry and the travelling motion during the long-travel reclaiming method.

Table E.2: Extra parameters used for the determination of the effective reclaiming utilization

Parameter	Description	Value	Unit
l_t	Pile length	325	[m]
w	Pile width	50	[m]
h	Pile height	18	[m]
α	Angle of repose	38	[°]
v_t	Travelling speed	10	[m/min]
a_t	Travel acceleration and deceleration	0.15	[m/min^2]

Figure E.5 shows the reclaiming capacities determined during an arbitrary time interval of 40 minutes for both reclaiming methods. For the long-travel reclaiming method, only at the end of a travelling movement when the bucket wheel reclaimer has to reverse, some reclaiming time is lost which leads to a drop of the average reclaiming capacity. For this case, an effective reclaiming utilization of 0.78 was reached.

From Figure E.5 can be concluded that for the slewing bench reclaiming method the reclaiming capacity fluctuates significantly. The time needed to set the new chip thickness was assumed to be 30 seconds. The net reclaiming capacity over the entire pile was 0.9 [kt/h] and together with the maximum capacity of 2 [kt/h] the effective reclaiming utilization becomes 0.45.

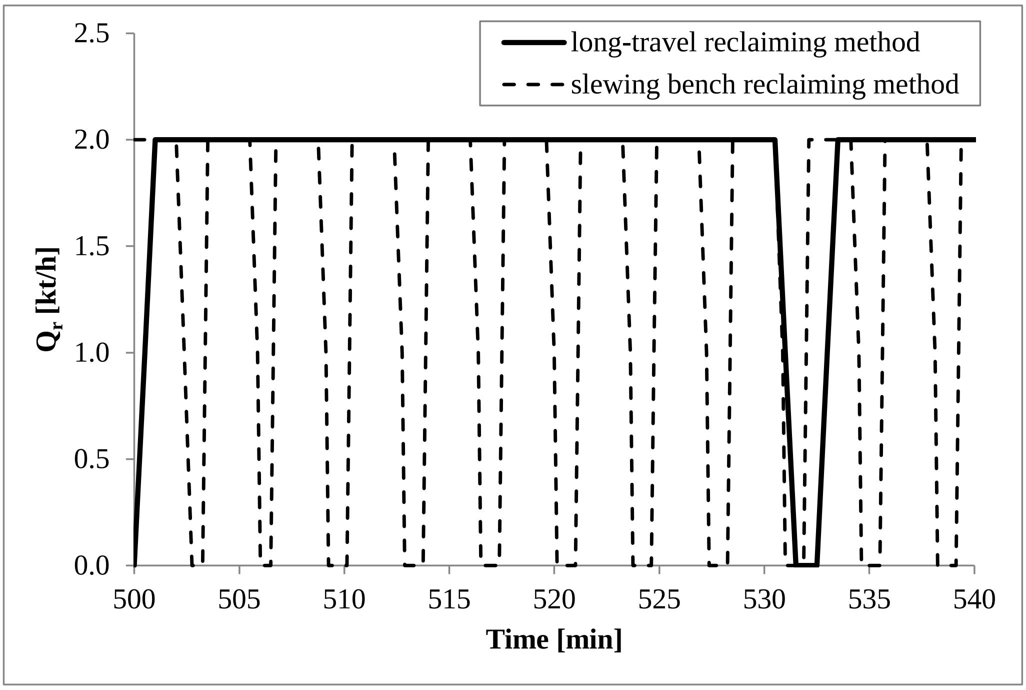

Figure E.5: Reclaiming capacities during an arbitrary time interval for both investigated reclaiming methods

For the long-travel reclaiming method the effective reclaiming utilization relates to the pile length. For longer piles the percentage of time that the reclaiming capacity drops decreases. To investigate the impact of the pile length on the effective reclaiming utilization, the pile length was varied between 50 and 350 meter. Figure E.6 shows the net reclaiming capacities needed ($Q_{r\text{-}net}$) to reclaim the entire pile versus the pile lengths. As expected, the effective reclaiming utilization decreases substantially for shorter piles. For long piles the effective reclaiming utilization can reach a value of 0.8 but for piles with short lengths the utilization can even be reduced until 0.4.

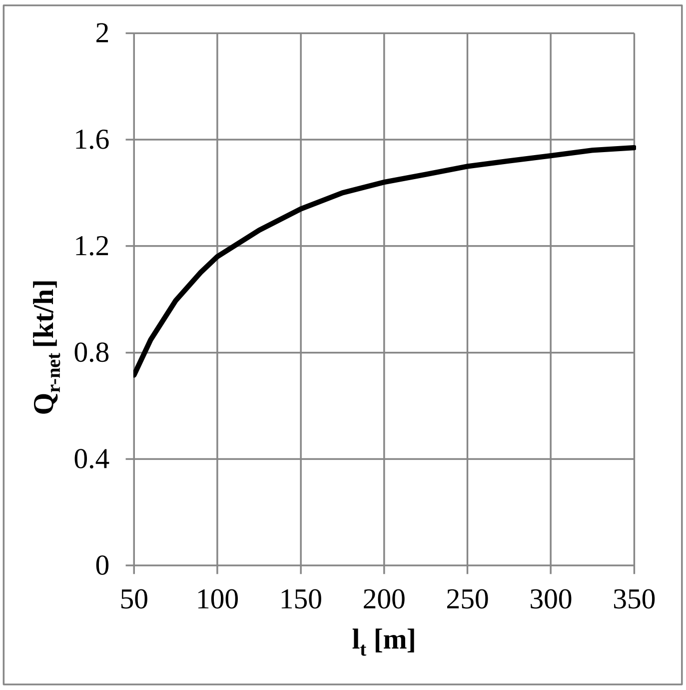

Figure E.6: Net reclaiming capacity over the entire pile versus the pile length for the long-travel reclaiming method

F. Investment costs determination

Stockyard machines manufactures and belt conveyor systems suppliers do not want to share their selling prices. That's why it was assumed that the machine's weight relates to the machine's investment cost. In this appendix, relations will be derived to determine the weight of stockyard machines. For belt conveyor systems, the investment costs will be based on the limited number of quotations from belt conveyor system suppliers.

F.1 Stockyard machine weight

From 75 stockyard machines (stackers, bucket wheel reclaimers and bucket wheel stacker-reclaimers) the machines weight, the boom length and the stacking and/or reclaiming capacity were gathered. From several sources like Wöhlbier (1977) and brochures from several manufactures (Tenova Takraf, ThyssenKrupp, Ameco and DeYing) these machine characteristics were collected. However, variation in the data was recovered due to the fact that this data comes from several manufactures and covers details of machines which were manufactured during several decades. Almost each machine has its specific boom length but some preferred boom lengths with a minimum variation can be recognized as well. Figure F.1 shows for bucket wheel stacker-reclaimers (A) and for bucket wheel reclaimers (B) the machines weight versus the machines capacity grouped for comparable values for the boom length. Note that the capacity of a stacker-reclaimer is the sum of the stacking and the reclaiming capacity.

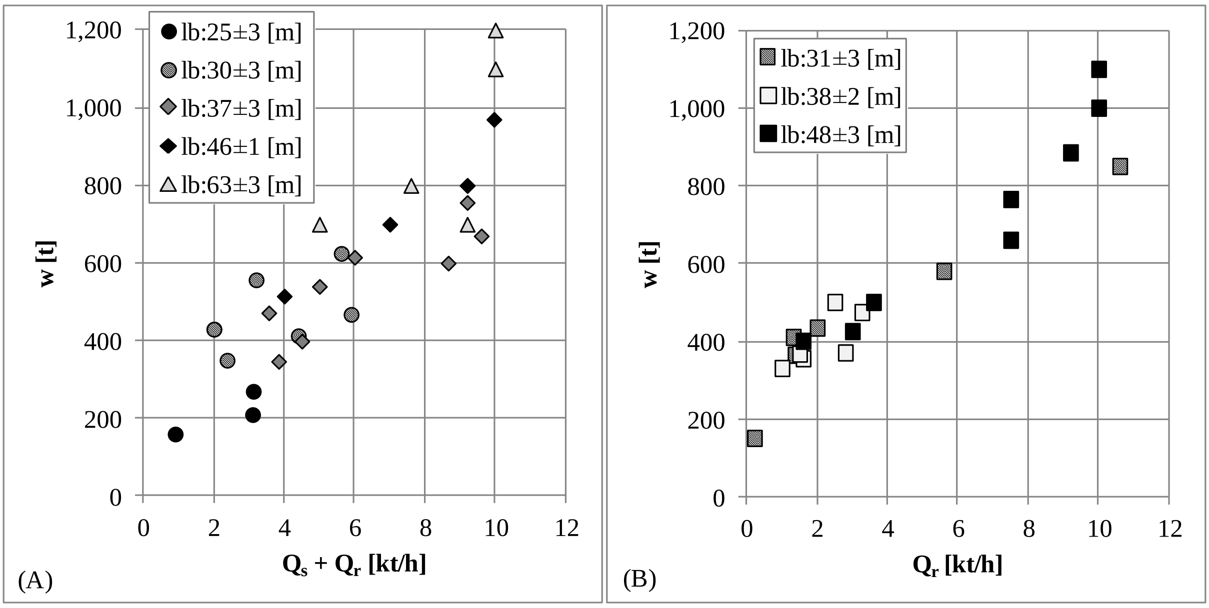

Figure F.1: Weight of the stockyard machine versus its capacity grouped for different boom lengths (average length ± limits); (A) bucket wheel stacker-reclaimers and (B) bucket wheel reclaimers

Despite the variation shown in Figure F.1 it is plausible to argue that the machine's weight relates to its capacity and to a minor extent to the boom length. For this research it was assumed that the machine weight relates to the product of the total capacity installed and the boom's length. For the investigated machines the weight was plotted versus the product defined and shown in Figure F.2.

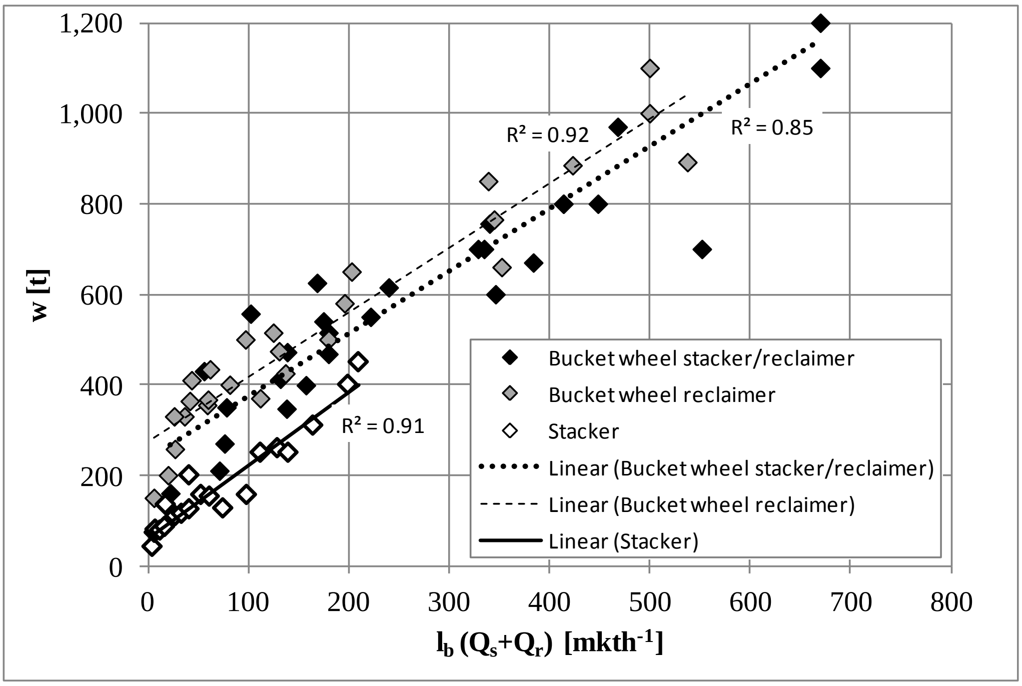

Figure F.2: Weight of stockyard machines versus the product of the boom length and machine's capacity

From the data points as shown in Figure F.2, relations between the stockyard machine's weight and the product of the boom length and capacity were derived using linear trend lines. Equation (6.6) describes the relations for these trend lines and this equation can be used to determine the machine's weight as function of boom length and capacity.

Note that despite the relatively high values for the correlation coefficients, which are shown in Figure F.2, these trend lines are based on historical data. It is recommeded to request machine manufactures for an up-to-date information to make the right selection for a real-world case. Finally, the stockyard machine investment costs can be determined by assuming a certain price per machine's weight. Several experts in the field of dry bulk terminal engineering use the following rule-of-thumb to estimate the stockyard machine's investment cost: a machine fully installed at the stockyard costs 6-8 times more in Euros than the machine's weight in kilograms.

F.2 Belt conveyor investment cost

Like it is the case for stockyard machines, it is expected that the investment cost for belt conveyors will increase when the transportation capacity will increase. As already mentioned in section 6.4.1 there is no model found that describes selling prices for belt conveyor systems as function of the transportation capacity. Belt conveyor system suppliers don't like to share their selling prices. Only a limited number of quotations were received where the investment costs per running meter could be derived from. The investment costs include the drive unit, the belt, idler sets, stringers and tensioning unit but exclude the civil works, sidewalks, covers, etc.

Only for six belt conveyor systems with a length between the 1 and 1.5 kilometer selling prices were provided. Yard belt conveyors, which are connected to stockyard machines, have normally this length. From these quotations the prices per meter were determined; values are shown as data points in Figure F.3. As it can be seen from this figure the prices per meter versus the transportation rate vary considerably. An upper and a lower limit were defined which will probably limit the maximum and minimum price per running meter versus the transportation capacity for troughed belt conveyors. Note that both limits were not validated due to the lack of real world data. The belt conveyor investment costs can be calculated by multiplying the total conveyor length with the price per running meter.

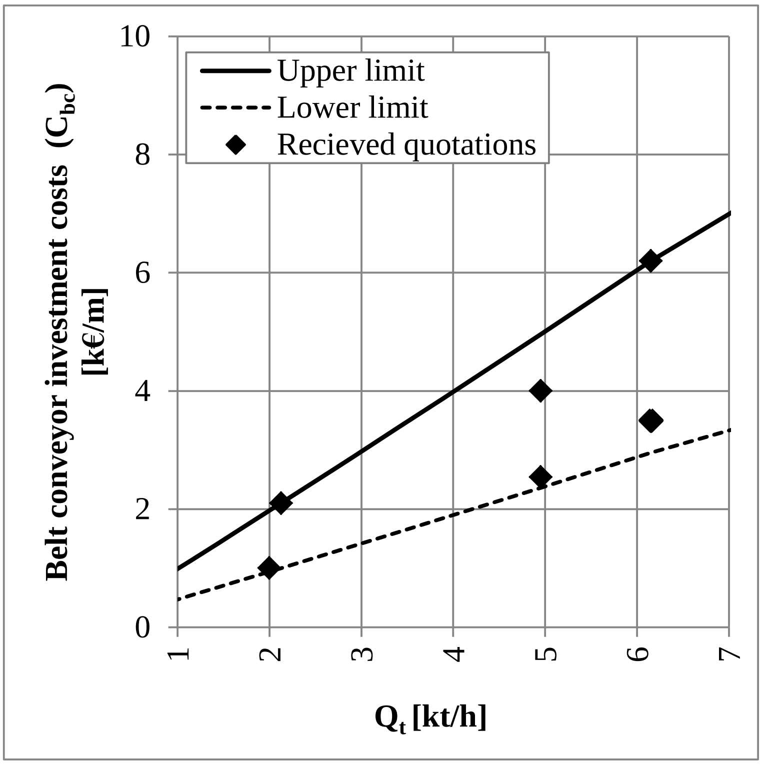

Figure F.3: Price per running meter for belt conveyor systems versus the transportation capacity for total lengths between 1 and 1.5 [km]

G. Validation data

The arrival data from 897 ships at terminal T2 was used to compose an input file for the validation study of the total terminal model. Table G.1 lists the ship number, the delivered shipload, the arrival time (relatively to the first ship in this dataset), the total storage time (T_s) of the shipload and the delivered material type.

Table G.1: Ship arrival data used for the validation of the terminal simulation model

ShipNr.	Shipload [t]	Arrival time [h]	T_s [h]	Material	ShipNr.	Shipload [t]	Arrival time [h]	T_s [h]	Material
1	108,280	0.0	1530	Coal	450	164,134	12503.8	3416	Coal
2	34,152	51.1	100	Iron Ore	451	8,706	12576.5	1684	Coal
3	136,473	70.4	756	Iron Ore	452	164,999	12603.6	3313	Coal
4	33,550	111.8	2612	Iron Ore	453	70,407	12639.9	695	Coal
5	72,139	113.1	2787	Coal	454	40,500	12690.3	439	Coal
6	69,674	157.1	1586	Coal	455	70,442	12806.3	5972	Coal
7	51,184	158.1	1236	Coal	456	36,111	12840.5	122	Coal
8	29,634	174.7	2498	Coal	457	90,558	12843.6	3998	Coal
9	41,186	188.7	1503	Coal	458	173,718	12964.1	4407	Coal
10	176,445	218.1	1286	Coal	459	39,076	12976.5	300	Iron Ore
11	76,959	247.3	1121	Iron Ore	460	49,990	13102.3	2113	Coal
12	4,650	251.7	1585	Coal	461	146,110	13113.3	3715	Coal
13	143,310	273.8	1114	Iron Ore	462	75,778	13272.8	6380	Coal
14	41,000	321.5	2752	Coal	463	40,255	13285.0	2002	Coal
15	168,806	337.0	1194	Coal	464	175,336	13297.8	1313	Coal
16	38,977	391.8	723	Coal	465	55,546	13366.6	4546	Coal
17	9,070	410.7	11114	Iron Ore	466	21,600	13401.6	250	Iron Ore
18	73,890	413.9	6666	Iron Ore	467	72,279	13486.0	2718	Coal
19	72,958	443.9	1310	Coal	468	72,688	13498.7	1691	Coal
20	50,000	459.4	8332	Iron Ore	469	87,651	13584.6	4116	Iron Ore
21	88,000	480.3	960	Coal	470	44,455	13586.7	5158	Coal
22	71,025	486.2	642	Coal	471	17,368	13652.0	234	Coal
23	144,451	517.3	1240	Coal	472	74,402	13682.3	5067	Coal
24	58,295	521.9	1805	Coal	473	175,358	13686.4	1726	Coal

ShipNr.	Shipload [t]	Arrival time [h]	T_s [h]	Material	ShipNr.	Shipload [t]	Arrival time [h]	T_s [h]	Material
25	170,723	541.4	4570	Iron Ore	474	138,103	13710.8	1000	Iron Ore
26	163,200	566.7	3652	Iron Ore	475	18,676	13721.5	5663	Coal
27	148,102	591.5	1327	Coal	476	189,870	13749.3	1846	Coal
28	95,051	631.3	1429	Iron Ore	477	169,426	13776.6	2785	Coal
29	177,840	661.3	1066	Iron Ore	478	104,700	13784.8	1523	Coal
30	74,144	710.4	1066	Iron Ore	479	75,153	13813.2	4557	Coal
31	151,881	755.3	925	Coal	480	51,813	13845.3	2574	Coal
32	250,010	781.2	1594	Iron Ore	481	45,000	13858.6	2104	Iron Ore
33	134,847	843.6	2124	Iron Ore	482	162,117	13870.8	3103	Coal
34	163,113	856.3	255	Coal	483	67,307	13883.3	1961	Coal
35	145,660	891.5	3369	Iron Ore	484	67,523	14034.9	7023	Coal
36	145,643	927.9	4054	Coal	485	44,027	14055.0	88	Coal
37	67,535	951.3	1344	Iron Ore	486	40,000	14069.8	132	Coal
38	173,926	966.3	2471	Iron Ore	487	174,722	14146.2	2716	Coal
39	223,688	1001.9	479	Coal	488	27,500	14171.8	250	Iron Ore
40	40,000	1042.6	11973	Iron Ore	489	72,414	14215.1	3303	Coal
41	79,700	1060.4	853	Iron Ore	490	120,314	14283.7	1165	Coal
42	37,508	1064.8	1292	Iron Ore	491	58,178	14292.2	2252	Iron Ore
43	50,000	1114.3	644	Coal	492	50,520	14292.8	1180	Iron Ore
44	70,609	1125.8	1448	Coal	493	25,087	14316.6	250	Iron Ore
45	69,263	1192.9	772	Coal	494	30,000	14329.8	105	Coal
46	252,694	1239.2	1645	Iron Ore	495	72,534	14335.3	1427	Coal
47	43,000	1241.2	1836	Iron Ore	496	34,000	14345.2	3592	Iron Ore
48	71,193	1291.5	2290	Iron Ore	497	156,246	14357.3	795	Coal
49	72,955	1299.9	2976	Coal	498	76,999	14377.9	4763	Iron Ore
50	161,603	1354.9	637	Coal	499	36,083	14417.6	1224	Coal
51	41,379	1380.8	2272	Iron Ore	500	52,528	14447.6	1420	Iron Ore
52	73,552	1383.2	3444	Coal	501	61,870	14482.7	3251	Coal
53	160,210	1399.7	770	Coal	502	36,929	14518.7	4211	Iron Ore
54	32,219	1409.9	25	Coal	503	69,141	14584.4	8274	Coal
55	5,740	1409.9	25	Coal	504	77,196	14603.5	3466	Coal
56	2,907	1417.9	25	Coal	505	20,258	14614.3	1364	Coal
57	1,333	1428.6	2781	Iron Ore	506	73,750	14659.8	1130	Coal
58	70,767	1483.0	23212	Coal	507	159,858	14674.8	4568	Coal
59	147,223	1610.4	1229	Iron Ore	508	80,729	14677.3	1000	Iron Ore
60	163,707	1613.9	1227	Coal	509	20,650	14742.2	250	Iron Ore
61	25,532	1649.9	79	Coal	510	26,530	14757.2	1852	Coal
62	34,650	1654.3	1759	Coal	511	144,743	14763.5	2708	Coal
63	69,705	1662.6	1698	Coal	512	67,516	14775.8	2313	Coal
64	162,916	1685.3	2028	Coal	513	36,940	14788.5	788	Coal
65	170,258	1690.8	2887	Coal	514	108,698	14798.1	4815	Coal
66	283,151	1697.8	646	Coal	515	75,165	14817.2	2140	Coal
67	55,940	1719.4	3088	Iron Ore	516	30,150	14847.1	250	Iron Ore
68	41,508	1747.9	623	Coal	517	76,493	14874.3	678	Coal
69	40,000	1750.8	2394	Iron Ore	518	67,510	14883.0	9445	Iron Ore
70	163,216	1764.2	2400	Iron Ore	519	46,042	14890.6	500	Iron Ore
71	150,279	1864.4	1187	Coal	520	26,241	14904.3	250	Iron Ore
72	67,695	1904.9	10358	Iron Ore	521	170,482	14940.7	2558	Coal
73	147,670	1922.4	3553	Coal	522	58,524	14949.8	741	Coal
74	62,400	1948.5	1873	Coal	523	18,743	14962.4	151	Coal
75	103,897	1969.8	1926	Coal	524	203,507	15027.8	1046	Coal
76	81,905	2009.7	1423	Iron Ore	525	71,890	15060.8	1651	Coal
77	43,961	2037.7	821	Iron Ore	526	75,845	15068.7	1299	Coal
78	247,363	2058.3	2351	Iron Ore	527	54,699	15072.7	25	Coal
79	165,757	2083.6	1264	Coal	528	22,237	15115.8	25	Coal
80	45,750	2086.3	1735	Iron Ore	529	115,101	15150.9	10227	Iron Ore
81	174,211	2125.4	401	Coal	530	161,971	15230.3	12084	Iron Ore
82	41,549	2155.1	11857	Iron Ore	531	104,750	15252.2	1023	Iron Ore
83	89,827	2194.3	430	Coal	532	70,280	15382.5	2089	Coal
84	81,724	2213.0	1262	Coal	533	39,286	15389.5	3461	Coal
85	70,768	2231.5	1051	Coal	534	49,456	15390.6	250	Iron Ore
86	44,450	2268.5	857	Coal	535	82,500	15427.3	12919	Coal
87	137,498	2304.0	1075	Iron Ore	536	69,117	15443.5	6219	Coal
88	139,252	2309.2	594	Coal	537	248,416	15449.0	8882	Coal
89	57,176	2322.0	1075	Iron Ore	538	172,601	15464.6	1714	Coal

ShipNr.	Shipload [t]	Arrival time [h]	T_s [h]	Material	ShipNr.	Shipload [t]	Arrival time [h]	T_s [h]	Material
90	201,556	2343.8	3004	Iron Ore	539	36,489	15486.5	9730	Coal
91	147,309	2358.0	1517	Coal	540	169,770	15501.6	1113	Coal
92	60,500	2400.8	922	Coal	541	68,186	15535.0	3766	Coal
93	135,708	2447.4	1660	Iron Ore	542	57,531	15550.2	5928	Iron Ore
94	167,854	2474.3	1619	Coal	543	172,304	15569.7	3066	Iron Ore
95	42,745	2523.6	820	Iron Ore	544	72,619	15604.1	5785	Coal
96	114,375	2569.3	448	Coal	545	29,493	15646.6	1682	Coal
97	144,887	2594.7	1581	Iron Ore	546	145,864	15666.4	203	Coal
98	92,596	2629.3	1578	Coal	547	164,824	15672.8	1293	Iron Ore
99	93,829	2692.2	1495	Coal	548	73,216	15689.3	3637	Coal
100	90,814	2694.4	1506	Coal	549	227,155	15705.5	2080	Coal
101	182,590	2705.3	1284	Coal	550	72,500	15724.7	1099	Coal
102	163,852	2725.1	2181	Iron Ore	551	168,317	15807.8	1768	Coal
103	74,545	2744.3	1256	Coal	552	163,641	15811.3	250	Iron Ore
104	165,013	2769.9	2336	Coal	553	21,485	15844.6	561	Coal
105	46,290	2815.7	1676	Coal	554	40,176	15845.6	950	Coal
106	70,001	2820.3	1561	Iron Ore	555	35,000	15858.4	4141	Iron Ore
107	104,021	2841.3	142	Iron Ore	556	176,010	15885.2	2205	Coal
108	80,350	2868.5	2121	Iron Ore	557	68,075	15919.2	250	Iron Ore
109	40,000	2881.9	550	Iron Ore	558	167,327	15962.7	1792	Coal
110	39,755	2895.8	1066	Coal	559	50,000	15969.2	3472	Coal
111	34,762	2901.2	2975	Coal	560	102,800	15980.7	1866	Coal
112	148,373	2929.8	1351	Coal	561	293,478	16046.1	2679	Coal
113	167,445	2939.5	504	Iron Ore	562	73,262	16058.0	2813	Coal
114	80,193	2946.2	1746	Coal	563	42,525	16071.5	1343	Coal
115	41,054	2989.4	3507	Coal	564	173,228	16103.9	1965	Coal
116	71,581	2994.4	3594	Coal	565	31,200	16153.8	84	Coal
117	71,624	2997.2	1541	Coal	566	134,623	16195.0	837	Coal
118	191,101	3027.5	1519	Coal	567	71,300	16197.8	6238	Iron Ore
119	38,266	3090.9	98	Iron Ore	568	73,522	16205.0	4288	Coal
120	51,842	3104.7	1652	Iron Ore	569	166,597	16268.6	2605	Iron Ore
121	167,480	3118.8	2121	Iron Ore	570	72,555	16293.2	1188	Iron Ore
122	172,077	3121.0	6255	Coal	571	161,278	16360.0	1000	Iron Ore
123	157,401	3143.7	10	Coal	572	170,477	16408.7	866	Coal
124	40,000	3190.1	3282	Iron Ore	573	38,925	16415.0	2280	Iron Ore
125	59,538	3233.5	899	Coal	574	76,990	16526.8	100	Iron Ore
126	73,100	3309.7	1542	Coal	575	54,879	16546.0	3551	Iron Ore
127	113,223	3312.6	1581	Coal	576	155,485	16557.6	2827	Coal
128	4,005	3330.6	6272	Iron Ore	577	70,300	16597.0	915	Coal
129	60,892	3356.5	2661	Coal	578	70,757	16626.3	6878	Coal
130	185,608	3389.9	2317	Coal	579	167,820	16626.8	6738	Coal
131	175,854	3453.3	2482	Coal	580	64,129	16627.4	4114	Coal
132	69,917	3454.3	2060	Coal	581	78,706	16647.3	1509	Iron Ore
133	30,645	3461.4	3213	Coal	582	177,993	16688.6	1067	Coal
134	173,135	3486.7	3349	Iron Ore	583	253,000	16706.4	1344	Iron Ore
135	142,691	3524.2	2942	Coal	584	53,967	16729.4	1293	Coal
136	257,141	3537.0	973	Coal	585	159,474	16740.8	1591	Coal
137	32,667	3538.6	1242	Coal	586	78,466	16774.8	7266	Iron Ore
138	159,899	3603.0	2972	Iron Ore	587	243,273	16830.0	2405	Iron Ore
139	71,169	3654.0	1843	Coal	588	40,000	16865.2	2768	Iron Ore
140	138,224	3672.8	1075	Coal	589	162,774	16900.7	1047	Iron Ore
141	70,525	3685.3	2848	Coal	590	88,035	16905.4	1423	Coal
142	83,651	3691.6	50	Coal	591	35,837	16919.4	1488	Iron Ore
143	19,741	3713.7	1617	Iron Ore	592	41,886	16967.5	1844	Iron Ore
144	72,140	3717.3	8595	Coal	593	131,132	16988.2	4690	Iron Ore
145	63,178	3730.8	2739	Coal	594	157,954	17018.1	1260	Coal
146	176,975	3760.5	1066	Coal	595	67,561	17043.2	1197	Coal
147	133,318	3778.6	2103	Iron Ore	596	69,732	17079.6	1302	Coal
148	154,569	3814.4	1286	Coal	597	164,056	17098.6	3176	Iron Ore
149	50,228	3822.9	1860	Coal	598	89,320	17136.3	1668	Coal
150	105,376	3826.3	962	Coal	599	57,407	17137.3	1237	Iron Ore
151	92,139	3863.0	1706	Iron Ore	600	145,537	17164.8	778	Coal
152	54,792	3889.3	1038	Iron Ore	601	43,089	17184.9	1045	Coal
153	75,083	3890.4	728	Iron Ore	602	56,531	17201.8	3313	Coal
154	142,821	3932.6	3313	Iron Ore	603	45,000	17214.3	1482	Coal

ShipNr.	Shipload [t]	Arrival time [h]	T_s [h]	Material	ShipNr.	Shipload [t]	Arrival time [h]	T_s [h]	Material
155	74,713	3934.5	1479	Coal	604	53,373	17253.3	2511	Coal
156	151,500	3972.8	2229	Coal	605	43,580	17310.2	445	Iron Ore
157	160,986	3976.6	2202	Iron Ore	606	50,012	17337.7	250	Iron Ore
158	98,830	3997.8	2446	Iron Ore	607	30,850	17340.5	1057	Coal
159	38,778	4022.8	1133	Coal	608	67,503	17378.6	2249	Coal
160	65,236	4046.3	5836	Coal	609	71,544	17397.8	1894	Coal
161	163,790	4069.9	1220	Coal	610	71,242	17418.9	6790	Coal
162	41,844	4093.6	1689	Iron Ore	611	161,889	17459.1	1234	Coal
163	33,524	4096.8	2350	Coal	612	79,400	17565.1	1834	Iron Ore
164	43,885	4136.9	838	Iron Ore	613	124,534	17572.3	1384	Coal
165	74,853	4163.8	1283	Iron Ore	614	163,092	17582.6	2187	Coal
166	146,271	4169.7	1363	Coal	615	164,666	17620.3	1614	Iron Ore
167	170,521	4183.7	1679	Coal	616	163,201	17683.3	2445	Coal
168	176,234	4211.2	2488	Iron Ore	617	155,890	17696.8	1522	Coal
169	17,000	4228.5	1221	Coal	618	51,009	17737.8	2833	Coal
170	48,238	4284.8	475	Iron Ore	619	122,498	17762.8	1723	Coal
171	41,709	4318.7	1171	Iron Ore	620	156,981	17834.3	1908	Coal
172	74,845	4324.4	627	Coal	621	80,115	17844.3	934	Coal
173	31,208	4379.6	1048	Coal	622	158,921	17845.2	727	Coal
174	156,113	4383.8	1145	Coal	623	21,620	17884.1	3377	Iron Ore
175	137,776	4408.5	1898	Iron Ore	624	37,830	17887.8	2184	Iron Ore
176	258,440	4422.5	984	Coal	625	35,400	17962.8	227	Coal
177	28,725	4433.4	5502	Iron Ore	626	48,109	17982.3	709	Iron Ore
178	30,560	4467.7	512	Coal	627	43,185	17994.3	845	Coal
179	62,300	4492.8	100	Coal	628	37,272	18005.0	250	Iron Ore
180	163,066	4517.8	1117	Coal	629	245,342	18009.6	5312	Iron Ore
181	215,642	4543.1	4379	Iron Ore	630	75,273	18030.5	5441	Iron Ore
182	152,009	4557.6	1325	Coal	631	69,027	18046.4	1104	Iron Ore
183	153,837	4572.6	3861	Coal	632	162,357	18119.9	7561	Iron Ore
184	83,819	4607.5	1781	Iron Ore	633	168,935	18205.3	431	Iron Ore
185	150,906	4643.2	8892	Coal	634	252,099	18218.6	2224	Coal
186	70,194	4662.2	12443	Coal	635	70,798	18225.8	1290	Coal
187	175,973	4667.8	3436	Coal	636	166,099	18266.2	3406	Coal
188	71,234	4719.5	10279	Iron Ore	637	79,528	18341.6	2629	Coal
189	241,995	4755.4	1716	Iron Ore	638	44,300	18342.3	846	Iron Ore
190	74,628	4778.3	2088	Coal	639	159,418	18344.8	1437	Coal
191	85,759	4802.0	881	Coal	640	42,714	18372.7	25	Iron Ore
192	148,712	4864.6	8791	Coal	641	164,871	18412.5	3250	Iron Ore
193	122,863	4904.1	5233	Coal	642	161,812	18416.6	1185	Coal
194	67,790	4912.1	2136	Iron Ore	643	73,412	18419.8	1344	Iron Ore
195	70,396	4919.9	1433	Iron Ore	644	177,989	18469.8	1555	Iron Ore
196	73,992	4930.3	1175	Iron Ore	645	39,000	18513.5	3289	Iron Ore
197	145,412	4955.3	2422	Coal	646	139,576	18543.8	1387	Coal
198	134,804	4991.5	3514	Coal	647	69,650	18554.0	11806	Coal
199	68,108	5027.7	2372	Coal	648	39,218	18582.9	25	Iron Ore
200	81,305	5029.6	1736	Iron Ore	649	31,647	18627.8	3253	Coal
201	74,834	5062.5	3647	Coal	650	145,590	18629.1	471	Coal
202	114,570	5102.3	3876	Coal	651	57,000	18688.7	2962	Iron Ore
203	75,294	5103.4	2199	Coal	652	145,753	18690.6	902	Coal
204	165,560	5153.0	2047	Iron Ore	653	64,845	18701.2	1849	Coal
205	147,442	5154.0	1223	Coal	654	29,600	18742.9	250	Iron Ore
206	41,638	5181.3	698	Coal	655	157,920	18764.7	2230	Coal
207	182,367	5200.1	535	Coal	656	160,414	18812.7	2090	Iron Ore
208	113,417	5229.1	3796	Iron Ore	657	172,403	18830.7	3891	Coal
209	143,608	5254.7	2634	Iron Ore	658	160,840	18837.4	2276	Iron Ore
210	122,852	5255.9	2944	Coal	659	74,245	18911.8	718	Coal
211	66,660	5338.5	2693	Coal	660	163,484	18912.1	1759	Coal
212	107,368	5351.3	1570	Coal	661	167,145	18949.2	1910	Coal
213	136,063	5390.3	2295	Coal	662	38,939	18952.6	587	Coal
214	167,578	5411.6	1305	Iron Ore	663	54,585	18990.6	4390	Iron Ore
215	51,414	5423.7	2069	Coal	664	31,673	18991.3	604	Coal
216	162,691	5452.3	1668	Iron Ore	665	75,000	19014.9	2676	Coal
217	172,141	5497.5	3179	Coal	666	168,420	19076.1	1568	Coal
218	82,496	5520.1	2744	Coal	667	58,000	19087.3	2431	Coal
219	60,986	5525.4	1824	Iron Ore	668	73,516	19106.9	2209	Iron Ore

ShipNr.	Shipload [t]	Arrival time [h]	T_s [h]	Material	ShipNr.	Shipload [t]	Arrival time [h]	T_s [h]	Material
220	170,926	5616.1	2295	Coal	669	59,655	19140.4	2614	Coal
221	105,413	5648.5	2032	Coal	670	103,309	19141.9	1221	Coal
222	91,009	5652.3	2419	Coal	671	159,369	19201.0	1805	Iron Ore
223	173,096	5675.0	1751	Iron Ore	672	175,998	19237.5	6427	Coal
224	43,490	5698.2	1820	Iron Ore	673	77,000	19245.8	6752	Iron Ore
225	80,502	5752.7	500	Iron Ore	674	171,745	19279.3	25	Iron Ore
226	154,297	5763.4	881	Coal	675	31,782	19308.0	2068	Coal
227	37,250	5797.9	1380	Coal	676	163,521	19320.8	5225	Iron Ore
228	50,000	5821.1	747	Iron Ore	677	33,200	19346.4	3209	Coal
229	145,905	5845.6	1712	Coal	678	170,081	19348.6	25	Coal
230	43,019	5848.4	2976	Iron Ore	679	45,599	19388.8	2578	Coal
231	114,960	5862.3	1011	Coal	680	166,811	19423.2	1712	Iron Ore
232	183,403	5895.3	2671	Coal	681	82,804	19459.2	1030	Coal
233	260,774	5898.8	500	Coal	682	31,803	19471.9	1675	Coal
234	81,246	5936.1	1156	Coal	683	24,282	19480.2	250	Iron Ore
235	35,460	5939.2	9742	Coal	684	49,761	19521.9	250	Iron Ore
236	167,364	5947.4	3651	Coal	685	77,034	19540.0	9478	Coal
237	75,263	6001.0	3827	Coal	686	68,985	19563.1	831	Iron Ore
238	158,842	6008.8	2122	Iron Ore	687	157,764	19576.8	3760	Coal
239	147,971	6070.2	3526	Iron Ore	688	165,985	19589.3	100	Coal
240	101,408	6074.0	2158	Coal	689	44,000	19624.0	1244	Coal
241	113,989	6100.5	3048	Iron Ore	690	78,699	19645.5	824	Iron Ore
242	168,905	6143.8	500	Iron Ore	691	37,187	19648.9	5207	Iron Ore
243	153,705	6146.9	5833	Coal	692	135,002	19672.4	750	Iron Ore
244	180,522	6193.3	57	Coal	693	141,947	19745.4	1747	Iron Ore
245	177,250	6198.0	2250	Coal	694	72,284	19759.3	2734	Coal
246	71,462	6249.4	3009	Coal	695	160,756	19761.1	1054	Coal
247	35,984	6296.1	3113	Iron Ore	696	70,000	19776.8	1624	Iron Ore
248	177,190	6312.3	1264	Coal	697	47,880	19833.3	50	Coal
249	71,578	6323.7	712	Coal	698	170,516	19833.7	1071	Iron Ore
250	171,788	6358.8	1023	Coal	699	35,494	19873.3	370	Iron Ore
251	121,121	6362.7	500	Coal	700	240,013	19875.4	3251	Coal
252	47,609	6385.2	566	Iron Ore	701	132,000	19898.7	1607	Coal
253	68,410	6440.2	10113	Coal	702	61,409	19921.4	5890	Coal
254	139,637	6445.5	2741	Iron Ore	703	311,759	20022.2	1081	Iron Ore
255	42,400	6458.4	249	Iron Ore	704	60,000	20042.8	1533	Iron Ore
256	258,495	6468.1	2097	Coal	705	55,101	20104.8	1079	Iron Ore
257	71,621	6486.3	669	Iron Ore	706	141,730	20168.3	2201	Iron Ore
258	102,300	6508.1	3122	Iron Ore	707	168,276	20180.6	437	Iron Ore
259	173,287	6555.8	5992	Coal	708	34,070	20182.4	3032	Coal
260	74,834	6578.2	100	Coal	709	50,000	20206.6	2118	Iron Ore
261	122,400	6641.0	500	Iron Ore	710	30,251	20235.9	757	Coal
262	43,495	6653.8	2677	Coal	711	72,306	20300.7	1233	Iron Ore
263	190,194	6666.4	4242	Iron Ore	712	168,099	20318.4	1648	Coal
264	72,142	6695.3	6155	Iron Ore	713	151,277	20331.6	2150	Iron Ore
265	131,860	6704.0	1205	Iron Ore	714	200,417	20368.5	8979	Iron Ore
266	83,053	6754.3	2333	Iron Ore	715	72,711	20443.1	1918	Coal
267	36,280	6781.0	4162	Coal	716	92,890	20451.9	139	Coal
268	161,975	6803.1	2454	Coal	717	54,515	20453.3	697	Coal
269	80,576	6820.2	150	Coal	718	42,127	20509.2	12999	Coal
270	47,408	6840.8	2338	Coal	719	257,476	20518.9	1714	Iron Ore
271	110,455	6852.9	2215	Coal	720	74,562	20667.1	3807	Coal
272	71,497	6931.1	571	Iron Ore	721	161,911	20704.6	1778	Coal
273	145,336	6968.1	3114	Coal	722	56,150	20715.4	250	Iron Ore
274	48,216	6977.4	1428	Coal	723	141,991	20727.8	5707	Iron Ore
275	146,729	7003.7	1587	Coal	724	20,387	20860.9	62	Iron Ore
276	73,748	7006.1	10534	Coal	725	144,786	20882.1	2283	Iron Ore
277	122,320	7045.3	808	Coal	726	160,404	20968.2	8098	Iron Ore
278	74,345	7067.5	5771	Coal	727	170,371	20999.8	9932	Iron Ore
279	161,664	7102.2	3322	Coal	728	107,207	21098.6	1322	Iron Ore
280	168,300	7102.8	4005	Iron Ore	729	86,089	21140.8	2278	Iron Ore
281	90,613	7106.8	1857	Iron Ore	730	127,513	21148.3	3945	Iron Ore
282	70,468	7137.4	2598	Coal	731	77,000	21154.6	5798	Iron Ore
283	156,881	7157.1	1749	Coal	732	62,382	21182.2	3492	Coal
284	58,277	7185.0	12409	Coal	733	309,974	21228.0	1864	Coal

ShipNr.	Shipload [t]	Arrival time [h]	T_s [h]	Material	ShipNr.	Shipload [t]	Arrival time [h]	T_s [h]	Material
285	55,145	7187.6	2914	Coal	734	257,465	21239.3	2396	Iron Ore
286	67,179	7211.8	3974	Coal	735	40,066	21278.3	5505	Iron Ore
287	171,245	7248.8	5183	Coal	736	73,825	21314.3	3664	Iron Ore
288	68,947	7264.4	3390	Coal	737	168,802	21348.6	100	Iron Ore
289	101,050	7290.5	2588	Coal	738	75,261	21349.4	2737	Coal
290	163,634	7323.4	3359	Coal	739	21,882	21358.0	7206	Iron Ore
291	42,426	7339.7	9953	Coal	740	150,919	21415.8	1897	Coal
292	72,135	7392.2	456	Coal	741	69,567	21437.6	5774	Iron Ore
293	40,000	7410.6	561	Iron Ore	742	168,610	21502.8	2239	Coal
294	141,402	7426.0	948	Coal	743	74,330	21511.6	2945	Coal
295	144,011	7442.1	3805	Iron Ore	744	35,000	21514.3	7104	Iron Ore
296	73,616	7460.8	1961	Iron Ore	745	21,910	21546.6	6366	Coal
297	32,034	7466.0	7241	Iron Ore	746	76,763	21549.8	3366	Coal
298	161,164	7501.6	7968	Iron Ore	747	25,000	21575.9	13208	Coal
299	122,671	7534.5	7141	Coal	748	72,003	21585.6	3342	Iron Ore
300	43,125	7583.3	2183	Coal	749	71,158	21626.8	3205	Iron Ore
301	122,174	7609.2	1613	Coal	750	164,452	21637.8	2951	Coal
302	25,084	7609.7	100	Coal	751	258,148	21648.7	2533	Coal
303	66,224	7661.5	150	Coal	752	10,094	21657.4	226	Coal
304	80,190	7662.8	6960	Coal	753	163,638	21720.1	1394	Iron Ore
305	174,086	7724.3	5895	Coal	754	143,069	21724.4	3339	Coal
306	249,447	7739.1	5762	Coal	755	35,356	21773.9	3531	Iron Ore
307	71,700	7761.7	9434	Coal	756	165,000	21782.4	8217	Coal
308	73,404	7777.7	4046	Iron Ore	757	131,974	21820.1	2268	Coal
309	173,677	7799.9	4954	Iron Ore	758	150,514	21822.2	9356	Coal
310	163,443	7808.8	4065	Iron Ore	759	123,941	21846.3	25	Coal
311	172,519	7899.5	3213	Iron Ore	760	183,400	21908.3	2704	Iron Ore
312	70,700	7907.0	100	Coal	761	135,003	21930.8	3997	Iron Ore
313	54,062	7971.2	6541	Iron Ore	762	158,066	21941.9	148	Coal
314	162,067	7983.5	1223	Iron Ore	763	174,308	21996.1	4700	Iron Ore
315	17,850	7993.3	4730	Iron Ore	764	108,197	21996.8	2966	Iron Ore
316	70,519	8031.3	2119	Iron Ore	765	6,500	22010.6	1097	Coal
317	72,945	8034.9	1977	Coal	766	202,960	22061.9	1980	Coal
318	148,507	8068.3	2832	Coal	767	73,943	22094.3	1260	Coal
319	70,565	8106.8	1693	Iron Ore	768	173,806	22122.2	4129	Coal
320	164,339	8121.6	6501	Coal	769	167,754	22150.7	5447	Iron Ore
321	110,000	8132.7	1299	Coal	770	101,499	22166.7	8483	Coal
322	74,172	8161.0	6585	Iron Ore	771	73,577	22196.1	100	Iron Ore
323	116,164	8169.4	425	Coal	772	161,960	22244.3	40	Iron Ore
324	42,700	8184.8	3425	Iron Ore	773	51,731	22280.4	5792	Iron Ore
325	173,654	8230.6	703	Coal	774	36,854	22396.9	1139	Coal
326	145,062	8258.3	100	Iron Ore	775	72,428	22403.1	6097	Coal
327	64,841	8285.4	1091	Coal	776	37,017	22415.6	2458	Coal
328	214,904	8307.9	4667	Iron Ore	777	72,858	22441.2	4001	Coal
329	140,609	8309.4	3923	Coal	778	69,725	22447.0	1130	Coal
330	138,792	8329.7	8497	Coal	779	45,000	22452.7	100	Iron Ore
331	22,300	8358.1	4286	Coal	780	220,000	22501.3	6660	Iron Ore
332	50,109	8359.1	2149	Coal	781	179,607	22513.9	2839	Coal
333	166,327	8411.2	3976	Coal	782	166,750	22553.2	533	Coal
334	137,953	8417.1	3065	Coal	783	69,549	22588.4	1923	Coal
335	43,394	8454.7	1786	Iron Ore	784	80,840	22592.8	3094	Iron Ore
336	136,931	8463.8	2396	Coal	785	157,835	22601.5	4016	Coal
337	235,710	8596.5	8217	Coal	786	149,830	22654.3	2245	Coal
338	99,236	8630.3	4171	Iron Ore	787	90,086	22741.9	1417	Iron Ore
339	46,692	8643.3	386	Coal	788	202,047	22753.2	796	Coal
340	30,838	8729.4	1231	Iron Ore	789	258,849	22763.2	1563	Coal
341	191,182	8742.4	2157	Coal	790	40,000	22793.6	1892	Coal
342	61,674	8751.7	500	Iron Ore	791	166,399	22805.1	1236	Iron Ore
343	1,926	8756.3	361	Iron Ore	792	78,144	22822.3	731	Iron Ore
344	69,190	8794.0	2698	Coal	793	174,293	22863.4	1008	Iron Ore
345	249,355	8849.6	695	Coal	794	43,720	22928.0	1766	Iron Ore
346	79,207	8866.6	6770	Coal	795	37,280	22947.9	4302	Coal
347	39,786	8892.4	825	Coal	796	54,989	22950.5	2085	Coal
348	77,495	8913.3	973	Coal	797	21,654	22975.6	1997	Coal
349	79,033	8951.8	2305	Coal	798	24,662	22982.2	9845	Iron Ore

ShipNr.	Shipload [t]	Arrival time [h]	T_s [h]	Material	ShipNr.	Shipload [t]	Arrival time [h]	T_s [h]	Material
350	37,205	8954.5	2730	Coal	799	56,026	23021.8	100	Iron Ore
351	70,350	8964.2	3153	Iron Ore	800	38,217	23042.9	877	Iron Ore
352	83,793	8988.0	6495	Coal	801	81,408	23043.3	2393	Iron Ore
353	40,000	9003.1	1128	Iron Ore	802	163,609	23062.9	2198	Coal
354	64,965	9020.2	288	Coal	803	77,877	23081.8	6547	Coal
355	168,267	9049.8	6673	Coal	804	75,285	23101.6	4157	Iron Ore
356	162,415	9079.0	1687	Coal	805	71,371	23148.9	1737	Coal
357	50,000	9137.6	500	Iron Ore	806	77,725	23235.9	1716	Coal
358	166,244	9150.3	891	Iron Ore	807	35,900	23264.1	100	Iron Ore
359	73,435	9217.9	13169	Coal	808	68,880	23277.3	2565	Coal
360	164,994	9218.5	909	Coal	809	18,093	23291.6	2015	Coal
361	39,494	9328.0	150	Coal	810	52,808	23308.2	100	Iron Ore
362	163,008	9336.9	5867	Coal	811	176,297	23321.8	10	Coal
363	69,416	9351.3	2602	Coal	812	160,119	23322.8	6244	Coal
364	158,553	9362.5	4697	Coal	813	42,266	23326.8	745	Coal
365	163,356	9396.9	691	Coal	814	92,933	23362.0	2284	Coal
366	125,964	9421.7	476	Coal	815	175,995	23378.7	1738	Coal
367	158,624	9440.4	1236	Coal	816	177,203	23411.0	3264	Iron Ore
368	151,638	9448.8	2875	Coal	817	178,129	23436.8	6432	Coal
369	251,816	9471.2	3530	Coal	818	199,966	23470.3	2795	Coal
370	50,173	9525.1	1411	Coal	819	75,370	23475.1	4625	Coal
371	168,305	9537.5	921	Coal	820	70,496	23519.6	4395	Iron Ore
372	60,225	9559.9	2504	Coal	821	147,836	23574.2	100	Iron Ore
373	54,540	9588.2	2186	Coal	822	23,853	23576.4	1454	Iron Ore
374	65,647	9610.7	1493	Coal	823	71,603	23612.8	1194	Coal
375	40,000	9613.0	748	Coal	824	165,305	23623.2	6261	Coal
376	58,623	9637.6	296	Iron Ore	825	112,584	23662.3	3358	Coal
377	27,000	9724.7	250	Iron Ore	826	81,243	23684.4	3415	Coal
378	35,735	9728.1	2616	Coal	827	44,000	23735.3	3000	Coal
379	41,023	9790.5	859	Coal	828	34,732	23759.8	8377	Coal
380	73,467	9807.4	5518	Coal	829	166,325	23770.8	1650	Coal
381	21,517	9886.8	150	Coal	830	43,181	23834.0	2410	Iron Ore
382	162,044	9889.3	2321	Coal	831	58,579	23834.3	2649	Coal
383	77,552	9935.1	825	Coal	832	69,184	23838.8	1211	Coal
384	65,997	9950.3	1006	Coal	833	26,389	23878.9	100	Iron Ore
385	21,665	10050.4	161	Coal	834	36,952	23909.4	3404	Coal
386	22,751	10057.2	1529	Coal	835	172,030	23918.9	6428	Coal
387	72,871	10091.1	4928	Coal	836	76,658	23980.3	4555	Iron Ore
388	48,900	10105.8	250	Iron Ore	837	69,543	23991.5	514	Coal
389	38,357	10110.5	250	Iron Ore	838	33,800	24023.3	539	Coal
390	170,886	10145.2	1953	Coal	839	42,761	24030.7	100	Iron Ore
391	65,998	10184.3	24429	Coal	840	151,412	24042.9	473	Coal
392	55,300	10219.5	500	Iron Ore	841	70,998	24132.2	2352	Coal
393	18,775	10245.7	1003	Coal	842	158,881	24142.7	1968	Coal
394	169,820	10255.8	725	Coal	843	138,848	24218.4	970	Coal
395	168,451	10305.0	3371	Coal	844	77,009	24316.2	1998	Coal
396	190,955	10329.8	1523	Iron Ore	845	171,980	24341.7	4156	Coal
397	77,046	10344.3	1329	Iron Ore	846	165,109	24344.4	2958	Coal
398	13,000	10366.3	100	Iron Ore	847	89,589	24458.8	2592	Coal
399	67,523	10394.2	1249	Coal	848	39,816	24466.7	2116	Iron Ore
400	70,044	10402.6	1888	Coal	849	181,599	24467.3	705	Coal
401	180,665	10414.9	2209	Coal	850	63,083	24468.8	2956	Coal
402	21,315	10434.2	547	Coal	851	71,832	24501.4	2557	Coal
403	164,970	10477.9	150	Coal	852	248,191	24505.4	2567	Coal
404	138,629	10531.1	2290	Coal	853	165,227	24554.9	465	Coal
405	30,000	10555.4	339	Coal	854	171,416	24602.8	2686	Coal
406	174,599	10567.2	14573	Coal	855	162,215	24612.8	1631	Iron Ore
407	45,882	10579.0	1639	Coal	856	44,000	24629.0	821	Iron Ore
408	170,451	10591.9	863	Coal	857	37,550	24675.5	5074	Iron Ore
409	165,395	10644.0	3469	Coal	858	166,104	24678.8	1311	Coal
410	140,599	10658.6	2591	Coal	859	19,225	24724.1	100	Iron Ore
411	78,208	10677.5	15506	Coal	860	38,498	24751.6	3633	Iron Ore
412	84,500	10726.3	2312	Coal	861	156,589	24765.6	2128	Iron Ore
413	70,624	10730.7	2919	Coal	862	162,745	24800.2	4651	Iron Ore
414	80,924	10787.3	15842	Coal	863	70,586	24803.8	4070	Iron Ore

ShipNr.	Shipload [t]	Arrival time [h]	T_s [h]	Material	ShipNr.	Shipload [t]	Arrival time [h]	T_s [h]	Material
415	35,776	10789.1	1108	Coal	864	39,491	24804.6	12144	Iron Ore
416	160,031	10803.1	1779	Coal	865	77,000	24848.2	3889	Iron Ore
417	75,329	10830.0	500	Iron Ore	866	168,571	25012.1	2100	Coal
418	163,379	10908.3	1846	Coal	867	73,875	25024.7	2176	Coal
419	40,607	10918.2	1633	Coal	868	75,928	25035.9	2810	Coal
420	37,400	10944.6	9516	Coal	869	152,312	25048.6	1419	Iron Ore
421	167,188	10955.7	4596	Coal	870	70,163	25128.3	4276	Coal
422	103,620	11014.7	2028	Coal	871	69,222	25149.8	3600	Coal
423	16,072	11067.2	5118	Coal	872	252,582	25161.1	2636	Iron Ore
424	56,120	11100.8	1817	Coal	873	24,750	25171.1	1046	Iron Ore
425	167,860	11174.0	3330	Coal	874	70,748	25221.5	6291	Iron Ore
426	170,294	11190.4	4884	Coal	875	74,758	25251.8	2493	Coal
427	73,248	11198.8	7472	Coal	876	42,960	25345.2	2171	Iron Ore
428	43,393	11211.1	905	Coal	877	73,288	25371.4	3271	Coal
429	163,568	11261.8	2343	Coal	878	16,000	25382.9	100	Iron Ore
430	52,851	11291.8	4468	Iron Ore	879	250,888	25460.1	1786	Coal
431	77,010	11378.8	5237	Coal	880	164,999	25465.4	3860	Iron Ore
432	167,634	11648.8	4464	Coal	881	128,886	25483.8	4313	Coal
433	160,486	11689.7	1357	Coal	882	140,000	25489.6	3586	Iron Ore
434	38,782	11715.4	25	Coal	883	150,611	25544.9	1003	Coal
435	4,054	11722.0	256	Coal	884	159,985	25625.4	1522	Coal
436	4,052	11730.6	1269	Coal	885	45,050	25636.8	1215	Coal
437	46,105	11775.4	2524	Coal	886	58,509	25676.7	250	Iron Ore
438	46,293	11787.0	2238	Coal	887	77,193	25834.3	2304	Iron Ore
439	163,272	11797.1	3810	Coal	888	77,941	25847.0	801	Coal
440	17,596	11855.9	2914	Coal	889	46,591	25847.9	1842	Coal
441	103,731	11906.7	1265	Coal	890	36,843	25857.0	4339	Coal
442	81,106	12032.1	1047	Coal	891	158,442	26008.2	1757	Coal
443	162,889	12144.8	1396	Coal	892	56,098	26018.4	4461	Coal
444	150,129	12172.4	4222	Coal	893	71,049	26024.2	1544	Coal
445	163,983	12318.0	2334	Iron Ore	894	166,930	26065.4	3469	Coal
446	35,000	12331.4	250	Iron Ore	895	73,117	26109.5	250	Iron Ore
447	160,854	12405.4	2350	Iron Ore	896	76,312	26115.5	3022	Coal
448	81,574	12418.1	8111	Coal	897	160,519	26122.6	1979	Coal
449	165,093	12491.8	13602	Coal					

Glossary

Capitals

A	Stockyard area	[m^2]
A_s	Crescent-shaped slice area during reclaiming	[m^2]
B	Bulk ship's beam	[m]
BB	Blending bed	
C_b	Costs per hour per berth	[€/h]
C_{bc}	Investment costs of belt conveyors	[M€]
C_{sm}	Investment costs of stockyard machines	[M€]
C_{tot}	Total investment costs	[M€]
C_{ws}	Costs per hour per waiting ship	[€/h]
CRS	Cyclic routes selection	
CPA	Clearing Pile's Area (stockyard procedure)	
D	Bulk ship's maximum draft	[m]
FCFS	First-Come-First-Served	
G1/2	Grade 1 / Grade 2	
IAT	Interarrival time	[h]
IATDist	Interarrival time distribution	
J	Route performance indicator	[-]
J_{cv}	Performance indicator that relates to number of belt conveyors	[-]
J_{rl}	Performance indicator that relates to route length	[-]
J_{tp}	Performance indicator that relates to number of transfer points	[-]
KPI	Key Performance indicator	
L_r	Route length	[m]
L_s	Ship length	[m]
L_l	Stockyard lane length	[m]
L_q	Quay length	[m]
N	Number of layers in the pile's cross-section	[-]

NED	Negative exponential distribution	
PRS	Preferred routes selection	
Q	Terminal (un)loading rate	[kt/h]
Q_c	Crane unloading rate	[kt/h]
Q_{qcv}	Quay conveyor transportation rate	[kt/h]
Q_s	Stacking capacity	[kt/h]
Q_r	Reclaiming capacity	[kt/h]
$Q_{r\text{-}net}$	Net reclaiming capacity	[kt/h]
Q_t	Transportation rate	[kt/h]
REL	Relocation of piles (stockyard procedure)	
SlDist	Shipload distribution	
T1-T5	Investigated dry bulk terminals	
TC	Total quay cost per hour	[€/h]
T_sDist	Storage time distribution	
W	Average time a unit spends in queuing system	[h]
W_{ship}	Average ship port time	[h]
W_{train}	Average train port time	[h]
W_s	Service time	[h]
$W_{s\text{-}ship}$	Average ship service time	[h]
$W_{s\text{-}train}$	Average train service time	[h]
W_t	Waiting time	[h]

Non capitals

a_s	Slewing acceleration	[rad/min^2]
b	Empirical blending ratio factor	[-]
c	Number of cranes	[-]
c_u	Number of customers	[-]
c_X	coefficient of variation for the interarrival time X	[-]
c_Y	coefficient of variation for the service time Y	[-]
d	Separation distance between piles	[m]
dwt	Ship's deadweight	[kt]
e_n	Constant for the determination machine's weight	[-]
f_l	Landside equipment installation factor	[-]
f_{ql}	Quay length factor	[ktm^{-1}y^{-1}]
$f_{qc,c}$	Fraction of time that a quay crane was active	[-]
f_r	Reclaiming equipment installation factor	[-]
f_s	Seaside equipment installation factor	[-]
f_{st}	Sacking equipment installation factor	[-]
h_s	Slice height	[m]
k	Distribution coefficient for Erlang distributions	[-]
l_b	Stockyard machine's boom length	[m]
m	Mass	[t]
m_{rel}	Relocated mass per year	[Mt/y]
$\dot{m}$	Annual throughput	[Mt/y]
n	Number of servers	[-]
n_b	Number of berths	[-]
n_c	Number of cranes	[-]
n_{cv}	Number of belt conveyors	[-]
n_d	Number of operating days	[-]
n_h	Number of operational hours per day	[-]

n_i	Number of interruptions	[-]
n_l	Number of lanes	[-]
n_s	Number of ships	[-]
n_{tp}	Number of transfer points	[-]
p	Average value for a bulk material property	
q	Average value for a bulk material property after blending/homogenizing	
r_{bw}	Radius of the bucket wheel	[m]
s	Storage factor	[$tm^{-2}y^{-1}$]
sl	Shipload	[kt]
$v(\theta)$	Slewing speed as function of the slewing angle	[m/s]
w	Stockyard lane width	[m]

Greek capitals

$\Delta r(\theta)$	Chip thickness as function of the slewing angle	[m]
Δx	Chip thickness	[m]
Π_W	Delay probability	[-]
Φ	Weighing factor	[-]

Greek non capitals

α	Constants determined for ship dimensions	[-]
β_0	Regression parameter for the unloading rate	[kt/h]
β_{1-2}	Regression parameters for the unloading rate	[1/h]
δ	Regression parameter	[kt/h]
ε	Bed blending ratio	[-]
η	Through-ship efficiency factor	[-]
θ	Slewing angle	[rad]
λ	Arrival rate	[1/h]
μ	Service rate	[1/h]
ρ	Berth utilization	[-]
ρ_m	Bulk material density	[t/m^3]
σ	Standard deviation of the average bulk material property	[-]
σ_q	Standard deviation of a bulk property after blending	[-]
τ	Networks connectivity	[-]
χ^2	Chi-square value	[-]
$\chi^2_{0.05}$	Critical chi-square value for a 95% confidence interval	[-]
ω_r	Angular velocity of the bucket wheel	[rad/min]
ω_s	Slewing rotational velocity	[rad/min]

Samenvatting

Om aan de verwachte toename van overzeese handelsstromen van steenkolen en ijzerertsen te voldoen, moeten nieuwe droge bulk terminals worden gebouwd of bestaande terminals worden uitgebreid. Bovendien moeten terminals voldoen aan steeds strenger wordende milieueisen en zullen in de toekomst geconfronteerd worden met een gebrek aan geschikte haventerreinen en geschoold technisch personeel. Door een gebrek aan een alomvattende ontwerpmethode voor droge bulk terminals zijn huidige ontwerpen vooral gebaseerd op gemiddelde waardes, vuistregels en praktijk ervaringen. De in de literatuur voorgestelde waardes voor die vuistregels komen echter nauwelijks overeen met afgeleide kentallen van bestaande terminals. Bovendien leidt een ontwerp gebaseerd op vuistregels en gemiddelde waardes tot verschillende onbeantwoorde vragen.

Gedurende de dagelijkse operatie op terminals zijn er verschillende stochastische processen die de operatie beïnvloeden. Het te laat arriveren van schepen kan zorgen voor extra wachttijd van andere schepen wat weer resulteert in het moeten betalen van boetes aan eigenaren van die laatstgenoemde schepen. Andere stochastische processen zijn de variaties in sheepsladingen, opslagtijden van materialen en het storingsgedrag van machines. Deze stochastische processen moeten zeker meegenomen worden om geschikte ontwerpen te realiseren. In navolging van andere auteurs is simulatie toegepast om de stochastische variaties mee te nemen in het ontwerpproces.

Het modelleren en ontwerpen van droge bulk terminals als geheel is complex door de afhankelijkheden tussen de verschillende subsystemen (zoals de zee-en landzijde, opslagveld en het netwerk van bandtransporteurs). Dit wordt bijvoorbeeld duidelijk bij het toepassen van een veelgebruikte prestatieindicator: de gemiddelde wachttijd van schepen. Schepen kunnen moeten wachten door gebrek aan voldoende loscapaciteit aan de zeekade, of door de afwezigheid van ruimte om de materialen op te slaan, of omdat er geen opslagmachines beschikbaar zijn. De gekozen aanpak beschreven in deze dissertatie is het opdelen van de terminal in subsystemen, vervolgens elke subsysteem apart analyseren om uiteindelijk de subsystemen samen te voegen tot één model.

Voor elk subsysteem is een simulatiemodel ontwikkeld welke gebruikt is om de parameters (en de gevoeligheid van deze parameters) te onderzoeken die het ontwerpen van subsystemen bepalen. Per subsysteem zijn casussen, afgeleid van bestaande terminals, toegepast om het gebruik van de simulatiemodellen te demonstreren. Het totale terminal model omvat alle subsytemen. Dit model is gevalideerd met operationele gegevens en gebruikt voor de definitie en evaluatie van totale terminal ontwerpen.

Van 49 bestaande terminals zijn waardes bepaald voor potentiële ontwerprichtlijnen zoals de kadelengte factor en de opslagfactor. Deze waardes varieren aanzienlijk en komen nauwelijks overeen met de voorgestelde waardes in literatuur. Wanneer de waardes uit de literatuur gebruikt worden, zal dit leiden tot ondergedimensioneerde kadelengtes en over-gedimensioneerde opslagvelden. Bovendien zijn voor het selecteren van nieuwe machines de bezettingsgraden van bestaande machines niet zomaar toepasbaar. Dit komt door de grote variatie van deze bezettingsgraden.

Ondanks dat veel onderzoekers het modeleren van de zee-en landzijde van container terminals hebben onderzocht, hebben droge bulk terminals aanzienlijk minder belangstelling gekregen in de wetenschapelijke literatuur. Daarnaast komen de in praktijk gemeten verdelingen, die de variatie beschrijven van de tussenaankomst- en servicetijden van schepen, nauwelijks overeen met de door verschillende auteurs voorgestelde verdelingen. Wanneer de voorgestelde verdelingen gebruikt worden, leidt dit tot verkeerde ontwerpspecificaties. De in deze dissertatie beschreven simulatiemodellen zijn zo ontworpen dat historische gegevens als invoer gebruikt kunnen worden.

Het zeezijde model, dat ook gebruikt kan worden voor de landzijde, is ontworpen om zeekade layouts te evalueren en specifieke procedures aan de zeekade te beoordelen. Een zeekade layout bestaat uit een specificatie van de lengte van de zeekade, het aantal ligplaatsen en het aantal plus capaciteit van kranen en kadebanden. Vooral het gebruik van de continue kade-operatie, waarbij kranen zich over de kade kunnen verplaatsen om op verschillende ligplaatsen werk te verzetten, resulteert in een hogere bezettingsgraad van kranen en ligplaatsen. Hierdoor is minder kadelengte nodig in vergelijk met de discrete kade-operatie waarbij elke kraan slechts op één ligplaats kan worden ingezet. Een andere bevinding is dat het aantal kadebanden met bijhorende transport capaciteit nauwkeurig gespecificeerd moet worden om te voorkomen dat kranen vertraagd worden bij het teglijkertijd lossen van hetzelfde materiaal.

De opslagfactor, welke de verhouding aangeeft tussen de jaarlijkse doorvoer en de grootte van het opslagveld, is afgeleid om inzicht te krijgen welke parameters van invloed zijn op de grootte van het opslagveld. De belangrijkste parameters zijn de verhouding massa per vierkante meter en het aantal keren dat het opslagveld gebruikt wordt gedurende een bepaalde tijd. Door de onbalans tussen de binnenkomende en vertrekkende ladingen varieert de hoeveelheid opgeslagen tonnen gedurende de tijd. Het opslagmodel is ontwikkeld om deze stochastische processen mee te nemen bij het bepalen van de benodigde opslagveld. Ook specifieke opslag procedures zoals het verdelen van een lading over meerdere hopen, het vrijmaken van opslagruimte direct na het afvoeren van een deel van een hoop én het verkassen van kleine hoopjes om een grote vrije ruimte te creëeren, zijn in dit opslagmodel geïmplementeerd. Simulaties hebben aangetoond dat deze opslag procedures leiden tot een aanzienlijke vermindering van de grootte van het opslagveld.

Op het opslagveld zijn doorgaans machines geïnstalleerd voor het opslaan en afgraven van droge bulk materialen. Om tot een goede machine selectie te komen, zijn de eigenschappen van deze machines bepaald. Wanneer materialen gemengd moeten worden, hangt het mengeffect af van de gebruikte opslagmethode en de geïnstalleerde afgraaf machine. In het algemeen wordt een beter mengeffect bereikt wanneer lagen van verschillende materialen verdeeld zijn over de dwarsdoorsnede van de hoop en wanneer deze menghopen vanaf de zijkant worden afgegraven. In een casus is de selectie van de opslagmethode en afgraaf machine gedemonstreerd voor het mengen van steenkolen die geleverd moeten worden aan een kolencentrale.

Gebruikelijke machines op opslagvelden zijn stacker-reclaimers maar ook losse stackers en reclaimers worden toegepast. Simulatie is gebruikt voor de selectie van deze machines om het niet tegelijkertijd opslaan en afgraven door stacker-reclaimers mee te nemen. Stacker-reclaimers hebben een hogere afgraafcapaciteit nodig dan wanneer losse machines worden ingezet om toch dezelfde prestatie te leveren. De investeringskosten voor stacker-reclaimers inclusief de bijhorende bandtransporteurs zijn, ondanks de hogere afgraafcapaciteit, lager dan de totale investeringskosten wanneer losse machines worden ingezet. Simulaties toonden aan dat de afgraafcapaciteit van stacker-reclaimers kan worden gereduceerd wanneer hopen binnen het bereik van twee machines worden opgeslagen. Een andere variant om de afgraafcapaciteit te verlagen is om het lossen van zeeschepen tijdelijk te onderbreken en treinen tussendoor te beladen.

Voor het transport van droge bulk materialen op de terminal is vaak een netwerk, waarbinnen zich verschillende bandtransporteurs bevinden, geïnstalleerd. Terminal operators streven naar uitgebreide, flexibele netwerken om meerder transporten op hetzelfde moment te kunnen uitvoeren. Daarom zijn deze netwerken uitgevoerd met een groot aantal overstortpunten om aansluitingen tussen verschillende bandtransporteurs te realiseren. Deze overstortpunten hebben echter extra aandrijfvermogen nodig; de materialen moeten immers omhoog getransporteerd worden om te kunnen worden gestort op onderliggende bandtransporteurs. Tevens zijn opstortpunten kostbaar om te realiseren, en vragen overstortpunten extra onderhoud (door slijtage) en extra opruim-werkzaamheden (door het morsen tijdens de overstort).

Het transport netwerk model is ontwikkeld om netwerken van bandtransporteurs te beoordelen. Zoals verwacht toonden simulaties aan dat een toename van het aantal verbindingen in een netwerk leidt tot een verbetering van de terminal prestatie. Het installeren van meer dan 75% van het maximale aantal verbindingen in een netwerk brengt echter geen merkbare verbetering tot stand. Een andere bevinding was dat een netwerk uitgevoerd met reversibele bandtransporteurs slechter presteerde dan een netwerk uitgevoerd met bandtransporteurs welke één richting op draaien. De reden hiervoor is dat het aantal transporten dat tegelijkertijd kon worden uitgevoerd was gereduceerd.

Verder was het transport netwerk model gebruikt om verschillende procedures voor het kiezen van transport routes te toetsen. In de eerste procedure werden alle routes achter elkaar gekozen. Bij de tweede procedure werden routes met een hoge prestatieindicator als eerste geselecteerd. Deze prestatieindicator was gedefinieerd als het gewogen product van de lengte van de route, het aantal bandtransporteurs en het aantal overstortpunten. Simulaties toonden aan dat het steeds opnieuw kiezen van voorkeursroutes (dus met hogere waardes voor de prestatieindicator) leidde tot een toename van de gemiddelde verblijftijd van schepen. Deze voorkeursroutes verhinderden namelijk dat meerdere routes tegelijkertijd gebruikt werden.

De toevoegingen aan bestaande ontwerpmethodes kunnen als volgt worden beschreven; een eerste ontwerp kan gemaakt worden door de bestaande ontwerpmethodes toe te passen. Vervolgens wordt dit ontwerp geïntegreerd in ontwikkelde simulatiemodellen. Stochastische variaties van bijv. aankomst en opslagprocessen worden toegevoegd en de bijhorende prestaties gemeten. Indien deze afwijken van de vereiste prestaties of om alternatieven ontwerpen te genereren kunnen verschillende operationele procedures worden onderzocht. Voorbeelden zijn het toepassen van een continue kade layout waarbij kranen ingezet worden op meerdere schepen, of het toepassen van verschillende procedures op het opslagveld. Ook kan een reductie van het aantal en capaciteit van machines en van de complexiteit van het bandtransporteur netwerk worden onderzocht door toepassing van het totale terminal simulatie model.

Summary

To meet the expected increase of the seaborne trade flows for coal and iron ore new dry bulk terminals have to be built or existing terminals need to be expanded. Furthermore, terminals have to comply with stringent environmental requirements and will face a shortage of port area and skilled personnel. Due to the absence of a comprehensive design method for dry bulk terminals, designs are nowadays forced to be based on average values, rules-of-thumb and practical experiences. However, the suggested values for rules-of-thumb match poorly with derived terminal characteristics and the impact of stochastic variations on terminal designs is hardly considered. A formulation of designs using rules-of-thumb and average values resulted in many questions unanswered.

During daily operation several stochastic processes affect the terminal operation. The late arrivals of ships may cause extra waiting times for other ships resulting in paying demurrage penalties to ship-owners. Other stochastic processes are the variations in shiploads, storage times of cargo at stockyards and equipment breakdown behavior. These stochastic processes must be considered as well to realize adequate designs. In accordance to other authors discrete event simulation is used to take the stochastic variations into account.

Modeling and designing terminals as a whole is complicated due to the dependencies between the terminal subsystems. For example, a typical performance indicator is the average ship waiting time. Ships may wait due to limited service capacity at the terminal's seaside, due to the absence of available storage area or due to the fact that all stockyard machines are occupied. The approach followed in this thesis is a decomposition of the terminal in subsystems (seaside, landside, stockyard and the belt conveyor network). Each subsystem was analyzed separately and at the end, the subsystems were combined.

For each subsystem a discrete-event simulation model was developed to assess which parameters affect the subsystem's design. Per subsystem case studies, usually derived from

existing terminals, were used to demonstrate the application of the simulation model. The total terminal model covers all subsystems. This model was validated using real-world operational data and was used for the formulation and evaluation of total terminal designs.

From 49 existing dry bulk terminals values for potential factors like the quay length factor and the storage factor were determined. These values vary significantly and do hardly correspond with values suggested in literature. Using the literature values will lead to undersized quay lengths and oversized stockyards. Also the derived equipment utilizations cannot be used for machine specification due to the large variation.

Although many researchers discussed the modeling of the seaside and landside operation for container terminals, dry bulk terminals have received significant less attention in literature. Measured interarrival time and service time distributions show hardly a fit with distributions proposed by several authors. Using the proposed distributions will lead to incorrect designs. The simulation models were developed in such a way that historical data can be used as input.

The seaside model, which can also be applied for the terminal's landside, was developed to evaluate seaside layouts and to assess quay operational procedures. A seaside design contains a certain length for the quay, a number of berths and a number and capacity of cranes. Especially the continuous quay operation, where cranes move alongside the quay to serve ships at different berths, results in a higher utilization for cranes and berths. This results that less quay length is required compared to the discrete quay layout where cranes are allocated to berths. Another finding is that the number and transportation rate of the quay conveyors needs to be determined precisely to prevent a slow slown of the crane operation when multiple cranes unload the same material at the same time.

The storage factor, which is the ratio between the terminal's annual throughput and the stockyard size, was derived analytically to get insight which parameters affect stockyard sizing. The main important parameters are the ratio mass per square meter and the number of replenishments per year. Due to the imbalance between the incoming and outgoing streams of bulk materials, the amount of cargo that is stored at the stockyard varies during time. The stockyard model was developed to take these stochastic variations into account. Also specific stockyard procedures like the distribution of material across multiple piles, clearing the pile's area directly after reclaiming a part of the pile and the relocation of small piles to make a large free location were implemented in the stockyard model. Simulation experiments have shown that applying these operational procedures will result in a significant reduction of the stockyard size needed.

Machines installed at the stockyard have to facilitate stacking and reclaiming of dry bulk materials. To obtain a correct machine selection, machine characteristics were determined. When the materials need to be blended, the blending effect that can be achieved relates to the stacking method and the installed reclaimer type. Generally, the better blending effect is realized when layers of different materials are spread over the pile's cross section and piles are reclaimed from the face side. The selection of the stacking method and the reclaiming machine was demonstrated in a case study where coal has to be blended before being transported to a power plant.

At stockyards stacker-reclaimers or individual stackers and reclaimers are often installed. Simulation was used for a correct machine type selection to take the impossibility of stacking and reclaiming at the same time by stacker-reclaimers into account. Stacker-reclaimers require higher capacities than individual machines to meet a comparable performance. However, the investment costs for stacker-reclaimers together with related belt conveyors are less compared to single stackers and reclaimers. Simulation results also proved that the reclaiming capacity for stacker-reclaimers can be reduced when piles are stored in reach of two machines. Another variant to reduce the reclaiming capacity required is to interrupt ship servicing in favor of train loading.

To transport dry bulk material at terminals, networks which contain several belt conveyors are generally installed. Terminal operators strive for extended, flexible networks to perform multiple transportation activities at the same time. That’s why a large number of transfer points are often installed to realize multiple connections between belt conveyors. However, these transfer points require extra power because the material must be conveyed up to be dumped onto other belt conveyors. Furthermore, transfer points are expensive to realize, require extra maintenance (due to wear) and extra cleaning activities (spillage during transfer).

The transport network model is developed to assess belt conveyor networks. As expected, simulation experiments have shown that an increase of the number of connections in a belt conveyor network leads to an improvement of the terminal performance. Nevertheless, installing more than 75% of the maximum number of transfer points in a network will not bring a notable improvement anymore. Another finding was that a network that contained bi-way belt conveyors performed significantly worse than a network equipped with single-way belt conveyors due to the reduced number of possible transport activities at the same time.

The transport network model was also applied to evaluate route selection procedures. The first procedure was the cyclic routes selection where all routes were assigned in succession. For the second selection procedure, routes with a high performance indicator (which is defined as a weighted product of the route length, the number of belt conveyors and the number of transfer points) were selected at first. Simulation results have shown that the selection of preferred routes increased the average ship port times. Better performing routes hinder the use of other routes at the same time.

The additions to existing design methods can be formulated as follows; a first design can be determined by applying existing design methods. Subsequently, this design should be integrated in the simulation models developed. Stochastic variations (e.g, ship arrival and storage processes) should be included and the corresponding performances are measured. If these deviate from performance predefined or to formulate alternative designs, several terminal operational procedures can be investigated. Examples are the continuous quay layout where (un)loading machines are used for servicing several ships, or applying specific stockyard operational procedures. The reduction of the number and capacities of machines and complexity of the belt conveyor network can be investigated as well using the total terminal model developed.

Biography

Teus van Vianen was born on the 31st of January, 1980 in Brandwijk, the Netherlands. He obtained his VWO diploma in 1998, after which he started his studies in mechanical engineering at the Hogeschool Brabant in Breda. In 2002 he obtained his BSc degree (cum laude) and continued his studies at Delft University of Technology. In July 2005, he finished his Master thesis and graduated under the supervision of Prof. Rijsenbrij within the Transport Engineering and Logistics group, at the 3ME faculty.

After his studies, he worked for five years in the machinery industry, two years as a project engineer and three years as a project manager. In June 2010, he returned to the academic world and started his PhD project “Simulation-integrated Design of Dry Bulk Terminals”. During his research, the parameters that affect a dry bulk terminal design were discovered, the sensitivity for these parameters on designs were determined and simulation tools were developed to support the design process. This research has led to several scientific publications and oral presentations in international conferences. In May 2014, Teus started his own consultancy firm (Exspecta) to provide professional advices to terminal operators, terminal designers or equipment manufactures and to implement the simulation models developed in real-world applications.

TRAIL Thesis Series

The following list contains the most recent dissertations in the TRAIL Thesis Series. For a complete overview of more than 100 titles see the TRAIL website: www.rsTRAIL.nl.

The TRAIL Thesis Series is a series of the Netherlands TRAIL Research School on transport, infrastructure and logistics.

Vianen, T. van, *Simulation-integrated Design of Dry Bulk Terminals,* T2015/1, January 2015, TRAIL Thesis Series, the Netherlands

Risto, M., *Cooperative In-Vehicle Advice: A study into drivers' ability and willingness to follow tactical driver advice,* T2014/10, December 2014, TRAIL Thesis Series, the Netherlands

Djukic, T., *Dynamic OD Demand Estimation and Prediction for Dynamic Traffic Management*, T2014/9, November 2014, TRAIL Thesis Series, the Netherlands

Chen, C., *Task Complexity and Time Pressure: Impacts on activity-travel choices,* T2014/8, November 2014, TRAIL Thesis Series, the Netherlands

Wang, Y., *Optimal Trajectory Planning and Train Scheduling for Railway Systems,* T2014/7, November 2014, TRAIL Thesis Series, the Netherlands

Wang, M., *Generic Model Predictive Control Framework for Advanced Driver Assistance Systems,* T2014/6, October 2014, TRAIL Thesis Series, the Netherlands

Kecman, P., *Models for Predictive Railway Traffic Management*, T2014/5, October 2014, TRAIL Thesis Series, the Netherlands

Davarynejad, M., *Deploying Evolutionary Metaheuristics for Global Optimization*, T2014/4, June 2014, TRAIL Thesis Series, the Netherlands

Li, J., *Characteristics of Chinese Driver Behavior*, T2014/3, June 2014, TRAIL Thesis Series, the Netherlands

Mouter, N., *Cost-Benefit Analysis in Practice: A study of the way Cost-Benefit Analysis is perceived by key actors in the Dutch appraisal practice for spatial-infrastructure projects*, T2014/2, June 2014, TRAIL Thesis Series, the Netherlands

Ohazulike, A., *Road Pricing mechanism: A game theoretic and multi-level approach*, T2014/1, January 2014, TRAIL Thesis Series, the Netherlands

Cranenburgh, S. van, *Vacation Travel Behaviour in a Very Different Future*, T2013/12, November 2013, TRAIL Thesis Series, the Netherlands

Samsura, D.A.A., *Games and the City: Applying game-theoretical approaches to land and property development analysis*, T2013/11, November 2013, TRAIL Thesis Series, the Netherlands

Huijts, N., *Sustainable Energy Technology Acceptance: A psychological perspective*, T2013/10, September 2013, TRAIL Thesis Series, the Netherlands

Zhang, Mo, *A Freight Transport Model for Integrated Network, Service, and Policy Design*, T2013/9, August 2013, TRAIL Thesis Series, the Netherlands

Wijnen, R., *Decision Support for Collaborative Airport Planning*, T2013/8, April 2013, TRAIL Thesis Series, the Netherlands

Wageningen-Kessels, F.L.M. van, *Multi-Class Continuum Traffic Flow Models: Analysis and simulation methods*, T2013/7, March 2013, TRAIL Thesis Series, the Netherlands

Taneja, P., *The Flexible Port*, T2013/6, March 2013, TRAIL Thesis Series, the Netherlands

Yuan, Y., *Lagrangian Multi-Class Traffic State Estimation*, T2013/5, March 2013, TRAIL Thesis Series, the Netherlands

Schreiter, Th., *Vehicle-Class Specific Control of Freeway Traffic*, T2013/4, March 2013, TRAIL Thesis Series, the Netherlands

Zaerpour, N., *Efficient Management of Compact Storage Systems*, T2013/3, February 2013, TRAIL Thesis Series, the Netherlands

Huibregtse, O.L., *Robust Model-Based Optimization of Evacuation Guidance*, T2013/2, February 2013, TRAIL Thesis Series, the Netherlands

Fortuijn, L.G.H., *Turborotonde en turboplein: ontwerp, capaciteit en veiligheid*, T2013/1, January 2013, TRAIL Thesis Series, the Netherlands

Gharehgozli, A.H., *Developing New Methods for Efficient Container Stacking Operations*, T2012/7, November 2012, TRAIL Thesis Series, the Netherlands

Duin, R. van, *Logistics Concept Development in Multi-Actor Environments: Aligning stakeholders for successful development of public/private logistics systems by increased awareness of multi-actor objectives and perceptions,* T2012/6, October 2012, TRAIL Thesis Series, the Netherlands

Dicke-Ogenia, M., *Psychological Aspects of Travel Information Presentation: A psychological and ergonomic view on travellers' response to travel information,* T2012/5, October 2012, TRAIL Thesis Series, the Netherlands

Wismans, L.J.J., *Towards Sustainable Dynamic Traffic Management,* T2012/4, September 2012, TRAIL Thesis Series, the Netherlands

Hoogendoorn, R.G., *Swiftly before the World Collapses: Empirics and Modeling of Longitudinal Driving Behavior under Adverse Conditions*, T2012/3, July 2012, TRAIL Thesis Series, the Netherlands

Carmona Benitez, R., *The Design of a Large Scale Airline Network*, T2012/2, June 2012, TRAIL Thesis Series, the Netherlands